



**UNIVERSITÀ DEGLI STUDI
DI MILANO**

PHD COURSE IN TRANSLATIONAL MEDICINE

CICLE XXXV

PhD THESIS

MED/03

**Molecular study of chromatinopathies:
the case of Rubinstein-Taybi and Rett syndromes**

PhD student: **Elisabetta Di Fedè**

Matricola n°: R12526

Tutor: Professor Cristina Gervasini

PhD Coordinator: Professor Chiarella Sforza

Academic Year 2021/2022

Table of contents

LIST OF ABBREVIATIONS.....	5
FIGURE INDEX.....	7
TABLE INDEX.....	8
ABSTRACT.....	9
1. INTRODUCTION.....	10
1.1 CHROMATINOPATHIES.....	10
1.2 EPIGENETIC MODIFICATIONS.....	16
1.2.1 Histone acetylation	16
1.2.1.1 Lysine acetyltransferases (KATs)	17
1.2.1.2 Histone deacetylases (HDACs)	18
1.2.1.3 HDAC inhibitors (HDACi)	19
1.2.2 Histone methylation.....	22
1.2.2.1 Lysine methyltransferases (KMTs)	22
1.2.2.2 Lysine demethylases (KDMs)	23
1.2.3 DNA methylation	24
1.2.3.1 DNA methyltransferases (DNMTs).....	24
1.2.3.2 TET proteins	25
1.3 RUBINSTEIN-TAYBI SYNDROME	25
1.3.1 Clinical aspects	26
1.3.1.1 Facial dysmorphisms	26
1.3.1.2 Skeletal anomalies	27
1.3.1.3 Growth delay.....	28
1.3.1.4 Intellectual disability and neurodevelopmental problems.....	29
1.3.1.5 Congenital anomalies and additional features	29
1.3.2 Molecular aspects	30
1.3.2.1 CBP and p300	30
1.3.2.2 Mutational spectrum	31
1.3.3 Genotype-phenotype correlation	32
1.4 RETT SYNDROME	33
1.4.1 Clinical aspects	34
1.4.2 Molecular aspects	34
1.4.3 Mutational spectrum and clinical heterogeneity.....	35
1.4.2.1 MeCP2	36
2. AIM OF THE THESIS.....	39
3. MATHERIAL AND METHODS	40

3.1 IN VITRO MODELS	40
3.1.1 Cell cultures.....	40
3.1.1.1 Lymphoblastoid cell lines (LCLs).....	40
3.1.1.2 Human embryonic Kidney (HEK) 293T cells and generated cell lines.....	41
3.1.2 AlphaLISA assay®	42
3.1.3 Immunocytochemistry	43
3.1.3.1 Immunofluorescence (IF)	43
3.1.3.2 TUNEL assay	44
3.1.4 Protein procedures	45
3.1.4.1 Protein extraction	45
3.1.4.2 Fractionation	45
3.1.4.3 Western blot.....	45
3.1.5 Proteomic analysis	46
3.1.5.1 Immunoprecipitation	46
3.1.5.2 Sample preparation and mass spectrometry analysis	46
3.2 DROSOPHILA MELANOGASTER MODEL	47
3.2.1 Stocks and feeding	47
3.2.2 Embryos flies immunostaining.....	47
3.2.3 Extraction of DNA for microbiota profiling	48
3.3 PATIENTS	49
3.3.1 Subjects and samples	49
3.3.1.1 Extraction of DNA from blood and saliva samples.....	49
3.3.1.2 Extraction of DNA for microbiota profiling	49
3.3.2 NGS analysis	50
3.3.2.1 RSTS multi gene panel sequencing	50
3.3.2.2 RSTS and RTT-like exome sequencing	50
3.3.2.3 Variants validation	50
3.3.2.4 16S rRNA gene sequencing of human gut microbiota	51
3.4 QUANTIFICATION AND STATISTICAL ANALYSIS	51
3.4.1 Data generated from LCLs assays.....	51
3.4.2 LC-MS/MS analysis	51
3.2.3 Microbiota profiling data from flies and human.....	52
4. RESULTS	53
4.1 EXPLORING POSSIBLE THERAPEUTIC APPROACH AND NEW GENOTYPE-PHENOTYPE CORRELATIONS FOR RUBINSTEIN-TAYBI SYNDROME (RSTS)	53

4.1.1 Dissecting HDACi effect as possible therapeutic approach	53
4.1.1.1 Exogenous HDACi exposure boosts acetylation in RSTS lymphoblastoid cell lines (LCLs)	53
4.1.1.2 Exogenous HDACi exposure leads to a partial rescue of RSTS phenotype in <i>Drosophila melanogaster</i> model	59
4.1.1.3 RSTS patients' microbiota profiling shows a depletion of bacteria procedures of endogenous HDACi	61
4.1.1.4 Microbiota profiling in <i>D. melanogaster</i> CBP mutants	66
4.1.2 NGS approach on RSTS patients without a molecular diagnosis	68
4.1.2.1 Genotype-phenotype correlation for <i>KMT2A</i> variants identified in six RSTS patients	68
4.1.2.2 Characterization of a HDAC2 variant identified in one RSTS patient.....	74
4.2 EXPANDING RETT SYNDROME LANDSCAPE	77
4.2.1 Identification of candidate genes from a WES study in Rett-like patients	77
4.2.1.1 Clinical presentation of three Rett-like patients.....	77
4.2.1.2 Variants identification and genotype-phenotype correlation	79
4.2.2 Exploring the role of SLC35F1	79
4.2.2.1 SLC35F1 cellular localization	79
4.2.2.2 SLC35F1 interactome	81
5. DISCUSSION	83
5.1 HDACi such as short chain fatty acids (SCFAs) could represent an epigenetic treatment for Rubinstein-Taybi syndrome (RSTS)	83
5.2 RSTS genotype-phenotype correlation for novel variants identified in a known chromatinopathy gene (<i>KMT2A</i>).....	84
5.3 Characterization of a pathogenetic variant found in a new chromatinopathy-related gene (<i>HDAC2</i>) in a RSTS patient.....	85
5.4 Identification of pathogenetic variants in <i>NBEA</i> , <i>DYNC1H1</i> and <i>SLC35F1</i> in Rett-like patients .	86
5.5 SLC35F1 is a cytoplasmic protein involved in ATP-dependent activity and rRNA binding	87
6. CONCLUSION.....	89
7. BIBLIOGRAPHY	90
RESEARCH INTEGRITY STATEMENT	107
APPENDIX 1 – Scientific work.....	108

LIST OF ABBREVIATIONS

5mC – 5-methylcytosine
5hmC – 5-hydroxymethylcytosine
ACMG – American College of Medical Genetics and Genomics
ACN - acetonitrile
AEDs – antiepileptic drugs
AmBic – ammonium bicarbonate
Amp - ampicillin
ASD – autism spectrum disorders
ASM – anti-seizure medications
CH1-3 – cysteine-histidine-rich regions
CNS – central nervous system
CTD – C-terminal domain
Del/ins – deletions/insertions
DMEM – Dulbecco’s modified eagle medium
DNMTs – DNA methyltransferases
DTT – dithiothreitol
E/I – excitatory/inhibitory
EEGs – electroencephalograms
ER – endoplasmic reticulum
ESCs – embryonic stem cells
EtOH – ethanol
FA – formic acid
FBS – fetal bovine serum
FDA – Food and Drug Administration
GERD – gastroesophageal reflux disease
GO – gene ontology
HD – healthy donors
HDACi – HDAC inhibitors
HEK – human embryonic kidney
HGVS – Human Genome Variation Society
IBD – inflammatory bowel disease
ID – intellectual disability
IF – immunofluorescence
IP – immunoprecipitation
IQ – intelligence quotient
KATs – lysine acetyltransferases
KD – knock down
KDACS – lysine deacetylases

KDMs – lysine demethylases
KID – kinase inducible domain
KMTs – lysine methyl transferases
LC-MS – liquid chromatography-mass spectrometry
LCLs – lymphoblastoid cell lines
LOF – loss of function
LSB – Laemmli sample buffer
MBD – methyl-binding domain
mESCs – mouse embryonic stem cells
min – minutes
mos – months
MRI – magnetic resonance imaging
MTBD – microtubule-binding domain
NaB – sodium butyrate
NAD⁺ – nicotinamide adenine dinucleotide
NCBD – nuclear binding coactivator domain
NDDs – neurodevelopmental disorders
NGS – next generation sequencing
NID – NcoR interaction domain
NLS – nuclear localization signal
NRID – nuclear receptor interaction domain
OFC – occipital frontal conference
PCoA – principal coordinates analysis
PD – Phylogenetic diversity
PDL – poly-D-lysine
P/S – penicillin/streptomycin
PHD – plant homeodomain
Pol II – RNA polymerase II
PTMs – post-translational modifications
RDP – Ribosomal Database Project
RT – room temperature
SAHA – suberoylanilide hydroxamic acid
SCFAs – short chain fatty acids
SD – standard deviation
SEM – standard error of the mean
TAZ1 – transcriptional adaptor zinc finger 1
TBP – TATA binding protein
TFA – trifluoroacetic acid
TRD – transcriptional repressor domain
TSA – tricostatin A
TUNEL – terminal deoxynucleotidyl transferase (TdT) dUTP Nick-End Labeling

VNS – vagal nerve stimulation
VPA – valproic acid
VUS – variant of uncertain significance
WES – whole exome sequencing
WGS – whole genome sequencing
yrs – years

FIGURE INDEX

Figure 1.1 Chromatinopathies.....	11
Figure 1.2 Transcriptional regulation of chromatin by acetylation.....	19
Figure 1.3 Butyrate in gut-brain axis.....	22
Figure 1.4 DNA methylation.....	25
Figure 1.5 RSTS features.....	28
Figure 1.6 CBP and p300 and their genes mutational spectrum.....	32
Figure 1.7 Structure of <i>MECP2</i> and protein domains involved in RTT.....	36
Figure 1.8 Molecular function of MeCP2 and its alteration in RTT.....	38
Figure 3.1 Schematic representation of the technology underlying AlphaLISA assay®	43
Figure 4.1. Histone acetylation on RSTS LCLs upon HDACi exposure.....	54
Figure 4.2. Insight on single-RSTS LCLs histone acetylation.....	55
Figure 4.3. Proliferation evaluation on RSTS LCLs after HDACi exposure.....	56
Figure 4.4. Cell death evaluation on RSTS LCLs after HDACi exposure.....	57
Figure 4.5. Insights on cell proliferation and cell death rate of RSTS LCLs upon HDAC inhibitors exposure.....	58
Figure 4.6. Correlation between HDACi-induced acetylation versus cell proliferation and apoptosis in RSTS LCLs.....	59
Figure 4.7. Partial developmental rescue of RSTS phenotype in <i>D. melanogaster</i> model (<i>nej</i>).....	60
Figure 4.8. Embryos survival and altered phenotypes upon HDACi treatments.....	61
Figure 4.9. Alpha and beta diversity in RSTS microbiota compared to HD.....	63
Figure 4.10. Microbial composition in HD and RSTS subjects.....	64
Figure 4.11. Alpha and beta diversity in <i>nej</i> ^{+/-} microbiota compared to <i>yw</i> flies.....	66
Figure 4.12. Microbial composition in <i>yw</i> and <i>nej</i> flies.....	67
Figure 4.13. Phenotypic features of patients #187, #243 and #251 with <i>KMT2A</i> variants.....	74

Figure 4.14. HDAC2 localization in patient derived lymphoblastoid cell line (LCL).....	75
Figure 4.15. Histone acetylation in patient #249 LCLs.....	76
Figure 4.16. Screening of SLC35F1 KO clones.....	79
Figure 4.17. Cellular localization of SLC35F1 in 293T cells.....	80
Figure 4.18. SLC35F1 IP check by western blot.....	81
Figure 4.19. Scatter plot of endogenous SLC35F1 IP MS data on 293T and KO samples.....	82

TABLE INDEX

Table 1.1 List of chromatinopathies' genes in Figure 1.1.....	11
Table 3.1 Patients-derived LCLs used in the present work.....	40
Table 3.2 Conditions of in vitro treatments used on <i>CREBBP</i> and <i>EP300</i> LCLs.....	41
Table 4.1. Nutritional values of the subjects enrolled in the study.....	62
Table 4.2. Bacterial composition in HD and RSTS groups.....	65
Table 4.3. <i>KMT2A</i> pathogenic variants detected in the described patients.....	68
Table 4.4. <i>KMT2A</i> pathogenic variants and phenotypic signs of the six described patients compared to the clinical features associated to RSTS and WDSTS.....	70
Table 4.5. Summarized WES results and phenotypic features of the three Rett-like patients negative for mutations in RTT known causative genes.....	78
Table 4.6. List of the top GO molecular functions enriched in differentially expressed proteins resulted from proteomic analysis.....	82

ABSTRACT

Background: Chromatinopathies are defined as a group of disorders displaying mutations in genes of the epigenetic apparatus and sharing clinical features such as intellectual disability and abnormal growth. Among them, Rubinstein-Taybi syndrome (RSTS) is characterized by CBP/p300 lysin-acetyltransferases deficit, while classic form of Rett syndrome (RTT) is caused by mutations in the reader *MECP2*. Both disorders show neurodevelopmental defects and 10 to 30% of patients remains without a molecular diagnosis.

Methods: In this work, we aim at deepening molecular aspects involving RSTS and RTT etiology and RSTS possible epigenetic treatments. Indeed, we tested exogenous histone deacetylase inhibitors (HDACi) in *in vitro* cellular models (lymphoblastoid cell lines derived from patients and healthy donors) and on a *Drosophila melanogaster* model of RSTS (*nej*) and wild type flies (*yw*), performing acetylation and viability assays and flies embryos immunostaining respectively. In parallel, we investigated endogenous HDACi in RSTS patients and in fruit flies models, assessing their microbiota. In addition, we applied whole exome sequencing (WES) analysis to RSTS and RTT-like probands negative for mutations in known associated genes and we then characterized two identified variants by genome editing techniques and functional analysis.

Results: In RSTS studies, we observed that patients gut microbiota is significantly depleted in butyrate-producing bacteria and we demonstrate that the effects of the HDACi butyrate, as well as the differences in microbiota composition, are conserved in *nej* flies. From WES study, we found in one RSTS and three RTT-like patients unreported variants in *HDAC2*, and *NBEA*, *DYNC1H1* and *SLC35F1* genes respectively, whose role is currently under investigation through *in vitro* models.

Conclusions: The study on microbiota composition could pave the way for novel therapeutic interventions for RSTS, while the identification of new RSTS and RTT genes could expand the genotype-phenotype correlation for these chromatinopathies, and characterization of new candidate genes could give insights into pathogenesis of these disorders.

1. INTRODUCTION

1.1 CHROMATINOPATHIES

In recent years the advent of genome-wide technologies, next generation sequencing (NGS) techniques such as sequencing of gene panels, whole exome (WES) or genome (WGS), led to the identification of an increasing number of a subgroup of diseases which in 2014 Fahrner and Bjornsson coined with the term of “Mendelian disorders of the epigenetic machinery” (Fahrner and Bjornsson, 2019). This group, also known as chromatinopathies, includes Mendelian diseases caused by mutations in genes of the epigenetic apparatus, which operates *in trans* on genes expression by regulating chromatin state. Indeed, an open or closed chromatin influences the DNA accessibility to transcriptional factors, thus controlling the transcription process (Jenuwein and Allis, 2001; Wolffe, 1994).

To date, 82 epigenetic disorders have been classified as Chromatinopathies, found to be caused by mutations in 70 genes of the epigenetic machinery (Fahrner and Bjornsson, 2019) (figure 1.1 and table 1.1). Despite the heterogeneity of this group of disorders, patients often display overlapping clinical signs, such as neurological dysfunctions, in particular intellectual disability (ID), growth abnormalities and in a minor fraction limb malformations (Bjornsson, 2015). Interestingly, many chromatin genes have been found mutated in conditions with shared neurological clinical features such as autism spectrum disorders (ASD) (De Rubeis et al., 2014), suggesting an important role of these genes in neurodevelopmental processes. In addition to clinical signs, many chromatinopathies also share a common etiology, since they are often characterized by haploinsufficiency and loss of function (LOF) mutations, as most of these disorders shows autosomal dominant inheritance and loss of a single allele, which can explain the dosage sensitivity observed (Bjornsson, 2015; Fahrner and Bjornsson, 2019). Thus, the interconnection between these epigenetic actors has been recently deepened investigating their co-expression, intolerance to variation and enrichment of neuronal genes (Boukas et al., 2019).

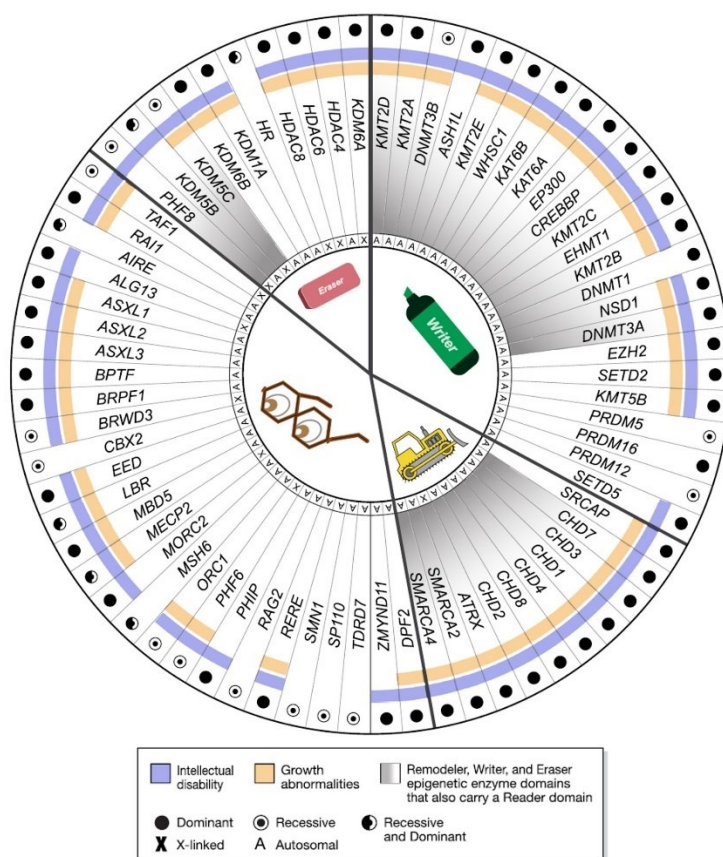


Figure 1.1 Chromatinopathies. Representation of 70 genes causing chromatinopathies, divided for main epigenetic domains (with icons of writer, eraser, reader, and remodeler) with marked coexistence of reader enzymatic domain (gray shades); inheritance is marked with circles (filled for dominant, partially filled for recessive and half-filled for both conditions), chromosome location is defined by letters A (autosome) and X (X chromosome) and phenotypic features by blue (ID) and orange (growth anomalies). Adapted from “Fahrner and Bjornsson, 2019”.

Table 1.1 List of chromatinopathies’ genes in figure 1.1

GENE	DISORDER	FUNCTION	INHERITANCE
<i>SETD5</i>	Mental Retardation, Autosomal Dominant 23 (OMIM #615761)	Writer	AD
<i>PRDM12</i>	Neuropathy, hereditary sensory and autonomic, type VIII (OMIM #616488)	Writer	AR
<i>PRDM16</i>	Dilated cardiomyopathy, left ventricular noncompaction 8 (OMIM #615373)	Writer	AD

<i>PRDM5</i>	Brittle cornea syndrome 2 (OMIM #614170)	Writer	AR
<i>KMT5B</i>	Mental Retardation, Autosomal Dominant 51 (OMIM #617788)	Writer	AD
<i>SETD2</i>	Luscan-Lumish syndrome (OMIM #616831)	Writer	AD
<i>EZH2</i>	Weaver syndrome (OMIM #277590)	Writer	AD
<i>DNMT3A</i>	Acute myeloid leukemia, somatic (OMIM #601626), Heyn-Sproul-Jackson syndrome (OMIM #618724), Tatton-Brown-Rahman syndrome (OMIM #615879)	Writer/Reader	AD
<i>NSD1</i>	Sotos syndrome (OMIM #117550)	Writer/Reader	AD
<i>DNMT1</i>	Cerebellar ataxia, deafness, and narcolepsy, autosomal dominant (OMIM #604121), Neuropathy, hereditary sensory, type IE (OMIM #614116)	Writer/Reader	AD
<i>KMT2B</i>	Childhood-onset dystonia 28 (OMIM #617284)	Writer/Reader	AD
<i>EHMT1</i>	Kleefstra syndrome 1 (OMIM #610253)	Writer/Reader	AD
<i>KMT2C</i>	Kleefstra syndrome 2 (OMIM #617768)	Writer/Reader	AD
<i>CREBBP</i>	Rubinstein-Taybi syndrome 1 (OMIM #180849)	Writer/Reader	AD
<i>EP300</i>	Rubinstein-Taybi syndrome 2 (OMIM #613684)	Writer/Reader	AD
<i>KAT6A</i>	Arboleda-Tham syndrome (OMIM #616268)	Writer/Reader	AD
<i>KAT6B</i>	Say-Barber-Biesecker-Young-Simpson or Ohdo syndrome (OMIM #603736)	Writer/Reader	AD
<i>WHSC1</i>	Wolf-Hirschhorn syndrome (OMIM #194190)	Writer/Reader	AD
<i>KMT2E</i>	KMT2E-deficiency or O'Donnell-Luria-Rodan syndrome (OMIM #618512)	Writer/Reader	AD
<i>ASH1L</i>	Mental retardation, autosomal dominant 52 (OMIM #617796)	Writer/Reader	AD

<i>DNMT3B</i>	Immunodeficiency-centromeric instability-facial anomalies syndrome 1 (OMIM #242860)	Writer/Reader	AR
<i>KMT2A</i>	Wiedemann-Steiner syndrome (OMIM #605130):	Writer/Reader	AD
<i>KMT2D</i>	Kabuki syndrome 1 (OMIM #147920):	Writer/Reader	AD
<i>KDM6A</i>	Kabuki Syndrome 2 (OMIM #300867)	Eraser	XLD
<i>HDAC4</i>	Brachydactyly-mental retardation syndrome (OMIM #600430)	Eraser	AD
<i>HDAC6</i>	Chondrodysplasia with platyspondyly, distinctive brachydactyly, hydrocephaly, and microphthalmia (OMIM #300863)	Eraser	XLD
<i>HDAC8</i>	Cornelia de Lange syndrome 5 (OMIM #300882)	Eraser	XLD
<i>HR</i>	Alopecia universalis (OMIM #203655); Atrichia with papular lesions (OMIM #209500); Hypotrichosis 4 (OMIM #146550)	Eraser	AR; AR; AD
<i>KDM1A</i>	Cleft palate, psychomotor retardation, and distinctive facial features (OMIM #616728)	Eraser	AD
<i>KDM6B</i>	Neurodevelopmental disorder with coarse facies and mild distal skeletal abnormalities (OMIM #618505)	Eraser	AD
<i>KDM5C</i>	Mental retardation, X-linked, syndromic, Claes-Jensen type (OMIM #300534)	Eraser/Reader	XLR
<i>KDM5B</i>	Mental retardation, autosomal recessive 65 (OMIM #618109)	Eraser/Reader	AD/AR
<i>PHF8</i>	Mental retardation syndrome, X-linked, Siderius type (OMIM #300263)	Eraser/Reader	XLR
<i>ASXL1</i>	Bohring-Opitz (BOPS, OMIM #605039)	Reader	AD
<i>ASXL2</i>	Shashi-Pena syndrome (OMIM #617190)	Reader	AD
<i>ASXL3</i>	Bainbridge-Ropers syndrome (OMIM #615485)	Reader	AD
<i>DPF2</i>	Coffin-Siris syndrome 7 (CSS7, OMIM #618027)	Reader	AD

<i>TAF1</i>	Mental Retardation X-Linked Syndromic 33 (OMIM #300966)	Reader	XLR
<i>RAI1</i>	Smith-Magenis syndrome (OMIM #182290)	Reader	AD
<i>AIRE</i>	Autoimmune Polyendocrine syndrome type I (OMIM #240300)	Reader	AD/AR
<i>ALG13</i>	Early Infantile Epileptic Encephalopathy-36 (OMIM #300884)	Reader	XLD
<i>BPTF</i>	Neurodevelopmental disorder with dysmorphic facies and distal limb anomalies (OMIM #617755)	Reader	AD
<i>BRPF1</i>	Intellectual developmental disorder with dysmorphic facies and ptosis (OMIM #617333)	Reader	AD
<i>BRWD3</i>	X-linked Mental Retardation 93 (OMIM #300659)	Reader	XLR
<i>CBX2</i>	46 XY Sex reversal 5 (OMIM #613080)	Reader	AR
<i>EED</i>	Cohen-Gibson syndrome (OMIM #617561)	Reader	AD
<i>LBR</i>	Pelger-Huet anomaly (OMIM #169400); PHA with musculoskeletal findings (OMIM #618019); Greenberg skeletal dysplasia (OMIM #215140)	Reader	AD; AR; AR
<i>MBD5</i>	Mental Retardation Autosomal Dominant (OMIM #156200)	Reader	AD
<i>MECP2</i>	Rett syndrome (OMIM #312750) or MECP2 Duplication syndrome or X-linked Syndromic Mental Retardation, Lubs type (OMIM #300260)	Reader	XLD (XLR)
<i>MORC2</i>	Charcot-Maire-Tooth disease type 2Z (OMIM #616688)	Reader	AD
<i>MSH6</i>	Hereditary Nonpolyposis Colorectal Cancer type 5 (OMIM #614350); Mismatch repair cancer syndrome (OMIM # 276300)	Reader	AD; AR
<i>ORC1</i>	Meier-Gorlin syndrome 1 (OMIM #224690)	Reader	AR
<i>PHF6</i>	Borjeson-Forssmann-Lehmann syndrome (OMIM #301900)	Reader	XLR

<i>PHIP</i>	Developmental Delay Intellectual Disability Obesity and Dysmorphism or Chung-Jansen syndrome (OMIM #617991)	Reader	AD
<i>RAG2</i>	Omenn syndrome and Severe Combined Immunodeficiency (OMIM #603554, #601457)	Reader	AR
<i>RERE</i>	Neurodevelopmental disorder with or without other anomalies (OMIM #616975):	Reader	AD
<i>SMN1</i>	Spinal Muscular Atrophy (OMIM #253300, #253550, #253400, #271150)	Reader	AR
<i>SP110</i>	Hepatic Venooclusive disease with immunodeficiency (OMIM #235550)	Reader	AR
<i>TDRD7</i>	Cataract 36 (OMIM #613887)	Reader	AR
<i>ZMYND11</i>	Mental Retardation Autosomal Dominant 30 (OMIM #616083)	Reader	AD
<i>SMARCA4</i>	Coffin-Siris syndrome-4 (OMIM #614609)	Remodeler/Reader	AD
<i>SMARCA2</i>	Nicolaides-Baraitser syndrome-4 (OMIM #601358)	Remodeler/Reader	AD
<i>ATRX</i>	Alpha-thalassemia myelodysplasia syndrome, somatic (OMIM #300448); Alpha-thalassemia/mental retardation syndrome (OMIM #301040); Mental retardation-hypotonic facies syndrome, X-linked (OMIM #309580)	Remodeler/Reader	AD XLD
<i>CHD2</i>	Epileptic encephalopathy, childhood-onset (OMIM #615369)	Remodeler/Reader	AD
<i>CHD8</i>	Autism susceptibility 8 (OMIM #615032)	Remodeler/Reader	AD
<i>CHD4</i>	Sifrim-Hitz-Weiss syndrome (OMIM #617159)	Remodeler/Reader	AD
<i>CHD1</i>	Pilarowski-Bjornsson syndrome (617682)	Remodeler/Reader	AD
<i>CHD3</i>	Snijders Blok-Campeau syndrome (OMIM #618205)	Remodeler/Reader	AD

<i>CHD7</i>	CHARGE syndrome (OMIM #214800); Hypogonadotropic hypogonadism 5 with or without anosmia (OMIM #612370)	Remodeler/Reader	AD
<i>SRCAP</i>	Floating Harbor syndrome (OMIM #136140)	Remodeler	AD

1.2 EPIGENETIC MODIFICATIONS

Chromatinopathies causative genes can be classified in four different not mutually exclusive categories, depending on the activities exerted by their respective protein domains. In fact, proteins encoded by epigenetic system genes can act as writers, erasers, readers, remodelers or as a combination of these roles. Writers and erasers have opposite function, respectively placing or removing epigenetic marks on specific genomic regions, making them reversible; these marks can be recognized by readers, whose domains can be part of the same protein with chromatin modifying domains, while chromatin remodelers can favor DNA-protein interactions regulating DNA accessibility through nucleosomes displacement in an ATP-dependent manner (Fahrner and Bjornsson, 2014). These epigenetic modifications are dynamic processes fundamental in cell identity maintenance, development, metabolism, and environmental response (Cavalli and Heard, 2019).

These epigenetic mechanisms can involve covalent modification on histone proteins or DNA. Among histone post-translational modifications (PTMs) there are acetylation, methylation, ubiquitination, phosphorylation, sumoylation, ADP-ribosylation, deamination and proline isomerization (Kouzarides, 2007), occurring at N-terminal histone tails. In this way, PTMs can alter the DNA association to nucleosomes leading to the chromatin opening or closure, which respectively corresponds to a more or less accessible state resulting in active or repressed transcription.

1.2.1 Histone acetylation

Acetylation is strictly regulated by lysine acetyltransferases (KATs, also referred to as HATs) and lysine deacetylases (KDACs, also referred to as HDACs), respectively writers and erasers of the epigenetic machinery. KATs transfer the acetyl portion of acetyl-CoA to histone lysine, neutralizing the positive charge of the amino acid and consequently reducing its affinity to

DNA whose conformation thus changes and makes promoters more accessible for transcription (figure 1.2). On the contrary, HDACs remove acetyl moiety at lysine tails restoring a compacted chromatin state (Wang et al., 2009b).

1.2.1.1 Lysine acetyltransferases (KATs)

To date, known proteins with endogenous KAT activity are p300/CBP, GCN5 (PCAF and GCN5) and MYST families (HBO1, KAT6B, MOF, MOZ or KAT6A, TIP60), ATAC2, ATAT1, CLOCK, ESCO1 and ESCO2, HAT1 and MCM3AP. Their function is exploited at enhancers, promoters, and gene bodies of genes with an active transcriptional state (figure 1.2). For instance, a more relaxed chromatin is associated with acetylated histone 4 lysine 16 (H4K16ac); the RNA polymerase II (Pol II) release for active transcription is marked by the acetylation of histone 3 lysine 27 (H3K27ac) and histone acetylation can recruit other proteins with acetyl-binding bromodomain and protein complexes. KATs themselves can act also in molecular complexes and not only on chromatin, as over 2000 target proteins have been identified, such as transcription factors (e.g. C/EBP α , FOXO1, p53), and they can be regulated by PTMs and metabolites essential for their function (i.e. acetyl-CoA). These enzymes result key regulators of many pathways and processes for cellular homeostasis, such as transcription, DNA repair, DNA replication and chromosome condensation, thus it is not surprising their involvement both in physiological and pathological conditions, from embryonic development to neurological disorders and cancer (Kouzarides, 2007; Sheikh and Akhtar, 2019).

The importance of KATs in embryonic development is underlined by the early lethality displayed by mouse models deficient for this class of writers. This was observed for *p300*, characterized by anomalies in neurulation, cardiac development, and cell proliferation (Yao et al., 1998), and *Cbp* null mice, exhibiting neural tube closure defects and defective hematopoiesis (Tanaka et al., 2000). Lack of *Gcn5* in mouse embryos caused growth retardation and dorsal mesoderm lineages failure, a phenotype which presented more pronounced severity when also *Pcaf* was depleted (Xu et al., 2000). In *Hbo1*^{-/-} embryos was observed a developmental arrest due to degeneration of mesenchyme and structural anomalies in blood vessels and somites (Kueh et al., 2011); *Mof*^{-/-} embryos couldn't reach implantation stage (Thomas et al., 2008); *Moz* resulted essential for hematopoietic stem cells maintenance and differentiation (Katsumoto et al., 2006) and *Tip60* for blastocyst-gastrula transition during embryogenesis (Hu et al., 2009).

1.2.1.2 Histone deacetylases (HDACs)

Antagonistic enzymes of KATs are HDACs (figure 1.2), which are grouped in four different classes based on the homology to the proteins found in *Saccharomyces cerevisiae*: class I (HDAC1, HDAC2, HDAC3 and HDAC8), class IIa (HDAC4, HDAC5, HDAC7 and HDAC9) and IIb (HDAC6 and HDAC10), class III (SIRT1, SIRT2, SIRT3, SIRT4, SIRT5, SIRT6 and SIRT7) and class IV (HDAC11). They use different cofactor for catalysis, with class I, II and IV requiring zinc while class III nicotinamide adenine dinucleotide (NAD⁺) (Ali et al., 2018). Class I HDACs are expressed ubiquitously, they are mainly localized into the nucleus, and often found acting as corepressors in multi-molecular protein complexes such as Sin3, NuRD, CoREST, PRC2 (HDAC1 and HDAC2) and SMRT/N-CoR (HDAC3). Class IIa enzymes show a localization not restricted to the nucleus and a more specific expression pattern: HDAC4 is enriched in brain and skeleton, HDAC5 and HDAC9 in muscles and HDAC7 in endothelial cells and T-cell precursors. They can carry out their repressor activity by either recruiting class I HDACs or interacting with other transcriptional factors, while little is known so far about class IIb and IV HDACs: HDAC6 is an important cytoplasmatic deacetylase in mammals targeting cytoskeletal proteins, while HDAC11 is expressed in different tissues but insights into its function are still poor. HDACs can be regulated by PTMs and protein-protein interaction, they are fundamental in acetylation balance maintenance and, similarly to KATs, they can regulate other proteins PTMs and alter gene transcription, impacting on human health and disease (Haberland et al., 2009; Park and Kim, 2020; Seto and Yoshida, 2014).

Indeed, as it has been reported for KATs, not all *in vivo* models depleted for these enzymes reach adulthood making clear their importance for embryogenesis and cardiac development. For instance, mice lacking *Hdac1* died at embryonic day 9.5, while *Hdac2*^{-/-} mice died during the perinatal period due to severe heart malformations (Montgomery et al., 2007); *Hdac3* null embryos showed gastrulation anomalies (Montgomery et al., 2008); *Hdac5* and *Hdac9* compound mutants displayed lethal cardiac abnormalities (Chang et al., 2004), while cardiovascular system disruption led to early lethality in *Hdac7*^{-/-} mice embryos (Chang et al., 2006).

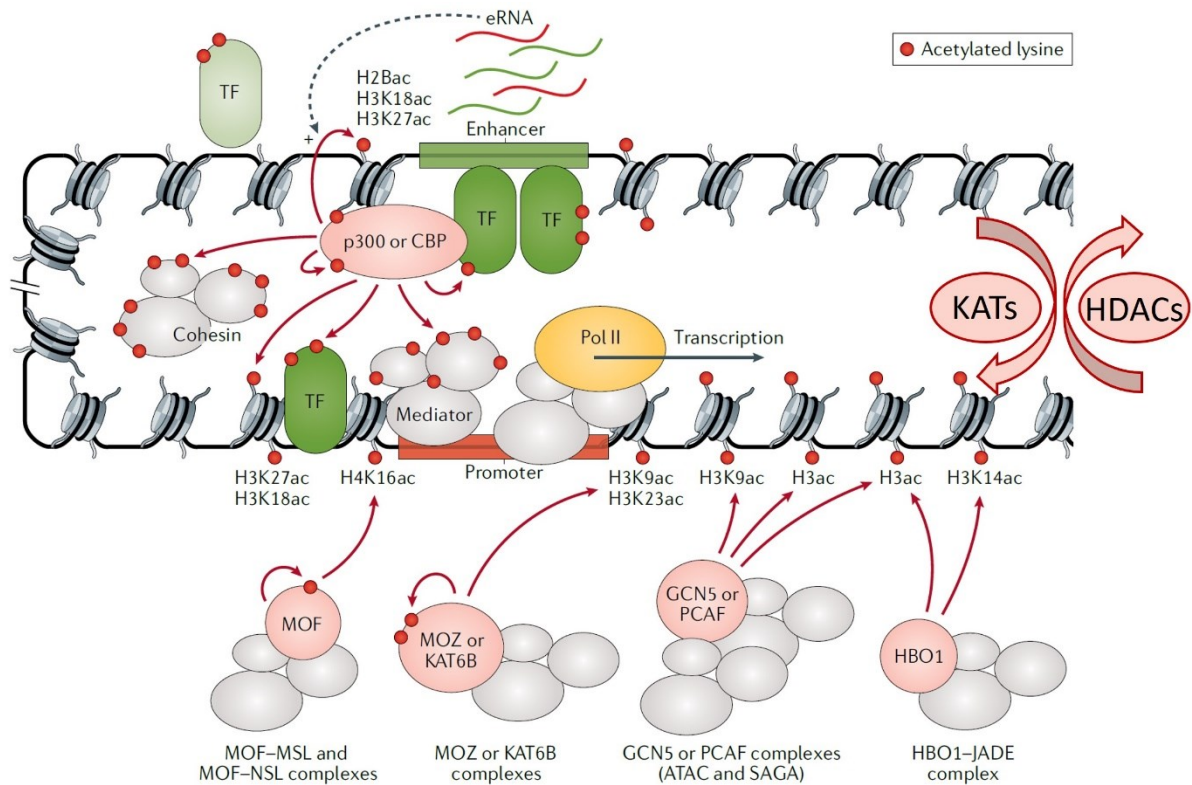


Figure 1.2 Transcriptional regulation of chromatin by acetylation. Representation of KATs complexes (CBP or p300, MOF, MOZ or KAT6B, GCN5 or PCAF and HBO1) acetylating lysines of histone (H3ac, H3K9ac, H3K14ac, H3K18ac, H3K27ac) and non-histone proteins (transcription factor, TF; promoter; mediator, cohesin), promoting RNA polymerase II (Pol II) activity and thus transcription, whose function antagonized the one exerted by HDACs which remove acetylated lysines. Adapted from “Sheikh and Akhtar, 2019”.

1.2.1.3 HDAC inhibitors (HDACi)

Histone acetylation can be modulated by a novel class of compounds called HDAC inhibitors (HDACi), which have been used for different pathological conditions characterized by ipoacetylation in order to prevent histone deacetylation and restore a balance in chromatin conformation and consequent gene expression (Schölz et al., 2015). Their activity is exploited blocking the interaction between the enzymatic catalytic site and its substrate and most of them recognizes multiple HDAC isoforms, lacking high specificity. HDACi can be classified into four groups based on their chemical composition: hydroxamic acid, short chain fatty acids (SCFAs), benzamide, and cyclic peptide.

HDACi belonging to the first mentioned group act on HDAC of class I and II, and among these compounds there are trichostatin A (TSA), the first discovered in 1990 which led *in vitro* to histone hyperacetylation and expression of tumor suppressor genes, and suberoylanilide

hydroxamic acid (SAHA), the first HDACi approved for the treatment of cutaneous T-cell lymphoma by Food and Drug Administration (FDA), which has been observed to cause also growth arrest, block of differentiation and apoptosis also in lymphoblastic leukemia cell lines (Duvic et al., 2007; Li et al., 2016; Schölz et al., 2015; Seto and Yoshida, 2014).

SCFAs are characterized by a short half-life, lower potency, and target mainly class I HDACs. Among these HDACi, valproic acid (VPA) acts on HDAC1-3, it induces hyperacetylation both *in vitro* and *in vivo*, and consequently activates transcriptional programs leading to apoptosis and reduction of cell proliferation (Göttlicher et al., 2001). VPA is widely used as anticonvulsant, mood stabilizer, and as treatment for other neurological disorders, as well as it is known to have antitumor properties (Bradbury et al., 2005; Emrich et al., 1981; Perucca, 2002; Phiel et al., 2001). Sodium butyrate (NaB) is another SCFAs which inhibits class I HDACs and its use in clinics was shown to have implications in different aspects of human health. Its properties can be exploited in cancer therapy and prevention, since butyrate induces caspase activation and apoptosis in human myeloid leukemia cells, provokes autophagic cell death, has antiangiogenic and antimetastatic effects, and protective function against colorectal cancer (Bordonaro et al., 2008; Deroanne et al., 2002; Rosato et al., 2001; Shao et al., 2004). In addition, this SCFA was observed to have anti-inflammatory effects (e.g. in inflammatory bowel disease, IBD), to improve insulin sensitivity (Gao et al., 2009; Hallert et al., 2003), and to exert a neuroprotective role. In detail, NaB and derivatives of butyric acid showed positive effects *in vivo* for cerebral ischemia, Huntington's disease, synaptic plasticity and long-term memory (Gardian et al., 2005; Kim et al., 2009; Vecsey et al., 2007).

Among benzamide derivatives there are MS-275 and CI-994 which are potent HDACi with antiproliferative and antitumor activity, while the two main cyclic peptides are apicidin and depsipeptide, a natural compound with cytotoxic activity in cancer cell lines (Bhalla, 2005; Seto and Yoshida, 2014).

Interestingly, a link between modulation of acetylation and metabolism is present, since acetyl-CoA functions both as acetyl donor for KATs and key metabolite sensitive to nutrients, as observed in starving cells showing a consistent reduction of acetyl-CoA and global acetylation (Mariño et al., 2014). This interplay was also observed during neuronal processes: inhibition of acetyl-CoA synthase short chain 2 (ACSS2), which converts acetate to acetyl-CoA and interacts with CBP, led to a reduction of H3K27ac and consequently a decreased

expression of genes for neuronal differentiation, and ACSS2 knockdown (KD) in murine brain caused memory and learning deficits (Mews et al., 2017).

In recent times, acetylation has been found to be modulated also by the microbiota (i.e. commensal microbial community), which can produce SCFAs, such as acetate, propionate and butyrate, with a known role of HDACi (Simon et al., 2012). They are bacterial metabolic products mainly from carbohydrates (e.g. dietary fiber) processed in the intestinal lumen by colonocytes. Among the produced SCFAs, butyrate is the most required by these cells for energy metabolism and it is metabolized by *Faecalibacterium prausnitzii* and *Roseburia* spp. in the cluster of Firmicutes according to two pathways of bacterial fermentation: butyryl-CoA can be phosphorylated and converted to butyrate, or CoA portion can be transferred to external acetate, resulting in the formation of butyrate and acetyl-CoA (figure 1.3) (Liu et al., 2018). In addition, growing evidence indicates that butyrate has beneficial role for brain in the context of microbiota-gut-brain axis for instance controlling cholinergic enteric neurons (Soret et al., 2010), regulating appetite through the activation of the vagus nerve and the hypothalamus (van de Wouw et al., 2017), and acting on insulin sensitivity in neural circuit (Selkrig et al., 2014).

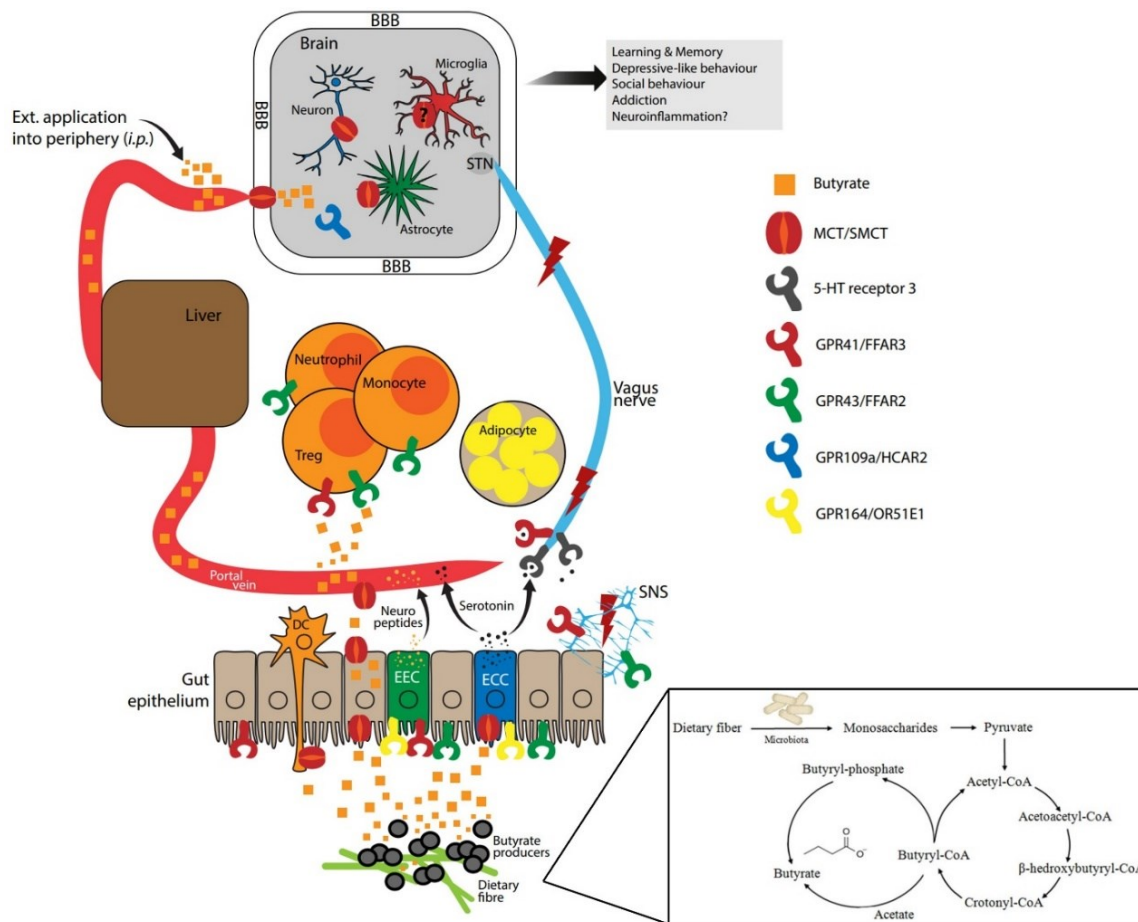


Figure 1.3 Butyrate in gut-brain axis. Schematic summary of butyrate biosynthesis from microbiota, absorption by gut epithelium, metabolism, and effects on brain function.

Adapted from “Stilling et al., 2016” and “Liu et al., 2018”.

1.2.2 Histone Methylation

Histone methylation can be found at residues of lysine (K) or arginine (R) and consists in the addition of up to three methyl groups (mono-, bi- or trimethylation) donated from S-adenosyl methionine to histone. This reaction is catalyzed by lysine methyl transferases (KMTs), while the removal of such modification is performed by lysine demethylases (KDMs). Contrary to histone acetylation, these epigenetic modifications can lead to transcriptional either activation or repression.

1.2.2.1 Lysine methyl transferases (KMTs)

KMTs result more specific than KATs, modifying one or two lysines on a particular histone, mainly histone H3. The methylated histone sites associated to transcriptionally active programs are lysine 4 of histone 3 (H3K4) methylated by KMT2A-E (MLL1-5), PRDM9, SET1A and B, SET7/9, SETMAR and SMYD1-3 (Gu and Lee, 2013); H3K36 methylated by ASH1L, NSD1-

3, SMYD2 and SETD2 (Lam et al., 2022) and H3K79, a non-tail site methylated by DOT1L, the only known non-SET domain containing KMTs (Ljungman et al., 2019). The ones associated to transcriptional repression are methylated lysine 9 of histone 3 (H3K9me) catalyzed by SUV39H1 (KMT1A) and 2 (KMT1B), EHMT2 (KMT1C/G9A) and 1 (KMT2D/GLP), KMT1E (SETDB1) and F (SETDB2) (Padeken et al., 2022); H3K27me catalyzed by the PRC2 component EZH2 (Wiles and Selker, 2017) and H4K20me catalyzed by KMT5B (SUV420H1) and C (SUV420H2), and SET8 (KMT5A) (Jørgensen et al., 2013). Another histone residue involved in gene regulation which can be methylated is the arginine, in particular arginine 17 of histone 3 (H3R17) and H4R3, methylated by PRMT1 (Guccione and Richard, 2019). KMTs and the deposition of their respective histone modifications are fundamental for demarking transcribed or active gene and genes that would become active (e.g. H3K4me3); inactive promoters (e.g. H3K27me3 or H3K9me3); gene bodies for regulating transcriptional elongation (e.g. H3K36me3 or H3K27me3); repetitive genomic elements for maintaining genomic stability and heterochromatin integrity (e.g. H3K9me2/H3K9me3 or H4K20me3) and bivalent chromatin (e.g. H3K4me3 and H3K27me3), which poise developmental genes for maintaining them repressed until signals for differentiation occur and genes can rapidly undergo transcriptional activation (Allis and Jenuwein, 2016; Atlasi and Stunnenberg, 2017; Black et al., 2012; Voigt et al., 2013).

1.2.2.2 Lysine demethylases (KDMs)

As well as for histone acetylation, also histone methylation is reversible and, along with KMTs, lysine demethylases (KDMs) have site specificity. Indeed, demethylation of H3K4 is exerted by LSD family, homologue of nuclear FAD-dependent amine oxidase (LSD1 and 2 or KDM1A and B) and another class of demethylases, Fe(II)/ α -ketoglutarate-dependent oxygenases containing Jumonji domains known as KDM5A-D (or JARID1A-D); H3K9 demethylation is carried out by KDM2A and B, and KDM4A-D, while H3K36 methylation is erased by KDM2A and B, and KDM4A and C (Allis and Jenuwein, 2016; Kouzarides, 2007).

Both KMTs and KDMs can also interact with DNA, transcription factors, Pol II and noncoding RNAs contributing to stem cell homeostasis, fate determination and differentiation (Smith and Meissner, 2013). The important role of genes encoding these writers and erasers can be inferred also from mice models lacking any of these epigenetic components. Among others, homozygous deletion of *Kmt2a*, *Kmt2b*, *Kmt2d*, *Ezh2*, *Kmt1d* or *Kdm1a* in mice led to growth

retardation and early embryonic lethality, while *Kmt2e*^{-/-} mice died in the postnatal period displaying hematopoietic impairment such as *Kmt2a*^{-/-} and *Kmt2b*^{-/-} animals (Goldsworthy et al., 2013; Lee et al., 2013; O'Carroll et al., 2001; Tachibana et al., 2005; Wang et al., 2009a; Yu et al., 1995).

1.2.3 DNA methylation

Another fundamental epigenetic modification which influences gene expression is DNA methylation, occurring at the fifth position of cytosine (5-methylcytosine, 5mC) located in repetitive genomic regions or in CpG dinucleotides dense regions (CpG islands), preferentially at 5' end nearby promoters of housekeeping and genes with tissue-specific expression. DNA methylation is mediated by DNA methyltransferases (DNMTs), including DNMT1, DNMT3A, DNMT3B and DNMT3L (Smith and Meissner, 2013), a process which can be reverted by methylcytosine dioxygenase TET proteins (TET1, TET2 and TET3) (Hackett et al., 2013) (figure 1.4).

1.2.3.1 DNA methyltransferases (DNMTs)

DNA methylation is a heritable process which is exploited during mitosis by DNMT1: it re-establishes methylation of CpGs in daughter cells recognizing hemimethylated sites marked by H3K9me, thanks to the E3 ubiquitin protein ligase UHRF1 which binds the parental strand and orient DNMT1 on newly synthesized DNA after replication. Although CpG islands at promoters of housekeeping or developmental genes show hypomethylation, some promoters gain DNA methylation during development thanks to *de novo* methyltransferase activity exploited by DNMT3A and DNMT3B (Smith and Meissner, 2013) (figure 1.4).

DNA methylation leads to transcriptional repression either preventing the binding of transcriptional factors to DNA due to the presence of 5mC or targeting promoters in concert with other proteins of repressive complexes. Indeed, DNMT3A and DNMT3B can be recruited by MeCP2, which recognizes methylated CpG islands, together with HDACs (Jones et al., 1998) and EHMT2, the methyltransferase associated to H3K9me2 (Dong et al., 2008), resulting in stable silencing of promoters.

Furthermore, the fundamental role of DNA methyltransferases in development became clear when it was observed that murine KO models for these enzymes showed embryonic (in *Dnmt1*^{-/-} and *Dnmt3b*^{-/-} mice) or postnatal lethality (in *Dnmt3a*^{-/-} mouse) (Li et al., 1992; Okano et al., 1999).

1.2.3.2 TET proteins

TET proteins are responsible of the enzymatic demethylation, catalyzing the oxidation of 5mC to 5-hydroxymethylcytosine (5hmC), the first intermediate of this reverse process. Tet1 and Tet2 are highly expressed in embryonic stem cells (ESCs), while Tet3 was shown to demethylate paternal genome in mouse zygote (Gu et al., 2011; Ito et al., 2010) (figure 1.4). Lack of Tet1 and Tet2 in mice was shown to be compatible with embryo development, although hypermethylation and imprinting anomalies were observed (Dawlaty et al., 2013), while depletion of all three TET in mouse ESCs (mESCs) led to differentiation defects (Dawlaty et al., 2014).

Interestingly, studies also showed that the presence at CpG islands of DNA methylation and histone marks such as H3K27me3 and H3K4me3 is mutually exclusive: loss of TET proteins caused loss of bivalency at promoters, increasing DNA methylation thus reducing H3K27me3 and H3K4me3 (Kong et al., 2016; Weber et al., 2007).

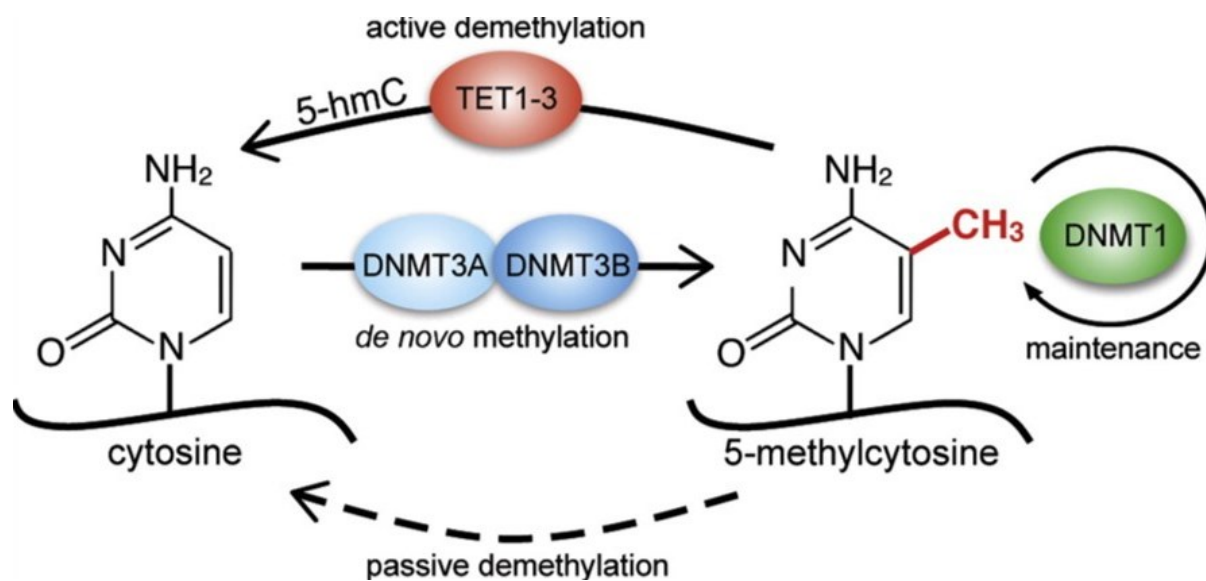


Figure 1.4 DNA methylation. Representation of main actors involved in DNA methylation (DNMT1/3A/3B) and demethylation (TET1-3). Adapted from “Ambrosi et al., 2017”

1.3 RUBINSTEIN-TAYBI SYNDROME

Rubinstein-Taybi syndrome (RSTS, OMIM #180849, #613684) is a rare autosomal dominant disorder belonging to the chromatinopathies group described for the first time in 1963 by the pediatrician Dr Jack Herbert and radiologist Dr Hooshang Taybi. They reported seven children (five males and two females) characterized by intellectual disability, short stature, peculiar dysmorphisms, and broad thumbs and halluces, feature which initially gave name to the

syndrome (“broad thumb-hallux syndrome”) (Rubinstein and Taybi, 1963). RSTS has an estimated incidence of 1:125,000 newborns, without a difference between males and females, and occurs generally *de novo*, although rare familial cases were described (Bartsch et al., 2010; Hennekam, 2006). This syndrome is mainly characterized by ID, postnatal growth deficiency with excessive weight gain in adolescence, distinctive dysmorphisms, skeletal abnormalities (e.g. broad thumbs and big toes) with a wide spectrum of multiple congenital anomalies and phenotypically heterogeneous variability (Hennekam, 2006).

RSTS is caused by pathogenic variants in one of two so far known highly conserved genes: *CREBBP* (16p13.3) coding for cAMP response element binding protein (CREB) binding protein (also known as CBP) (Petrif et al., 1995) and *EP300*, coding for E1A-associated protein p300, mapping on chromosome 22q13.2 and identified in 2005 (Roelfsema et al., 2005). *CREBBP* is considered the “major gene” as found mutated in almost 60% RSTS patients (RSTS1, OMIM #180849), while *EP300* gene mutations have been described in a minor fraction of patients (RSTS2, OMIM #613684) (Fergelot et al., 2016), leaving about 30% of patients without a molecular diagnosis.

1.3.1 Clinical aspects

Despite the clinical heterogeneity characterizing RSTS phenotype, these patients present peculiar features whose recognition can help geneticists in the diagnostic process, and they include the following categories: typical facial dysmorphisms, skeletal anomalies, growth delay, ID and neurodevelopmental problems, congenital anomalies, and additional features such as feeding problems, among others (Spena et al., 2015a).

1.3.1.1 Facial dysmorphisms

Children affected display microcephaly (>50%), arched eyebrows, downslanting of palpebral fissures (>80%), long eyelashes, epicanthal folds, ptosis, low set ears, broad nose, and long columella below *alae nasi* (>90%). A peculiar RSTS features which can be appreciated late in childhood is the “grimacing smile”, a typical smile associated with the closure of the eyes (figure 1.5A). Often in the newborns hypertelorism, upslanted palpebral fissures, depressed nose, microretrognathia and capillary hemangioma are reported, while clinical signs such as low implantation hairline, deviated nasal septum and small mouth with thin upper lip seem less frequent. Other abnormalities reported include dental and ocular defects such as talon cusps (>90%), arched palate (>80%), dental caries (>15%), hypodontia (30%), supernumerary

teeth (15%), strabismus (>60%), refractive errors (>40%), nasolacrimal duct obstruction (>30%) and more rarely cataracts, hypoplasia of the optic nerve, coloboma and glaucoma risk (Cohen et al., 2020; Van Gils et al., 2021; Hennekam et al., 1990; Milani et al., 2015; Pérez-Grijalba et al., 2019; Spina et al., 2015b; Tekendo-Ngongang et al., 2020).

1.3.1.2 Skeletal anomalies

Among skeletal anomalies, a peculiar RSTS signs are extremities abnormalities regarding hands and feet. 99% of RSTS patients display broad thumbs and big toes and about one third of them show radial deviation (figure 1.5B). Other anomalies include large or duplicated distal phalanges (>30%), which can lead to overlapping toes, clinodactyly of the fifth finger, persistence of fetal fingertip pads, flat feet and less frequently polydactyly, partial syndactyly of II-III of toes and III-IV of finger and absence of the distal phalanx of the hallux. From radiological examinations a delayed bone age is often observed (>70%), and besides hands and feet anomalies, in RSTS patients the following skeletal defects are described: congenital or acquired scoliosis, kyphosis or lordosis, an higher risk of fractures due to bones fragility, cervical vertebral fusion, C1-C2 instability, slipped capital femoral epiphysis and costal agenesis (Cohen et al., 2020; Van Gils et al., 2021; Hennekam et al., 1990; Negri et al., 2015; Pérez-Grijalba et al., 2019; Spina et al., 2015a; Tekendo-Ngongang et al., 2020).

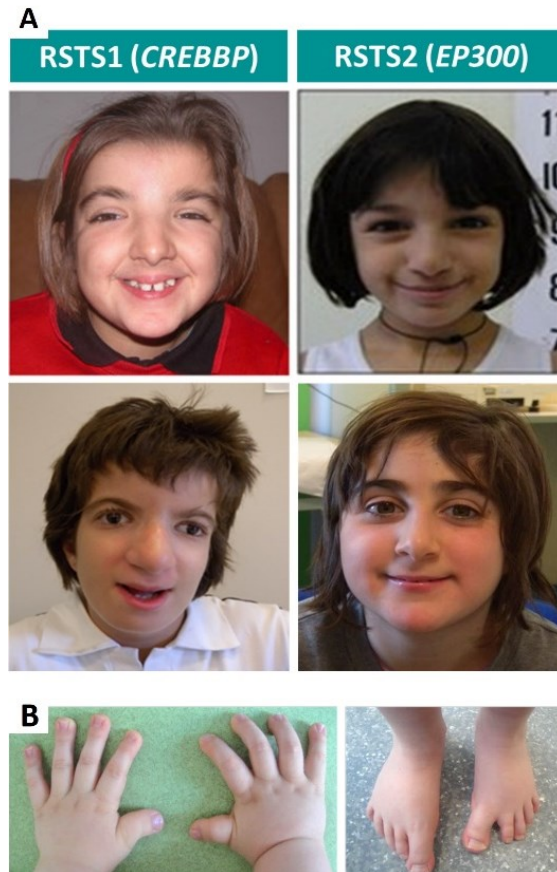


Figure 1.5 RSTS features. A) Example of RSTS *facies* of RSTS1 and RSTS2 patients with mutations in *CREBBP* and *EP300* respectively; B) detail of skeletal anomalies typical of RSTS involving hands and feet. Adapted from "Bentivegna et al., 2006; Van Gils et al., 2021; Negri et al., 2015"

1.3.1.3 Growth delay

Intrauterine growth results normal in both females and males, with birth measurements around the 50th percentile: average height, weight and occipital frontal conference (OFC) are respectively 49.7 cm, 3.3 kg and 34.2 cm for males, and 48.6 cm, 2.97 kg and 32.2 cm for females. However, an inflection in the growth curve can be observed since the first months of life, especially in weight values, probably due to the presence of feeding problems (>80%), gastroesophageal reflux (>60%), hypotonia and frequent respiratory infections. Curiously, a gain of weight and the absence of pubertal spurt are often observed, respectively increasing the risk of obesity during childhood for boys and at puberty for girls and causing the reduced stature (Beets et al., 2014).

1.3.1.4 Intellectual disability and neurodevelopmental problems

Intellectual disability is present in all RSTS patients, who usually display a moderate mental retardation with a variable intelligence quotient (IQ) (25-79). Peculiar aspects observed for RSTS are that fluid reasoning in these patients is higher than IQ, and that patients with mutations in *EP300* show a milder ID. Almost all RSTS are characterized by psychomotor impairment due to hypotonia and by speech delay (>90%), and despite this they show discreet emotional and social interactions. However, behavioral problems are reported, including mood instability, hyperactivity, attention deficits, noise intolerance and aggressive behavior (also self-injury), symptomatology which can get worse with age, with patients that can display obsessive-compulsive behavior, anxiety, autism spectrum disorder and stereotypies. Anomalies in electroencephalograms (EEGs) are often reported (>60%) while seizures and brain malformations (e.g. agenesis of corpus callosum, spinal cord, Dandy-Walker and Chiari type I malformations) occur in less than one fourth of patients (Ajmone et al., 2018; Fergelot et al., 2016; Galéra et al., 2009; Hennekam et al., 1990; López et al., 2018; Spena et al., 2015c; Waite et al., 2015).

1.3.1.5 Congenital anomalies and additional features

Cardiac defects and vascular anomalies are frequently reported in RSTS patients (>25%), ranging from patent ductus arteriosus, atrial/ventricular septal defect, aortic or pulmonary stenosis and aortic bicuspidism to pseudotruncus and left heart hypoplasia (Cohen et al., 2020; Fergelot et al., 2016; Loomba and Geddes, 2015; Pérez-Grijalba et al., 2019; Stevens and Bhakta, 1995).

Genitourinary abnormalities include cryptorchidism in males (>75%), hypermenorrhea and metrorrhagia in females (Spena et al., 2015a). In addition, more than 25% of patients display renal anomalies such as pyelectasis, renal or pyloric duplication, hydronephrosis and renal agenesis and recurrent renal infections (Cohen et al., 2020; Fergelot et al., 2016; Milani et al., 2015; Pérez-Grijalba et al., 2019).

Dermatological features are another RSTS sign, in particular hirsutism (>75%), keloid or hypertrophic scars (>15%), supernumerary nipples, capillary hemangiomas, ingrown nails, paronychia, and hypertrichosis (>75%) (Hennekam, 2006; Van De Kar et al., 2014).

Additional RSTS features are hypothyroidism, growth hormone deficiency, pituitary hypoplasia and immunological deficits affecting B cells (Milani et al., 2015; Saettini et al., 2020).

To date, in RSTS patients are reported tumors deriving from the neural crest (e.g. neuroblastoma, medulloblastoma, meningioma) and hematological malignancies such as leukemia and non-Hodgkin's lymphoma. Interestingly, a study in a wide Dutch RSTS cohort by Boot and colleagues associated to RSTS an increased risk of developing tumors (>10%), in particular meningiomas and benign tumors such as pilomatrixomas, although a defined genotype-phenotype correlation is still missing (Boot et al., 2018; Van Gils et al., 2021; Milani et al., 2015).

Since most of RSTS clinical signs occurs during the postnatal period, there are few antenatal marks suitable for RSTS diagnosis, but among them, a higher incidence of pre-eclampsia is described for mothers of carriers of pathogenetic variant in *EP300* (>20%) (Bartholdi et al., 2007; Cohen et al., 2020; Fergelot et al., 2016; Negri et al., 2015, 2016; Steegers et al., 2010).

1.3.2 Molecular aspects

RSTS patients in almost 60% of cases result positive for mutations in *CREBBP* (55-75%) causing RSTS1 or *EP300* (8-11%) causing RSTS2, generally occurring *de novo*, although somatic mosaicisms and familial forms were reported (Bartsch et al., 2010; Gucev et al., 2019; De Vries et al., 2016). These two causative genes have 31 exons and encode respectively for CBP (or KAT3A) and its homolog p300 (or KAT3B), two KATs writers of the epigenetic machinery involved in chromatin opening and transcriptional activation able to acetylate histone and non-histone proteins.

1.3.2.1 CBP and p300

CBP and p300 are two nuclear transcriptional coactivators with high protein homology, which are evolutionarily conserved even in distant species such as *Drosophila melanogaster* and *Caenorhabditis elegans*, especially at functional domains (Akimaru et al., 1997a). These two proteins share indeed a nuclear receptor interaction domain (NRID) at the N-terminal; a KIX domain which allows CBP to interact with CREB by kinase inducible domain (KID) and with other transcription factors (e.g. BRCA-1, p53); a Bromo domain which binds lysine residues; a KAT domain which represents the enzymatic core; three cysteine-histidine-rich regions (CH1-3) for protein-protein interaction (e.g. TFIIB, RNA helicase A, p53, viral oncoprotein E1A) made

up of four zinc finger motives (CH1 contains transcriptional adaptor zinc finger 1 TAZ1, CH3 contains TAZ2 and ZZ zinc finger motif, and CH2 a plant homeodomain PHD); and at the C-terminal a interferon-binding transactivation domain (IBiD) containing a nuclear binding coactivator domain (NCBD) and a glutamine-rich domain (Breen and Mapp, 2018; Dancy and Cole, 2015; Giles et al., 1998; Valor et al., 2013) (figure 1.6A). CBP and p300 can thus regulate gene expression acetylating both histones at lysine N-terminal tails and other protein such as transcription factors (e.g. TATA binding protein TBP and TFIIB) forming a complex with RNA Pol II and recruiting the transcriptional machinery to promoters (Bedford et al., 2010; Iyer et al., 2004; Wang et al., 2008). In addition, these two KATs are fundamental not only in transcription process but they also acetylate protein involved in DNA replication and repair (Dutto et al., 2019), making CBP and p300 crucial for growth, proliferation, and development (Goodman and Smolik, 2000).

Indeed, *Cbp*^{-/-} or *p300*^{-/-} mice showed embryonic lethality (Tanaka et al., 1997), as well as *p300*^{+/-} mutants (Yao et al., 1998), while *Cbp* heterozygous mice were viable, showing skeletal and cardiac abnormalities, growth retardation and memory deficits (Oike et al., 1999). These genes were proven to be involved in many functions such as hematopoiesis, synaptic plasticity and long-term memory, neurogenesis, and behavior, as proven by their loss of function in mice (Alarcón et al., 2004; Kasper et al., 2002; Kung et al., 2000; Lopez-Atalaya et al., 2011; Wood et al., 2006; Zheng et al., 2016).

1.3.2.2 Mutational spectrum

According to LOVD and HGMD databases, almost 500 pathogenetic variants in *CREBBP* are reported causing RSTS1. Chromosomal rearrangements occur in 20% of cases, while most of genetic alterations correspond to point mutations, including frameshift, nonsense, missense and splicing mutations in order of frequency, in addition to a minor fraction of deletions and duplications (figure 1.6B) (Van Gils et al., 2021; Pérez-Grijalba et al., 2019; Petrif et al., 1995; Rusconi et al., 2015; Spina et al., 2015c; Tsai et al., 2011).

In *EP300* are referenced 118 pathogenetic variants as causative of RSTS2, with a mutational spectrum similar to the one described for *CREBBP*, with >80% of point mutations such as frameshift, nonsense, missense and splicing mutations, while large rearrangements including deletions of the entire gene represent 10% of cases (Figure 1.6C) (Bartholdi et al., 2007; Cohen

et al., 2020; Cross et al., 2020; Fergelot et al., 2016; Van Gils et al., 2021; Negri et al., 2015, 2016; Roelfsema et al., 2005; Tsai et al., 2011).

A mutational hotspot in *CREBBP* or *EP300* was not reported, although more than a half of missense mutations in *CREBBP* and almost all in *EP300* affect the catalytic domain of their protein products (Cross et al., 2020).

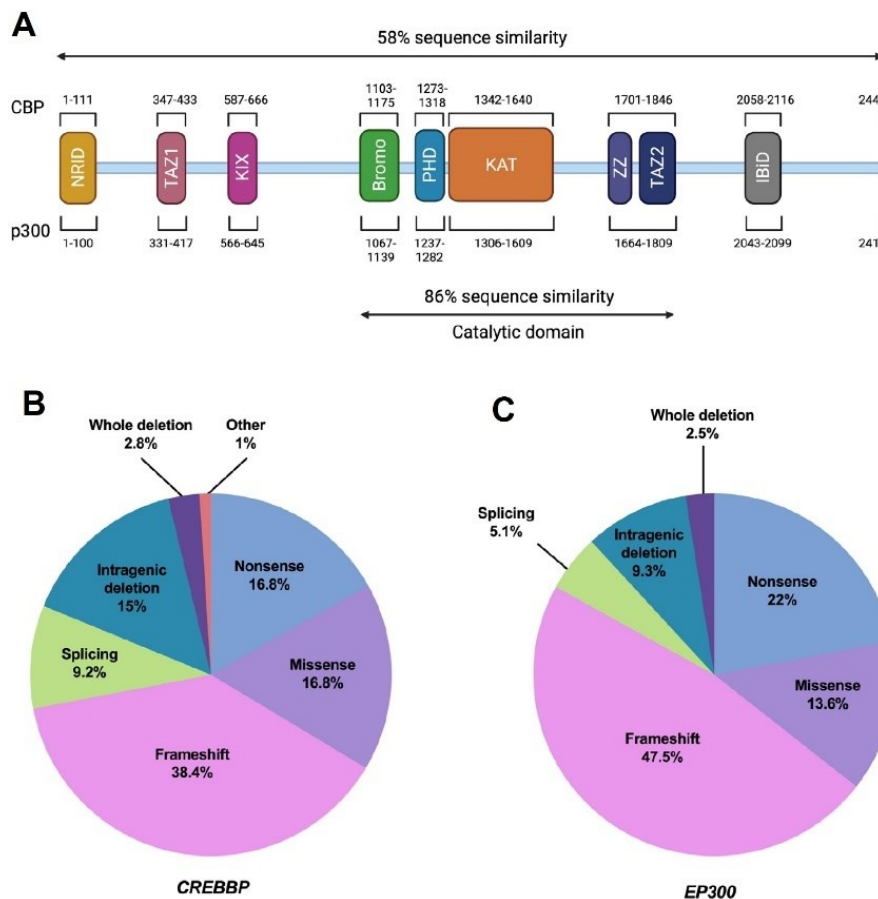


Figure 1.6 CBP and p300 and their genes mutational spectrum. A) CBP and p300 protein domains (nuclear receptor interaction domain, NRID or RID; zinc finger transcriptional adapters, TAZ1 and TAZ2; kinase inducible domain-interacting domain, KIX; plant homeodomain, PHD; bromodomain, Bromo; lysine acetyltransferase domain, KAT; zinc finger motif, ZZ; interferon-binding transactivation domain, IBiD) with corresponding amino acidic length and similarity sequence; B-C) pie charts of mutations in *CREBBP* (B) and *EP300* (C) reported in literature and in HGMDPro and LOVD databases. Adapted from “Van Gils et al., 2021”.

1.3.3 Genotype-phenotype correlation

Patients displaying RSTS phenotype can be carriers of pathogenetic variants in *CREBBP* or *EP300* with a notable difference in mutation frequency affecting these two genes as cited

above. This difference seems to be reflected also by slightly divergent phenotypic features with *EP300* patients displaying milder clinical signs involving ID, hands and feet anomalies and presence of ASD-like behavior, and showing an association with pre-eclampsia and higher frequency of microcephaly (Fergelot et al., 2016).

Interestingly, due to clinical heterogeneity of RSTS and chromatinopathies, patients clinically diagnosed as RSTS were found positive for mutations in other genes of the epigenetic machinery and patients without a RSTS phenotype were reported having pathogenetic variants in *CREBBP* or *EP300*. In the first scenario RSTS patients negative for known causative genes were found positive for mutations in genes causing Bohring-Opitz syndrome (BOPS, OMIM #605039), Kabuki syndrome (KS1, OMIM #147920; KS2 OMIM #300867), Wiedemann-Steiner syndrome (WDSTS, OMIM #605130), Brachydactyly-Mental Retardation syndrome (BDMR, OMIM #600430) and Luscan-Lumish syndrome (LLS, OMIM #616831) (Negri et al., 2019; Squeo et al., 2020), while in the second case mutations in *EP300/CREBBP* were described for few patients displaying a phenotype resembling Cornelia de Lange syndrome (CdLS1, OMIM #122470; CdLS2, OMIM #300590; CdLS3, OMIM #610759; CdLS4, OMIM #614701; CdLS5, OMIM #300882) (Aoi et al., 2019; Cucco et al., 2020; Squeo et al., 2020; Tang et al., 2019; Woods et al., 2014), another chromatinopathy.

1.4 RETT SYNDROME

Rett syndrome (RTT, OMIM #312750) is a X-linked neurodevelopmental disorder first described in 1966 by the physician Andreas Rett (Rett, 1966). This syndrome affects 1:10,000 newborns, representing the second cause of ID in females, and it is characterized by 6-18 months of overtly normal development followed by a neurological regression and peculiar neurological features (Neul et al., 2010).

Almost 95% of RTT patients have pathogenetic variants in methyl CpG binding protein 2 (*MECP2*), a reader of the epigenetic machinery located at Xq28 chromosome, whose protein product is involved in chromatin regulation (Amir et al., 1999). In addition to *MECP2*, other causative genes were identified and associated to RTT variant forms and Rett-like phenotypes, such as Cyclin-dependent kinase-like 5 (*CDKL5*) and Forkhead box G1 (*FOXP1*), located respectively on chromosome Xp22 and 14q12 (Ariani et al., 2008; Weaving et al., 2004).

1.4.1 Clinical aspects

RTT diagnosis criteria were originally given in 1994 (Hagberg and Skjeldal, 1994) and then updated in 2010 (Neul et al., 2010). Main features of this neurological disorder include a profound cognitive impairment, communication dysfunction, stereotypic movements, and a pervasive growth failure. Classic RTT patients with *MECP2* mutations display a peculiar clinical presentation based on age of onset of specific signs. In fact, a phase of early onset between 6-18 months can be identified, which is defined by microcephaly, hypotonia, delays in gross motor skills and less social interaction (in particular lack of interest in others). This is usually followed by a rapid regression within the first three years of life, in which RTT patients can show ASD-like clinical manifestations (i.e. social withdrawal, loss of acquired language skills and eye contact avoidance) and hand stereotypies, motor dysfunction due to ataxia and respiratory anomalies. A plateau phase can follow and last for the rest of patients' lives, with a reduction of ASD-like signs and an improvement of emotional contact, although prominent seizures and autonomic dysfunction can be present. In the end a later motor deterioration can occur with stable seizures control, communication abilities and hands skills, but a decrease or loss of mobility characterized by spasticity, dystonia, and muscular weakness (Leonard et al., 2017; Percy et al., 2010).

1.4.2 Molecular aspects

In 95% of cases of classic RTT patients result carries of a pathogenetic variant in *MECP2* which causes a LOF of the protein product MeCP2, a chromatin-associated protein (Percy et al., 2010). Since these mutations in sporadic cases usually have paternal origin and X inactivation in females can lead to early lethality or to a severe phenotype characterized by congenital encephalopathy, this syndrome rarely affects males (Schüle et al., 2008; Trappe et al., 2001). When it does, males RTT patients have mutations not causing a complete LOF and they display a wide range of neurological impairments, other than cases of somatic mosaicism and associated Klinefelter syndrome that were reported (Schwartzman et al., 2001; Topçu et al., 2002; Villard, 2007).

MECP2 has four exons and the second undergoes to alternative splicing, generating two protein isoforms (MeCP2_e1, whose mRNA lacks exon 2, and MeCP2_e2) (figure 1.7A). MeCP2_e1 with 24 amino acids is the one that mutated causes RTT phenotype since it is more

expressed in both human and murine brain and mutations in *MECP2_e2* specific exon 2 were not reported (Yasui et al., 2014).

1.4.3 Mutational spectrum and clinical heterogeneity

Among pathogenetic variants found in RTT patients, it was observed that missense variants are concentrated in the methyl-binding domain (MBD), transcriptional repressor domain (TRD) and in the C-terminal domain (CTD) of *MECP2*, while truncating or frameshift mutations are spread along the gene (figure 1.7B) (Krishnaraj et al., 2017). In addition, more than a half of patients with *MECP2* mutations have these variants localized at eight mutational hotspots (corresponding to R106W, R133C, T158M, R168X, R255X, R270X, R294X and R306C amino acidic nonsense mutations) whose associated phenotypes show high variability, while 15% of mutations are deletions/insertions (del/ins), duplications or chromosome rearrangements (Neul et al., 2008; Percy et al., 2010).

In addition to classic RTT, other atypical or variant forms were described, caused in 70% of cases by *MECP2* mutations, highlighting the clinical heterogeneity characterizing this syndrome (Percy et al., 2010). The Zappella or preserved speech variant is associated to a specific missense mutation or a C-terminal deletion affecting *MECP2*. These patients display a prolonged plateau phase, a milder reduction of hand skills, a recovery of language after regression, milder ID and less frequent typical RTT signs (e.g. epilepsy, autonomic dysfunction, reduced head circumference) (Neul et al., 2010; Zappella, 1992). The Hanefeld variant or early seizure variant, later known as CDKL5 disorder, is more often caused by mutations in *CDKL5* coding for a kinase which is involved in the phosphorylation of different targets (i.e. MeCP2 and DNMT1) regulating gene expression and DNA methylation, in the regulation of mRNA splicing and actin/dendritic arborization (Kadam et al., 2019; Kilstrup-Nielsen et al., 2012). Affected patients show an early onset of seizures usually before regression phase with infantile spasms and refractory myoclonic epilepsy and less frequent typical RTT signs (Fehr et al., 2013; Neul et al., 2010). Rolando variant or congenital variant is mainly caused by pathogenetic variants in *FOXG1*, which has a specific expression in the fetal brain and encodes for a regulator of forebrain development, involved in cell proliferation, neurogenesis, neuronal differentiation, patterning of cerebral cortex and circuit assembly (Akol et al., 2022). Patients with congenital variant show severe postnatal microcephaly, initial abnormal development characterized by severe psychomotor delay and inability to walk, early regression, lack of typical RTT signs (e.g. eye gaze), presence of RTT autonomic anomalies and

specific movement abnormalities such as tongue stereotypies and jerky movements of limbs (Ariani et al., 2008; Neul et al., 2010). In addition, about 3-5% of patients with RTT phenotypes result negative for mutation in these known causative genes and in the last years many genes associated with RTT-like phenotypes were identified and it was observed that their protein products are involved in transcription, chromatin regulation and neuronal processes such as synaptic function, ion channels and neurotransmitters (Ehrhart et al., 2018).

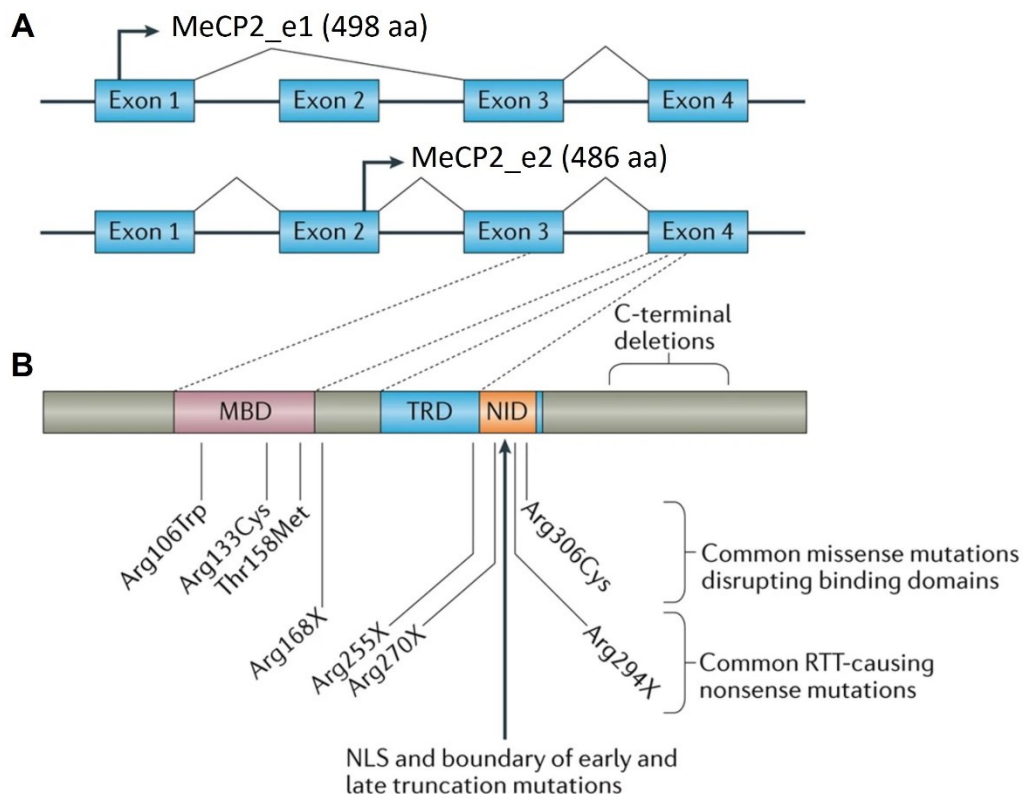


Figure 1.7 Structure of *MECP2* and protein domains involved in RTT. A) Two mRNA isoforms of *MECP2* (*MECP2_e1* and *MECP2_e2*) differing for inclusion/exclusion of exon 2; B) MeCP2 functional domains and marked mutational hotspots. Adapted from “Leonard et al., 2017”.

1.4.2.1 MeCP2

MeCP2 is a nuclear protein made up of four main domains: MBD, TRD containing the NCoR interaction domain (NID) and the CTD (figure 1.7B). The first one mediates the binding to methylated CpG with adjacent fragments containing A/T bases and to non-methylated DNA (Galvão and Thomas, 2005; Klose et al., 2005). The role of transcriptional repressor is exploited by MeCP2 thanks to the TRD, which recruits the SMRT/NCoR-mSin3A-HDAC repressing complexes, linking DNA methylation to chromatin remodeling, and other proteins

- e.g. YB1 (Nan et al., 1998; Young et al., 2005). In the end, also CTD seems to have essential functions since mouse models lacking this domain showed RTT phenotypes (Shahbazian et al., 2002).

MeCP2 is an epigenetic reader which activates/represses transcription, via CREB1 interaction or recruiting co-repressor complexes, it regulates chromatin compaction, alternative splicing by YB1 interaction and miRNA processing, preventing the assembly of DROSHA-DGCR8 complex by DGCR8 sequestration (figure 1.8) (Ip et al., 2018; Lyst and Bird, 2015). MeCP2 shows a tissue- and time-specific expression following the maturation of central nervous system (CNS), with higher levels detected postnatally (Shahbazian et al., 2002). Indeed, this aspect together with the reduced brain volume displayed by RTT patients, is associated with the observation of RTT neurons being more packed and smaller, with shorter and fewer dendritic spines (Armstrong et al., 1995). In addition, MeCP2 can be considered a multifunctional hub which integrates different processes underpinning neuronal function. For instance, loss of this protein in mice was shown to cause impairment of neuronal differentiation in early development, of neuronal maturation, connectivity and excitatory/inhibitory (E/I) balance (Cohen and Greenberg, 2008; Nelson and Valakh, 2015). Homozygous mice for *Mecp2* loss, before dying between 6 and 12 weeks, exhibited physical deterioration, abnormal behavior and overweight for the first weeks of life, followed by hyperactivity and weight reduction at later stage of disease, while *Mecp2*^{+/-} females were viable but showed reduced activity, ataxia and impaired behavior (Chen et al., 2001; Guy et al., 2001; Krishnan et al., 2017).

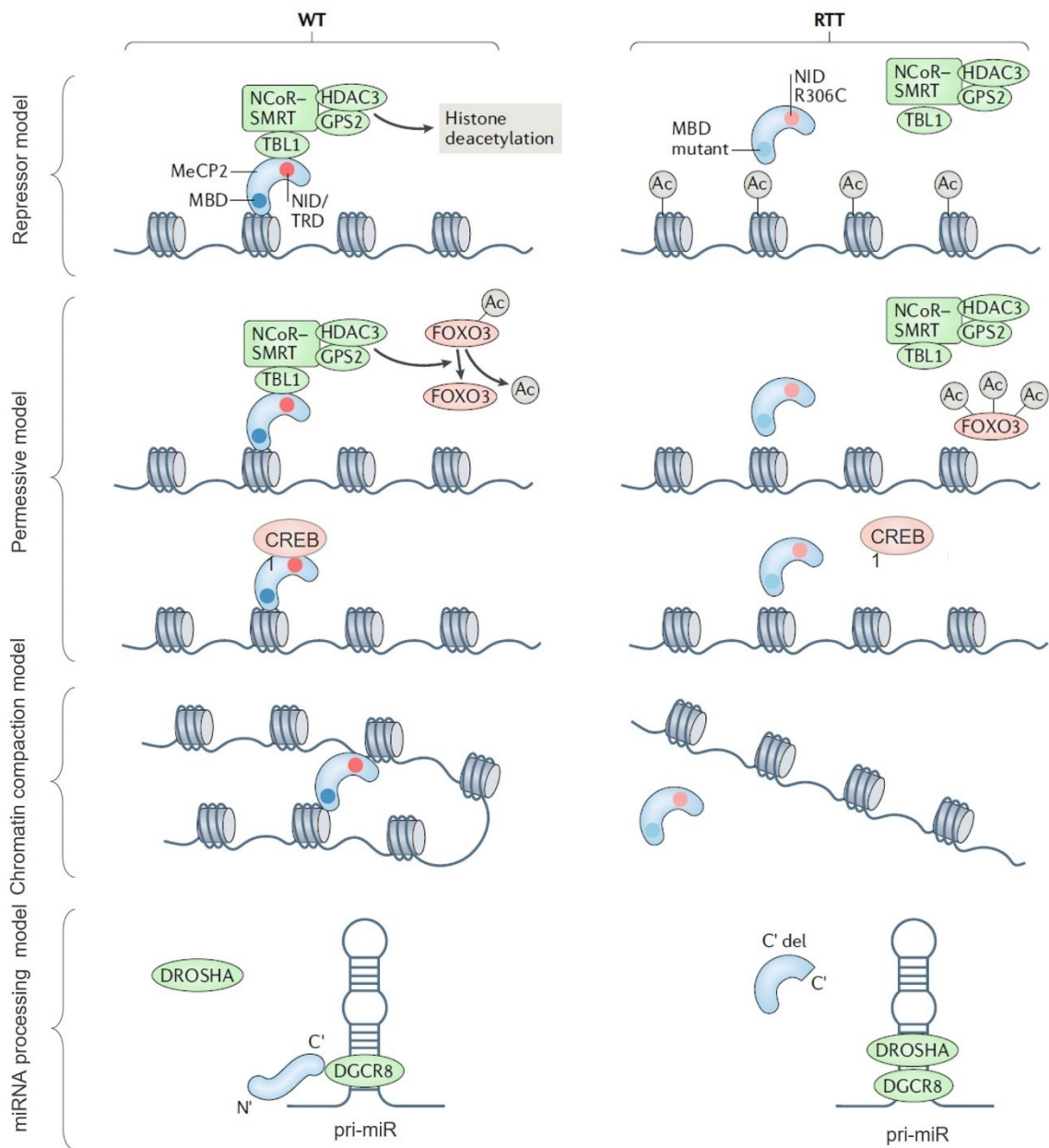


Figure 1.8 Molecular function of MeCP2 and its alteration in RTT. MeCP2 in wild type (wt) condition has repressive or transcriptionally active function recruiting co-repressors such as NCoR-SMRT complex through TRD/NID domain (red dot), transducin β -like protein 1 (TBL1) and HDAC3, to methylated DNA by MBD domain (blue dot) or co-activator as CREB1; MeCP2 can also compacts chromatin and binds through the Carboxyl terminus (C') DGCR8, preventing the formation of a complex with DROSHA, and the pri-miR processing into miRNA. Adapted from "Ip et al., 2018".

2. AIM OF THE THESIS

Chromatinopathies are a group of Mendelian overlapping disorders characterized by clinical heterogeneity. Rubinstein-Taybi (RSTS) and Rett syndromes (RTT) belong to this group, sharing phenotypic features such as intellectual disability and growth delay. A fraction of RSTS and RTT patients remains without a molecular diagnosis.

In this work we explored two different thus complementary approaches for the study of chromatinopathies. For RSTS we investigated possible therapeutic strategies deepening the knowledge on syndrome etiopathogenesis starting from the known established molecular mechanisms, while for both RSTS and RTT we identified new causative genes leading to the study of related pathogenetic findings.

Since a therapeutic approach is still missing for RSTS patients, which show a defect in histone acetylation, we first focused on molecular aspects underlying the etiology of this disorder to explore possible epigenetic treatments to restore acetylation/deacetylation balance. Our strategy forecasted the investigation of exogenous HDACi effects *in vitro* on lymphoblastoid cell lines derived from patients and *in vivo* on a RSTS *Drosophila melanogaster* model. Then we assessed the microbiota of RSTS patients and flies for investigating the presence of bacteria producers of SCFAs with HDACi activity.

In the last decade NGS approach and in detail whole exome sequencing (WES) have been crucial for getting solved many cases, especially for rare disorders such as chromatinopathies. Indeed, we wanted to exploit these techniques for RSTS and RTT-like patients who displayed phenotypes resembling those syndromes but resulted negative for known causative genes. Thus, we aimed at obtaining a molecular diagnosis for these patients and at expanding genotype-phenotype correlation for RSTS and RTT, deepening also molecular aspects underlying newly identified variants.

The experiments performed during my PhD program and the relevant results are reported in the present thesis and in the enclosed papers (see Appendix 1).

3. MATERIALS AND METHODS

3.1 IN VITRO MODELS

3.1.1 Cell cultures

3.1.1.1 Lymphoblastoid cell lines (LCLs)

Lymphoblastoid cell lines (LCLs) from nine different RSTS patients (four carrying *CREBBP* mutations, four carrying *EP300* mutations, and one carrying *HDAC2* mutation listed in table 3.1) (Lopez-Atalaya et al., 2012; Negri et al., 2015, 2016; Spena et al., 2015b) and seven healthy donors (HD) were obtained in collaboration with the Gaslini Genetic Bank service (Telethon Network of Genetic Biobanks) and their use was approved by Ethics Committee of Università degli Studi di Milano (Comitato Etico number 99/20, 17 November 2020). Cells were maintained in RPMI 1640 culture medium supplemented with L-glutamine, 20% fetal bovine serum (FBS) and 1% penicillin/streptomycin (P/S), and cultured in an incubator with 5% CO₂ at 37°C. *CREBBP*, *EP300* and HD LCLs were exposed to Tricostatin A (TSA, 2 µM for 2h), Suberoylanilide hydroxamic acid (SAHA, 2 µM for 24h), Valproic acid (VPA, 2 mM for 24h), Sodium butyrate (NaB, 5 mM for 24h), and their respective vehicles (water or DMSO) as indicated in table 3.2 (Chang et al., 2018; Chriett et al., 2019; Freese et al., 2019; Göttlicher et al., 2001; Schölz et al., 2015; Tarasenko et al., 2018), in order to evaluate the response to HDACi exposure, in term of both acetylation pattern, through AlphaLISA® assay, and cytotoxicity, exploring the cell proliferation and cell death by immunocytochemistry (Ki67 and TUNEL assay respectively). *HDAC2* and HD LCLs were tested for AlphaLISA® assay and immunofluorescence (IF).

Table 3.1 Patients-derived LCLs used in the present work.

Gene	LCLs	cDNA change	Protein change	Mutation type	Reference
<i>CREBBP</i>	RSTS 114	c.4485-7G>C	p.(R1428_G1465del) p.(F1379_G1465del)	Splicing	Lopez-Atalaya et al. 2012
	RSTS 120	c.5837dupC	p.(P1947Tfs*19)	Frameshift	Spena et al. 2015
	RSTS 122	c.4394+5G>T	p.(R1428_G1465del) p.(F1379_G1465del)	Splicing	Spena et al. 2015
	RSTS 176	c.4508A>T	p.(Y1503F)	Missense (KAT)	Spena et al. 2015

EP300	RSTS 25	c.41_51delinsT	p.(K141fs*31)	Frameshift	Negri et al. 2015
	RSTS 39	c.4640dupA	p.(N1547Kfs*3)	Frameshift	Negri et al. 2016
	RSTS 54	c.669dupT	p.(Q223Sfs*19)	Frameshift	Negri et al. 2015
	RT010-15	c.4763T>C	p.(M1588T)	Missense (KAT)	this study
HDAC2	#249	c.1330_1333del	p.(K444Lfs*61)	Frameshift	this study

Table 3.2 Conditions of in vitro treatments used on *CREBBP* and *EP300* LCLs.

Treatment	TSA	SAHA	VPA	NaB
Against	Class I, IIa, IIb HDAC	Class I, IIa, IIb HDAC	Class I (HDAC1, HDAC2, HDAC3)	Class I HDAC
Vehicle	DMSO	DMSO	H ₂ O	H ₂ O
Time	2h	24h	24h	24h
Dosage	1 - 2 - 5 μ M	1 - 2 - 10 μ M	0,5 - 1 - 2 mM	1 - 2 - 5 mM
Reference	Schölz et al., 2015; Chang et al., 2018; Freese et al., 2019	Schölz et al., 2015; Freese et al., 2019; Tarasenko et al., 2018	Schölz et al., 2015; Chang et al., 2018; Tarasenko et al., 2018; Gottlicher et al., 2001	Schölz et al., 2015; Chang et al., 2018; Chriett et al., 2019

3.1.1.2 Human Embryonic Kidney (HEK) 293T cells and generated cell lines

Human Embryonic Kidney (HEK) 293T cells and *SLC35F1* KO lines were maintained in Dulbecco's Modified Eagle Medium (DMEM) supplemented with 10% FBS and 1% P/S, at 37°C with 5% CO₂.

In collaboration with Prof. Pasini laboratory of the Department of Experimental Oncology at European Institute of Oncology (IEO), *SLC35F1* KO clones were generated performing calcium phosphate transfection with 10 μ g of Px458 plasmid (#48138 Addgene) containing Cas9 and sgRNAs and a mixture of CaCl₂ 2 M and HBS solution.

For targeting *SLC35F1* (NM_001029858.4) the following gRNAs were annealed and ligated to the digested plasmid: *SLC35F1* Exon 2 5'-CACCGATGTTAATCTCTGTGGCCCT-3' and 5'-

AAACAGGGCCACAGAGATTAACATC-3'; *SLC35F1* Exon 7 5'-CACCGAGTCTGCTGTGAGCAAGGAG-3' and 5'-AAACCTCCTTGCTCACAGCAGACTC-3'. Briefly, Px458 was digested with BbsI enzyme and NE buffer 2.1 according to manufacturer's protocol (New England BioLabs); diluted (1:200) and previously annealed sgRNAs (by T4 DNA ligase and its buffer supplemented with ATP, New England BioLabs) were ligated to 50 ng of digested plasmid with T7 ligase and Stick together DNA ligase buffer for 30 min at RT according to New England BioLabs' instructions. DH5 α competent cells were incubated with ligation product on ice for 30 min, they were heat shocked for 45 seconds at 42°C and reincubated on ice for additional 15 min. They were resuspended in 300 μ l of LB medium, incubated for at least 45 min at 37°C, plated into agar plates supplemented with antibiotic (Ampicillin - Amp) and incubated overnight at 37°C. Colonies were picked and individually inoculated into 10 ml of LB with Amp, grown overnight at 37°C and minipreps were performed according to NucleoSpin[®] Plasmid (NoLid) protocol's (Macherey-Nagel). After plasmid sequencing for checking sgRNAs, cells were expanded through inoculation into 200 ml of LB with Amp, cells were grown overnight at 37°C and midipreps were performed with NucleoBond[®] Xtra Midi/Maxi kit (Macherey-Nagel).

After transfection, high GFP-positive cells were sorted, 750/1500/3000 cells were seeded into a 15cm dish and after 10 days clones were picked and screened by western blot. Positive clones were also confirmed by PCR and Sanger sequencing. Primers used for PCR were the following: *SLC35F1* Exon 2 5'-TCTCAGTAATCATTGCACCTTCC-3' and 5'-TACAGTTTTGCCTATACATGCAG-3'; *SLC35F1* Exon 7 5'-CATCAGTGAATAGGGGAAAAGAG-3' and 5'-TGTGAATACCTAAATCATGGAGG-3'.

3.1.2 AlphaLISA assay[®]

LCLs pellets were obtained by centrifugation and frozen at -80°C. An amount of ~10,000 cells/well resuspended in 60 μ l of culture media was used in order to perform AlphaLISA[®] assay (figure 3.1) according to manufacturer's protocol (PerkinElmer). Briefly, cells were incubated 15 minutes (min) with Cell-Histone Lysis buffer and 10 min with Cell-Histone Extraction buffer; 30 μ l of lysates were incubated with 10 μ l of Acceptor mix 1h at room temperature (RT) and then 10 μ l of Donor mix was added overnight at RT. Replicates were tested with both AlphaLISA Acetylated-Histone H3 Lysine 27 (H3K27ac) Cellular Detection Kit and AlphaLISA unmodified Histone H3 Lysine 4 (H3K4) Cellular Detection Kit for normalization.

PerkinElmer EnSight™ plate reader was used for the detection of the chemiluminescent signal.

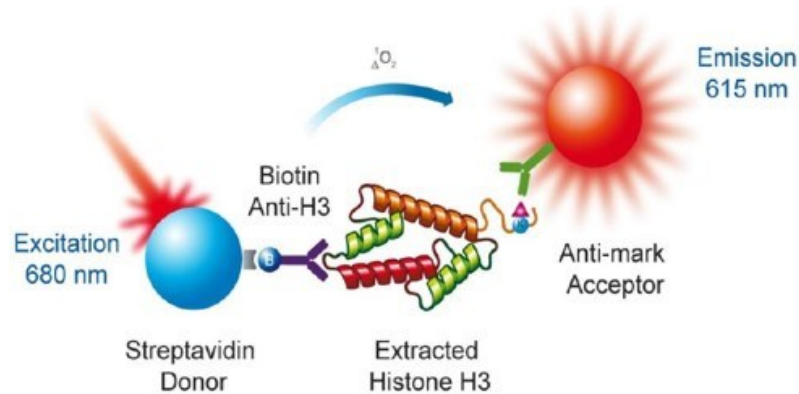


Figure 3.1 Schematic representation of the technology underlying AlphaLISA assay® (adapted from PerkinElmer, Inc)

3.1.3 Immunocytochemistry

At least 1.5×10^4 cells of LCLs were seeded in duplicate on SuperFrost Plus slides through 5 min of cytopspin at 500 rpm, while 1×10^5 cells of 293T and *SLC35F1* KO were seeded on slides coated with poly-D-lysine (PDL) in 24-well plate overnight. Seeded cells were washed with PBS, incubated with PFA 4% (10 min for LCLs, 20 min for 293T and *SLC35F1* KO cells) at RT and then washed again. Slides were stored at 4°C until immunofluorescence (IF) or TUNEL assays were performed.

3.1.3.1 Immunofluorescence (IF)

Briefly, for IF assay LCLs slides samples were put in a wet chamber and cells permeabilized with PBT buffer (PBS and 0.2% Triton) for 10 min at RT and non-specific sites were blocked by slide incubation with PBT supplemented with 10% FBS for 30 min at RT. Slides were first incubated overnight at 4°C with the primary antibody rabbit anti-Ki67 (1:400, #9129 Cell Signaling) or rabbit anti-HDAC2 (1:500, #ab137364 Abcam), washed with PBT and then incubated with Alexa-488 anti-Rabbit secondary antibody (1:250) for 2h. Slides were washed with PBT and water and mounted with EverBrite Mounting Medium with DAPI (Biotium).

293T and *SLC35F1* KO slides were permeabilized with PBS and 0.5% Triton for 20 min on ice, washed with PBS and blocked with PBS supplemented with 0.05% Triton and 10% FBS for 1h at RT. Incubation with primary antibody rabbit anti-*SLC35F1* (1:200, #HPA019576 Sigma Aldrich) was performed overnight at 4°C in PBS with 0.005% Triton and 1% FBS. The day after the incubation with primary antibody Goat anti-Lamin A/C in (1:200) for 1h at RT and

following washes were performed. Slides were incubated with Alexa-488 anti-Rabbit (1:400), Alexa-647 anti-Goat (1:400) and Phalloidin-TRITC (1:1000) for 1h at RT in the dark. After PBS washes, slides were incubated with DAPI (1:5000) for 5 min at RT in the dark, washed and mounted with DABCO Mounting Medium.

Microscopic images for Ki67 assay were acquired by NanoZoomer S60 Digital Slide Scanner at 20x and 80x magnification and two randomly selected fields for each experimental group at 20x were selected for blinded cells counts by three different operators. The images were analyzed with ImageJ software and the number of Ki67+ cells were normalized on the total cells number per image.

IF slides for HDAC2 were acquired by A1/A1R confocal microscopy (ten images of fields randomly selected for each sample) at 63x, analyzed with ImageJ software for blinded counting by three different operators. HDAC2 localization was divided into five degrees, where 0 meant lack of HDAC2 signal in the nucleus while 4 an abundance. Values assigned to each degree (HDAC2+ cells) were normalized on the total cell number in every acquired image.

All LCLs microscopic images were acquired at the Advanced Microscopy Facility Platform-UNitech NOLIMITS of the University of Milan. IF images from 293T and *SLC35F1* KO slides were obtained by SP8 Leica confocal microscope at 63x at IEO Imaging Unit.

3.1.3.2 TUNEL assay

Terminal deoxynucleotidyl transferase (TdT) dUTP Nick-End Labeling (TUNEL) assay (Roche Diagnostics) was performed using In Situ Cell Death Detection kit, AP, in order to detect apoptotic cells, according to manufacturer's protocol. Cells, previously seeded on slides were incubated with a permeabilization solution (0.1% Triton 100X and 0.1% sodium citrate) for 2 min at 4°C, then washed with PBS and incubated with TUNEL mixture (composed by Enzyme Solution added to Label Solution) in a wet chamber for 1h at 37°C. After 3 PBS washes, slides were incubated with Converter AP for 30 min at 37°C and then with Substrate Solution (2% NBT/BCIP Stock solution in NBT/BCIP Buffer) for 10 min at RT and dark. Finally, following PBS washes, mounted with DABCO Mounting Medium and brightfield microscopic images of apoptotic cells (TUNEL+) were acquired and analyzed with ImageJ software. Brightfield slides images were acquired by NanoZoomer S60 Digital Slide Scanner at 20x and 80x magnification and two randomly selected fields for each experimental group at 20x were selected for

blinded cells counts by three different operators. The number of TUNEL+ cells was normalized on the total cells number per image.

3.1.4 Protein procedures

3.1.4.1 Protein extraction

Cellular pellets were washed two times in PBS and centrifuged 5 min 2,500-3,000 rpm at 4°C, resuspended in cold S300 buffer (50 mM HEPES pH 7.6, 300 mM NaCl, 0.1% NP40, 2 mM MgCl₂, 10% glycerol) supplemented with protease inhibitors (Leupeptin and Apolipoprotein) and left on ice for 20-30 min. Samples were sonicated for 10 cycles (30s ON/30s OFF) at 4°C in a water bath sonicator (Biorupter), centrifuged at maximum speed (13,000 rpm) for 10 min at 4°C and the supernatant was quantified with Bradford assay (Bio-Rad) following the manufacturer's instructions. Protein samples were finally denatured in Laemmli sample buffer 4x (LSB) supplemented with dithiothreitol (DTT) and boiled for 10 min at 95°C before they could be loaded on gel.

3.1.4.2 Fractionation

293T cellular pellets were split equally in two recipients: for total lysate (Total) and cytoplasm/nuclei fraction. Pellet for total lysate was resuspended in S300 buffer for protein extraction for 30 min on ice.

Pellet for cytoplasm/nuclei fraction was washed in cold hypotonic buffer (10 mM Tris HCl pH 7.6, 1.5 mM MgCl₂, 10 mM KCl, 340 mM sucrose) 5 min at 2,500 rpm at 4°C and resuspended in hypotonic buffer (1:5) and put on ice for 10-15 min. Then 1/30 of Triton X100 10% was rapidly added to the solution which was left on ice for 5 min and centrifuged at maximum speed for one minute at 4°C. At this point supernatant was collected for cytoplasmic fraction (Cytosol), while cellular pellet corresponding to nuclei fraction was washed again in hypotonic buffer, lysed in S300 buffer, and left resting on ice for 30 min. Nuclei and total lysate were sonicated and centrifuged at maximum speed for 10 min at 4°C for removing debris. After quantification LSB with DTT was added to fractions.

3.1.4.3 Western blot

Denatured protein samples were separated by SDS-PAGE (Running buffer 1x diluted from 10x made of 3% Tris HCl, 14,4% Glycine and 1% SDS), transferred to nitrocellulose membranes and the transfer (Transfer buffer 1x made of 20% methanol and 10% Transfer buffer 10x which was composed of 3% Tris HCl and 14,4% Glycine) was checked by Ponceau staining.

Membranes were washed with TBS (TBS 1x diluted from 10x made of 3% Tris HCl, 8,7% NaCl and 0,2% KCl) supplemented with 0.1% Tween (TBS-T), blocked for 1h at RT with 5% milk in TBS-T and then with primary antibody diluted in blocking solution for 1h at RT (mouse anti-GAPDH 1:1000) or overnight at 4°C (rabbit anti-SLC35F1 1:1000). After washing, membranes were incubated with horseradish peroxidase (HRP)-conjugated secondary antibody (anti-rabbit or anti-mouse, Bio-Rad) diluted in 5% milk in TBS-T for 1h at RT, they were washed again and chemiluminescence signals were detected through ECL (Bio-Rad) incubation and captured by Chemidoc Imaging System.

3.1.5 Proteomic analysis

3.1.5.1 Immunoprecipitation

For immunoprecipitation (IP), 293T and *SLC35F1* KO cells from five 15 cm dishes per sample were collected and cellular pellets were washed with PBS 1x. They were lysed in S150 buffer (50 mM HEPES pH 7.6, 150 mM NaCl, 0.1% NP40, 2 mM MgCl₂, 10% glycerol and used to immunoprecipitate endogenous SLC35F1. Briefly, lysate (~5 mg) was incubated with 30 µg/ml of primary antibody anti-SLC35F1. IgG were used as negative control of the immunoprecipitation. After addition of 35 µL of Sepharose Protein A beads and incubation for 1 h at 4°C, beads were washed with 50 mM HEPES pH 7.6, 150 mM NaCl, 0.1% NP-40. Immunocomplexes were eluted in LSB and resolved on pre-cast 4–12% NuPage gels (Invitrogen, CA), stained with Coomassie Brilliant Blue and samples were prepared for mass spectrometry (MS).

3.1.5.2 Sample preparation and mass spectrometry analysis

After SDS-PAGE separation of SLC35F1 IP duplicates, the precast gel was stained with Coomassie Brilliant Blue overnight at RT, then it was washed with water and bands were cut for samples preparation by in-gel digestion. Briefly, gel pieces (1mm x 1mm for each band) were kept overnight at 4°C in destaining solution (25 mM ammonium bicarbonate - AmBic and 50% ethanol- EtOH), they were then dehydrated twice with 100% EtOH for 10 min at RT, dried with SpeedVac for 5 min, rehydrated with Reduction buffer (10 mM DTT in 50 mM AmBic) and incubated for 1h at 56°C. After discarding the liquid, gel pieces were incubated with Alkylation buffer (55 mM iodoacetamide in 50 mM AmBic) in the dark for 45 min, washed and dehydrated twice for 10 min with Digestion buffer (50 mM AmBic in milliQ water, pH 8) and 100% EtOH respectively (the last dehydration was repeated twice). Samples were dried

in SpeedVac (Savant) for 5 min and a double digestion was performed: GluC (Promega) solution (in 50 mM AmBic) was added for 20 min on ice, the excess removed, and gel pieces were incubated with Digestion buffer overnight at 37°C. Digestion was stopped with 4% final of trifluoroacetic acid (TFA), the liquid saved and the second digestion was performed with Trypsin/LysC mix (Promega) (in 50 mM AmBic) and previous steps were repeated. Peptides were extracted incubating gel pieces twice shaking for 10 min at RT with Extraction buffer (3% TFA and 30% acetonitrile - ACN) and 100% ACN and liquid was saved at every step. Samples were dried in SpeedVac until they reached the 10-20% of their original volume. In the meantime, stagetips (Pierce, Thermo Fisher Scientific) were prepared through a wash with 50% ACN and two washes with Buffer A (0.1% formic acid - FA). Samples were resuspended in 50 µl of 0.1% TFA and 2% ACN and loaded on stagetips two times. Two washes in Buffer A and the elution with Buffer B (80% ACN) were performed. In the end, samples were dried on SpeedVac until they reached a volume of 1 µl and then resuspended with 0,1% Formic acid to 8 uL and were loaded on the plate. 6 uL out of 8 were run on Q Exactive™ Plus Hybrid Quadrupole-Orbitrap™ Mass Spectrometer (Thermo Fisher Scientific).

3.2 DROSOPHILA MELANOGASTER MODEL

3.2.1 Stocks and feeding

Studies on *D. melanogaster* model were carried out in collaboration with Applied Biology laboratory (Prof. Vaccari) at the Department of Biosciences (University of Milan). In this study were used *D. melanogaster* yellow white (*yw*) strain as control and $w[*]P\{w[+mC]=lacW\}nej[P]/FM7c$ known as *nejire* or *nej* (*nejP/+*) mutant strain, which mimics a loss of function mutant due to its P-element 347bp upstream of the second exon of *nej* gene (Akimaru et al., 1997b). Fruit flies were maintained at 25°C and raised into vials containing a standard food medium of yeast, cornmeal, molasses, agar, propionic acid, tegosept, and water. In addition, *nej* mutants were balanced over FM7, *kr-GAL4 UAS-GFP* chromosome to identify homozygous animals in sibling crosses. For HDACi treatment, 2.5 mM VPA and 20 mM NaB were diluted in food under 65°C and before solidification to avoid heat damages.

Adult *nej* flies were synchronized by life cycle and fed with mock, VPA or NaB for four days.

3.2.2 Embryos flies immunostaining

Adult flies were placed in cages for 4h and then removed, after 8h fertilized eggs were collected and stained (Ashburner, 1989). In details, we proceeded with collection,

dechoriation and fixation of embryos with a mixture of 4% paraformaldehyde and heptane. Embryos were washed, permeabilized and blocked with PBT (PBS containing 0.1% Triton X-100 and 1% BSA) for 3 h. Incubation with primary antibody anti-wg (1:50) was performed overnight and the one with secondary goat anti-mouse-Cy3 (1:500) for 2 h. Images were acquired with a Nikon AR1 confocal microscope using a 10X objective.

3.2.3 Extraction of DNA for microbiota profiling

To avoid environmental contamination adult fly guts of *yw* and *nej* flies were dissected. Flies were anesthetized on ice for 5 min in a dish, then transferred to the dissection dish and put in 50 µL-drop of cold PBS; wings and legs were removed, and insect head was gently separated from the body by surgical forceps. To expose the foregut, the abdominal cuticle needed to be cut and dissected out, the hindgut pulled out and to free the gastrointestinal tract, fly head and Malpighian tubes were removed. Three undamaged dissected guts for experimental condition were transferred in 100µl of cold PBS and kept at -80°C. Bacterial DNA was extracted from 15 *nej* and 15 *yw* flies by QIAamp DNA Microbiome Kit, specific for low biomass samples. After adding lysis buffer, benzonase and beads to samples the lysis was carried out in the TissueLyser LT instrument, lysates were processed in QIAamp UCP Mini Columns according to manufacturer's protocol. DNA was eluted for library preparation (Illumina 16S Metagenomic Sequencing Library Preparation) and sequencing (2x250 bp paired-end run), which was performed on the Illumina platform (MiSeq) after library quantification by DNA High Sensitivity Qubit kit and Agilent 2100 Bioanalyzer System, in collaboration with Dr. Fazio at the University of Milano-Bicocca.

16S rRNA gene sequences were processed through PANDAseq and Quantitative Insights Into Microbial Ecology (QIIME) pipeline (release 1.8.0) (Caporaso et al., 2010; Masella et al., 2012). They were assembled into Operational Taxonomic Unit (OTUs) with 97% identity level and singletons were discarded as considered chimeras-like. Ribosomal Database Project (RDP) classifier (Wang et al., 2007) was used against Greengenes database (version 13_8; ftp://greengenes.microbio.me/greengenes_release/gg_13_8_otus, accessed on 22 February 2021) with 0.5 threshold for identity for assigning taxonomy. Alpha-diversity was obtained through the number of OTUs, Chao1, Shannon diversity and Phylogenetic Diversity (PD) whole tree metrics, while beta-diversity was computed using unweighted and weighted UniFrac distances and principal coordinates analysis (PCoA) (Lozupone et al., 2011).

3.3 PATIENTS

3.3.1 Subjects and samples

Patients with initial diagnosis of Rubinstein-Taybi syndrome were clinically assessed and diagnosed by a single expert clinical geneticist, while Rett-like patients were recruited by Prof. Vignoli among the ones attending RTT Clinic at the Adolescent Neuro-Psychiatry Unit of ASST Santi Paolo Carlo Hospital (University of Milan).

Concerning RSTS microbiota evaluation, we collected stool samples and three-days dietary surveys from 23 RSTS patients and 16 healthy donors represented by their healthy siblings in collaboration with “Associazione RTS Una Vita Speciale ONLUS”. Exclusion criteria for this study were antibiotic and/or pro-prebiotic treatments in the previous three months; inclusion criteria for RSTS patients were confirmed clinical diagnosis with (20/23) or without (3/23) molecular confirmation of *CREBBP/EP300* mutations. Written informed consent was obtained and Ethics Committee of San Paolo Hospital in Milan approved this study (Comitato Etico Milano Area 1, Protocol number 2019/EM/076, 2 May 2019).

3.3.1.1 Extraction of DNA from blood and saliva samples

For DNA samples collection, genomic DNA for sequencing was extracted from peripheral blood in EDTA and saliva samples (additionally to blood for some patients), using QIAamp DNA Blood Mini Kit (Qiagen) or with Wizard® Genomic DNA Purification Kit (Promega) and Quick-DNA Miniprep Plus Kit (Zymo Research) respectively. Patients (and their parents when possible) underwent genetic analysis and then they were carefully phenotypically re-evaluated by two geneticists with a deep expertise in RSTS and RTT diagnosis respectively.

3.3.1.2 Extraction of DNA for microbiota profiling

In collaboration with Prof. Borghi and her Microbiology laboratory at the Department of Health Sciences (University of Milan), bacterial genomic DNA was extracted from stool samples by Spin tool DNA kit as previously described (Verduci et al., 2018) and according to the manufacturer’s instructions. Briefly, fecal samples were homogenized in the lysis buffer for DNases inactivation and TissueLyser LT was used for lysing completely bacterial cells through the addition of Zirconia Beads II. After mixing the lysates with InviAdsorb reagent, bacterial DNA was eventually eluted in 100µl of buffer.

3.3.2 NGS analysis

3.3.2.1 RSTS multi gene panel sequencing

DNA from 30 clinically diagnosed RSTS patients (five of them described in this work: #208, #221, #243, #250, #251) were analyzed through a custom-made gene panel sequencing comprehensive of 68 chromatinopathies genes in collaboration with “IRCSS Casa Sollievo della Sofferenza” (San Giovanni Rotondo, Italy). Exploiting Agilent’s SureDesign tool, a HaloPlex Target Enrichment NGS panel was generated, and libraries were prepared according to manufacturer’s guidelines using the human reference genome GRCh37/hg19. Libraries were amplified, quantified and sequenced on MiSeq System using MiSeq Reagent Kit V2-500 cycles reaching 151 bp paired-end reads. After quality check, reads were aligned to the human genome GRCh37/hg19. Identification and annotation of variants were performed exploiting GATK v. 3.8 and ANNOVAR respectively, and they were pursued after interrogating ClinVar, dbSNP v. 150, ExAC v. 0.3, Exome Variant Server, gnomAD, HRC and Kaviar.

3.3.2.2 RSTS and RTT-like exome sequencing

Whole exome sequencing (WES) was performed for nine clinically diagnosed RSTS (#187 and #249 and their parents) and three RTT-like patients (#1, #2, #3 and their parents). Agilent SureSelect V7 kit was used for libraries preparation and exome enrichment according to manufacturer’s protocol, libraries quality was checked and run (150 bp paired-end) on Illumina HiSeq 3000 at CRS4 facility. The average coverage was 75x, with 97% covered at least 10x. Reads were aligned to human reference genome GRCh37/hg19 through Burrows-Wheeler Aligner (BWA MEM) and variants were identified by GATK Haplotype Caller module, classified using dbSNP146 and annotated with KGGSeq. For retrieving variants were exploited dbNSFP v.3.0, dbSNP, ENSEMBL, ESP6500 (release SI-V2), ExAC and gnomAD, GENCODE, RefGene, UCSC, OMIM and ClinVar, 1000 Genome Project (release 05/2013) and for predictions of aminoacidic changes were used different models (FATHMM, LTR, Pathogenic variantTaster, Pathogenic variantAssessor, PolyPhen2 and SIFT). Variants identified were filtered for pattern of inheritance, features of the gene and MAF < 1% referred to dbSNP138, dbSNP141, ESP6500, ExAC, gnomAD and 1000 Genomes).

3.3.2.3 Variants validation

Subsequently, variants were evaluated for their phenotypic and biological impact. Candidate variants were reported according to Human Genome Variation Society (HGVS) nomenclature

guidelines and their significance according to American College of Medical Genetics and Genomics (ACMG) criteria using InterVar and Varsome tools. Finally, all variants of interest were confirmed by PCR amplification, ruled following the protocol for GoTaq Flexi DNA Polymerase (Promega), and Sanger sequencing and segregation analysis were performed in the available family trios.

3.3.2.4 16S rRNA gene sequencing of human gut microbiota

25 ng of DNA extracted from RSTS stool samples was used for library preparation accordingly to manufacturer's protocol (Illumina 16S Metagenomic Sequencing Library Preparation). Libraries were quantified, pooled and sequenced on a MiSeq platform. Sequencing were performed as described above for flies gut samples.

3.4 QUANTIFICATION AND STATISTICAL ANALYSIS

3.4.1 Data generated from LCLs assays

Data were analyzed using Prism software (GraphPad Software) and expressed as mean \pm Standard Deviation (SD) or \pm Standard Error of the Mean (SEM). Student's t tests were used to compare means between groups in AlphaLISA assay on RSTS or HDAC2 and HD LCLs for evaluating acetylation pattern and the variance among HDAC2, RSTS and HD LCLs acetylation was compared using one-way ANOVA. Data from Ki67 and TUNEL assays for LCLs proliferation and death rate investigation were compared using Student's t test as statistical tool. Correlation between HDACi-induced acetylation and proliferative or apoptotic cells was calculated using Pearson correlation coefficient ($-1 < r < 1$) and Pearson correlation p value. Multiple t-test was used for comparing means of cells counts (HDAC2+ cells) for five degrees of nuclear localization, with significant p value determined through Holm-Sidak method as *post-hoc* test ($\alpha = 0.05$). For all these statistical analyses p values < 0.05 were considered significant (*p < 0.05 ; **p < 0.01 ; ***p < 0.001).

3.4.2 LC-MS/MS analysis

Raw data files were analyzed using the peptide search engine Andromeda, which is integrated into the MaxQuant software environment (version 2.1.4.0) (Tyanova et al., 2016), with the following parameters: human protein database, Oxidation (M), Acetyl (Protein N-term), as variable modifications, peptide false discovery rate (FDR) 0.01, maximum peptide posterior error probability (PEP) 1, protein FDR 0.05, minimum peptides 2, at least 1 unique, minimum length peptide 6 amino acids. Statistical analysis was performed by using Perseus software

included in MaxQuant package. T-test and ANOVA statistical analysis were performed applying $p\text{Value} < 0,05$. The matrix was then exported to GraphPad for visualization.

3.4.3 Microbiota profiling data from flies and human

Statistical tool applied to alpha-diversity indices was Monte Carlo-base test in which were used 9999 random permutations. Microbial community composition of subjects within beta-diversity analysis was compared with PERMANOVA test (adonis function) in the vegan R package version 2.0-10. Pairwise t-test from “rstatix” package version 0.6.0 (RStudio software version 1.2.1335; R version 3.6.3) was applied for assessing differences in taxonomic relative abundances. For all microbiota analyses p values < 0.05 were considered significant.

4. RESULTS

4.1 EXPLORING POSSIBLE THERAPEUTIC APPROACH AND NEW GENOTYPE-PHENOTYPE CORRELATIONS FOR RUBINSTEIN-TAYBI SYNDROME (RSTS)

4.1.1 Dissecting HDACi effect as a possible therapeutic approach

4.1.1.1 Exogenous HDACi exposure boosts acetylation in RSTS lymphoblastoid cell lines (LCLs)

We exposed LCLs derived from eight RSTS patients with *CREBBP* (n.4) or *EP300* (n.4) confirmed mutations (table 3.1) and seven healthy donors (HD) to four different HDACi: Tricostatin A (TSA), Suberoylanilide hydroxamic acid (SAHA), Valproic acid (VPA), Sodium butyrate (NaB). We analyzed by AlphaLISA[®] assay the acetylation levels of lysine 27 of histone H3 (H3K27Ac) in LCLs upon seven different conditions: HDACi treatments (TSA, SAHA, VPA or NaB), exposure to vehicle (H₂O or DMSO) and untreated cells (figure 4.1). We observed that all compounds increase histone acetylation in RSTS LCLs compared to HD LCLs, particularly VPA ($p < 0.01$), and with a considerable increment in treated samples compared to untreated ones (figure 4.1A).

In addition, as shown in Figure 4.1B, HDACi exposure induced a patient-specific acetylation response when compared to treated HD LCLs. TSA 2 μ M increased acetylation levels significantly in LCLs RSTS 176 ($p < 0.001$), RSTS 25 ($p < 0.001$) and RSTS 39 ($p < 0.01$), while SAHA 2 μ M on RSTS 176 and RSTS 25 ($p < 0.001$). VPA 2 mM exposure showed highly significant effect on RSTS 114, RSTS 120, RSTS 176, and RSTS 54 ($p < 0.001$) as well as NaB 5mM for RSTS 176 and RSTS 39 ($p < 0.001$), RSTS 54, and RT010-15 ($p < 0.05$).

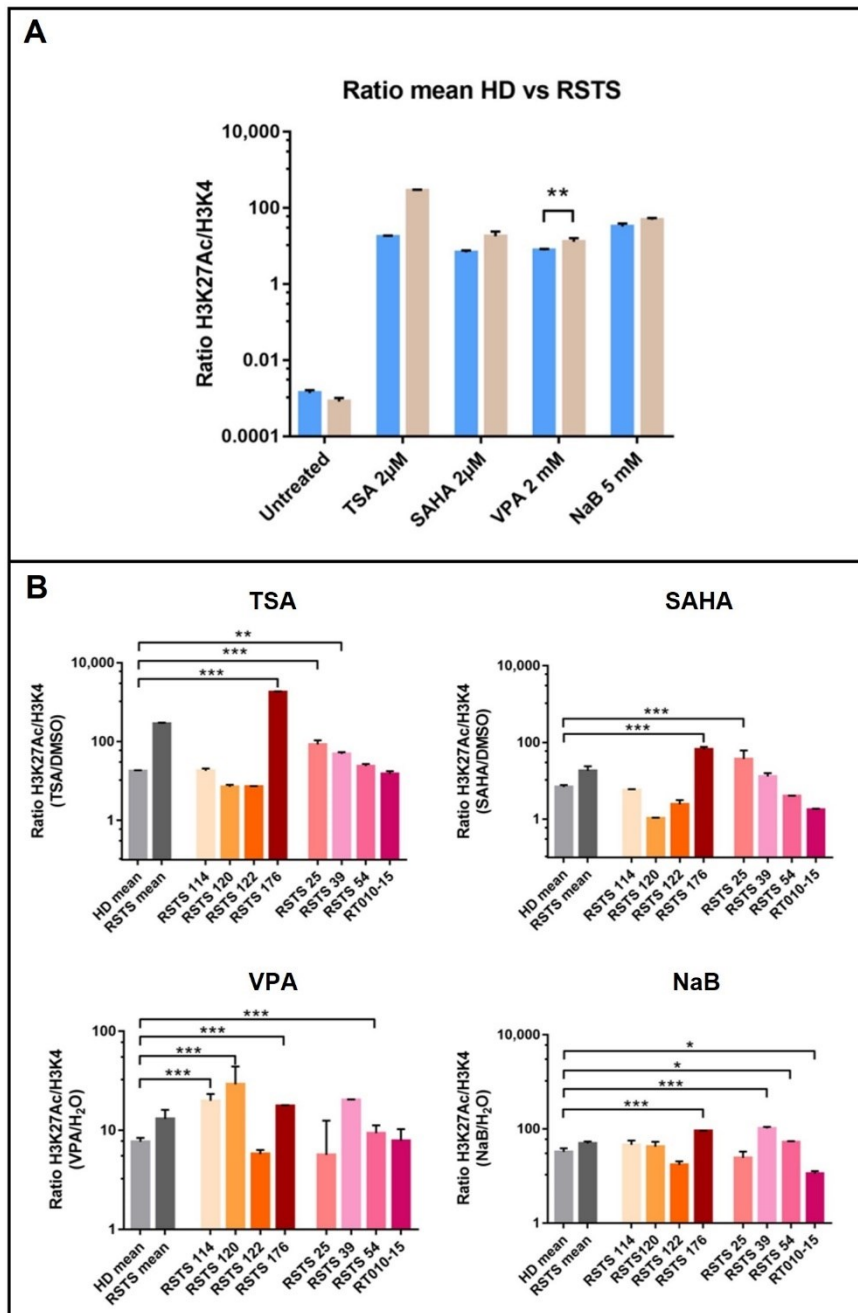


Figure 4.1. Histone acetylation on RSTS LCLs upon HDACi exposure. AlphaLISA® data showing H3K27 acetylation (H3K27Ac) levels normalized on H3K4 unmodified (on Log scale, Y-axis); acetylation values resulted from HDACi exposure are expressed as ratio between HDACi and respective vehicle (H₂O or DMSO); on X-axis list of treatment conditions or untreated/treated single LCL or LCLs means. A) Means of values of H3K27Ac in healthy donors (HD, in blue) and patients LCLs (RSTS, in pale brown) untreated and exposed to four different HDACi at specific indicated dosage (TSA, SAHA, VPA and NaB). B) Values of H3K27Ac in eight RSTS LCLs (*CREBBP* LCLs in shades of red, *EP300* LCLs in shades of pink) after exposure with HDACi, compared to treated HD and RSTS means (in

shades of grey). Groups were compared using Student's *t*-test as statistical method (**p* < 0.05; ***p* < 0.01; ****p* < 0.001). Adapted from "Di Fede et al., 2021" (see Appendix 1).

Interestingly, analysis of single-RSTS patient response to HDACi compared to its untreated condition showed that at least one exogenous HDACi significantly increased H3K27ac and RSTS LCLs response was variable among different HDACi treatments (figure 4.2).

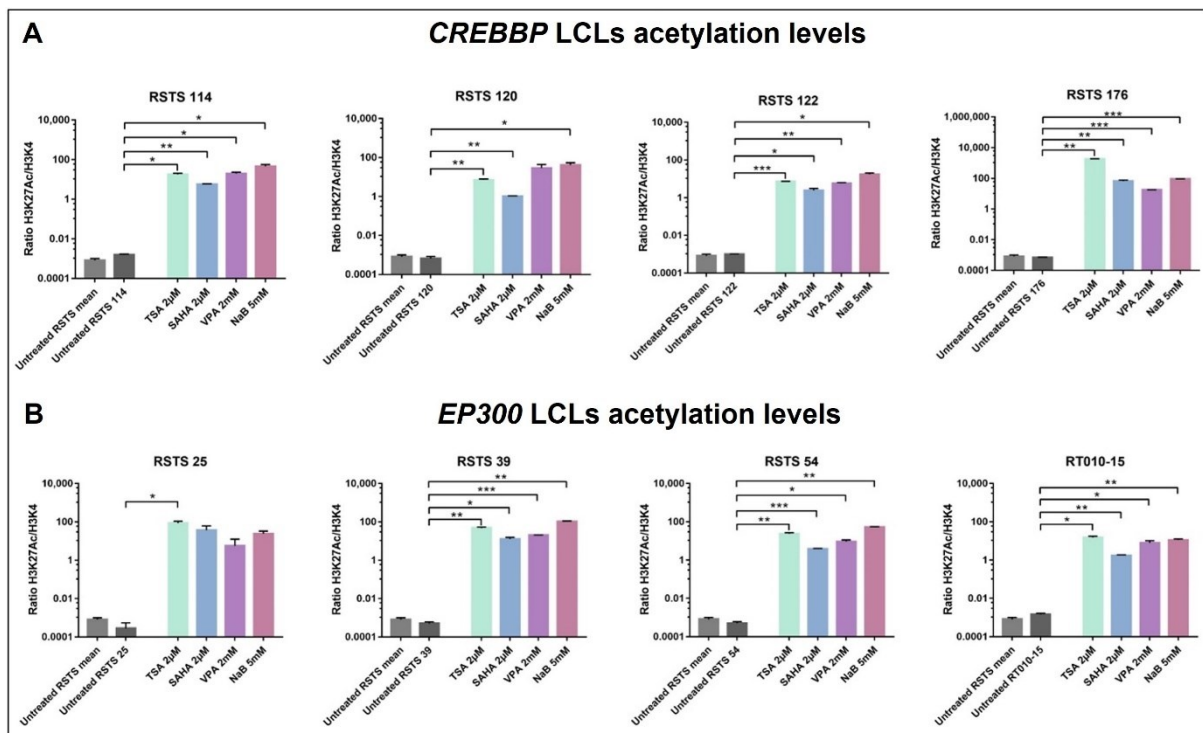


Figure 4.2. Insight on single-RSTS LCLs histone acetylation. Single-RSTS response (A *CREBBP* group and B *EP300* LCLs) to the four compounds (TSA, SAHA, VPA and NaB, in light green, light blue, violet and pink bars, respectively) compared to untreated RSTS means and untreated single-RSTS condition (in shades of grey); groups were compared using Student's *t*-test as statistical method (* *p* < 0.05; ***p* < 0.01; *** *p* < 0.001). Adapted from "Di Fede et al., 2021" (see Appendix 1).

In order to investigate compounds effect on cell-cycle regulation, cell proliferation and cell death were assessed upon HDACi exposure with Ki67 (figure 4.3A-C) and TUNEL assays, (figure 4.4A-C) respectively. Significant changes in proliferation rate occurred in case of exposure to SAHA and DMSO (*p* < 0.05) in RSTS cells compared to HD (figure 4.3B), as well as for increase of apoptotic cells with DMSO treatment (*p* < 0.001) (figure 4.4B). For both assays, we did not observe a significant correlation with H3K27 acetylation (figure 4.3C and 4.4C).

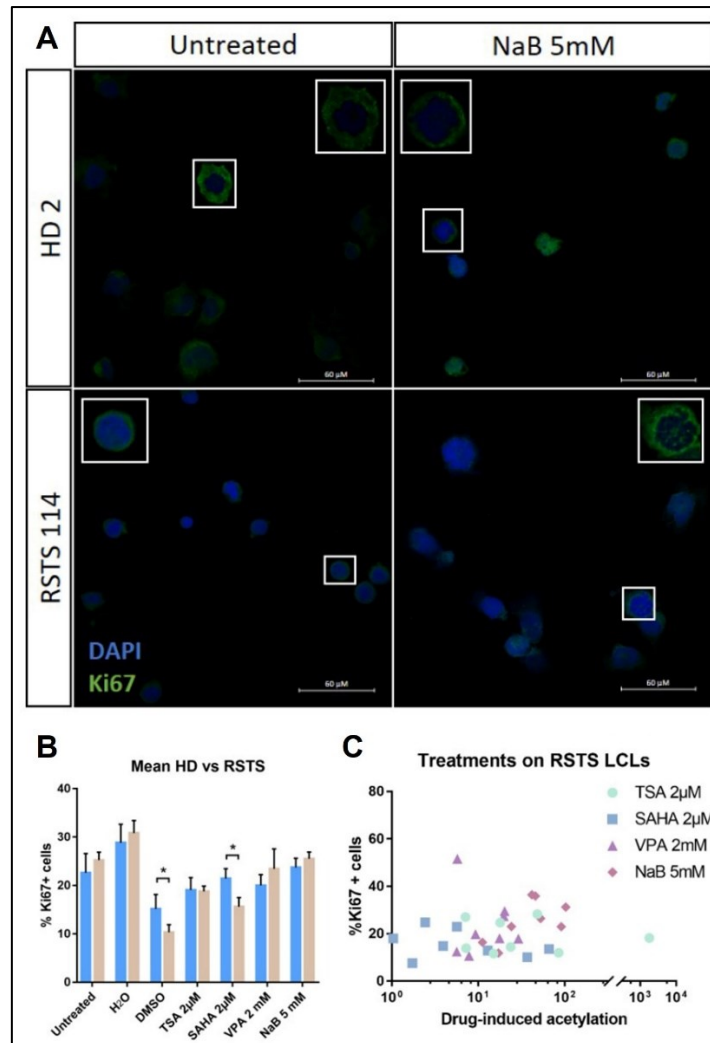


Figure 4.3. Proliferation evaluation on RSTS LCLs after HDACi exposure. Cell proliferation analysis (A-C) of RSTS LCLs compared to HD LCLs. A) Confocal 60x images resulting from Ki67 assay performed on HD LCL (HD2) and RSTS LCL (RSTS 114) untreated and treated with NaB 5mM; DAPI (blue) and Ki67 (green signal) mark respectively cell nuclei and proliferative cells; Insets show 100x cell magnification. B) Cell proliferation rate of Ki67 positive cells (% Ki67+ cells, on Y-axis, \pm SD) of RSTS LCLs compared to HD LCLs upon untreated condition, treatment with vehicles (H₂O and DMSO) and HDACi exposure (TSA 2μM, SAHA 2μM, VPA 2mM and NaB 5mM) (X-axis). C) Correlation overview between cell proliferation rate (% Ki67+ cells, on Y-axis) and HDACi-induced acetylation (X-axis) in RSTS LCLs. Cell proliferation rate of groups was compared using Student's *t*-test as statistical method (**p* < 0.05; ***p* < 0.01; ****p* < 0.001). Adapted from "Di Fede et al., 2021" (see Appendix 1).

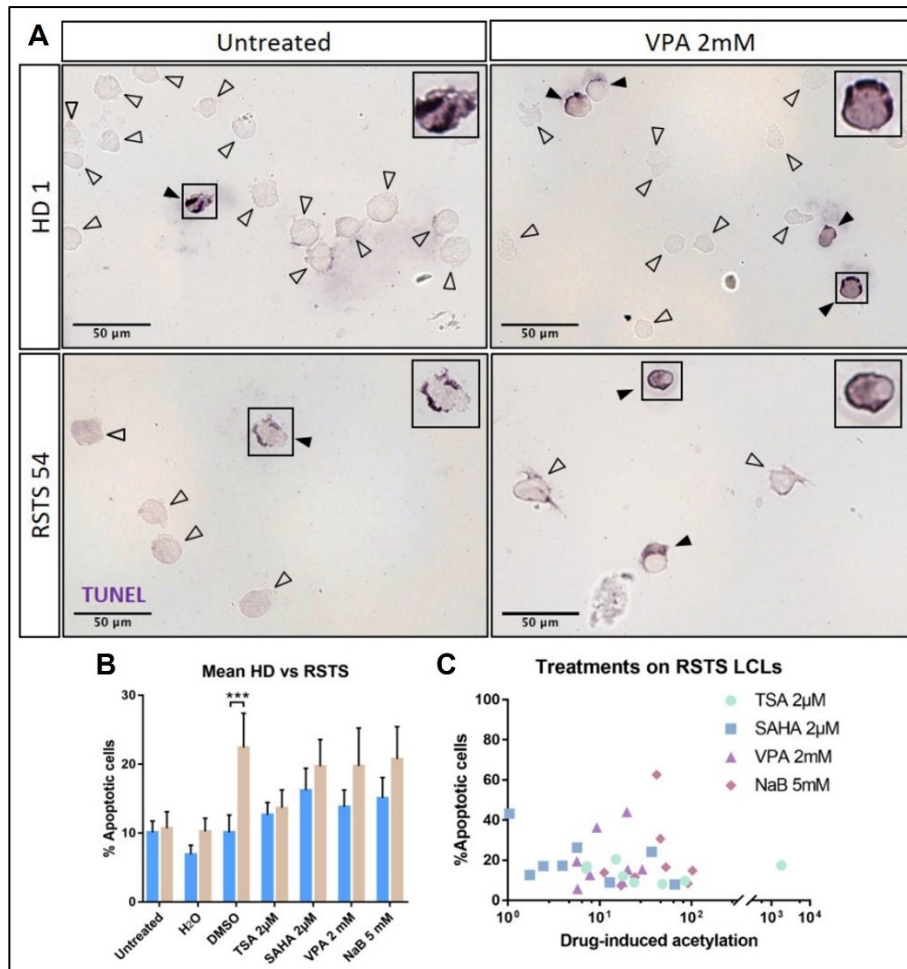


Figure 4.4. Cell death evaluation on RSTS LCLs after HDACi exposure. Cell death analysis (A-C) of RSTS LCLs compared to HD LCLs. A) Brightfield 40x images resulting from TUNEL assay performed on HD LCL (HD1) and RSTS LCL (RSTS 54) untreated and treated with VPA 2mM, with TUNEL positive/apoptotic (deep purple) and negative cells pointed respectively with black and empty arrowheads; Insets show 80x cell magnification. B) Cell death rate of TUNEL positive cells (% Apoptotic cells, on Y-axis, \pm SD) of RSTS LCLs compared to HD LCLs upon untreated condition, treatment with vehicles (H₂O and DMSO) and HDACi exposure (TSA 2μM, SAHA 2μM, VPA 2mM and NaB 5mM) (X-axis). C) Correlation overview between cell death rate (% Apoptotic cells, on Y-axis) and HDACi-induced acetylation (X-axis) in RSTS LCLs. Cell death rate of groups was compared using Student's *t*-test as statistical method (**p* < 0.05; ***p* < 0.01; ****p* < 0.001). Adapted from "Di Fede et al., 2021" (see Appendix 1).

Ki67 assay revealed variable proliferation in response to HDACi treatment among different RSTS LCLs, observing statistical significance for RSTS 25 (*p* < 0.05) and RT010-15 (*p* < 0.01) exposed to SAHA, RSTS 122 exposed to VPA and RSTS 114, RSTS 120, RSTS 122 to NaB

compared to HD LCLs (figure 4.5A). TUNEL assay showed patient and drug-specific response to HDACi in term of cell death too: TSA and SAHA increased percentage of apoptotic cells in RT010-15 ($p < 0.05$) and RSTS 120 ($p < 0.01$) respectively, significant values were observed for RSTS 114 ($p < 0.001$), RSTS 122 ($p < 0.05$) and RSTS 54 ($p < 0.01$) exposed to VPA, and for RSTS 114 ($p < 0.05$) and RSTS 120 ($p < 0.001$) treated with NaB, compared to controls (figure 4.5B).

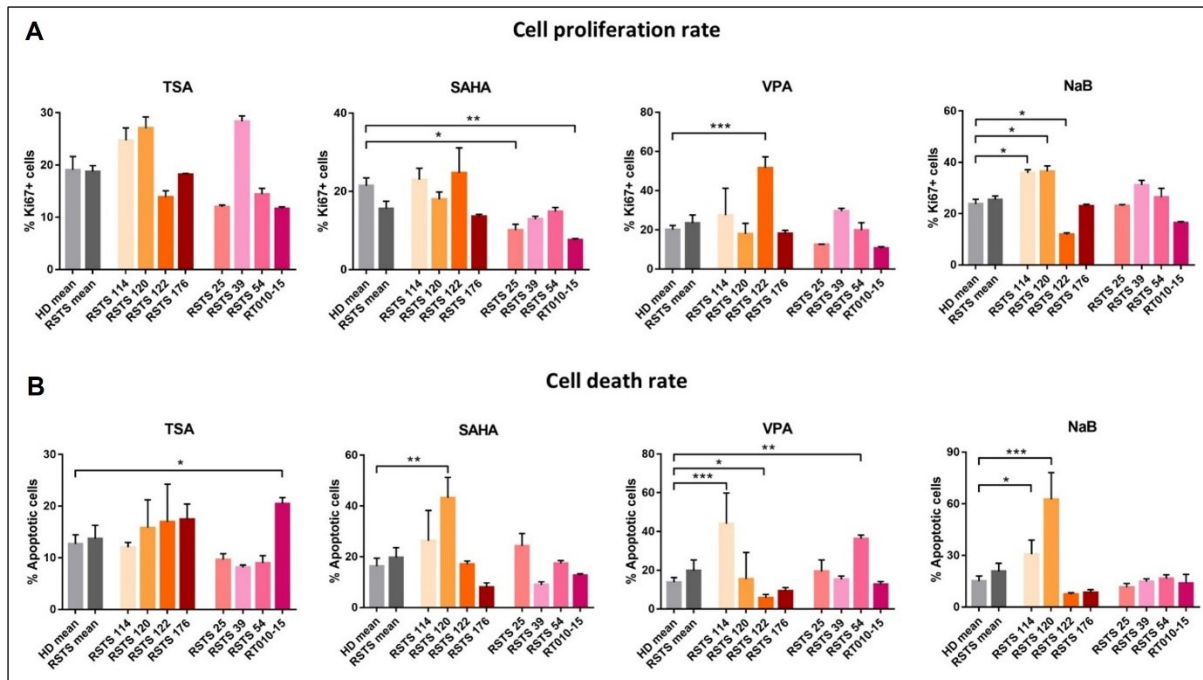


Figure 4.5. Insights on cell proliferation and cell death rate of RSTS LCLs upon HDAC inhibitors exposure. Cell proliferation (A) and cell death (B) analysis on eight RSTS LCLs (*CREBBP* LCLs in shades of red, *EP300* LCLs in shades of pink) after exposure with four HDACi (TSA, SAHA, VPA and NaB). A) Cell proliferation rate of Ki67 positive cells (% Ki67+ cells, on Y-axis) and B) cell death rate of TUNEL positive cells (% Apoptotic cells, on Y-axis) of single RSTS LCLs compared to treated HD and RSTS means (in shades of grey). Student's *t*-test was applied as statistical method (* $p < 0.05$; ** $p < 0.01$; *** $p < 0.001$). Adapted from “Di Fede et al., 2021” (see Appendix 1).

We found no correlation between cell proliferation and drug-induced acetylation (Pearson correlation $p > 0.05$; figure 4.6A), with treatments with TSA 2 μ M and VPA 2 mM showing a very weak negative correlation ($r = -0.03$ and $r = -0.11$ respectively), SAHA 2 μ M a weak negative correlation ($r = -0.3$), while NaB 5 mM a moderate positive correlation ($r = 0.45$). No significant correlation was observed neither between apoptosis rate and HDACi-induced acetylation (Pearson correlation $p > 0.05$; figure 4.6B): TSA 2 μ M and VPA 2 mM showed, respectively, a weak and a very weak positive correlation ($r = 0.3$ and $r = 0.11$), while SAHA 2

μM and NaB 5 mM shared a very weak negative correlation ($r = -0.038$ and $r = -0.06$ respectively).

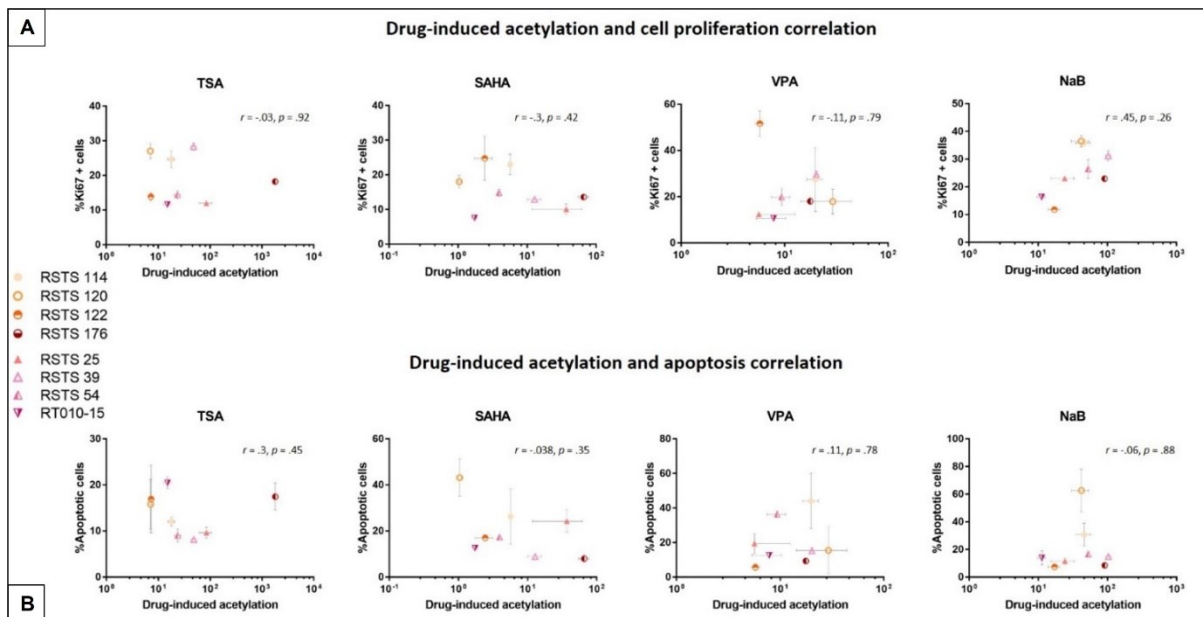


Figure 4.6. Correlation between HDACi-induced acetylation versus cell proliferation and apoptosis in RSTS LCLs. A) Correlation between cell proliferation rate (% Ki67+ cells, on Y-axis of upper graphics) or B) cell death rate (% Apoptotic cells, on Y-axis of lower graphics) and drug-induced acetylation (X-axis) in RSTS LCLs exposed to four HDACi (TSA, SAHA, VPA and NaB); Pearson correlation coefficient ($-1 < r < 1$) and Pearson correlation p value (significant for $p < 0.05$) were used for statistical analysis. Adapted from “Di Fede et al., 2021” (see Appendix 1).

4.1.1.2 Exogenous HDACi exposure leads to a partial rescue of RSTS phenotype in *Drosophila melanogaster* model

We set up a *Drosophila melanogaster* model for RSTS, mutant in the CBP homolog *nejire* (*nej*), and exploited this *in vivo* model for the investigation of exogenous HDACi effects on RSTS pathogenesis. We confirmed that null embryos for CBP show early lethality due to abnormal embryonic development (Akimaru et al., 1997a, 1997b) (figure 4.7).

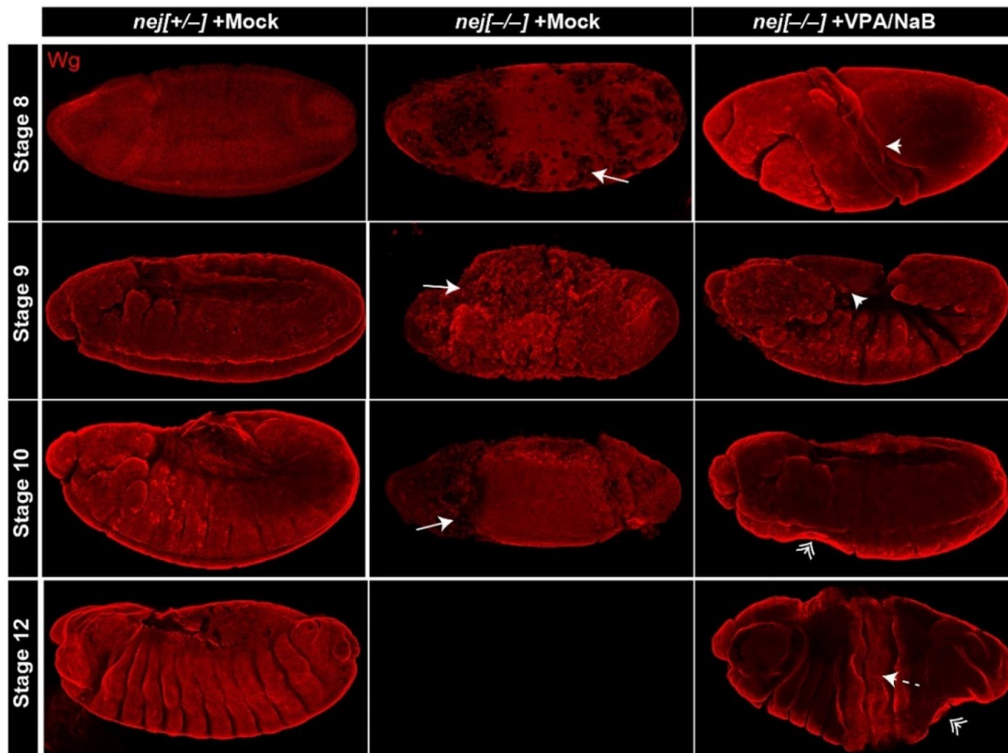


Figure 4.7. Partial developmental rescue of RSTS phenotype in *D. melanogaster* model (*nej*). Developmental and morphological defects in *nej* mutant embryos detected with wingless (*wg*) staining. Representative confocal images from stages 8 to 12 are shown, in which defects detected in *nej*^{-/-} mutant embryos include loss or uneven *wg* staining (arrow) and twists (arrowhead), bottlenecks (double arrowheads) or cracks (dashed arrow) after VPA or NaB parental feeding. Adapted from “Di Fede et al., 2021” (see Appendix 1).

In details, we assessed morphology of embryos deposited by females at stages 8-12 through wingless (*wg*) immunostaining and we observed that majority of *nej*^{-/-} flies did not survive beyond stage 10 due to the twisting of the embryo (Akimaru et al., 1997b) (figure 4.7 and 4.8A). After feeding parental females with food supplemented with NaB or VPA, *nej*^{-/-} embryos showed a partial rescue of the embryonic development, particularly evident at stage 10 ($p < 0.01$), although they still displayed a bottlenecked and cracked phenotype (figure 4.7 and 4.8B). Strikingly, F1 *nej*^{-/-} generation of HDACi-treated flies reached stage 12 since segmentation occurred due a milder twisting of the embryo phenotype (figure 4.7), suggesting that exogenous HDACi can counteract developmental defects due to CBP loss *in vivo*.

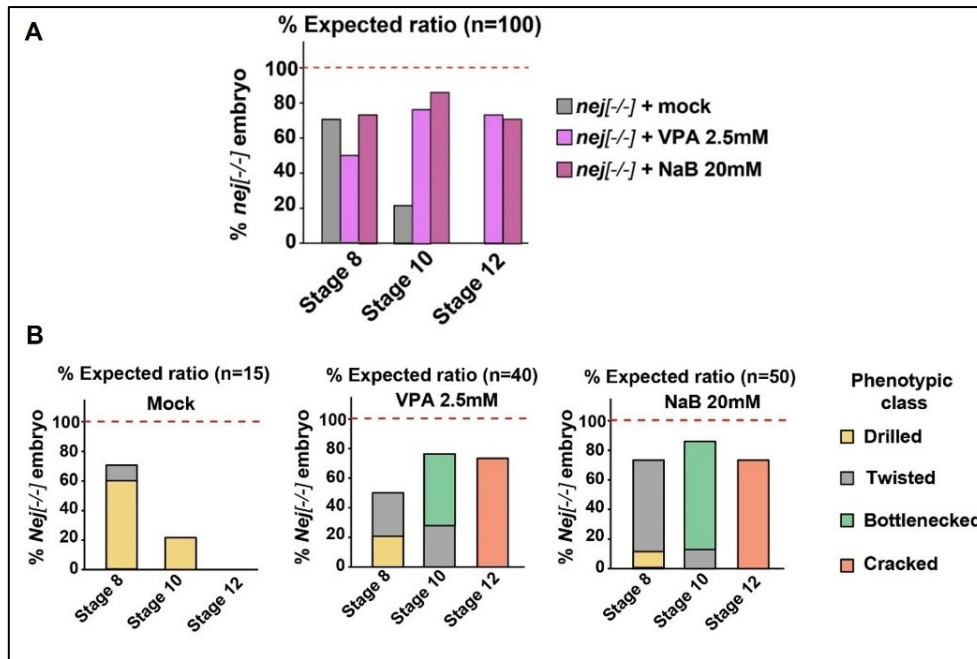


Figure 4.8. Embryos survival and altered phenotypes upon HDACi treatments. Quantification of *nej* mutant embryos (A) and their altered phenotypes (B) in untreated or treated conditions (with VPA or NaB). *nej* groups were compared using Student t-test as statistical tool ($p < 0.05$ considered significant). Adapted from “Di Fede et al., 2021” (see Appendix 1).

4.1.1.3 RSTS patients’ microbiota profiling shows a depletion of bacteria producers of endogenous HDACi

We enrolled 23 RSTS patients (12 females and 11 males, average age 10.2 ± 6.4 years) and 16 HD siblings (6 females and 10 males, average age 12.7 ± 7.2 years) for evaluating patients commensal microbiota and in particular SCFAs production since their known role of HDACi. From dietary survey did not emerge any differences in macronutrients intake, except for a lower energy intake in RSTS patients compared to controls ($p = 0.0054$) (table 4.1).

Table 4.1. Nutritional values of the subjects enrolled in the study. Daily intake of energy and macronutrients of patients (RSTS) and healthy donors (HD); values are expressed as mean, with standard deviation among parentheses. Mann-Whitney test was applied as statistical tool (p-value significant for <0.05, **p < 0.01).

Variable	HD Mean (SD)	RSTS Mean (SD)	p-value	Reference values
Energy intake			**	boys:1330-4020
kcal	1528 (343)	1185 (294)	0.0054	girls:1220-3550 kcal (AR)
Proteins			**	
g	60.8 (17.97)	46.22 (13.21)	0.0079	16-50 g (AR)
% energy	15.93 (3.35)	15.72 (3.29)	0.8990	12-15% (RI)
Lipids				
g	51.55 (15.05)	43.73 (13)	0.0609	20-35% (RI)
% energy	30.36 (6.96)	33.16 (5.38)	0.1206	
Carbohydrates			**	
g	209.4 (60.81)	158.8 (41.48)	0.0054	45-60% (RI)
% energy	54.29 (7.62)	53.65 (5.48)	0.5626	
Total fiber				
g	20.41 (420.05)	17.33 (13.4)	0.4369	8.40 g/1000 kcal (AI)
g/1000 Kcal	12.87 (10.35)	14.54 (9.19)	0.2065	

AR. average requirement; RI. reference intake; AI. adequate intake.

Concerning microbiota analysis, alpha-diversity did not show any significant differences for richness (figure 4.9A), and richness and evenness (figure 4.9B), while beta-diversity showed significant changes in microbiota between RSTS and HD, relative to unweighted and weighted Unifrac distances (p = 0.013 and p = 0.022 respectively) (figure 4.9C).

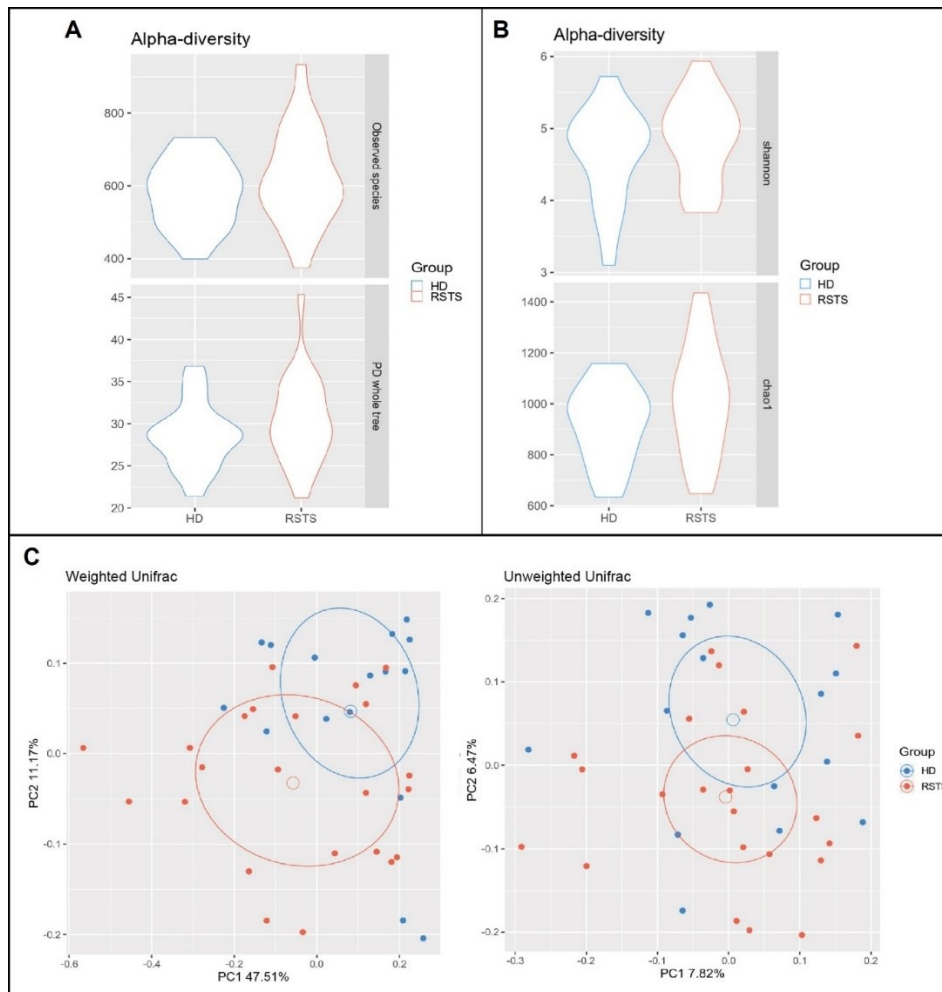


Figure 4.9. Alpha and beta diversity in RSTS microbiota compared to HD. A-B) Violin plots showing no differences in alpha-diversity in terms of biodiversity values between RSTS and HD according to observed species ($p = 0.255$) and PD whole tree ($p = 0.279$) (A), and Shannon ($p = 0.287$) and Chao1 ($p = 0.151$) diversity indices (B). C) Beta-diversity represented by Principal Coordinate Analysis (PCoA) of weighted and unweighted Unifrac distances of microbial communities showed statistical differences calculated by *Adonis* test ($p < 0.05$ considered significant). Adapted from “Di Fede et al., 2021” (see Appendix 1).

Relative abundance of Firmicutes phylum, *Ruminococcaceae* family and *Faecalibacterium* spp., a SCFAs-producer, was decreased in RSTS (58%, 32.2% and 3.3% respectively) compared to HD (73.4%, 41.9% and 9.8%) in a significant manner ($p = 0.019$, $p = 0.049$ and $p = 0.001$) (figure 4.10A and table 4.2). An opposite trend resulted for *Bacteroidaceae* family and *Bacteroides* spp., and *Oscillospira* spp. which were enriched in RSTS (21.1% and 5.1% respectively) compared to controls (10.3% and 2.4%) with p value < 0.05 ($p = 0.021$ and $p = 0.007$) (figure 4.10A and table 4.2). In addition, contrary to the significant enrichment of

Oscillospira spp., the significant decrease in *Faecalibacterium* spp. was demonstrated to be environment-independent as shown by the matched-pair analysis on RSTS-siblings (Wilcoxon signed-rank test, $p = 0.0021$) (figure 4.10B).

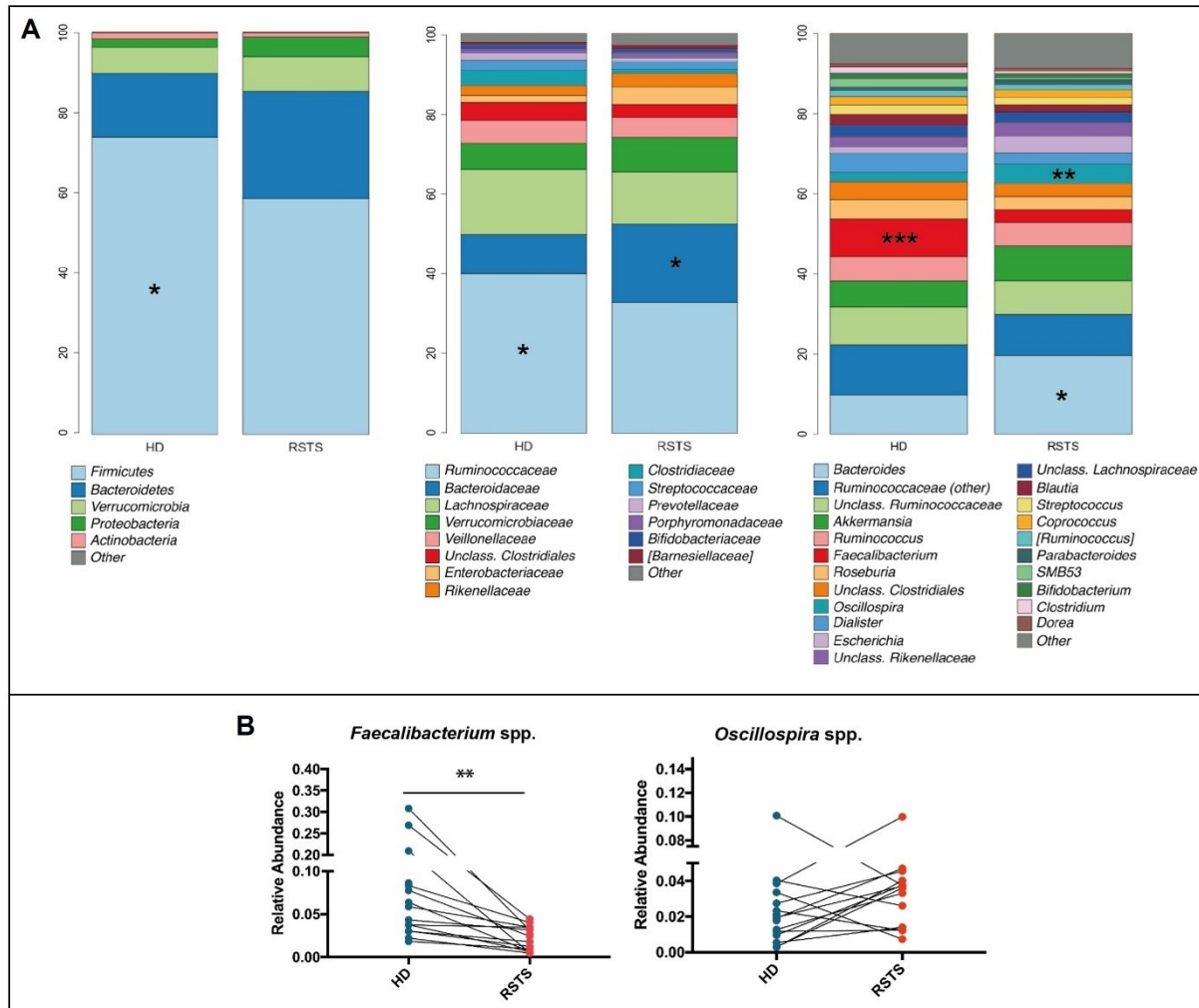


Figure 4.10. Microbial composition in HD and RSTS subjects. A) Relative abundances were shown at different phylogenetic levels, according to phylum-family-genus order; “Other” represented taxa which were present with a frequency < 1%. B) Focus on comparison between relative abundances of *Faecalibacterium* spp. and *Oscillospira* spp. in matched RSTS patients/siblings (n = 16) by Wilcoxon signed rank test. P value < 0.05 were considered significant (* $p < 0.05$; ** $p < 0.01$; *** $p < 0.001$). Adapted from “Di Fede et al., 2021” (see Appendix 1).

Table 4.2. Bacterial composition in HD and RSTS groups. Bacterial groups were divided into phylum, family and genus phylogenetic levels and values were expressed as average relative abundance (\pm SD), with p values significant for $p < 0.05$ (* $p < 0.05$; ** $p < 0.01$; *** $p < 0.005$).

TAXONOMIC LEVEL			HD	RSTS	p-value
Phylum	Family	Genus			
<i>FIRMICUTES</i>			73.4 \pm 15.6	58.5 \pm 18.8	0.019 *
	<i>Ruminococcaceae</i>		41.9 \pm 15.1	32.2 \pm 13.9	0.049 *
		<i>Faecalibacterium</i>	9.8 \pm 2.2	3.3 \pm 3.8	0.001 ***
		<i>Ruminococcus</i>	6.4 \pm 5.1	6.4 \pm 4.9	0.877
		<i>Oscillospira</i>	2.4 \pm 2.4	5.1 \pm 5.0	0.007 **
		<i>Ruminococcaceae (other)</i>	13.3 \pm 15.9	8.2 \pm 10.2	0.746
		<i>Unclass. Ruminococcaceae</i>	9.6 \pm 9.0	9.0 \pm 10.1	0.525
	<i>Lachnospiraceae</i>		16.2 \pm 7.2	13.1 \pm 7.3	0.187
		<i>Roseburia</i>	5.2 \pm 5.8	3.4 \pm 4.9	0.053
		<i>Blautia</i>	2.5 \pm 3.3	1.8 \pm 1.3	0.855
		<i>Coprococcus</i>	2.2 \pm 1.4	2.0 \pm 2.4	0.168
		<i>Clostridium</i>	1.1 \pm 1.6	0.6 \pm 1.1	0.263
		<i>Dorea</i>	0.8 \pm 0.9	0.8 \pm 1.0	0.855
		<i>Unclass. Lachnospiraceae</i>	3.3 \pm 3.4	2.7 \pm 2.1	0.471
	<i>Veillonellaceae</i>		6.0 \pm 6.1	5.1 \pm 5.4	0.703
		<i>Dialister</i>	5.1 \pm 5.9	3.1 \pm 4.9	0.501
	<i>Clostridiaceae</i>		2.4 \pm 3.8	0.9 \pm 1.2	0.095
		<i>Clostridium</i>	1.1 \pm 1.6	0.6 \pm 1.1	0.263
	<i>Unclassified Clostridiales</i>		4.8 \pm 6.7	3.6 \pm 5.9	0.746
	<i>Streptococcaceae</i>		1.0 \pm 2.0	1.8 \pm 2.7	0.315
		<i>Streptococcus</i>	1.0 \pm 2.0	1.7 \pm 2.7	0.641
<i>BACTEROIDETES</i>			16.8 \pm 14	28.7 \pm 21	0.065

<i>Bacteroidaceae</i>	10.3 ± 10.3	21.1 ± 16.3	0.021	*
<i>Bacteroides</i>	10.3 ± 10.3	21.1 ± 16.3	0.021	*
<i>Rikenellaceae</i>	2.6 ± 2.5	3.7 ± 3.3	0.220	
<i>Unclass. Rikenellaceae</i>	2.5 ± 2.4	3.6 ± 3.3	0.263	
<i>Prevotellaceae</i>	2.0 ± 4.4	0.9 ± 3.0	0.110	
<i>Prevotella</i>	2.1 ± 4.4	0.8 ± 3.0	0.115	
<i>Porphyromonadaceae</i>	0.8 ± 1.4	1.6 ± 2.2	0.177	
<i>Parabacteroides</i>	1.4 ± 2.2	1.5 ± 2.3	0.217	
VERRUCOMICROBIA	6.8 ± 14.7	9.4 ± 10.1	0.056	
<i>Verrucomicrobiaceae</i>	6.8 ± 14.7	9.4 ± 10.1	0.056	
<i>Akkermansia</i>	6.8 ± 14.7	9.4 ± 10.1	0.056	
PROTEOBACTERIA	1.2 ± 1.5	2.1 ± 2.1	0.061	
<i>Enterobacteriaceae</i>	1.0 ± 1.5	1.5 ± 2.2	0.358	
<i>Escherichia</i>	0.8 ± 1.2	1.3 ± 2.2	0.263	
ACTINOBACTERIA	1.6 ± 2.2	1.1 ± 1.9	0.621	
<i>Bifidobacteriaceae</i>	1.4 ± 2.2	1.0 ± 1.9	0.724	
<i>Bifidobacterium</i>	1.4 ± 2.2	1.1 ± 1.9	0.724	

4.1.1.4 Microbiota profiling in *D. melanogaster* CBP mutants

Microbiota analysis was performed on *nej^{+/-}* and *yw* flies as control (five replicates were done, each one made of three dissected guts, for a total of 15 flies per groups used), since homozygous CBP mutants did not reach adulthood. Analysis of alpha and beta diversity (figure 4.11) showed respectively a significative enrichment of less abundant species in *nej* compared to *yw* flies according to Chao1 index ($p = 0.005$) (figure 4.11A), and a clear discernment within mutants and wild type files microbiota (both rare and abundant species were considered) as resulted from unweighted UniFrac distance ($p = 0.007$) (figure 4.11B).

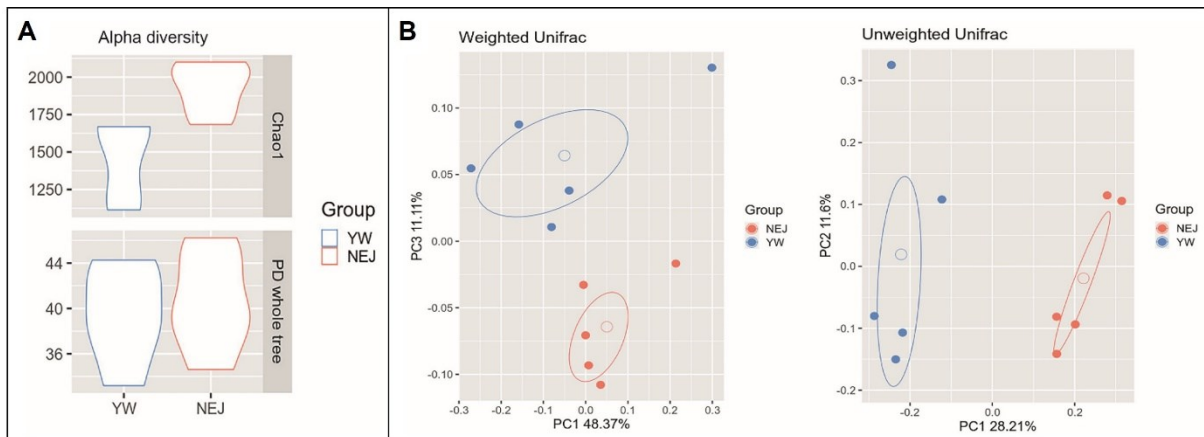


Figure 4.11. Alpha and beta diversity in *nej*^{+/-} microbiota compared to *yw* flies. A) Violin plot of alpha-diversity showing significant difference in term of Chao1 biodiversity values, while according to PD whole tree metric any difference was found between the two groups ($p = 0.668$). B) Beta-diversity represented by PCoA showed statistical differences in unweighted Unifrac distances of microbial communities and no difference in weighted values ($p = 0.216$), calculated by *Adonis* test ($p < 0.05$ considered significant). Adapted from “Di Fede et al., 2021” (see Appendix 1).

Indeed, we observed an increased relative abundance of Firmicutes phylum and *Lactobacillaceae* family in *nej* flies (64.7% and 58.8% respectively) compared to wild type animals (53.9% and 7.5% respectively), and concurrently a decreased in Proteobacteria and *Enterococcaceae* in mutants (31.6% and 0.2%) compared to *yw* flies (41.1% and 12.9%) (figure 4.12).

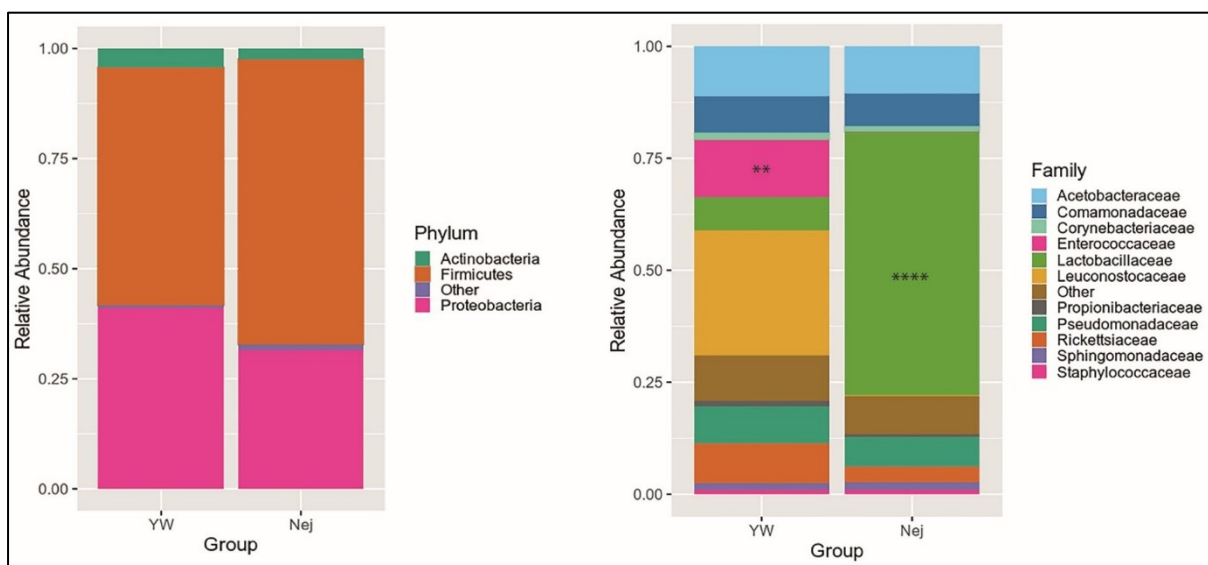


Figure 4.12. Microbial composition in *yw* and *nej* flies. Relative abundances were shown at phylum and family levels, with significant *Lactobacillaceae* and *Enterococcaceae*

abundances ($p = 0.0000254$ and $p = 0.00784$ respectively); “Other” represented taxa which were present with a frequency $< 1\%$. P value < 0.05 were considered significant (** $p < 0.01$; **** $p < 0.001$). Adapted from “Di Fede et al., 2021” (see Appendix 1).

4.1.2 NGS approach on RSTS patients without a molecular diagnosis

4.1.2.1 Genotype-phenotype correlation for KMT2A variants identified in six RSTS patients

We found six novel heterozygous variants in Lysin methyl transferase 2A (*KMT2A*) gene in six patients (5/30 tested by multi gene panel sequencing and 1/10 analyzed by WES with initial diagnosis of RSTS (table 4.3)). In particular, patients #208 and #250 were found to be carriers of two different mutations in exon 3, a nucleotide substitution (c.553C>T) and a 21 nucleotides insertion (c.1697_1717dup), respectively. The first was predicted to cause a premature stop codon p.(R185*), the second an aminoacidic in frame duplication p.(L566_L572dup). Three different variants in exon 6 were identified in patients #187, #251 and #243: a single nucleotide change (c.3596G>A) and two deletions (c.3603del and c.3632_3634+2del) which were predicted to cause a premature stop codon p.(W1199*), a frameshift p.(S1202Pfs*12) and incorrect splicing respectively. Finally, a four nucleotides duplication in exon 7 (c.3897_3900dup), leading to a frameshift p.(L1303Sfs24*) was found in patient #221. All the variants here described were *de novo*, except for patients #250 and #221, whose parents were not available.

Table 4.3. *KMT2A* pathogenic variants detected in the described patients. Position (at genomic, gene and protein level) and inheritance of the pathogenic variants were indicated.

Pt	Position	Exon	Nucleotide change	Protein change	Inheritance
RSTS-208	chr11:118342427	3	c.553C>T	p.(R185*)	<i>de novo</i>
RSTS-250	chr11:118343566	3	c.1697_1717dup	p.(L566_L572dup)	NA (unavailable parents)
RSTS-187	chr11:118350915	6	c.3596G>A	p.(W1199*)	<i>de novo</i>
RSTS-251	chr11:118350921	6	c.3603del	p.(S1202Pfs*12)	<i>de novo</i>
RSTS-243	chr11:118350948	6	c.3632_3634+2del	p.?	<i>de novo</i>
RSTS-221	chr11:118352691	7	c.3897_3900dup	p.(L1303Sfs24*)	NA (adopted child)

According to ACMG criteria (Richards et al., 2015), variants found in patients #208, #187, #251, #243 were considered pathogenic (PVS1, PM2, PP3), in patient #221 likely

pathogenetic (PVS1, PM2), while the one found in patient #250 was classified as a variant of uncertain significance (VUS) (PM2, PM4, BP4) probably considering the unknown impact on gene product.

Patients were also clinically re-evaluated and table 4.4 summarizes the clinical features of the six patients here described (three of them represented in figure 4.13), comparing the clinical signs of each patient to the typical features of RSTS and Wiedemann-Steiner (WDSTS, OMIM #605130), the chromatinopathy known to be caused by mutations in *KMT2A*. RSTS and WDSTS shares many phenotypic features such as ID, growth delay and peculiar dysmorphisms, also evident in our patients after the clinical re-evaluation. For instance, all our patients here described showed RSTS typical signs such as columella (6/6), broad thumbs and hallux (4/6 and 5/6 respectively), ptosis (4/6) and features mainly associated to WDSTS such as narrow palpebral fissures (5/6), wide nasal tip (4/6) and hirsutism (3/6) (figure 4.13).

Table 4.4. *KMT2A* pathogenic variants and phenotypic signs of the six described patients compared to the clinical features associated to RSTS and WDSTS.

Clinical signs were reported as NA (not assessed), + (present, >30%), – (absent or unreported) and +/- (present in few cases, 5-30%).

	RSTS	WDSTS	RSTS-208	RSTS-250	RSTS-187	RSTS-251	RSTS-243	RSTS-221
<i>KMT2A</i> pathogenic variant NG_027813.1 (NM_001197104.2)			c.553C>T p.(R185*)	c.1697_1717dup p.(L566_L572dup)	c.3596G>A p.(W1199*)	c.3603del p.(S1202Pfs*12)	c.3632_3634+2del p.?	c.3897_3900dup p.(L1303Sfs24*)
Date of birth			22/10/2006	17/09/2003	01/01/2002	16/07/1994	20/07/1993	12/07/2010
Sex			M	M	M	F	M	M
Dysmorphisms								
Long eyelashes	89% +	81% +	+	+	+	+	+	+
Synophrys	5-30% +/-	>30% +	-	-	+	-	+	+
Ptosis	<82% +	31% +	+	+	-	+	+	-
Downslanting palpebral fissures	75% +	64% +	+	+	-	-	+	+
Thick eyebrows	>30% +	64% +	+	-	+	+/-	+	-
Narrow palpebral fissures	-	74% +	+	+	-	+	+	+
Hypertelorism	5% +/-	71% +	+	-	telecanthus	+	telecanthus	+
Columella below the alae nasi	89% +	-	+	+	+/-	+	NA	+

Wide nasal bridge	-	68% +	+	+	-	+	+	-
Grimacing smile	80% +	-	+	-	+/-	-	NA	+
High-arched palate	75% +	>30% +	+	NA	NA	-	+	+
Micrognathia	57% +	>30% +	-	+	-	-	+	+
Low set ears	>30% +	46% +	+	+	+/-	-	-	-
Strabismus	60-71% +	-	-	-	-	-	+	-
Flammeus nevus/angioma	5-30% +/-	-	-	NA	-	-	-	NA
Growth failure								
IUGR	-	>30% +	-	-	-	NA	-	unknown
PNGR	73% +	38% +	+	-	+/-	NA	+	+
Intellectual disability	98% +	98% +	+++	++	+	+	+	+++
Speech delay/absence	90% +	82% +	-	+	+	+	+	+
Behavioral problems	41% +	42% +	+	+	+		++	NA
Vision problems								
Myopia	9% +/-	-	-	-	-	NA	-	-
Teeth anomalies	>30% +	-	-	-	NA	NA	+	-

Musculoskeletal anomalies								
Broad thumbs	91% +	-	-	+	+/-	-	+	+
Angulated thumbs	42% +	-	+	-	-	-	-	+
Broad halluces	92% +	-	+	+	+	-	+	+
Clinodactyly	5-30% +/-	23% +/-	-	-	-	-	+	-
Brachydactyly	5-30% +/-	45% +	-	-	-	-	-	+
Microcephaly	63% +	-	-	+ (relative)	-	NA	-	+
Delayed bone age	74% +	34% +	-	NA	-	NA	-	-
Hypotonia	70% +	73% +	-	NA	-	NA	+	+
Organ anomalies								
Cryptorchidism	78-100% +	-	-	-	-	-	-	mobile testis
Heart defect	24-38% +/-	29% +/-	-	-	-	-	-	-
Brain anomalies								
Abnormal corpus callosum	17% +/-	14% +/-	-	NA	-	NA	-	-
Seizures	25% +/-	9% +/-	-	NA	-	-	-	-
Hirsutism	>30% +	>30% +	-	-	+	NA	+	+

Keloids/naevi	24% +/-	-	-	NA	-	-	-	-
Pilomatrixoma	5-30% +/-	-	-	NA	-	-	-	-
Frequent infections	75% +	-	-	NA	-	NA	-	-
Feeding problems	80% +	53% +	-	NA	-	NA	+	+
Gastroesophageal reflux	68% +	-	-	NA	+	NA	-	-
Others			Prominent eyes; thin upper lip; C2-C3 vertebral fusion; cerebellar vermis hypoplasia; organomegaly	thin upper lip; autism spectrum disorder; epileptiform abnormalities in the left fronto-temporal region	early puberty (treated)	thin lips	thin lips; hearing loss; altered fine motor abilities; born at 35 weeks; pregnancy with a threatened miscarriage	thin lips; kyphosis; abnormal ears

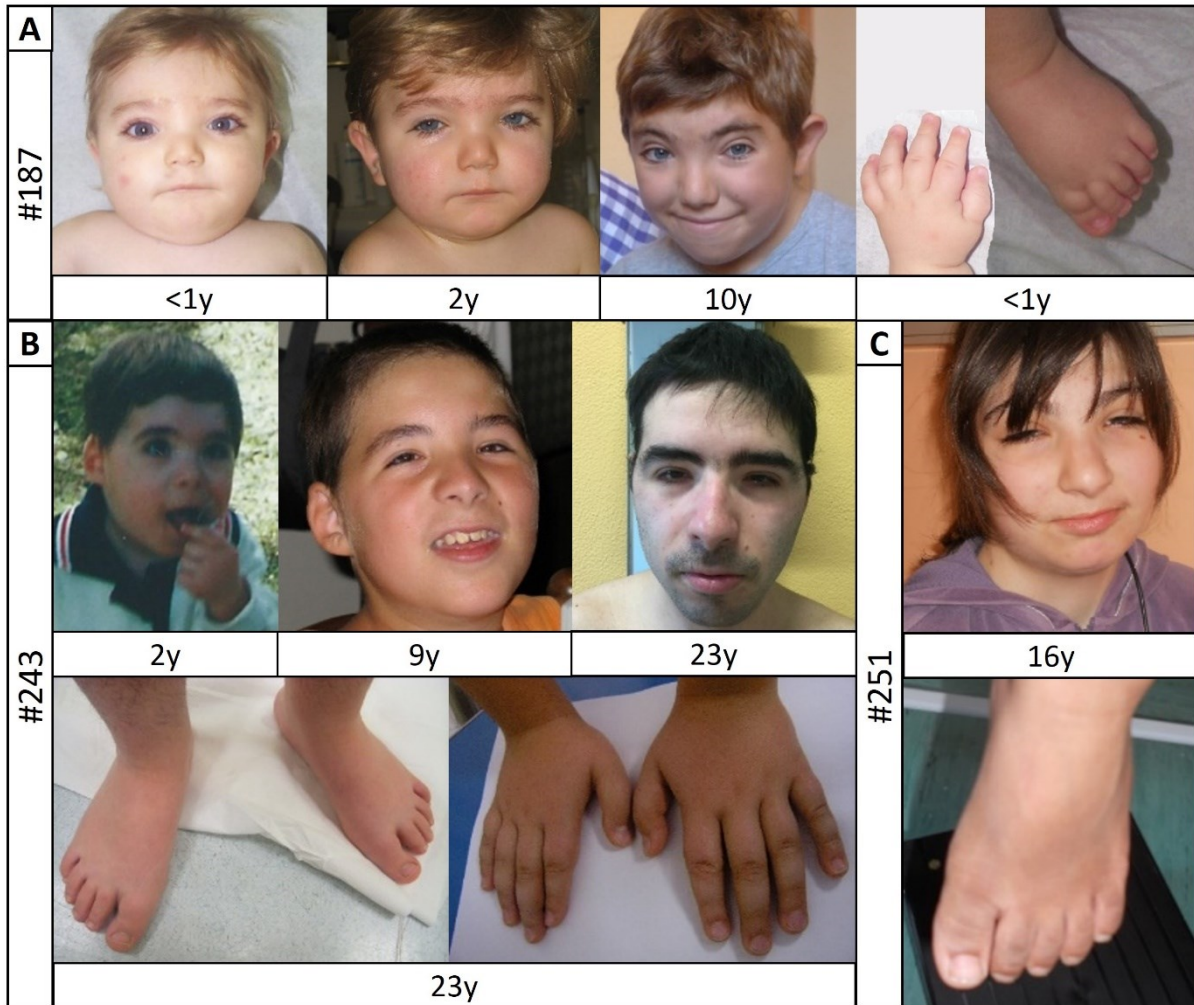


Figure 4.13. Phenotypic features of patients #187, #243 and #251 with *KMT2A* variants. Facies of A) patient #187 in neonatal period with particular of hand and foot, at 2 and 10 years, B) patient #243 at 2, at 9 and 23 years with details of hands/feet and C) patient #251 at 16 years with particular of one foot. Adapted from “Di Fede et al., 2020” (see Appendix 1).

4.1.2.2 Characterization of a *HDAC2* variant identified in one *RSTS* patient

Among nine patients with initial diagnosis of *RSTS* but negative for known causative genes, we found by WES one patient (#249) carrier of a *de novo* pathogenetic variant in *HDAC2*. The patient displayed some *RSTS* features such as ID, growth delay, peculiar dysmorphisms, broad halluces, speech and feeding problems and recurrent infections. From trio blood and patient saliva samples we found a deletion of four nucleotides (c.1330_1333del) which was predicted to cause the frameshift p.(K444Lfs*61) and affect the nuclear localization signal (NLS) of the protein. For this reason, we performed immunocytochemistry on LCLs derived from patient

and HD to investigate HDAC2 intracellular presence (figure 4.14). After setting up five degrees of nuclear localization (from degree 4 to degree 0) as illustrated in figure 4.14B, we observed a mis-localization of HDAC2 in patient #249 compared to HD LCLs (figure 4.14A and 4.14C). Degree 0-2 resulted significantly frequent in patient LCL compared to HD LCLs ($p < 0.05$ for degree 0, $p < 0.001$ for degree 1 and $p < 0.01$ for degree 2), meaning that HDAC2 nuclear presence in #249 LCL was poorer than in controls (figure 4.14C).

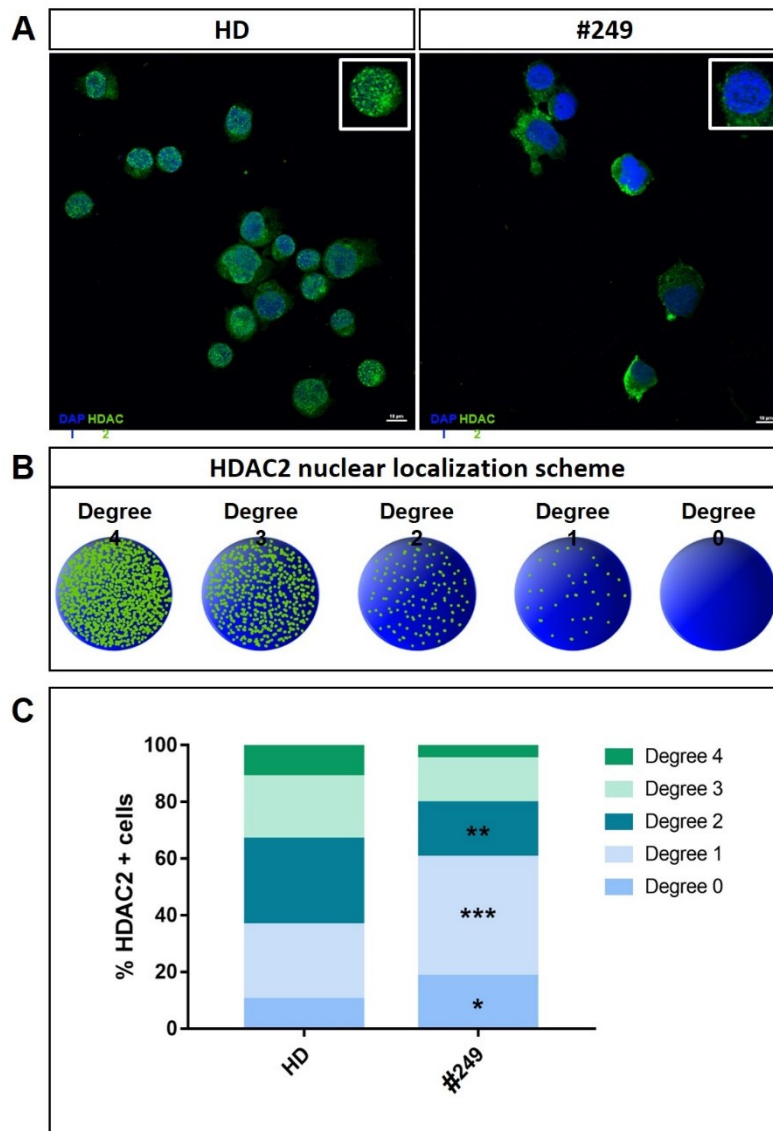


Figure 4.14. HDAC2 localization in patient derived lymphoblastoid cell line (LCL). A) 60x confocal images showing an example of HDAC2 immunocytochemistry on HD LCL and patient LCL (#249); HDAC2 is marked with green signal and nuclei with blue (DAPI); Insets show cell magnification of degree 4 (in HD box) and degree 0 (in #249 box) of HDAC2 nuclear localization. B) Schematic representation of degrees set for evaluation of HDAC2 presence in nucleus, from most abundant (Degree 4) to absent (Degree 0). C) Frequency

of HDAC2 positive cells (% HDAC2+ cells, on Y-axis) into the five degrees of nuclear localization (in shapes from green for Degree 4 to blue for Degree 0) observed in patient (#249) and HD LCLs (on X-axis); multiple *t*-tests were used as statistical method (* $p < 0.05$; ** $p < 0.01$; *** $p < 0.001$).

In addition, to assess whether the newly identified variant in *HDAC2* affects epigenetic functions, we performed AlphaLISA assay on #249 LCLs. We compared their histone acetylation levels (H3K27Ac) with the ones detected in LCLs derived from HD and RSTS patients with mutation in the major gene *CREBBP* (figure 4.15). We found significant difference in acetylation pattern among the three groups ($p < 0.01$) (figure 4.15A) and, in details, we observed higher H3K27Ac in LCL of our patient with *HDAC2* mutation than in LCLs derived from either HD ($p < 0.05$) or RSTS patients ($p < 0.001$) (figure 4.15B).

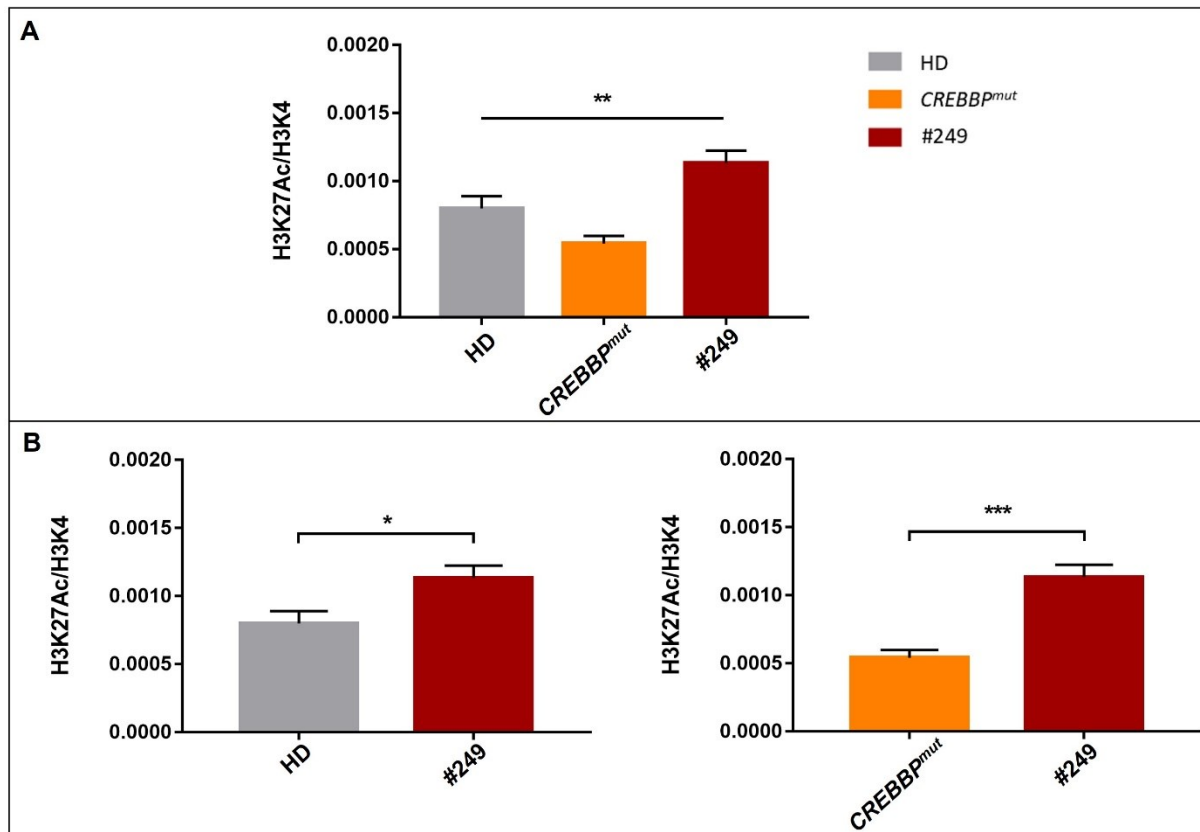


Figure 4.15. Histone acetylation in patient #249 LCLs. Acetylation of lysin 27 of histone 3 (H3K27Ac) normalized on unmodified lysin 4 of histone 3 (H3K4) (H3k27Ac/H3K4, on Y-axis) in LCLs derived from healthy donors (HD, grey bar), three RSTS patients with mutation in *CREBBP* (*CREBBP*^{mut}, orange bar) and patient #249 (red bar) (on X-axis), assessed by AlphaLISA assay. A) Means of histone acetylation values of the three groups, whose variance was compared using one-way ANOVA, and B) insight on acetylation

pattern of patient #249 with *HDAC2* pathogenetic variant compared with HD (on the left) and RSTS patients with *CREBBP* mutations (on the right) (Student's *t*-test was used as statistical method) (* $p < 0.05$; ** $p < 0.01$; *** $p < 0.001$).

4.2 EXPANDING RETT SYNDROME LANDSCAPE

4.2.1 Identification of candidate genes from a WES study in Rett-like patients

We performed WES trio analysis on three patients (except for patient #2 for whom only the father was tested) who attended the RTT Clinic at the Child and Adolescent Neuro-Psychiatry Unit of ASST Santi Paolo Carlo Hospital (University of Milan, Italy). They displayed phenotypic features resembling Rett syndrome but were found negative for mutations in known causative gene (*MECP2*) or genes causing known variant forms (*CDKL5* and *FOXG1*), therefore they underwent to NGS approach.

4.2.1.1 Clinical presentation of three Rett-like patients

In detail, patient #1 was a 28-year-old female, born to non-consanguineous parents after an uneventful pregnancy, with birth measurements around the 50th percentile. Her development was normal until age 24 months (mos) when she showed psychomotor regression. She displayed monthly generalized epilepsy with onset at age 4 years (yrs), severe ID, absent speech, hands stereotypies, sleep problems, occurrences of apnea and hyperventilation, moderate scoliosis since age 15 yrs, constipation, growth parameters below the average at the time of the last evaluation and normal magnetic resonance imaging (MRI).

Patient #2 was a 52-year-old woman, born to unrelated parents after regular pregnancy and with an average body weight. After a normal development at 4 mos she presented febrile clonic seizures subsequently to vaccine administration, which were partially controlled with Phenobarbital. During the first years of life, she displayed an epileptic and developmental encephalopathy with daily frequent multiple seizure types (tonic, tonic-clonic and clonic seizures) whose attempt to treat with anti-seizure medications (ASMs) failed. In addition, she showed sporadic status epilepticus which was resolved with Phenytoin. After seizure onset she displayed global developmental delay, gait difficulties, limited speech, severe ID, microcephaly, spastic quadriplegia, gastro-esophageal reflux disease (GERD), severe constipation and hands stereotypies. Pachygyria and a global slowing of cerebral activity were observed from brain MRI and interictal EEG respectively.

The third patient (#3) was a 27-year-old woman born by caesarean section from non-consanguineous parents. From 3 mos a global developmental delay was observed, and she displayed drug resistant generalized tonic and tonic-clonic seizures, except from age 4 to 9 yrs, which could not be controlled by antiepileptic drugs (AEDs) or vagal nerve stimulation (VNS). She had severe ID, incapability to walk autonomously, hands stereotypies starting from age 2 yrs, spastic tetraplegia in adulthood and limited speech. From brain MRI emerged nonspecific abnormalities in the white matter and from EEG a diffusely slow background activity. The patient was affected by several respiratory infections and unfortunately recently passed away due to cardiac arrest.

Interestingly these three patients displayed clinical signs shared with Rett syndrome, summarized in table 4.5, such as severe ID, developmental delay, presence of seizures, stereotypies, speech and sleep problems.

Table 4.5. Summarized WES results and phenotypic features of the three Rett-like patients negative for mutations in RTT known causative genes.

	Patient #1	Patient #2	Patient #3
Gene	<i>NBEA</i>	<i>DYNC1H1</i>	<i>SLC35F1</i>
Nucleotide change	c.3221T>C c.7687C>T	c.10031G>A	c.1037T>C
Protein change	p.(M1074T) p.(R2563W)	p.(R3344Q)	p.(I346T)
Age	28 yrs	52 yrs	27 yrs
Sex	Female	Female	Female
ID	Severe	Severe	Severe
Developmental delay	Present	Present	Present
Seizures	Monthly generalized	Epileptic encephalopathy	Generalized and drug resistant
Stereotypies	Hands	Hands	Hands
Speech	Absent	Limited	Limited
Sleep problems	Present	Present	Present
MRI	Normal	Pachygyria	Nonspecific abnormalities in white matter

4.2.1.2 Variants identification and genotype-phenotype correlation

In patient #1 we identified two novel variants in *NBEA* gene: c.3221T>C and c.7687C>T, inherited from the mother and the father, respectively. The patient resulted compound heterozygote for these two missense variants which were predicted to cause the protein changes p.(M1074T) and p.(R2563W) respectively (table 4.5). *NBEA*, located at chromosome 13q13.3, encodes for neurobeachin, family member of the BEACH domain containing proteins, expressed in the brain and important for vesicle trafficking due to its scaffold functions. Interestingly, mutations in this gene are associated to a class of neurodevelopmental disorders (NDDs) displaying an early generalized epilepsy (Mulhern et al., 2018).

A *de novo* missense variant was found in patient #2 in *DYNC1H1* (Poirier et al., 2013) (table 4.5), located at chromosome 14q32.31 and coding for a subunit of the cytoplasmatic dynein, the main retrograde microtubule-based motor of the cell. Remarkably, diagnosis of *DYNC1H1*-NDDs is consistent with the clinical and molecular features displayed by our patient, having ID, peculiar CNS malformations and the pathogenetic variant located in the dynein motor domain (Poirier et al., 2013). Indeed, the mutation affects the microtubule-binding domain (MTBD) and consequently prevents dynein movements (Hoang et al., 2017).

In the end, patient #3 resulted heterozygous for a *de novo* and unreported missense variant in *SLC35F1* gene (table 4.5), predicted to be damaging and likely pathogenetic (PS2, PM2, PP3) according to prediction tools and ACMG guidelines. Interestingly, microdeletions involving a portion of chromosome 6 where *SLC35F1* maps, were recently associated to pediatric epilepsy (Szafranski et al., 2015), as reported for our patient.

4.2.2 Exploring the role of SLC35F1

4.2.2.1 SLC35F1 cellular localization

SLC35F1 has 8 exons and encodes for the F1 member of the solute carrier family 35, a transmembrane protein mainly expressed in the brain and a putative nucleoside sugar transporter, although its role currently needs to be elucidated. Thus, in order to characterize this protein, we generated *SLC35F1* KO lines by CRISPR/Cas9 genome editing using two sgRNAs targeting exon 2 and 7 in order to induce a macrodeletion and cause the absence of the protein product (figure 4.16A).

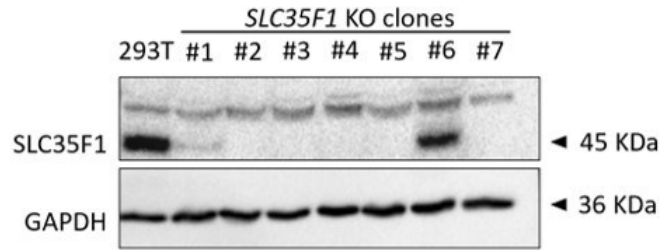


Figure 4.16. Screening of SLC35F1 KO clones. Western blot of SLC35F1 on lysates from KO clones (#1-7) compared to 293T cells, normalized on GAPDH expression.

In parallel we performed immunocytochemistry on 293T and KO cell lines (figure 4.17A) and 293T lysates fractionation (figure 4.17B) to define SLC35F1 cellular localization. Both assays showed the protein having a mainly cytoplasmatic compartmentalization, particularly interesting with the appearance of more brilliant protein dots just outside the nucleus (figure 4.17A).

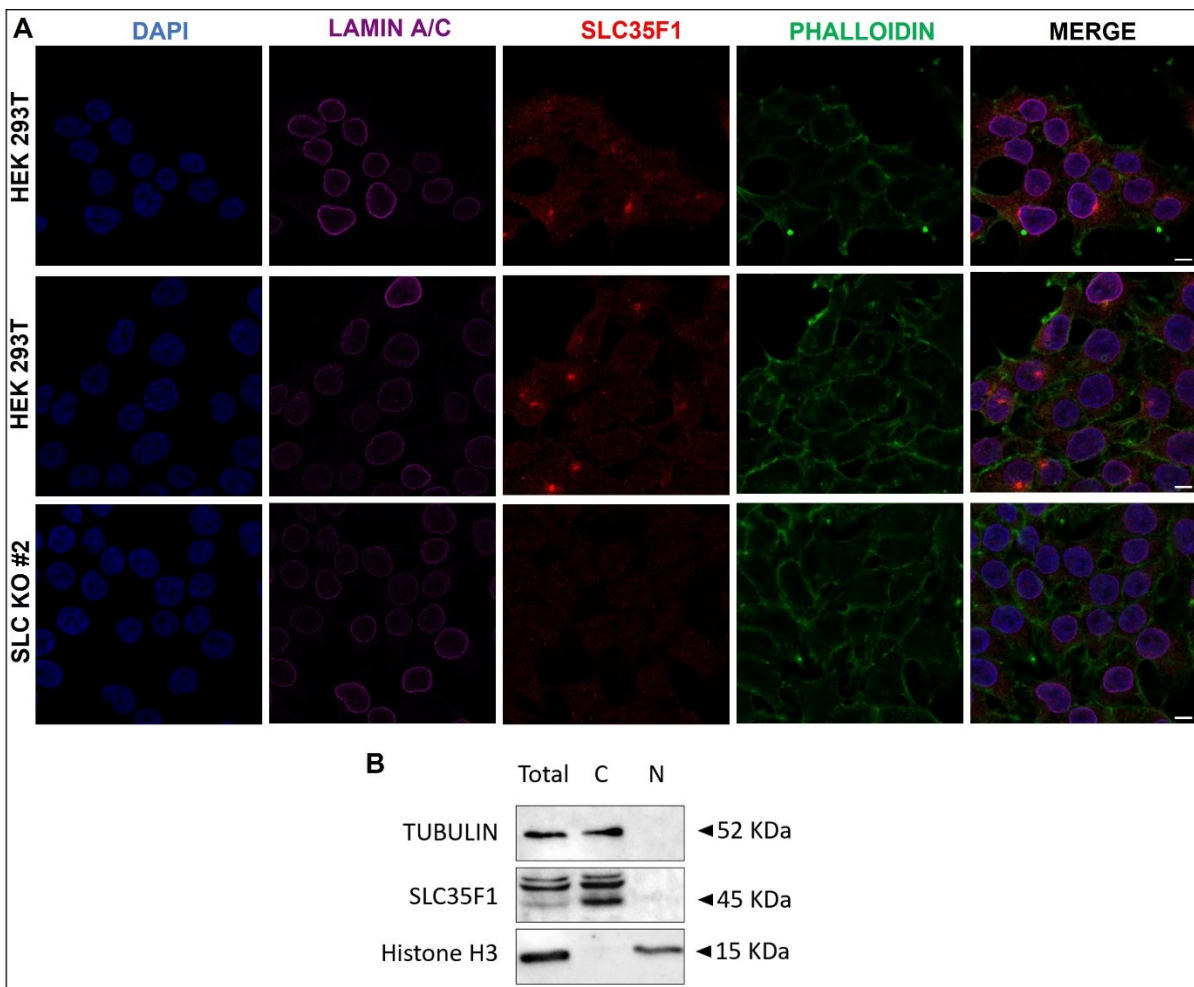


Figure 4.17. Cellular localization of SLC35F1 in 293T cells. A) SLC35F1 localization in two 293T replicates and KO clone #2 used as a negative control; cells were stained with DAPI

(blue), Lamin A/C (magenta), SLC35F1 (red), phalloidin (green) and acquired at confocal microscope with 60x magnification. B) Western blot of SLC35F1 protein (45 kDa) in 293T lysate fractionation (total, C = cytoplasmic fraction, N = nuclear fraction) compared to tubulin (52 kDa) and histone H3 (15 kDa).

4.2.2.2 SLC35F1 interactome

To identify interactors of SLC35F1, we collected lysates from 293T cells and KO line as a control, we performed an IP for the endogenous SLC35F1 (two biological replicates for each line), which was checked by western blot as shown by figure 4.18, and after samples preparation by Ingel digestion, proteomic analysis was performed by mass spectrometry (LC-MS/MS).

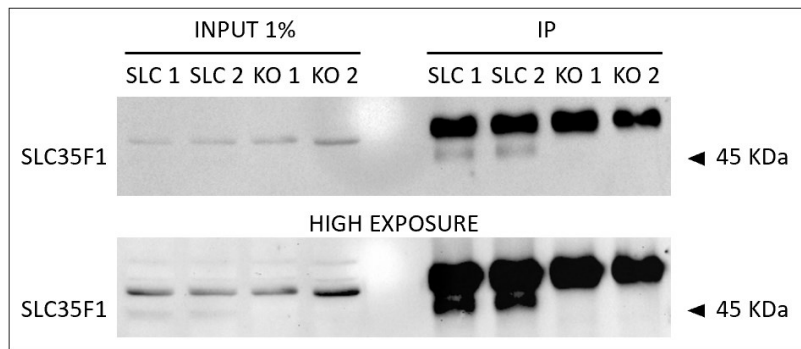


Figure 4.18. SLC35F1 IP check by western blot. Western blot performed on input (1%) and SLC35F1 IP of 293T samples (SLC 1 and SLC 2) and KO lines (KO 1 and KO2) used as a control, acquired at normal (upper image) and higher exposure (bottom image).

Differences in proteome abundance were observed by scatter plot (figure 4.19) comparing control (KO) and 293T cells. 371 proteins were identified, the proteomic analysis revealed 52 differentially expressed proteins with $p < 0.05$ and Gene Ontology (GO) analysis of these proteins showed an enrichment of proteins mostly involved in ATP-dependent activity and rRNA binding (table 4.6).

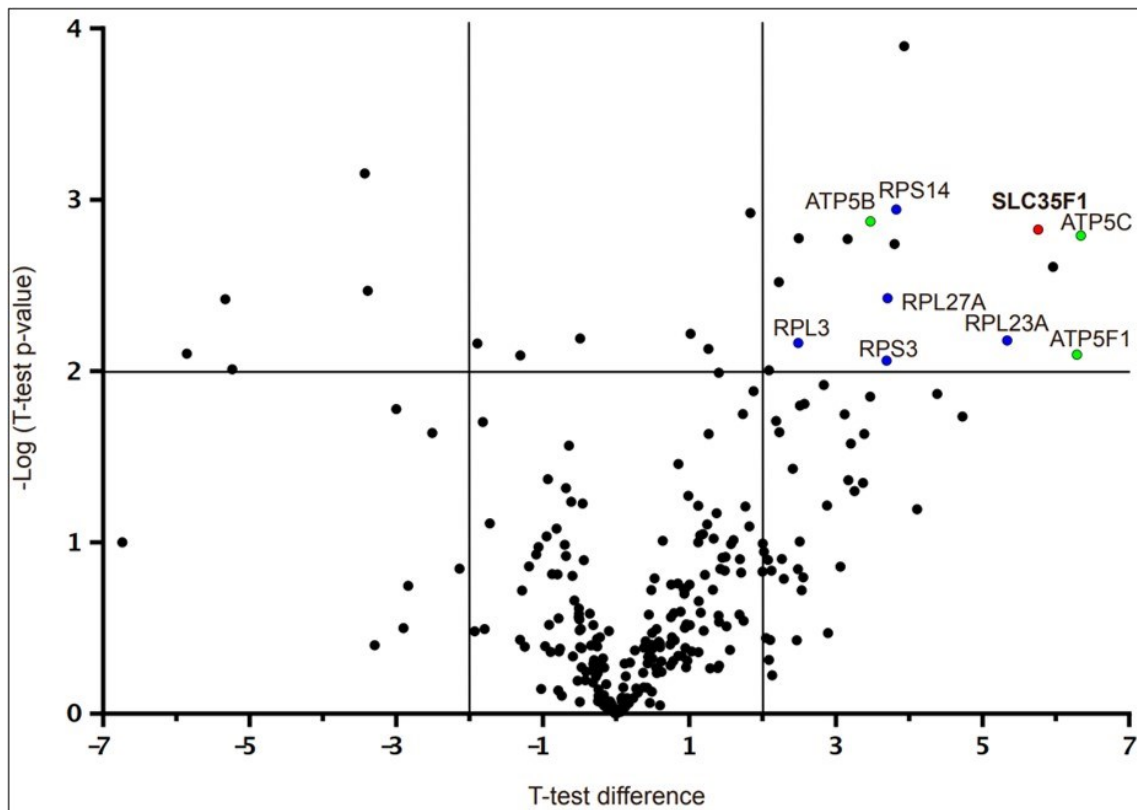


Figure 4.19. Scatter plot of endogenous SLC35F1 IP MS data on 293T and KO samples. Colored dots correspond to the bait (SLC35F1 in red) and to most significant interactors (in blue ribosomal proteins, in green ATP synthase subunits).

Table 4.6. List of the top GO molecular functions enriched in differentially expressed proteins resulted from proteomic analysis.

GO ID	GO TERM	P-VALUE	FROM INPUT
GO:0005198	structural molecule activity	1.068E-18	26/52
GO:0003735	structural constituent of ribosome	1.143E-15	14/52
GO:0019843	rRNA binding	1.362E-15	11/52
GO:0140657	ATP-dependent activity	5.615E-8	13/52
GO:0046933	proton-transporting ATP synthase activity, rotational mechanism	3.026E-7	4/52
GO:0015078	proton transmembrane transporter activity	6.494E-7	7/52
GO:0030527	structural constituent of chromatin	9.366E-7	6/52
GO:0015252	proton channel activity	1.230E-6	4/52
GO:0070181	small ribosomal subunit rRNA binding	3.890E-6	3/52
GO:0005200	structural constituent of cytoskeleton	4.095E-6	6/52

5. DISCUSSION

5.1 HDACi such as short chain fatty acids (SCFAs) could represent an epigenetic treatment for Rubinstein-Taybi syndrome (RSTS)

Nowadays therapeutic options for RSTS patients forecast surgical interventions for malformations, prevention of comorbidities or behavioral support. As a future therapeutic approach, it is though interesting to explore the acetylation modulation, since RSTS patients show an imbalance in acetylation and HDACi are well-known and already used for neurological disorders (Cobos et al., 2019). In this work we indeed investigated the effect of exogenous and endogenous HDACi in different experimental models, focusing on SCFAs active in HDAC inhibition.

In our RSTS *in vitro* model, RSTS cell lines showed a general boost in histone acetylation levels upon exogenous HDACi exposure (figure 4.1). Importantly, albeit HDACi can induce dose-dependent apoptosis (De Schutter and Nuyts, 2009; Yuan et al., 2019) we did not observe a significant correlation of HDACi-induced acetylation with neither cell proliferation nor cell death (figure 4.3-4.6). These findings show that HDACi treatments in RSTS cells are effective in modulating the acetylation pattern without notable impact on cell viability at sub-toxic concentrations. Interestingly, exposure to these exogenous compounds led to a patient-specific response variability (figure 4.2) which could address the study of this rare disorder to the field of personalized medicine.

In parallel, studies on *Drosophila* model highlighted the role of CBP in signaling pathways fundamental for embryogenesis (figure 4.7) (Akimaru et al., 1997b; Tanaka et al., 1997). Since we observed the HDAC inhibitors response *in vitro*, we investigated their effect *in vivo*, feeding parental fruit flies with these compounds. Strikingly, we observed a partial rescue of embryonic development and pattern in F1 generation embryos upon valproic acid (VPA) or sodium butyrate (NaB) supplement, thus implying that dietary modulation by administration of epigenetic treatments could improve RSTS phenotype *in vivo* (figure 4.7 and 4.8).

Among the exogenous HDACi tested, NaB is also a well-known short chain fatty acid (SCFA) produced by commensal gut microbial community (Davie, 2003). This evidence led us investigating the relationship between endogenous HDACi and RSTS microbiota. Thus, after performing microbiota profiling of RSTS patients and their healthy siblings, we did not observed differences in nutrients intake (especially dietary fibers which are substrates for

SCFA production) and alpha-diversity, while beta-diversity showed significant changes between the two groups (table 4.1 and figure 4.9). In details, a depletion of SCFAs-producing bacteria (*Faecalibacterium* genus) was observed in RSTS microbiota (figure 4.10 and table 4.2), consistent with the low abundance of this genus characterizing other neurodevelopmental disorders (e.g. autism spectrum disorder, Rett and Down syndrome) (Borghi and Vignoli, 2019; Louis and Flint, 2009).

Exploiting the heterozygous CBP mutant flies, we explored the existence of microbiota differences also in the *in vivo* model comparing *nej^{+/-}* to wild type flies. Despite the species-specificity and the few genera composing *Drosophila* microbiota due to the absence of an anoxic compartment in their gut, among the taxa identified we observed significant changes in abundances involving Firmicutes (*Lactobacillaceae* family) and Proteobacteria (*Enterococcaceae* family) (figure 4.12). Interestingly, the alteration of these genera is associated to changes in behavior, gut homeostasis, and growth (Fast et al., 2018; Sharon et al., 2010; Shin et al., 2011) and these findings suggest that microbiota-host interaction studied in RSTS patients could be shaped in *D. melanogaster*.

It is known that epigenetic modifications (i.e. methylation and acetylation) can be regulated by microbiota in a diet-dependent manner (Krautkramer et al., 2016) and HDACi administration in term of nutritional approach was already used in several diseases, from epilepsy to cancer (Chang et al., 2015; Shingler et al., 2019). Recently this approach was explored also for a chromatinopathy which shares some features with RSTS: in a mouse model of Kabuki syndrome (OMIM #147920, #300867) a ketogenic diet led to HDACi production ameliorating neurological activity and behavior (Benjamin et al., 2017).

In our study we investigated HDACi effects in a RSTS *Drosophila* model, however the reproductive nature of these animals should be considered. Indeed, in this case the HDACi administration was possible before birth since they are oviparous animals, while for mammals a therapeutic intervention should be explored postnatally when the CNS development is ongoing, as maternal HDACi can affect embryogenesis crossing the placenta.

5.2 RSTS genotype-phenotype correlation for novel variants identified in a known chromatinopathy gene (*KMT2A*)

In six clinically diagnosed RSTS patients negative for mutations in *CREBBP* or *EP300* we found six unreported variants in *KMT2A* gene by NGS-based genes panel and WES analysis. Among

these variants, 5/6 resulted likely pathogenetic or pathogenetic and 4/6 were *de novo* (parents of two patients were unavailable). Interestingly, *KMT2A* is another writer of the epigenetic machinery, encoding for a protein that favors the opening of the chromatin, as CBP and p300 do. Nevertheless, this gene is also associated to another chromatinopathy, the Wiedemann-Steiner syndrome (WDSTS, OMIM #605130), described for the first time in 1989 by Wiedemann (Wiedemann et al., 1989) and characterized by hypertrichosis *cubiti*, intellectual disability (ID) and developmental delay, a distinctive facial appearance and short stature (Jones et al., 2012). In our patients typical RSTS signs were more marked in childhood, but also WDSTS specific features were present, which complicated the diagnosis and made a clinical reevaluation indispensable. Indeed, although these syndromes display peculiar phenotypic signs, WDSTS shares with RSTS some clinical features such as growth retardation, ID, limb abnormalities and specific dysmorphisms (table 4.4 and figure 4.13). According to this work and previous ones, in which *KMT2A* variants were identified in patients clinically diagnosed with Coffin-Siris (CSS, OMIM #135900, #614608, #614607, #614609, #616938, #615866, #617808, #618362, #618027, #618506), Cornelia de Lange (CdLS, OMIM #122470, #300590, #610759, #614701, #300882), Kabuki (KS, OMIM #147920, #300867) and Rubinstein-Taybi syndromes (Bramswig et al., 2015; Negri et al., 2019; Parenti et al., 2017; Sobreira et al., 2017; Yuan et al., 2015), pathogenic variants in a same “epi-gene” could be responsible for overlapping and/or slightly different clinical presentation cases. This significant phenotypic overlap among chromatinopathies likely reflects the interconnected pathways involved in the complex regulation of balance between open and closed chromatin (Fahrner and Bjornsson, 2019; Kleefstra et al., 2014).

5.3 Characterization of a pathogenetic variant found in a new chromatinopathy-related gene (*HDAC2*) in a RSTS patient

We identified by WES a *de novo* and unreported pathogenetic variant in *HDAC2* gene (NM_001527.4: c.1330_1333del; p.K444Lfs*61) in another patient clinically diagnosed with RSTS but not carrying mutations in known causative genes. *HDAC2* encodes for a class I histone deacetylase mainly localized into the nucleus and often found in protein complexes involved in transcriptional regulation (You et al., 2001). Characterizing this variant in LCLs derived from the patient, we found that it caused a protein nuclear mis-localization (figure 4.14), in line with prediction tools since the variant affected nuclear localization signal, and

increased acetylation levels in patient LCLs compared to HD and to LCLs derived from patients with *CREBBP* mutations (figure 4.15).

To date, are known three neurodevelopmental disorders caused by mutations in genes encoding for HDACs. Deletions at chromosome localization 2q37 or point mutations in *HDAC4* gene are causative of Brachydactyly mental retardation syndrome (BDMR, OMIM #600430) (Villavicencio-Lorini et al., 2013; Williams et al., 2010), *HDAC6* is reported as causative gene of Chondrodysplasia with platyspondyly, distinctive brachydactyly, hydrocephaly and microphthalmia (OMIM #300863) (Simon et al., 2010), and pathogenetic variants in *HDAC8* are causative of Cornelia de Lange syndrome 5 (CdLS5, OMIM #300882) (Deardorff et al., 2012).

Currently, any syndrome is associated to *HDAC2* mutations and, so far, only other two heterozygous *de novo* variants in *HDAC2* were reported: c.83G>A and c.93G>A (NM_001527.3) predicted to cause respectively the substitutions p.(G28D) and p.(M31I) (Martínez et al., 2017; Wagner et al., 2019). Both were missense variants affecting the histone deacetylase domain and thus likely pathogenetic. The first mutation was identified in a patient belonging to a syndromic intellectual disability cohort, who displayed ID, developmental regression, ASD and stereotypic behavior, hyperactivity, speech problems, hypotonia and seizures (Martínez et al., 2017). The second patient was clinically diagnosed with CdLS, showing developmental and growth delay, peculiar dysmorphisms, skeletal anomalies (e.g. polydactyly), heart defects (e.g. tetralogy of Fallot), urogenital anomalies (cryptorchidism and hypoplastic genitalia), gastrointestinal and feeding problems (Wagner et al., 2019). Our patient shared some phenotypic features such as some dysmorphisms, ID, growth delay, congenital defects, and speech problems, although a higher number of cases are needed for a deeper genotype-phenotype correlation due to the clinical heterogeneity characterizing chromatinopathies.

5.4 Identification of pathogenetic variants in *NBEA*, *DYNC1H1* and *SLC35F1* in Rett-like patients

We performed trio WES on three Rett-like patients, who were previously tested for known Rett syndrome-associated genes but resulted negative, remaining without a molecular diagnosis. Clinical evaluation of these patients showed how they shared overlapping clinical features such as a global developmental delay and regression, ID, hands stereotypies,

seizures, absent or limited language ability and sleep problems (table 4.5). Interestingly, we identified four missense variants in three different genes: patient #1 resulted compound heterozygous for two novel variants in *NBEA*, patient #2 was carrier of a *de novo* variant in *DYNC1H1* and patient #3 for an unreported *de novo* variant in *SLC35F1* (table 4.5).

For 2/3 patients we gave insights into genotype-phenotype correlations as the identified mutated genes were already associated to two class of known neurodevelopmental disorders (Mulhern et al., 2018; Poirier et al., 2013). *NBEA* and *DYNC1H1* encodes for a protein with vesicle trafficking function and a cytoskeletal motor protein respectively, and in recent years many genes which were found mutated in individuals with Rett-like phenotypes were involved in gene regulation, RNA transcription and translation, neurotransmission, transport and channel activity (Ehrhart et al., 2018). Contrary to the other two genes just discussed, mutations in *SLC35F1* were not associated to any disorder yet, although microdeletions encompassing its chromosomal location were recently described in patients with pediatric epilepsy and similar phenotypes to the one displayed by our patient (Szafranski et al., 2015). In addition, in several cohorts of Rett-like patients were identified mutations in other SLC family members, such as *SLC6A1*, *SLC35A2* and *SLC39A13*, genes already associated to other conditions (Myoclonic-atonic epilepsy and schizophrenia, Early onset epileptic encephalopathy and Congenital disorder of glycosylation type II, Recessive Ehlers-Danlos syndrome-like spondylocheirodysplasia respectively) (Lopes et al., 2016; Lucariello et al., 2016; Sajan et al., 2017; Vidal et al., 2017). These findings could open to the possibility that *SLC35F1* could have a role in pathogenesis of neurodevelopmental disorders such as Rett-like syndrome.

5.5 SLC35F1 is a cytoplasmic protein involved in ATP-dependent activity and rRNA binding

SLC35F1, the gene found mutated in patient #3, encodes for the F1 member of solute carrier family 35, a putative nucleoside sugar transporter and a transmembrane protein mainly expressed in the brain. This protein is considered an orphan transporter due to the fact that its substrate specificity and function need to be still determined. Curiously, despite the clear relevance of solute carrier family in health and disease, this family is less studied compared to other gene families, showing the greatest publication asymmetry (César-Razquin et al., 2015). Thus, since little is known about *SLC35F1*, we investigated its role starting with the characterization of its cellular localization and its interactome by LC-MS/MS, exploiting the

generation of *SLC35F1* KO lines. We observed that the protein localized mainly in the cytoplasmic compartment, with peculiar dots appearance outside the nucleus appreciable by immunofluorescence (figure 17). In addition, interactome analysis revealed as major interactors subunits of ATP synthase and ribosomal proteins (figure 4.19 and table 4.6).

According to protein databases, *SLC35F1* belongs to a family of nucleotide sugar transporters, whose activity mainly consists in the transport of substrates for glycosylation across the endoplasmic reticulum (ER) and Golgi lipid bilayer membranes (Song, 2013), although data on *SLC35F1* biological function have been not reported yet. Surprisingly, significant *SLC35F1* interactors identified by MS resulted *ATP5B*, *ATP5C* and *ATP5F1* which are subunits of the F_1F_0 ATP synthase or Complex V, a multisubunit complex acting as ATP-driven proton pumps. F-type ATPase are made of a catalytic core (F_1), which *ATP5B* and *ATP5C* belong to, and a membrane proton channel (F_0) composed by three subunits including *ATP5F1* (Forgac, 2007; Vlasov et al., 2022). *SLC35F1* resulted to interact also with several ribosomal proteins such as *RPS3*, *RPS14*, *RPL3*, *RPL23A* and *RPL27A*, components of cytosolic ribosome involved in translation and biosynthesis of macromolecules. In addition, since different transporters often work together due to shared substrate specificities, having another member of SLC family among *SLC35F1* significant interactors it could be interesting (Lin et al., 2015). In particular *SLC25A5* (or adenine nucleotide translocator 2, *ANT2*) is ubiquitously expressed, with higher expression in brain and muscle, and contributes to ADP/ATP exchange between mitochondria and cytoplasm (Chen et al., 1990). Interestingly, deletions of *SLC25A5* gene were associated to X-linked non-syndromic ID in males and mitochondrial nucleotide exchange was proposed as novel pathway related to ID (Vandewalle et al., 2013), although a characterization also of this protein is still lacking. This relationship and, above all, *SLC35F1* role should be deepened to identify its substrate and function with particularly attention to neurodevelopmental context.

6. CONCLUSION

In this work we used two different approaches for studying chromatinopathies RSTS and RTT syndromes.

For RSTS patients with *CREBPP* or *EP300* mutations we focused on a possible therapeutic strategy, identifying in HDACi a concrete option for the epigenetic modulation of this syndrome. Investigating microbiota of RSTS patients and fruit flies model, we found differences in microbial composition compared to controls and strikingly, a depletion of bacteria producers of the endogenous HDACi butyrate, which can be regulated by diet, was found in RSTS samples. Interestingly, *in vitro* model showed that HDACi drugs were not cytotoxic for patients cell lines, with a patient-specific response which suggest a possible application in the field of personalized medicine. Finally, HDACi should be taken into account for repurposing for RSTS future therapy, since *in vivo* model showed a partial rescue of embryonic development in mutant flies embryos, suggesting that nutritional intervention could ameliorate RSTS traits.

For RSTS and RTT-like patients without a molecular diagnosis we used an NGS-based approach, which led to the identification of novel variants in genes associated to another chromatinopathy and other neurodevelopmental disorders for RSTS and RTT-like patients respectively, elucidating genotype-phenotype correlation for disorders with overlapping phenotypes. In addition, molecular investigation of a variant in a gene not previously associated to chromatinopathies for a RSTS patient, and the characterization of a protein encoded by a new candidate gene for RTT-like syndrome, represented preliminary findings for disclosing pathogenetic mechanisms underlying these neurodevelopmental disorders.

Thus, the results showed in this work could represent a starting point for the investigation of these newly identified candidate genes in a neuronal context, in order to elucidate the neurocognitive aspects known to be relevant for these syndromes.

7. BIBLIOGRAPHY

Ajmone, P.F., Avignone, S., Gervasini, C., Giacobbe, A., Monti, F., Costantino, A., Esposito, S., Marchisio, P., Triulzi, F., and Milani, D. (2018). Rubinstein-Taybi syndrome: New neuroradiological and neuropsychiatric insights from a multidisciplinary approach. *Am. J. Med. Genet. B. Neuropsychiatr. Genet.* *177*, 406–415.

Akimaru, H., Chen, Y., Dai, P., Hou, D.-X., Nonaka, M., Smolik, S.M., Armstrong, S., Goodman, R.H., and Ishii, S. (1997a). *Drosophila* CBP is a co-activator of cubitus interruptus in hedgehog signalling. *Nature* *386*, 735–738.

Akimaru, H., Hou, D.-X., and Ishii, S. (1997b). *Drosophila* CBP is required for dorsal-dependent twist gene expression. *Nat. Genet.* *17*, 211–214.

Akol, I., Gather, F., and Vogel, T. (2022). Paving Therapeutic Avenues for FOXG1 Syndrome: Untangling Genotypes and Phenotypes from a Molecular Perspective. *Int. J. Mol. Sci.* *23*.

Alarcón, J.M., Malleret, G., Touzani, K., Vronskaya, S., Ishii, S., Kandel, E.R., and Barco, A. (2004). Chromatin acetylation, memory, and LTP are impaired in CBP^{+/-} mice: A model for the cognitive deficit in Rubinstein-Taybi syndrome and its amelioration. *Neuron* *42*, 947–959.

Ali, I., Conrad, R.J., Verdin, E., and Ott, M. (2018). Lysine Acetylation Goes Global: From Epigenetics to Metabolism and Therapeutics. *Chem. Rev.* *118*, 1216–1252.

Allis, C.D., and Jenuwein, T. (2016). The molecular hallmarks of epigenetic control. *Nat. Rev. Genet.* *17*, 487–500.

Ambrosi, C., Manzo, M., and Baubec, T. (2017). Dynamics and Context-Dependent Roles of DNA Methylation. *J. Mol. Biol.* *429*, 1459–1475.

Amir, R.E., Van Den Veyver, I.B., Wan, M., Tran, C.Q., Francke, U., and Zoghbi, H.Y. (1999). Rett syndrome is caused by mutations in X-linked MECP2, encoding methyl-CpG-binding protein 2. *Nat. Genet.* *23*, 185–188.

Aoi, H., Mizuguchi, T., Ceroni, J.R., Kim, V.E.H., Furquim, I., Honjo, R.S., Iwaki, T., Suzuki, T., Sekiguchi, F., Uchiyama, Y., et al. (2019). Comprehensive genetic analysis of 57 families with clinically suspected Cornelia de Lange syndrome. *J. Hum. Genet.* *64*, 967–978.

Ariani, F., Hayek, G., Rondinella, D., Artuso, R., Mencarelli, M.A., Spanhol-Rosseto, A., Pollazzon, M., Buoni, S., Spiga, O., Ricciardi, S., et al. (2008). FOXG1 is responsible for the congenital variant of Rett syndrome. *Am. J. Hum. Genet.* *83*, 89–93.

Armstrong, D., Dunn, J.K., Antalffy, B., and Trivedi, R. (1995). Selective dendritic alterations in the cortex of Rett syndrome. *J. Neuropathol. Exp. Neurol.* *54*, 195–201.

Ashburner, M. (1989). *Drosophila: A laboratory handbook* (Cold spring harbor laboratory press).

Atlasi, Y., and Stunnenberg, H.G. (2017). The interplay of epigenetic marks during stem cell differentiation and development. *Nat. Rev. Genet.* *18*, 643–658.

Bartholdi, D., Roelfsema, J.H., Papadia, F., Breuning, M.H., Niedrist, D., Hennekam, R.C., Schinzel, A., and Peters, D.J.M. (2007). Genetic heterogeneity in Rubinstein-Taybi syndrome:

delineation of the phenotype of the first patients carrying mutations in EP300. *J. Med. Genet.* **44**, 327–333.

Bartsch, O., Kress, W., Kempf, O., Lechno, S., Haaf, T., and Zechner, U. (2010). Inheritance and variable expression in Rubinstein-Taybi syndrome. *Am. J. Med. Genet. A* **152A**, 2254–2261.

Bedford, D.C., Kasper, L.H., Fukuyama, T., and Brindle, P.K. (2010). Target gene context influences the transcriptional requirement for the KAT3 family of CBP and p300 histone acetyltransferases. *Epigenetics* **5**, 9–15.

Beets, L., Rodríguez-Fonseca, C., and Hennekam, R.C. (2014). Growth charts for individuals with Rubinstein-Taybi syndrome. *Am. J. Med. Genet. Part A* **164**, 2300–2309.

Benjamin, J.S., Pilarowski, G.O., Carosso, G.A., Zhang, L., Huso, D.L., Goff, L.A., Vernon, H.J., Hansen, K.D., and Bjornsson, H.T. (2017). A ketogenic diet rescues hippocampal memory defects in a mouse model of Kabuki syndrome. *Proc. Natl. Acad. Sci. U. S. A.* **114**, 125–130.

Bentivegna, A., Milani, D., Gervasini, C., Castronovo, P., Mottadelli, F., Manzini, S., Colapietro, P., Giordano, L., Atzeri, F., Divizia, M.T., et al. (2006). Rubinstein-Taybi Syndrome: spectrum of CREBBP mutations in Italian patients. *BMC Med. Genet.* **7**, 77.

Bhalla, K.N. (2005). Epigenetic and chromatin modifiers as targeted therapy of hematologic malignancies. *J. Clin. Oncol.* **23**, 3971–3993.

Bjornsson, H.T. (2015). The Mendelian disorders of the epigenetic machinery. *Genome Res.* **25**.

Black, J.C., Van Rechem, C., and Whetstine, J.R. (2012). Histone lysine methylation dynamics: establishment, regulation, and biological impact. *Mol. Cell* **48**, 491–507.

Boot, M. V., van Belzen, M.J., Overbeek, L.I., Hijmering, N., Mendeville, M., Waisfisz, Q., Wesseling, P., Hennekam, R.C., and de Jong, D. (2018). Benign and malignant tumors in Rubinstein-Taybi syndrome. *Am. J. Med. Genet. Part A* **176**, 597–608.

Bordonaro, M., Lazarova, D.L., and Sartorelli, A.C. (2008). Butyrate and Wnt signaling: a possible solution to the puzzle of dietary fiber and colon cancer risk? *Cell Cycle* **7**, 1178–1183.

Borghi, E., and Vignoli, A. (2019). Rett Syndrome and Other Neurodevelopmental Disorders Share Common Changes in Gut Microbial Community: A Descriptive Review. *Int. J. Mol. Sci.* **20**.

Boukas, L., Havrilla, J.M., Hickey, P.F., Quinlan, A.R., Bjornsson, H.T., and Hansen, K.D. (2019). Coexpression patterns define epigenetic regulators associated with neurological dysfunction. *Genome Res.* **29**, 532–542.

Bradbury, C.A., Khanim, F.L., Hayden, R., Bunce, C.M., White, D.A., Drayson, M.T., Craddock, C., and Turner, B.M. (2005). Histone deacetylases in acute myeloid leukaemia show a distinctive pattern of expression that changes selectively in response to deacetylase inhibitors. *Leukemia* **19**, 1751–1759.

Bramswig, N.C., Lüdecke, H.J., Alanay, Y., Albrecht, B., Barthelmie, A., Boduroglu, K., Braunholz, D., Caliebe, A., Chrzanowska, K.H., Czeschik, J.C., et al. (2015). Exome sequencing unravels unexpected differential diagnoses in individuals with the tentative diagnosis of

- Coffin-Siris and Nicolaides-Baraitser syndromes. *Hum. Genet.* *134*, 553–568.
- Breen, M.E., and Mapp, A.K. (2018). Modulating the masters: chemical tools to dissect CBP and p300 function. *Curr. Opin. Chem. Biol.* *45*, 195–203.
- Caporaso, J.G., Kuczynski, J., Stombaugh, J., Bittinger, K., Bushman, F.D., Costello, E.K., Fierer, N., Pěa, A.G., Goodrich, J.K., Gordon, J.I., et al. (2010). QIIME allows analysis of high-throughput community sequencing data. *Nat. Methods* *7*, 335–336.
- Cavalli, G., and Heard, E. (2019). Advances in epigenetics link genetics to the environment and disease. *Nature* *571*, 489–499.
- César-Razquin, A., Snijder, B., Frappier-Brinton, T., Isserlin, R., Gyimesi, G., Bai, X., Reithmeier, R.A., Hepworth, D., Hediger, M.A., Edwards, A.M., et al. (2015). A Call for Systematic Research on Solute Carriers. *Cell* *162*, 478–487.
- Chang, M.C., Chen, Y.J., Lian, Y.C., Chang, B.E., Huang, C.C., Huang, W.L., Pan, Y.H., and Jeng, J.H. (2018). Butyrate stimulates histone H3 acetylation, 8-isoprostane production, RANKL expression, and regulated osteoprotegerin expression/secretion in MG-63 osteoblastic cells. *Int. J. Mol. Sci.* *19*.
- Chang, P., Zuckermann, A.M.E., Williams, S., Close, A.J., Cano-Jaimez, M., McEvoy, J.P., Spencer, J., Walker, M.C., and Williams, R.S.B. (2015). Seizure control by derivatives of medium chain fatty acids associated with the ketogenic diet show novel branching-point structure for enhanced potency. *J. Pharmacol. Exp. Ther.* *352*, 43–52.
- Chang, S., McKinsey, T.A., Zhang, C.L., Richardson, J.A., Hill, J.A., and Olson, E.N. (2004). Histone deacetylases 5 and 9 govern responsiveness of the heart to a subset of stress signals and play redundant roles in heart development. *Mol. Cell. Biol.* *24*, 8467–8476.
- Chang, S., Young, B.D., Li, S., Qi, X., Richardson, J.A., and Olson, E.N. (2006). Histone deacetylase 7 maintains vascular integrity by repressing matrix metalloproteinase 10. *Cell* *126*, 321–334.
- Chen, R.Z., Akbarian, S., Tudor, M., and Jaenisch, R. (2001). Deficiency of methyl-CpG binding protein-2 in CNS neurons results in a Rett-like phenotype in mice. *Nat. Genet.* *27*, 327–331.
- Chen, S.T., Chang, C. Der, Huebner, K., Ku, D.H., McFarland, M., DeRiel, J.K., Baserga, R., and Wurzel, J. (1990). A human ADP/ATP translocase gene has seven pseudogenes and localizes to chromosome X. *Somat. Cell Mol. Genet.* *16*, 143–149.
- Chriett, S., Dąbek, A., Wojtala, M., Vidal, H., Balcerczyk, A., and Pirola, L. (2019). Prominent action of butyrate over β -hydroxybutyrate as histone deacetylase inhibitor, transcriptional modulator and anti-inflammatory molecule. *Sci. Rep.* *9*, 742.
- Cobos, S.N., Bennett, S.A., and Torrente, M.P. (2019). The impact of histone post-translational modifications in neurodegenerative diseases. *Biochim. Biophys. Acta - Mol. Basis Dis.* *1865*, 1982–1991.
- Cohen, S., and Greenberg, M.E. (2008). Communication between the synapse and the nucleus in neuronal development, plasticity, and disease. *Annu. Rev. Cell Dev. Biol.* *24*, 183–209.
- Cohen, J.L., Schrier Vergano, S.A., Mazzola, S., Strong, A., Keena, B., McDougall, C., Ritter, A.,

Li, D., Bedoukian, E.C., Burke, L.W., et al. (2020). EP300-related Rubinstein-Taybi syndrome: Highlighted rare phenotypic findings and a genotype-phenotype meta-analysis of 74 patients. *Am. J. Med. Genet. A* *182*, 2926–2938.

Cross, E., Duncan-Flavell, P.J., Howarth, R.J., Hobbs, J.I., Thomas, N.S., and Bunyan, D.J. (2020). Screening of a large Rubinstein-Taybi cohort identified many novel variants and emphasizes the importance of the CREBBP histone acetyltransferase domain. *Am. J. Med. Genet. A* *182*, 2508–2520.

Cucco, F., Sarogni, P., Rossato, S., Alpa, M., Patimo, A., Latorre, A., Magnani, C., Puisac, B., Ramos, F.J., Pié, J., et al. (2020). Pathogenic variants in EP300 and ANKRD11 in patients with phenotypes overlapping Cornelia de Lange syndrome. *Am. J. Med. Genet. A* *182*, 1690–1696.

Dancy, B.M., and Cole, P.A. (2015). Protein Lysine Acetylation by p300/CBP. *Chem. Rev.* *115*, 2419–2452.

Davie, J.R. (2003). Inhibition of Histone Deacetylase Activity by Butyrate. *J. Nutr.* *133*, 2485S–2493S.

Dawlaty, M.M., Breiling, A., Le, T., Raddatz, G., Barrasa, M.I., Cheng, A.W., Gao, Q., Powell, B.E., Li, Z., Xu, M., et al. (2013). Combined deficiency of Tet1 and Tet2 causes epigenetic abnormalities but is compatible with postnatal development. *Dev. Cell* *24*, 310–323.

Dawlaty, M.M., Breiling, A., Le, T., Barrasa, M.I., Raddatz, G., Gao, Q., Powell, B.E., Cheng, A.W., Faull, K.F., Lyko, F., et al. (2014). Loss of Tet enzymes compromises proper differentiation of embryonic stem cells. *Dev. Cell* *29*, 102–111.

Deardorff, M.A., Bando, M., Nakato, R., Watrin, E., Itoh, T., Minamino, M., Saitoh, K., Komata, M., Katou, Y., Clark, D., et al. (2012). HDAC8 mutations in Cornelia de Lange syndrome affect the cohesin acetylation cycle. *Nature* *489*, 313–317.

Deroanne, C.F., Bonjean, K., Servotte, S., Devy, L., Colige, A., Clause, N., Blacher, S., Verdin, E., Foidart, J.M., Nusgens, B. V., et al. (2002). Histone deacetylases inhibitors as anti-angiogenic agents altering vascular endothelial growth factor signaling. *Oncogene* *21*, 427–436.

Dong, K.B., Maksakova, I.A., Mohn, F., Leung, D., Appanah, R., Lee, S., Yang, H.W., Lam, L.L., Mager, D.L., Schübeler, D., et al. (2008). DNA methylation in ES cells requires the lysine methyltransferase G9a but not its catalytic activity. *EMBO J.* *27*, 2691–2701.

Dutto, I., Scalera, C., Tillhon, M., Ticli, G., Passaniti, G., Cazzalini, O., Savio, M., Stivala, L.A., Gervasini, C., Larizza, L., et al. (2019). Mutations in CREBBP and EP300 genes affect DNA repair of oxidative damage in Rubinstein-Taybi syndrome cells. *Carcinogenesis* *1–10*.

Duvic, M., Talpur, R., Ni, X., Zhang, C., Hazarika, P., Kelly, C., Chiao, J.H., Reilly, J.F., Ricker, J.L., Richon, V.M., et al. (2007). Phase 2 trial of oral vorinostat (suberoylanilide hydroxamic acid, SAHA) for refractory cutaneous T-cell lymphoma (CTCL). *Blood* *109*, 31–39.

Ehrhart, F., Sangani, N.B., and Curfs, L.M.G. (2018). Current developments in the genetics of Rett and Rett-like syndrome. *Curr. Opin. Psychiatry* *31*, 103–108.

Emrich, H.M., Von Zerssen, D., Kissling, W., and Moeller, H.J. (1981). Therapeutic effect of valproate in mania. *Am. J. Psychiatry* *138*, 256.

- Fahrner, J.A., and Bjornsson, H.T. (2014). Mendelian Disorders of the Epigenetic Machinery: Tipping the Balance of Chromatin States. *Annu. Rev. Genomics Hum. Genet.* *15*, 269–293.
- Fahrner, J.A., and Bjornsson, H.T. (2019). Mendelian disorders of the epigenetic machinery: postnatal malleability and therapeutic prospects. *Hum. Mol. Genet.*
- Fast, D., Duggal, A., and Foley, E. (2018). Monoassociation with *Lactobacillus plantarum* Disrupts Intestinal Homeostasis in Adult *Drosophila melanogaster*. *MBio* *9*.
- Fehr, S., Wilson, M., Downs, J., Williams, S., Murgia, A., Sartori, S., Vecchi, M., Ho, G., Polli, R., Psoni, S., et al. (2013). The CDKL5 disorder is an independent clinical entity associated with early-onset encephalopathy. *Eur. J. Hum. Genet.* *21*, 266–273.
- Fergelot, P., Van Belzen, M., Van Gils, J., Afenjar, A., Armour, C.M., Arveiler, B., Beets, L., Burglen, L., Busa, T., Collet, M., et al. (2016). Phenotype and genotype in 52 patients with Rubinstein-Taybi syndrome caused by EP300 mutations. *Am. J. Med. Genet. A* *170*, 3069–3082.
- Forgac, M. (2007). Vacuolar ATPases: rotary proton pumps in physiology and pathophysiology. *Nat. Rev. Mol. Cell Biol.* *8*, 917–929.
- Freese, K., Seitz, T., Dietrich, P., Lee, S.M.L., Thasler, W.E., Bosserhoff, A., and Hellerbrand, C. (2019). Histone deacetylase expressions in hepatocellular carcinoma and functional effects of histone deacetylase inhibitors on liver cancer cells in vitro. *Cancers (Basel)*. *11*.
- Galéra, C., Taupiac, E., Fraise, S., Naudion, S., Toussaint, E., Rooryck-Thambo, C., Delrue, M.A., Arveiler, B., Lacombe, D., and Bouvard, M.P. (2009). Socio-behavioral characteristics of children with Rubinstein-Taybi syndrome. *J. Autism Dev. Disord.* *39*, 1252–1260.
- Galvão, T.C., and Thomas, J.O. (2005). Structure-specific binding of MeCP2 to four-way junction DNA through its methyl CpG-binding domain. *Nucleic Acids Res.* *33*, 6603–6609.
- Gao, Z., Yin, J., Zhang, J., Ward, R.E., Martin, R.J., Lefevre, M., Cefalu, W.T., and Ye, J. (2009). Butyrate improves insulin sensitivity and increases energy expenditure in mice. *Diabetes* *58*, 1509–1517.
- Gardian, G., Browne, S.E., Choi, D.K., Klivenyi, P., Gregorio, J., Kubilus, J.K., Ryu, H., Langley, B., Ratan, R.R., Ferrante, R.J., et al. (2005). Neuroprotective effects of phenylbutyrate in the N171-82Q transgenic mouse model of Huntington's disease. *J. Biol. Chem.* *280*, 556–563.
- Giles, R.H., Dauwerse, H.G., Van Ommen, G.J.B., and Breuning, M.H. (1998). Do human chromosomal bands 16p13 and 22q11-13 share ancestral origins? *Am. J. Hum. Genet.* *63*, 1240–1242.
- Van Gils, J., Magdinier, F., Fergelot, P., and Lacombe, D. (2021). Rubinstein-Taybi Syndrome: A Model of Epigenetic Disorder. *Genes (Basel)*. *12*.
- Goldsworthy, M., Absalom, N.L., Schröter, D., Matthews, H.C., Bogani, D., Moir, L., Long, A., Church, C., Hugill, A., Anstee, Q.M., et al. (2013). Mutations in Mll2, an H3K4 methyltransferase, result in insulin resistance and impaired glucose tolerance in mice. *PLoS One* *8*.
- Goodman, R.H., and Smolik, S. (2000). CBP/p300 in cell growth, transformation, and

development. *Genes Dev.* *14*, 1553–1577.

Göttlicher, M., Minucci, S., Zhu, P., Krämer, O.H., Schimpf, A., Giavara, S., Sleeman, J.P., Lo Coco, F., Nervi, C., Pelicci, P.G., et al. (2001). Valproic acid defines a novel class of HDAC inhibitors inducing differentiation of transformed cells. *EMBO J.* *20*, 6969–6978.

Gu, B., and Lee, M.G. (2013). Histone H3 lysine 4 methyltransferases and demethylases in self-renewal and differentiation of stem cells. *Cell Biosci.* *3*.

Gu, T.P., Guo, F., Yang, H., Wu, H.P., Xu, G.F., Liu, W., Xie, Z.G., Shi, L., He, X., Jin, S.G., et al. (2011). The role of Tet3 DNA dioxygenase in epigenetic reprogramming by oocytes. *Nature* *477*, 606–612.

Guccione, E., and Richard, S. (2019). The regulation, functions and clinical relevance of arginine methylation. *Nat. Rev. Mol. Cell Biol.* *20*, 642–657.

Gucev, Z.S., Tasic, V.B., Saveski, A., Polenakovic, M.H., Laban, N.B., Zechner, U., and Bartsch, O. (2019). Tissue-specific mosaicism in a patient with Rubinstein-Taybi syndrome and CREBBP exon 1 duplication. *Clin. Dysmorphol.* *28*, 140–142.

Guy, J., Hendrich, B., Holmes, M., Martin, J.E., and Bird, A. (2001). A mouse *Mecp2*-null mutation causes neurological symptoms that mimic Rett syndrome. *Nat. Genet.* *27*, 322–326.

Haberland, M., Montgomery, R.L., and Olson, E.N. (2009). The many roles of histone deacetylases in development and physiology: implications for disease and therapy. *Nat. Rev. Genet.* *10*, 32–42.

Hackett, J.A., Sengupta, R., Zylicz, J.J., Murakami, K., Lee, C., Down, T.A., and Surani, M.A. (2013). Germline DNA demethylation dynamics and imprint erasure through 5-hydroxymethylcytosine. *Science* *339*, 448–452.

Hagberg, B.A., and Skjeldal, O.H. (1994). Rett variants: a suggested model for inclusion criteria. *Pediatr. Neurol.* *11*, 5–11.

Hallert, C., Björck, I., Nyman, M., Pousette, A., Grännö, C., and Svensson, H. (2003). Increasing fecal butyrate in ulcerative colitis patients by diet: controlled pilot study. *Inflamm. Bowel Dis.* *9*, 116–121.

Hennekam, R.C.M. (2006). Rubinstein-Taybi syndrome. *Eur. J. Hum. Genet.* *14*, 981–985.

Hennekam, R.C.M., Van den Boogaard, M.J., Sibbles, B.J., and Van Spijker, H.G. (1990). Rubinstein-Taybi syndrome in The Netherlands. *Am. J. Med. Genet. Suppl.* *6*, 17–29.

Hoang, H.T., Schlager, M.A., Carter, A.P., and Bullock, S.L. (2017). *DYNC1H1* mutations associated with neurological diseases compromise processivity of dynein-dynactin-cargo adaptor complexes. *Proc. Natl. Acad. Sci. U. S. A.* *114*, E1597–E1606.

Hu, Y., Fisher, J.B., Koprowski, S., McAllister, D., Kim, M.S., and Lough, J. (2009). Homozygous disruption of the *Tip60* gene causes early embryonic lethality. *Dev. Dyn.* *238*, 2912–2921.

Ip, J.P.K., Mellios, N., and Sur, M. (2018). Rett syndrome: insights into genetic, molecular and circuit mechanisms. *Nat. Rev. Neurosci.* *19*, 368–382.

Ito, S., Dalessio, A.C., Taranova, O. V., Hong, K., Sowers, L.C., and Zhang, Y. (2010). Role of Tet

proteins in 5mC to 5hmC conversion, ES-cell self-renewal and inner cell mass specification. *Nature* **466**, 1129–1133.

Iyer, N.G., Özdag, H., and Caldas, C. (2004). p300/CBP and cancer. *Oncogene* **23**, 4225–4231.

Jenuwein, T., and Allis, C.D. (2001). Translating the histone code. *Science* **293**, 1074–1080.

Jones, P.L., Veenstra, G.J.C., Wade, P.A., Vermaak, D., Kass, S.U., Landsberger, N., Strouboulis, J., and Wolffe, A.P. (1998). Methylated DNA and MeCP2 recruit histone deacetylase to repress transcription. *Nat. Genet.* **19**, 187–191.

Jones, W.D., Dafou, D., McEntagart, M., Woollard, W.J., Elmslie, F. V., Holder-Espinasse, M., Irving, M., Saggat, A.K., Smithson, S., Trembath, R.C., et al. (2012). De novo mutations in MLL cause Wiedemann-Steiner syndrome. *Am. J. Hum. Genet.* **91**, 358–364.

Jørgensen, S., Schotta, G., and Sørensen, C.S. (2013). Histone H4 Lysine 20 methylation: key player in epigenetic regulation of genomic integrity. *Nucleic Acids Res.* **41**, 2797.

Kadam, S.D., Sullivan, B.J., Goyal, A., Blue, M.E., and Smith-Hicks, C. (2019). Rett Syndrome and CDKL5 Deficiency Disorder: From Bench to Clinic. *Int. J. Mol. Sci.* **20**.

Van De Kar, A.L., Houge, G., Shaw, A.C., De Jong, D., Van Belzen, M.J., Peters, D.J.M., and Hennekam, R.C.M. (2014). Keloids in Rubinstein-Taybi syndrome: a clinical study. *Br. J. Dermatol.* **171**, 615–621.

Kasper, L.H., Boussouar, F., Ney, P.A., Jackson, C.W., Rehg, J., Van Deursen, J.M., and Brindle, P.K. (2002). A transcription-factor-binding surface of coactivator p300 is required for haematopoiesis. *Nature* **419**, 738–743.

Katsumoto, T., Aikawa, Y., Iwama, A., Ueda, S., Ichikawa, H., Ochiya, T., and Kitabayashi, I. (2006). MOZ is essential for maintenance of hematopoietic stem cells. *Genes Dev.* **20**, 1321–1330.

Kilstrup-Nielsen, C., Rusconi, L., La Montanara, P., Ciceri, D., Bergo, A., Bedogni, F., and Landsberger, N. (2012). What we know and would like to know about CDKL5 and its involvement in epileptic encephalopathy. *Neural Plast.* **2012**.

Kim, H.J., Leeds, P., and Chuang, D.M. (2009). The HDAC inhibitor, sodium butyrate, stimulates neurogenesis in the ischemic brain. *J. Neurochem.* **110**, 1226–1240.

Kleefstra, T., Schenck, A., Kramer, J.M., and Van Bokhoven, H. (2014). The genetics of cognitive epigenetics. *Neuropharmacology* **80**, 83–94.

Klose, R.J., Sarraf, S.A., Schmiedeberg, L., McDermott, S.M., Stancheva, I., and Bird, A.P. (2005). DNA binding selectivity of MeCP2 due to a requirement for A/T sequences adjacent to methyl-CpG. *Mol. Cell* **19**, 667–678.

Kong, L., Tan, L., Lv, R., Shi, Z., Xiong, L., Wu, F., Rabidou, K., Smith, M., He, C., Zhang, L., et al. (2016). A primary role of TET proteins in establishment and maintenance of De Novo bivalency at CpG islands. *Nucleic Acids Res.* **44**.

Kouzarides, T. (2007). Chromatin modifications and their function. *Cell* **128**, 693–705.

Krautkramer, K.A., Kreznar, J.H., Romano, K.A., Vivas, E.I., Barrett-Wilt, G.A., Rabaglia, M.E.,

Keller, M.P., Attie, A.D., Rey, F.E., and Denu, J.M. (2016). Diet-Microbiota Interactions Mediate Global Epigenetic Programming in Multiple Host Tissues. *Mol. Cell* 64, 982–992.

Krishnan, K., Lau, B.Y.B., Ewall, G., Huang, Z.J., and Shea, S.D. (2017). MECP2 regulates cortical plasticity underlying a learned behaviour in adult female mice. *Nat. Commun.* 8.

Krishnaraj, R., Ho, G., and Christodoulou, J. (2017). RettBASE: Rett syndrome database update. *Hum. Mutat.* 38, 922–931.

Kueh, A.J., Dixon, M.P., Voss, A.K., and Thomas, T. (2011). HBO1 is required for H3K14 acetylation and normal transcriptional activity during embryonic development. *Mol. Cell. Biol.* 31, 845–860.

Kung, A.L., Rebel, V.I., Bronson, R.T., Ch'ng, L.E., Sieff, C.A., Livingston, D.M., and Yao, T.P. (2000). Gene dose-dependent control of hematopoiesis and hematologic tumor suppression by CBP. *Genes Dev.* 14, 272.

Lam, U.T.F., Tan, B.K.Y., Poh, J.J.X., and Chen, E.S. (2022). Structural and functional specificity of H3K36 methylation. *Epigenetics Chromatin* 2022 151 15, 1–20.

Lee, J.E., Wang, C., Xu, S., Cho, Y.W., Wang, L., Feng, X., Baldrige, A., Sartorelli, V., Zhuang, L., Peng, W., et al. (2013). H3K4 mono- and di-methyltransferase MLL4 is required for enhancer activation during cell differentiation. *Elife* 2.

Leonard, H., Cobb, S., and Downs, J. (2017). Clinical and biological progress over 50 years in Rett syndrome. *Nat. Rev. Neurol.* 13, 37–51.

Li, E., Bestor, T.H., and Jaenisch, R. (1992). Targeted mutation of the DNA methyltransferase gene results in embryonic lethality. *Cell* 69, 915–926.

Li, Y., Zhao, K., Yao, C., Kahwash, S., Tang, Y., Zhang, G., Patterson, K., Wang, Q.E., and Zhao, W. (2016). Givinostat, a type II histone deacetylase inhibitor, induces potent caspase-dependent apoptosis in human lymphoblastic leukemia. *Genes Cancer* 7, 292–300.

Lin, L., Yee, S.W., Kim, R.B., and Giacomini, K.M. (2015). SLC Transporters as Therapeutic Targets: Emerging Opportunities. *Nat. Rev. Drug Discov.* 14, 543.

Liu, H., Wang, J., He, T., Becker, S., Zhang, G., Li, D., and Ma, X. (2018). Butyrate: A Double-Edged Sword for Health? *Adv. Nutr.* 9, 21–29.

Ljungman, M., Parks, L., Hulbatte, R., and Bedi, K. (2019). The role of H3K79 methylation in transcription and the DNA damage response. *Mutat. Res. Rev. Mutat. Res.* 780, 48–54.

Looma, R.S., and Geddes, G. (2015). Tricuspid atresia and pulmonary atresia in a child with Rubinstein-Taybi syndrome. *Ann. Pediatr. Cardiol.* 8, 157–160.

Lopes, F., Barbosa, M., Ameer, A., Soares, G., De Sá, J., Dias, A.I., Oliveira, G., Cabral, P., Temudo, T., Calado, E., et al. (2016). Identification of novel genetic causes of Rett syndrome-like phenotypes. *J. Med. Genet.* 53, 190–199.

Lopez-Atalaya, J.P., Ciccarelli, A., Viosca, J., Valor, L.M., Jimenez-Minchan, M., Canals, S., Giustetto, M., and Barco, A. (2011). CBP is required for environmental enrichment-induced neurogenesis and cognitive enhancement. *EMBO J.* 30, 4287–4298.

- Lopez-Atalaya, J.P., Gervasini, C., Mottadelli, F., Spena, S., Piccione, M., Scarano, G., Selicorni, A., Barco, A., and Larizza, L. (2012). Histone acetylation deficits in lymphoblastoid cell lines from patients with Rubinstein-Taybi syndrome. *J. Med. Genet.* *49*, 66–74.
- López, M., García-Oguiza, A., Armstrong, J., García-Cobaleda, I., García-Miñaur, S., Santos-Simarro, F., Seidel, V., and Domínguez-Garrido, E. (2018). Rubinstein-Taybi 2 associated to novel EP300 mutations: deepening the clinical and genetic spectrum. *BMC Med. Genet.* *19*, 36.
- Louis, P., and Flint, H.J. (2009). Diversity, metabolism and microbial ecology of butyrate-producing bacteria from the human large intestine. *FEMS Microbiol. Lett.* *294*, 1–8.
- Lozupone, C., Lladser, M.E., Knights, D., Stombaugh, J., and Knight, R. (2011). UniFrac: an effective distance metric for microbial community comparison. *ISME J.* *5*, 169–172.
- Lucariello, M., Vidal, E., Vidal, S., Saez, M., Roa, L., Huertas, D., Pineda, M., Dalfó, E., Dopazo, J., Jurado, P., et al. (2016). Whole exome sequencing of Rett syndrome-like patients reveals the mutational diversity of the clinical phenotype. *Hum. Genet.* *135*, 1343–1354.
- Lyst, M.J., and Bird, A. (2015). Rett syndrome: a complex disorder with simple roots. *Nat. Rev. Genet.* *16*, 261–274.
- Mariño, G., Pietrocola, F., Eisenberg, T., Kong, Y., Malik, S.A., Andryushkova, A., Schroeder, S., Pendl, T., Harger, A., Niso-Santano, M., et al. (2014). Regulation of autophagy by cytosolic acetyl-coenzyme A. *Mol. Cell* *53*, 710–725.
- Martínez, F., Caro-Llopis, A., Roselló, M., Oltra, S., Mayo, S., Monfort, S., and Orellana, C. (2017). High diagnostic yield of syndromic intellectual disability by targeted next-generation sequencing. *J. Med. Genet.* *54*, 87–92.
- Masella, A.P., Bartram, A.K., Trzaskowski, J.M., Brown, D.G., and Neufeld, J.D. (2012). PANDAseq: paired-end assembler for illumina sequences. *BMC Bioinformatics* *13*, 31.
- Mews, P., Donahue, G., Drake, A.M., Luczak, V., Abel, T., and Berger, S.L. (2017). Acetyl-CoA synthetase regulates histone acetylation and hippocampal memory. *Nature* *546*, 381–386.
- Milani, D., Manzoni, F., Pezzani, L., Ajmone, P., Gervasini, C., Menni, F., and Esposito, S. (2015). Rubinstein-Taybi syndrome: clinical features, genetic basis, diagnosis, and management. *Ital. J. Pediatr.* *41*, 4.
- Montgomery, R.L., Davis, C.A., Potthoff, M.J., Haberland, M., Fielitz, J., Qi, X., Hill, J.A., Richardson, J.A., and Olson, E.N. (2007). Histone deacetylases 1 and 2 redundantly regulate cardiac morphogenesis, growth, and contractility. *Genes Dev.* *21*, 1790–1802.
- Montgomery, R.L., Potthoff, M.J., Haberland, M., Qi, X., Matsuzaki, S., Humphries, K.M., Richardson, J.A., Bassel-Duby, R., and Olson, E.N. (2008). Maintenance of cardiac energy metabolism by histone deacetylase 3 in mice. *J. Clin. Invest.* *118*, 3588–3597.
- Mulhern, M.S., Stumpel, C., Stong, N., Brunner, H.G., Bier, L., Lippa, N., Riviello, J., Rouhl, R.P.W., Kempers, M., Pfundt, R., et al. (2018). NBEA: developmental disease gene with early generalized epilepsy phenotypes. *Ann. Neurol.* *84*, 788.
- Nan, X., Ng, H.H., Johnson, C.A., Laherty, C.D., Turner, B.M., Eisenman, R.N., and Bird, A.

(1998). Transcriptional repression by the methyl-CpG-binding protein MeCP2 involves a histone deacetylase complex. *Nature* **393**, 386–389.

Negri, G., Milani, D., Colapietro, P., Forzano, F., Della Monica, M., Rusconi, D., Consonni, L., Caffi, L.G., Finelli, P., Scarano, G., et al. (2015). Clinical and molecular characterization of Rubinstein-Taybi syndrome patients carrying distinct novel mutations of the EP300 gene. *Clin. Genet.* **87**, 148–154.

Negri, G., Magini, P., Milani, D., Colapietro, P., Rusconi, D., Scarano, E., Bonati, M., Priolo, M., Crippa, M., Mazzanti, L., et al. (2016). From Whole Gene Deletion to Point Mutations of EP300-Positive Rubinstein-Taybi Patients: New Insights into the Mutational Spectrum and Peculiar Clinical Hallmarks. *Hum. Mutat.* **37**, 175–183.

Negri, G., Magini, P., Milani, D., Crippa, M., Biamino, E., Piccione, M., Sotgiu, S., Perrià, C., Vitiello, G., Frontali, M., et al. (2019). Exploring by whole exome sequencing patients with initial diagnosis of Rubinstein-Taybi syndrome: the interconnections of epigenetic machinery disorders. *Hum. Genet.* **138**.

Nelson, S.B., and Valakh, V. (2015). Excitatory/Inhibitory Balance and Circuit Homeostasis in Autism Spectrum Disorders. *Neuron* **87**, 684–698.

Neul, J.L., Fang, P., Barrish, J., Lane, J., Caeg, E.B., Smith, E.O., Zoghbi, H., Percy, A., and Glaze, D.G. (2008). Specific mutations in methyl-CpG-binding protein 2 confer different severity in Rett syndrome. *Neurology* **70**, 1313–1321.

Neul, J.L., Kaufmann, W.E., Glaze, D.G., Christodoulou, J., Clarke, A.J., Bahi-Buisson, N., Leonard, H., Bailey, M.E.S., Schanen, N.C., Zappella, M., et al. (2010). Rett syndrome: revised diagnostic criteria and nomenclature. *Ann. Neurol.* **68**, 944–950.

O'Carroll, D., Erhardt, S., Pagani, M., Barton, S.C., Surani, M.A., and Jenuwein, T. (2001). The polycomb-group gene *Ezh2* is required for early mouse development. *Mol. Cell. Biol.* **21**, 4330–4336.

Oike, Y., Hata, A., Mamiya, T., Kaname, T., Noda, Y., Suzuki, M., Yasue, H., Nabeshima, T., Araki, K., and Yamamura, K. (1999). Truncated CBP protein leads to classical Rubinstein-Taybi syndrome phenotypes in mice: implications for a dominant-negative mechanism. *Hum. Mol. Genet.* **8**, 387–396.

Okano, M., Bell, D.W., Haber, D.A., and Li, E. (1999). DNA methyltransferases *Dnmt3a* and *Dnmt3b* are essential for de novo methylation and mammalian development. *Cell* **99**, 247–257.

Padeken, J., Methot, S.P., and Gasser, S.M. (2022). Establishment of H3K9-methylated heterochromatin and its functions in tissue differentiation and maintenance. *Nat. Rev. Mol. Cell Biol.* **2022** 1–18.

Parenti, I., Teresa-Rodrigo, M.E., Pozojevic, J., Ruiz Gil, S., Bader, I., Braunholz, D., Bramswig, N.C., Gervasini, C., Larizza, L., Pfeiffer, L., et al. (2017). Mutations in chromatin regulators functionally link Cornelia de Lange syndrome and clinically overlapping phenotypes. *Hum. Genet.* **136**, 307–320.

Park, S.Y., and Kim, J.S. (2020). A short guide to histone deacetylases including recent progress on class II enzymes. *Exp. Mol. Med.* **52**, 204–212.

Percy, A.K., Neul, J.L., Glaze, D.G., Motil, K.J., Skinner, S.A., Khwaja, O., Lee, H.S., Lane, J.B., Barrish, J.O., Annese, F., et al. (2010). Rett syndrome diagnostic criteria: lessons from the Natural History Study. *Ann. Neurol.* *68*, 951–955.

Pérez-Grijalba, V., García-Oguiza, A., López, M., Armstrong, J., García-Miñaur, S., Mesa-Latorre, J.M., O'Callaghan, M., Pineda Marfa, M., Ramos-Arroyo, M.A., Santos-Simarro, F., et al. (2019). New insights into genetic variant spectrum and genotype-phenotype correlations of Rubinstein-Taybi syndrome in 39 CREBBP-positive patients. *Mol. Genet. Genomic Med.* *7*.

Perucca, E. (2002). Pharmacological and therapeutic properties of valproate: a summary after 35 years of clinical experience. *CNS Drugs* *16*, 695–714.

Petrif, F., Giles, R.H., Dauwerse, H.G., Saris, J.J., Hennekam, R.C.M., Masuno, M., Tommerup, N., van Ommen, G.J.B., Goodman, R.H., Peters, D.J.M., et al. (1995). Rubinstein-Taybi syndrome caused by mutations in the transcriptional co-activator CBP. *Nature* *376*, 348–351.

Phiel, C.J., Zhang, F., Huang, E.Y., Guenther, M.G., Lazar, M.A., and Klein, P.S. (2001). Histone deacetylase is a direct target of valproic acid, a potent anticonvulsant, mood stabilizer, and teratogen. *J. Biol. Chem.* *276*, 36734–36741.

Poirier, K., Lebrun, N., Broix, L., Tian, G., Saillour, Y., Boscheron, C., Parrini, E., Valence, S., Pierre, B. Saint, Oger, M., et al. (2013). Mutations in TUBG1, DYNC1H1, KIF5C and KIF2A cause malformations of cortical development and microcephaly. *Nat. Genet.* *45*, 639–647.

Rett, A. (1966). [On a unusual brain atrophy syndrome in hyperammonemia in childhood] - PubMed. *Wiener Medizinische Wochenschrift* *116*, 723–726.

Richards, S., Aziz, N., Bale, S., Bick, D., Das, S., Gastier-Foster, J., Grody, W.W., Hegde, M., Lyon, E., Spector, E., et al. (2015). Standards and guidelines for the interpretation of sequence variants: a joint consensus recommendation of the American College of Medical Genetics and Genomics and the Association for Molecular Pathology. *Genet. Med.* *17*, 405–424.

Roelfsema, J.H., White, S.J., Ariyürek, Y., Bartholdi, D., Niedrist, D., Papadia, F., Bacino, C.A., Den Dunnen, J.T., Van Ommen, G.J.B., Breuning, M.H., et al. (2005). Genetic heterogeneity in Rubinstein-Taybi syndrome: mutations in both the CBP and EP300 genes cause disease. *Am. J. Hum. Genet.* *76*, 572–580.

Rosato, R.R., Wang, Z., Gopalkrishnan, R. V., Fisher, P.B., and Grant, S. (2001). Evidence of a functional role for the cyclin-dependent kinase-inhibitor p21WAF1/CIP1/MDA6 in promoting differentiation and preventing mitochondrial dysfunction and apoptosis induced by sodium butyrate in human myelomonocytic leukemia cells (U937). *Int. J. Oncol.* *19*, 181–191.

De Rubeis, S., He, X., Goldberg, A.P., Poultney, C.S., Samocha, K., Cicek, A.E., Kou, Y., Liu, L., Fromer, M., Walker, S., et al. (2014). Synaptic, transcriptional and chromatin genes disrupted in autism. *Nature* *515*, 209–215.

Rubinstein, J.H., and Taybi, H. (1963). Broad thumbs and toes and facial abnormalities. A possible mental retardation syndrome. *Am. J. Dis. Child.* *105*, 588–608.

Rusconi, D., Negri, G., Colapietro, P., Picinelli, C., Milani, D., Spena, S., Magnani, C., Silengo, M.C., Sorasio, L., Curtisova, V., et al. (2015). Characterization of 14 novel deletions underlying Rubinstein-Taybi syndrome: an update of the CREBBP deletion repertoire. *Hum. Genet.* *134*, 613–626.

- Saettini, F., Herriot, R., Prada, E., Nizon, M., Zama, D., Marzollo, A., Romaniouk, I., Lougaris, V., Cortesi, M., Morreale, A., et al. (2020). Prevalence of Immunological Defects in a Cohort of 97 Rubinstein-Taybi Syndrome Patients. *J. Clin. Immunol.* *40*, 851–860.
- Sajan, S.A., Jhangiani, S.N., Muzny, D.M., Gibbs, R.A., Lupski, J.R., Glaze, D.G., Kaufmann, W.E., Skinner, S.A., Annese, F., Friez, M.J., et al. (2017). Enrichment of mutations in chromatin regulators in people with Rett syndrome lacking mutations in MECP2. *Genet. Med.* *19*, 13–19.
- Schölz, C., Weinert, B.T., Wagner, S.A., Beli, P., Miyake, Y., Qi, J., Jensen, L.J., Streicher, W., McCarthy, A.R., Westwood, N.J., et al. (2015). Acetylation site specificities of lysine deacetylase inhibitors in human cells. *Nat. Biotechnol.* *33*, 415–425.
- Schüle, B., Armstrong, D.D., Vogel, H., Oviedo, A., and Francke, U. (2008). Severe congenital encephalopathy caused by MECP2 null mutations in males: central hypoxia and reduced neuronal dendritic structure. *Clin. Genet.* *74*, 116–126.
- De Schutter, H., and Nuyts, S. (2009). Radiosensitizing Potential of Epigenetic Anticancer Drugs. *Anticancer. Agents Med. Chem.* *9*, 99–108.
- Schwartzman, J.S., Bernardino, A., Nishimura, A., Gomes, R.R., and Zatz, M. (2001). Rett syndrome in a boy with a 47,XXY karyotype confirmed by a rare mutation in the MECP2 gene. *Neuropediatrics* *32*, 162–164.
- Selkig, J., Wong, P., Zhang, X., and Pettersson, S. (2014). Metabolic tinkering by the gut microbiome: Implications for brain development and function. *Gut Microbes* *5*.
- Seto, E., and Yoshida, M. (2014). Erasers of histone acetylation: the histone deacetylase enzymes. *Cold Spring Harb. Perspect. Biol.* *6*.
- Shahbazian, M.D., Young, J.I., Yuva-Paylor, L.A., Spencer, C.M., Antalffy, B.A., Noebels, J.L., Armstrong, D.L., Paylor, R., and Zoghbi, H.Y. (2002). Mice with truncated MeCP2 recapitulate many Rett syndrome features and display hyperacetylation of histone H3. *Neuron* *35*, 243–254.
- Shao, Y., Gao, Z., Marks, P.A., and Jiang, X. (2004). Apoptotic and autophagic cell death induced by histone deacetylase inhibitors. *Proc. Natl. Acad. Sci. U. S. A.* *101*, 18030–18035.
- Sharon, G., Segal, D., Ringo, J.M., Hefetz, A., Zilber-Rosenberg, I., and Rosenberg, E. (2010). Commensal bacteria play a role in mating preference of *Drosophila melanogaster*. *Proc. Natl. Acad. Sci. U. S. A.* *107*, 20051–20056.
- Sheikh, B.N., and Akhtar, A. (2019). The many lives of KATs - detectors, integrators and modulators of the cellular environment. *Nat. Rev. Genet.* *20*, 7–23.
- Shin, S.C., Kim, S.-H., You, H., Kim, B., Kim, A.C., Lee, K.-A., Yoon, J.-H., Ryu, J.-H., and Lee, W.-J. (2011). *Drosophila* microbiome modulates host developmental and metabolic homeostasis via insulin signaling. *Science* *334*, 670–674.
- Shingler, E., Perry, R., Mitchell, A., England, C., Perks, C., Herbert, G., Ness, A., and Atkinson, C. (2019). Dietary restriction during the treatment of cancer: results of a systematic scoping review. *BMC Cancer* *19*.
- Simon, D., Laloo, B., Barillot, M., Barnette, T., Blanchard, C., Rooryck, C., Marche, M.,

- Burgelin, I., Coupry, I., Chassaing, N., et al. (2010). A mutation in the 3'-UTR of the HDAC6 gene abolishing the post-transcriptional regulation mediated by hsa-miR-433 is linked to a new form of dominant X-linked chondrodysplasia. *Hum. Mol. Genet.* *19*, 2015–2027.
- Simon, G.M., Cheng, J., and Gordon, J.I. (2012). Quantitative assessment of the impact of the gut microbiota on lysine epsilon-acetylation of host proteins using gnotobiotic mice. *Proc. Natl. Acad. Sci. U. S. A.* *109*, 11133–11138.
- Smith, Z.D., and Meissner, A. (2013). DNA methylation: roles in mammalian development. *Nat. Rev. Genet.* *14*, 204–220.
- Sobreira, N., Brucato, M., Zhang, L., Ladd-Acosta, C., Ongaco, C., Romm, J., Doheny, K.F., Mingroni-Netto, R.C., Bertola, D., Kim, C.A., et al. (2017). Patients with a Kabuki syndrome phenotype demonstrate DNA methylation abnormalities. *Eur. J. Hum. Genet.* *25*, 1335–1344.
- Song, Z. (2013). Roles of the nucleotide sugar transporters (SLC35 family) in health and disease. *Mol. Aspects Med.* *34*, 590–600.
- Soret, R., Chevalier, J., De Coppet, P., Poupeau, G., Derkinderen, P., Segain, J.P., and Neunlist, M. (2010). Short-chain fatty acids regulate the enteric neurons and control gastrointestinal motility in rats. *Gastroenterology* *138*.
- Spena, S., Gervasini, C., and Milani, D. (2015a). Ultra-Rare Syndromes: The Example of Rubinstein–Taybi Syndrome. *J. Pediatr. Genet.* *04*, 177–186.
- Spena, S., Milani, D., Rusconi, D., Negri, G., Colapietro, P., Elcioglu, N., Bedeschi, F., Pilotta, A., Spaccini, L., Ficcadenti, A., et al. (2015b). Insights into genotype–phenotype correlations from CREBBP point mutation screening in a cohort of 46 Rubinstein–Taybi syndrome patients. *Clin. Genet.* *88*, 431–440.
- Spena, S., Milani, D., Rusconi, D., Negri, G., Colapietro, P., Elcioglu, N., Bedeschi, F., Pilotta, A., Spaccini, L., Ficcadenti, A., et al. (2015c). Insights into genotype-phenotype correlations from CREBBP point mutation screening in a cohort of 46 Rubinstein-Taybi syndrome patients. *Clin. Genet.* *88*, 431–440.
- Squeo, G.M., Augello, B., Massa, V., Milani, D., Colombo, E.A., Mazza, T., Castellana, S., Piccione, M., Maitz, S., Petracca, A., et al. (2020). Customised next-generation sequencing multigene panel to screen a large cohort of individuals with chromatin-related disorder. *J. Med. Genet.* *57*, 760–768.
- Stegers, E.A.P., Von Dadelszen, P., Duvekot, J.J., and Pijnenborg, R. (2010). Pre-eclampsia. *Lancet (London, England)* *376*, 631–644.
- Stevens, C.A., and Bhakta, M.G. (1995). Cardiac abnormalities in the Rubinstein-Taybi syndrome. *Am. J. Med. Genet.* *59*, 346–348.
- Stilling, R.M., van de Wouw, M., Clarke, G., Stanton, C., Dinan, T.G., and Cryan, J.F. (2016). The neuropharmacology of butyrate: The bread and butter of the microbiota-gut-brain axis? *Neurochem. Int.* *99*, 110–132.
- Szafranski, P., Von Allmen, G.K., Graham, B.H., Wilfong, A.A., Kang, S.H.L., Ferreira, J.A., Upton, S.J., Moeschler, J.B., Bi, W., Rosenfeld, J.A., et al. (2015). 6q22.1 microdeletion and susceptibility to pediatric epilepsy. *Eur. J. Hum. Genet.* *23*, 173–179.

- Tachibana, M., Ueda, J., Fukuda, M., Takeda, N., Ohta, T., Iwanari, H., Sakihama, T., Kodama, T., Hamakubo, T., and Shinkai, Y. (2005). Histone methyltransferases G9a and GLP form heteromeric complexes and are both crucial for methylation of euchromatin at H3-K9. *Genes Dev.* *19*, 815–826.
- Tanaka, Y., Naruse, I., Maekawa, T., Masuya, H., Shiroishi, T., and Ishii, S. (1997). Abnormal skeletal patterning in embryos lacking a single Cbp allele: a partial similarity with Rubinstein-Taybi syndrome. *Proc. Natl. Acad. Sci. U. S. A.* *94*, 10215–10220.
- Tanaka, Y., Naruse, I., Hongo, T., Xu, M.J., Nakahata, T., Maekawa, T., and Ishii, S. (2000). Extensive brain hemorrhage and embryonic lethality in a mouse null mutant of CREB-binding protein. *Mech. Dev.* *95*, 133–145.
- Tang, H., Guo, J., Linpeng, S., and Wu, L. (2019). Next generation sequencing identified two novel mutations in NIPBL and a frame shift mutation in CREBBP in three Chinese children. *Orphanet J. Rare Dis.* *14*.
- Tarasenko, N., Chekroun-Setti, H., Nudelman, A., and Rephaeli, A. (2018). Comparison of the anticancer properties of a novel valproic acid prodrug to leading histone deacetylase inhibitors. *J. Cell. Biochem.* *119*, 3417–3428.
- Tekendo-Ngongang, C., Owosela, B., Fleischer, N., Addissie, Y.A., Malonga, B., Badoe, E., Gupta, N., Moresco, A., Huckstadt, V., Ashaat, E.A., et al. (2020). Rubinstein-Taybi syndrome in diverse populations. *Am. J. Med. Genet. A* *182*, 2939–2950.
- Thomas, T., Dixon, M.P., Kueh, A.J., and Voss, A.K. (2008). Mof (MYST1 or KAT8) is essential for progression of embryonic development past the blastocyst stage and required for normal chromatin architecture. *Mol. Cell. Biol.* *28*, 5093–5105.
- Topçu, M., Akyerli, C., Sayi, A., Törüner, G.A., Koçoğlu, S.R., Cimbiş, M., and özçelik, T. (2002). Somatic mosaicism for a MECP2 mutation associated with classic Rett syndrome in a boy. *Eur. J. Hum. Genet.* *10*, 77–81.
- Trappe, R., Laccone, F., Cobilanschi, J., Meins, M., Huppke, P., Hanefeld, F., and Engel, W. (2001). MECP2 mutations in sporadic cases of Rett syndrome are almost exclusively of paternal origin. *Am. J. Hum. Genet.* *68*, 1093–1101.
- Tsai, A.C.H., J Dossett, C., Walton, C.S., E Cramer, A., Eng, P.A., Nowakowska, B.A., Pursley, A.N., Stankiewicz, P., Wiszniewska, J., and Cheung, S.W. (2011). Exon deletions of the EP300 and CREBBP genes in two children with Rubinstein-Taybi syndrome detected by aCGH. *Eur. J. Hum. Genet.* *19*, 43–49.
- Tyanova, S., Temu, T., and Cox, J. (2016). The MaxQuant computational platform for mass spectrometry-based shotgun proteomics. *Nat. Protoc.* *11*, 2301–2319.
- Valor, L., Viosca, J., Lopez-Atalaya, J., and Barco, A. (2013). Lysine acetyltransferases CBP and p300 as therapeutic targets in cognitive and neurodegenerative disorders. *Curr. Pharm. Des.* *19*, 5051–5064.
- Vandewalle, J., Bauters, M., Van Esch, H., Belet, S., Verbeeck, J., Fieremans, N., Holvoet, M., Vento, J., Spreiz, A., Kotzot, D., et al. (2013). The mitochondrial solute carrier SLC25A5 at Xq24 is a novel candidate gene for non-syndromic intellectual disability. *Hum. Genet.* *132*, 1177–1185.

Vecsey, C.G., Hawk, J.D., Lattal, K.M., Stein, J.M., Fabian, S.A., Attner, M.A., Cabrera, S.M., McDonough, C.B., Brindle, P.K., Abel, T., et al. (2007). Histone deacetylase inhibitors enhance memory and synaptic plasticity via CREB:CBP-dependent transcriptional activation. *J. Neurosci.* *27*, 6128–6140.

Verduci, E., Moretti, F., Bassanini, G., Banderali, G., Rovelli, V., Casiraghi, M.C., Morace, G., Borgo, F., and Borghi, E. (2018). Phenylketonuric diet negatively impacts on butyrate production. *Nutr. Metab. Cardiovasc. Dis.* *28*, 385–392.

Vidal, S., Brandi, N., Pacheco, P., Gerotina, E., Blasco, L., Trotta, J.R., Derdak, S., Del Mar O’Callaghan, M., Garcia-Cazorla, À., Pineda, M., et al. (2017). The utility of Next Generation Sequencing for molecular diagnostics in Rett syndrome. *Sci. Rep.* *7*.

Villard, L. (2007). MECP2 mutations in males. *J. Med. Genet.* *44*, 417–423.

Villavicencio-Lorini, P., Klopocki, E., Trimborn, M., Koll, R., Mundlos, S., and Horn, D. (2013). Phenotypic variant of Brachydactyly-mental retardation syndrome in a family with an inherited interstitial 2q37.3 microdeletion including HDAC4. *Eur. J. Hum. Genet.* *21*, 743–748.

Vlasov, A. V., Osipov, S.D., Bondarev, N.A., Uversky, V.N., Borshchevskiy, V.I., Yanyushin, M.F., Manukhov, I. V., Rogachev, A. V., Vlasova, A.D., Ilyinsky, N.S., et al. (2022). ATP synthase F O F 1 structure, function, and structure-based drug design. *Cell. Mol. Life Sci.* *79*.

Voigt, P., Tee, W.W., and Reinberg, D. (2013). A double take on bivalent promoters. *Genes Dev.* *27*, 1318–1338.

De Vries, T.I., Monroe, G.R., Van Belzen, M.J., Van Der Lans, C.A., Savelberg, S.M.C., Newman, W.G., Van Haaften, G., Nievelstein, R.A., and Van Haelst, M.M. (2016). Mosaic CREBBP mutation causes overlapping clinical features of Rubinstein-Taybi and Filippi syndromes. *Eur. J. Hum. Genet.* *24*, 1363–1366.

Wagner, V.F., Hillman, P.R., Britt, A.D., Ray, J.W., and Farach, L.S. (2019). A De novo HDAC2 variant in a patient with features consistent with Cornelia de Lange syndrome phenotype. *Am. J. Med. Genet. Part A* *179*, 852–856.

Waite, J., Moss, J., Beck, S.R., Richards, C., Nelson, L., Arron, K., Burbidge, C., Berg, K., and Oliver, C. (2015). Repetitive behavior in Rubinstein-Taybi syndrome: parallels with autism spectrum phenomenology. *J. Autism Dev. Disord.* *45*, 1238–1253.

Wang, J., Hevi, S., Kurash, J.K., Lei, H., Gay, F., Bajko, J., Su, H., Sun, W., Chang, H., Xu, G., et al. (2009a). The lysine demethylase LSD1 (KDM1) is required for maintenance of global DNA methylation. *Nat. Genet.* *41*, 125–129.

Wang, L., Tang, Y., Cole, P.A., and Marmorstein, R. (2008). Structure and chemistry of the p300/CBP and Rtt109 histone acetyltransferases: implications for histone acetyltransferase evolution and function. *Curr. Opin. Struct. Biol.* *18*, 741–747.

Wang, Q., Garrity, G.M., Tiedje, J.M., and Cole, J.R. (2007). Naive Bayesian classifier for rapid assignment of rRNA sequences into the new bacterial taxonomy. *Appl. Environ. Microbiol.* *73*, 5261–5267.

Wang, Z., Zang, C., Cui, K., Schones, D.E., Barski, A., Peng, W., and Zhao, K. (2009b). Genome-wide mapping of HATs and HDACs reveals distinct functions in active and inactive genes. *Cell*

138, 1019–1031.

Weaving, L.S., Christodoulou, J., Williamson, S.L., Friend, K.L., McKenzie, O.L.D., Archer, H., Evans, J., Clarke, A., Pelka, G.J., Tam, P.P.L., et al. (2004). Mutations of CDKL5 cause a severe neurodevelopmental disorder with infantile spasms and mental retardation. *Am. J. Hum. Genet.* 75, 1079–1093.

Weber, M., Hellmann, I., Stadler, M.B., Ramos, L., Pääbo, S., Rebhan, M., and Schübeler, D. (2007). Distribution, silencing potential and evolutionary impact of promoter DNA methylation in the human genome. *Nat. Genet.* 39, 457–466.

Wiedemann, H., Kunze, J., Grosse, H., and Dibbern, F. (1989). A syndrome of abnormal facies, short stature, and psychomotor retardation. *Atlas Clin. Syndr. A Vis. Aid to Diagnosis Clin. Pract. Physicians* 198–199.

Wiles, E.T., and Selker, E.U. (2017). H3K27 methylation: a promiscuous repressive chromatin mark. *Curr. Opin. Genet. Dev.* 43, 31.

Williams, S.R., Aldred, M.A., Der Kaloustian, V.M., Halal, F., Gowans, G., McLeod, D.R., Zondag, S., Toriello, H. V., Magenis, R.E., and Elsea, S.H. (2010). Haploinsufficiency of HDAC4 causes brachydactyly mental retardation syndrome, with brachydactyly type E, developmental delays, and behavioral problems. *Am. J. Hum. Genet.* 87, 219–228.

Wolffe, A.P. (1994). Nucleosome positioning and modification: chromatin structures that potentiate transcription. *Trends Biochem. Sci.* 19, 240–244.

Wood, M.A., Attner, M.A., Oliveira, A.M.M., Brindle, P.K., and Abel, T. (2006). A transcription factor-binding domain of the coactivator CBP is essential for long-term memory and the expression of specific target genes. *Learn. Mem.* 13, 609–617.

Woods, S.A., Robinson, H.B., Kohler, L.J., Agamanolis, D., Sterbenz, G., and Khalifa, M. (2014). Exome sequencing identifies a novel EP300 frame shift mutation in a patient with features that overlap Cornelia de Lange syndrome. *Am. J. Med. Genet. A* 164A, 251–258.

van de Wouw, M., Schellekens, H., Dinan, T.G., and Cryan, J.F. (2017). Microbiota-Gut-Brain Axis: Modulator of Host Metabolism and Appetite. *J. Nutr.* 147, 727–745.

Xu, W., Edmondson, D.G., Evrard, Y.A., Wakamiya, M., Behringer, R.R., and Roth, S.Y. (2000). Loss of Gcn5l2 leads to increased apoptosis and mesodermal defects during mouse development. *Nat. Genet.* 26, 229–232.

Yao, T.P., Oh, S.P., Fuchs, M., Zhou, N.D., Ch'ng, L.E., Newsome, D., Bronson, R.T., Li, E., Livingston, D.M., and Eckner, R. (1998). Gene dosage-dependent embryonic development and proliferation defects in mice lacking the transcriptional integrator p300. *Cell* 93, 361–372.

Yasui, D.H., Gonzales, M.L., Aflatooni, J.O., Crary, F.K., Hu, D.J., Gavino, B.J., Golub, M.S., Vincent, J.B., Schanen, N.C., Olson, C.O., et al. (2014). Mice with an isoform-ablating Mecp2 exon 1 mutation recapitulate the neurologic deficits of Rett syndrome. *Hum. Mol. Genet.* 23, 2447–2458.

You, A., Tong, J.K., Grozinger, C.M., and Schreiber, S.L. (2001). CoREST is an integral component of the CoREST- human histone deacetylase complex. *Proc. Natl. Acad. Sci. U. S. A.* 98, 1454–1458.

- Young, J.I., Hong, E.P., Castle, J.C., Crespo-Barreto, J., Bowman, A.B., Rose, M.F., Kang, D., Richman, R., Johnson, J.M., Berget, S., et al. (2005). Regulation of RNA splicing by the methylation-dependent transcriptional repressor methyl-CpG binding protein 2. *Proc. Natl. Acad. Sci. U. S. A.* *102*, 17551–17558.
- Yu, B.D., Hess, J.L., Horning, S.E., Brown, G.A.J., and Korsmeyer, S.J. (1995). Altered Hox expression and segmental identity in Mll-mutant mice. *Nature* *378*, 505–508.
- Yuan, B., Pehlivan, D., Karaca, E., Patel, N., Charng, W.-L., Gambin, T., Gonzaga-Jauregui, C., Sutton, V.R., Yesil, G., Bozdogan, S.T., et al. (2015). Global transcriptional disturbances underlie Cornelia de Lange syndrome and related phenotypes. *J. Clin. Invest.* *125*, 636–651.
- Yuan, X.G., Huang, Y.R., Yu, T., Jiang, H.W., Xu, Y., and Zhao, X.Y. (2019). Chidamide, a histone deacetylase inhibitor, induces growth arrest and apoptosis in multiple myeloma cells in a caspase-dependent manner. *Oncol. Lett.* *18*, 411–419.
- Zappella, M. (1992). The Rett girls with preserved speech. *Brain Dev.* *14*, 98–101.
- Zheng, F., Kasper, L.H., Bedford, D.C., Lerach, S., Teubner, B.J.W., and Brindle, P.K. (2016). Mutation of the CH1 Domain in the Histone Acetyltransferase CREBBP Results in Autism-Relevant Behaviors in Mice. *PLoS One* *11*.

RESEARCH INTEGRITY STATEMENT

All the principles of “The European Code of Conduct for Research Integrity” established by ALLEA (All European Academies, Berlin 2018) were followed for this PhD project:

quality of research was ensured by RELIABILITY;

research development, data production and communication were conducted with HONESTY;

RESPECT for colleagues, research participants, society and environment was shown;

research organization, publication, training and supervision were ruled by ACCOUNTABILITY.

This work respected the open access key as these results were and will be discussed to conferences for maintaining the dialogue among researcher open.

APPENDIX 1 – Scientific work



Expanding the phenotype associated to *KMT2A* variants: overlapping clinical signs between Wiedemann–Steiner and Rubinstein–Taybi syndromes

Elisabetta Di Fede¹ · Valentina Massa^{1,2} · Bartolomeo Augello³ · Gabriella Squeo³ · Emanuela Scarano⁴ · Anna Maria Perri⁴ · Rita Fischetto⁵ · Francesco Andrea Causio⁵ · Giuseppe Zampino⁶ · Maria Piccione⁷ · Elena Curridori⁸ · Tommaso Mazza⁹ · Stefano Castellana⁹ · Lidia Larizza¹⁰ · Filippo Ghelma¹¹ · Elisa Adele Colombo¹ · Maria Chiara Gandini¹ · Marco Castori³ · Giuseppe Merla³ · Donatella Milani¹² · Cristina Gervasini^{1,2}

Received: 24 March 2020 / Revised: 3 June 2020 / Accepted: 23 June 2020
© The Author(s) 2020. This article is published with open access

Abstract

Lysine-specific methyltransferase 2A (*KMT2A*) is responsible for methylation of histone H3 (K4H3me) and contributes to chromatin remodeling, acting as “writer” of the epigenetic machinery. Mutations in *KMT2A* were first reported in Wiedemann–Steiner syndrome (WDSTS). More recently, *KMT2A* variants have been described in probands with a specific clinical diagnosis comprised in the so-called chromatinopathies. Such conditions, including WDSTS, are a group of overlapping disorders caused by mutations in genes coding for the epigenetic machinery. Among them, Rubinstein–Taybi syndrome (RSTS) is mainly caused by heterozygous pathogenic variants in *CREBBP* or *EP300*. In this work, we used next generation sequencing (either by custom-made panel or by whole exome) to identify alternative causative genes in individuals with a RSTS-like phenotype negative to *CREBBP* and *EP300* mutational screening. In six patients we identified different novel unreported variants in *KMT2A* gene. The identified variants are *de novo* in at least four out of six tested individuals and all of them display some typical RSTS phenotypic features but also WDSTS specific signs. This study reinforces the concept that germline variants affecting the epigenetic machinery lead to a shared molecular effect (alteration of the chromatin state) determining superimposable clinical conditions.

These authors contributed equally: Donatella Milani, Cristina Gervasini

Supplementary information The online version of this article (<https://doi.org/10.1038/s41431-020-0679-8>) contains supplementary material, which is available to authorized users.

✉ Cristina Gervasini
cristina.gervasini@unimi.it

- 1 Genetica Medica e Biologia Applicata, Dipartimento di Scienze della Salute, Università degli Studi di Milano, Milano, Italy
- 2 “Aldo Ravelli” Center for Neurotechnology and Experimental Brain Therapeutics, Università degli Studi di Milano, Milano, Italy
- 3 Unità di Genetica Medica, IRCCS Casa Sollievo della Sofferenza, San Giovanni Rotondo, Italy
- 4 Ambulatorio di Malattie Rare, Sindromologia ed Auxologia U.O. Pediatria AOU S.Orsola-Malpighi, Bologna, Italy
- 5 U.O.C. Malattie Metaboliche Genetica Medica, PO Giovanni XXIII, AOU Policlinico Consorziale, Bari, Italy
- 6 Centro Malattie Rare e Difetti Congeniti, Fondazione Policlinico Universitario A. Gemelli, Università Cattolica, Roma, Italy

Introduction

Lysine-specific methyltransferase 2A (*KMT2A*, OMIM +159555) located at 11q23.3 contributes to chromatin

- 7 Dipartimento di scienze per la promozione della salute e la cura della madre e del bambino “G. D’Alessandro”, Università di Palermo, Palermo, Italy
- 8 Dipartimento di clinica pediatrica e malattie rare, Ospedale pediatrico Antonio Cao, Cagliari, Italy
- 9 Unit of Bioinformatics IRCCS Casa Sollievo della Sofferenza, San Giovanni Rotondo, Italy
- 10 Research Laboratory of Medical Cytogenetics and Molecular Genetics, IRCCS Istituto Auxologico Italiano, Milan, Italy
- 11 Dipartimento di Scienze della Salute, Università degli Studi di Milano, Milano, Italy
- 12 UOSD Pediatria ad alta intensità di cura, Fondazione IRCCS Cà Granda Ospedale Maggiore Policlinico Milano, Milano, Italy

opening, acting as “writer” of the epigenetic machinery. This gene encodes for a DNA-binding protein that methylates lysine 4 of histone H3 (K4H3me), which positively regulates transcription of multiple genes, including those involved in hematopoiesis and neuronal development [1]. *KMT2A* is expressed ubiquitously in human tissues and has been broadly studied in hematological diseases, since somatic translocations at its locus characterize a subset of acute leukemias [2]. More recently, heterozygous *KMT2A* loss-of-function and missense variants have been associated to Wiedemann–Steiner syndrome (WDSTS, OMIM #605130), described for the first time in 1989 by Wiedemann et al. [3] and characterized by hypertrichosis *cutibiti*, intellectual disability (ID) and developmental delay, a distinctive facial appearance and short stature [4].

Since 2012, pathogenic variants have been reported in patients with a typical WDSTS phenotype [4–11] and most of them generate a truncated protein. Additional variants have been annotated by exome sequencing performed for undiagnosed genetic disorders (<https://decipher.sanger.ac.uk/>). Studies in large cohorts of syndromic/non-syndromic ID and neurodevelopmental disorders with heterogeneous phenotype have led to the identification of further 32 *KMT2A* novel variants [12–15]. In addition, Li et al. have described 11 unreported mutations in a study comparing French and Chinese cohorts [15, 16]. Besides WDSTS, deleterious variants in *KMT2A* were also described in association with epilepsy [17], primary immunodeficiency [18], and eosinophilia [19].

Interestingly, five more patients carrying *KMT2A* variants were clinically diagnosed with Coffin–Siris syndrome (CSS, OMIM #135900, #614608, #614607, #614609, #616938, #615866, #617808, #618362, #618027, #618506) (pt #K2431) [20], Cornelia de Lange syndrome (CdLS, OMIM #122470, #300590, #610759, #614701, #300882) (pt CdLs #3 and pt #1) [21, 22], Kabuki syndrome (KS, OMIM #147920, #300867) (pts #KS8-KS29) [23], and Rubinstein–Taybi syndrome (RSTS, OMIM #180849, #613684) (pt #103) [24] respectively (Supplementary Table S1). To note, all the above-mentioned syndromes and WDSTS are typical epigenetic machinery disorders, also called chromatinopathies, a group of diseases caused by alterations in genes coding for components of the epigenetic apparatus termed “writers, erasers, readers, and remodelers” [25]. These proteins act in concert to control the chromatin opening and closing thus regulating gene expression by modification (i.e., methylation, acetylation, etc.) of histones and DNA.

As well as *KMT2A*, protein products of RSTS causative genes, CBP and p300, are “writers” of the epigenetic machinery. Both are ubiquitously expressed homologous proteins belonging to the KAT3 family of lysine acetyltransferases [26]. CBP and p300 are encoded by CREB

binding protein (*CREBBP*, also known as “CBP”) and E1A-associated protein p300 (*EP300*) respectively. Mutations in the “major gene” *CREBBP*, located at 16p13.3, are responsible for ~60% of RSTS patients [27], while almost 10% of RSTS cases have been diagnosed for pathogenic variants in *EP300*, mapping on chromosome 22q13.2 and called the “minor gene” [28]. RSTS is a rare (1:125,000) autosomal-dominant disorder which, generally, occurs *de novo* [29] and displays phenotypically heterogeneous variability. RSTS peculiar clinical picture includes postnatal growth deficiency, microcephaly, specific dysmorphisms, and skeletal abnormalities (e.g., broad thumbs and big toes). All these signs are hallmarks frequently used for clinical diagnosis, with a wide spectrum of multiple congenital anomalies [30].

To investigate the molecular basis of patients with a suspicious of RSTS diagnosis but without causative variants in *CREBBP* and *EP300*, we performed a whole exome/targeted next generation sequencing (NGS) identifying six different novel variants in *KMT2A*. The identified variants are *de novo* in at least four out of six tested patients (parents are unavailable in two families) and unreported. The clinical reevaluation of patients shows that they display some typical RSTS features but also various WDSTS specific signs with a peculiar global clinical presentation suggesting that different alterations of epigenetic machinery genes can converge to the same molecular effect (alteration opening/closing chromatin) to determine overlapping clinical conditions.

Materials and methods

Subjects

Individuals with RSTS initial diagnosis were clinically assessed and diagnosed by the respective clinical geneticist to enter genetic analysis and then carefully phenotypically reevaluated by a single geneticist with a deep expertise in RSTS diagnosis (DM). Informed consent was obtained from all enrolled subjects and families and this study was approved by the local institution ethical committee and review board.

CREBBP and *EP300* molecular analysis

A molecular multi-method approach based on a combination of multiple ligation-dependent probe amplification (MLPA) to detect whole gene or intragenic deletions and direct Sanger sequencing to identify point variants was applied. Genomic DNA was extracted from peripheral blood samples in EDTA using DNeasy Blood and Tissue Kit (Sigma-Aldrich, St. Louis, MO, USA) for MLPA

analysis, or with Wizard[®] Genomic DNA Purification Kit (Promega, Madison, WI, USA) for sequencing. MLPA analysis was performed with the SALSA MLPA commercially available kits (P313-A for *CREBBP* and P333-A1 for *EP300*) (MRC-Holland, Amsterdam, NL) according to the manufacturer's protocol. Amplified products were separated by capillary electrophoresis using an ABI PRISM 3700 Genetic Analyzer (Applied Biosystems, Foster City, CA, USA) and data were visually inspected using GeneMaker software v.1.5 (SoftGenetics, LLC, State College, PA, USA) and then deeply analyzed using Coffalyser (MRC-Holland). *CREBBP* amplicons encompassing coding regions and splicing junctions were amplified from the genomic DNA of patients #208 and #221 using GoTaQ Flexi DNA Polymerase (Promega) and primer's couples were designed with the public software Primer3 (<http://bioinfo.ut.ee/primer3-0.4.0/>) and OligoAnalyser 3.1 (<https://eu.idtdna.com/calc/analyzer>). Amplified fragments were sequenced with the same primers using the Big Dye Terminator v.1.1 or v.3.1 Cycle Sequencing Kit (Applied Biosystems) and the ABI PRISM 3130 sequencer (Applied Biosystems) according to the manufacturer's protocol. Electropherograms were analyzed with ChromasPro software 1.7.5 (Technelysium Pty Ltd., Queensland, AUS) considering the NG_009873.2 sequence as reference for *CREBBP*.

Multigene panel sequencing and data analysis

All the patients here described, except patient #187, have been tested by multigene panel sequencing. A customized HaloPlex Target Enrichment NGS panel (Agilent Technologies, Santa Clara, CA, USA) was generated using Agilent's SureDesign tool available at www.agilent.com/genomics/suredesign. A library of all the coding exons and intron–exon boundaries of 68 known genes associated with more than 40 OMIM entries, selected as classified as known chromatinopathies [25], was prepared using the HaloPlex HS Target Enrichment System (Agilent Technologies). Total genome target spanned 384 kb and was theoretically estimated to be completely covered (99.82%). A total of 17,470 amplicons were generated. Libraries were prepared according to the manufacturer's protocol using the human reference genome GRCh37/hg19. The library was then amplified by PCR to produce a sequencing-ready, target-enriched sample. Fragmented gDNA and final libraries were evaluated using High Sensitivity D1000 ScreenTape System on TapeStation 2200 (Agilent Technologies) and Qubit dsDNA Hs Assay Kits on Qubit[®] 4 Fluorometer (Thermo Fisher Scientific, Waltham, MA, USA) to quantify, according to the manufacturer's instructions. Sequencing was performed on Illumina MiSeq System, using the MiSeq Reagent Kit V2-500 cycles (Illumina, San Diego, CA,

USA), yielding 151 bp-long paired-end reads and achieving an average read depth of at least 400× for 11–22 samples and at least 20× per-base coverage in more than 98% of the targeted regions. Quality of sequences was preliminary checked with FastQC and trimmed using Trimmomatic (PMID: 24695404) if the quality of at least half-read was lower than 10 (phred quality score). Residual adapter sequences were removed by cutadapt (<https://cutadapt.readthedocs.io/en/stable/>). Preprocessed reads were aligned against the GRCh37/hg19 reference genome sequence by BWA-0.7.17 software. Depth of coverage statistics for the target regions were calculated by means of TEQC (<https://doi.org/10.18129/B9.bioc.TEQC>) and other custom scripts. Variants were identified by means of the Haplotype Caller tool of GATK v. 3.8 and were annotated with ANNOVAR, using RefSeq gene and transcript annotations (updated to Dec 2016). Variants were sought in the most important public collections, including dbSNP v. 150, ExAC v. 0.3, Exome Variant Server, gnomAD, HRC, Kaviar and ClinVar. Sequencing artefacts were controlled by matching individual-specific variants against an internal database of variants. Missense variants were fully annotated using dbNSFP v3.5 from which we have retrieved precomputed pathogenicity predictions and evolutionary conservation predictions and measures. The significance of candidate variants was classified according to American College of Medical Genetics and Genomics (ACMG) criteria using InterVar (<http://wintervar.wglab.org/>) (<https://doi.org/10.1016/j.ajhg.2017.01.004>) and Varsome (<https://varsome.com/>) (<https://doi.org/10.1093/bioinformatics/bty897>) tools.

Exome sequencing

Patient #187 and his parents has been tested by exome sequencing. Genomic DNA was extracted from whole blood for DNA library preparation and exome enrichment using the Agilent SureSelect V7 kit according to manufacturer instructions. Quality of post-amplification libraries was assessed using DNA 1000 chips on the BioAnalyzer 2100 (Agilent) and Qubit fluorimetric quantitation using Qubit dsDNA BR Assay Kits (Invitrogen by Thermo Fisher Scientific). An indexed 150 bp paired-end sequencing run was performed on an Illumina HiSeq 3000 instrument at CRS4 NGS facility. This approach achieved a 75× average coverage over the 36 Mb of genomic regions sequenced, with 97% regions covered at least 10×. Data analysis has been performed using an analysis pipeline based on public tools. In brief, paired-end sequence reads were aligned to the human genome (hg19) with the Burrows–Wheeler Aligner (BWA MEM) using default settings. Initial mappings were processed using the GATK framework (v4.1.0.0) according to their Best Practices recommendations. Variant sites were identified using GATK Haplotype

Table 1 *KMT2A* pathogenic variants and clinical signs of six described patients compared with typical features of RSTS and WDSTS. Sign + means present, sign - absent and sign +/- present in a few cases.

	RSTS	WDSTS	RSTS-208	RSTS-250	RSTS-187	RSTS-251	RSTS-243	RSTS-221
<i>KMT2A</i> pathogenic variant NG_027813.1 (NM_001197104.2) GRCh37/hg19								
Position			chr11:118342427	chr11:118343566	chr11:118350915	chr11:118350921	chr11:118350948	chr11:118352691
Exon			3	3	6	6	6	7
Inheritance			<i>De novo</i>	NA (unavailable parents)	<i>De novo</i>	<i>De novo</i>	<i>De novo</i>	NA (adopted child)
Date of birth			22/10/2006	17/09/2003	01/01/2002	16/07/1994	20/07/1993	12/07/2010
Sex			M	M	M	F	M	M
Dysmorphisms								
Long eyelashes	89% +	81% +	+	+	+	+	+	+
Synophrys	5-30% +/-	>30% +	-	-	+	-	+	+
Ptosis	<82% +	31% +	+	+	-	+	+	-
Downslanting palpebral fissures	75% +	64% +	+	+	-	-	+	+
Thick eyebrow	>30% +	64% +	+	-	+	+/-	+	-
Narrow palpebral fissures	-	74% +	+	+	-	+	+	+
Hyperthelorism	5% +/-	71% +	+	-	Telecanthus	+	Telecanthus	+
Columella below the alae nasi	89% +	-	+	+	+/-	+	NA	+
Wide nasal bridge	-	68% +	+	+	-	+	+	-
Grimacing smile	80% +	-	+	-	+/-	-	NA	+
High-arched palate	75% +	>30% +	+	NA	NA	-	+	+
Micrognathia	57% +	>30% +	-	+	-	-	+	+
Low set ears	>30% +	46% +	+	+	+/-	-	-	-
Strabismus	-	-	-	-	-	-	+	-

Table 1 (continued)

	RSTS	WDSTS	RSTS-208	RSTS-250	RSTS-187	RSTS-251	RSTS-243	RSTS-221
	60–71%							
Flammeus nevus/ angioma	+ 5–30% +/-	-	-	NA	-	-	-	NA
Growth failure								
IUGR	-	>30% +	-	-	-	NA	-	Unknown
PNGR	73% +	38% +	+	-	+/-	NA	+	+
Intellectual disability	98% +	98% +	+++	++	+	+	+	+++
Speech delay/absence	90% +	82% +	-	+	+	+	+	+
Behavioral problems	41% +	42% +	+	+	+		++	NA
Vision problems								
Myopia	9% +/-	-	-	-	-	NA	-	-
Teeth anomalies	>30% +	-	-	-	NA	NA	+	-
Musculoskeletal anomalies								
Broad thumbs	91% +	-	-	+	+/-	-	+	+
Angulated thumbs	42% +	-	+	-	-	-	-	+
Broad halluces	92% +	-	+	+	+	-	+	+
Clinodactyly	5–30% +/-	23% +/-	-	-	-	-	+	-
Brachydactyly	5–30% +/-	45% +	-	-	-	-	-	+
Microcephaly	63% +	-	-	+	-	NA	-	+
Delayed bone age	74% +	34% +	-	NA	-	NA	-	-
Hypotonia	70% +	73% +	-	NA	-	NA	+	+
Organ anomalies								

Table 1 (continued)

	RSTS	WDSTS	RSTS-208	RSTS-250	RSTS-187	RSTS-251	RSTS-243	RSTS-221
Cryptorchidism	78–100% +	–	–	–	–	–	–	Mobile testis
Heart defect	24–38% +/-	29% +/-	–	–	–	–	–	–
Brain anomalies								
Abnormal corpus callosum	17% +/-	14% +/-	–	NA	–	NA	–	–
Seizures	25% +/-	9% +/-	–	NA	–	–	–	–
Hirsutism	>30% +	>30% +	–	–	+	NA	+	+
Keloids/naevi	24% +/-	–	–	NA	–	–	–	–
Pilomatricoma	5–30% +/-	–	–	NA	–	–	–	–
Frequent infections	75% +	–	–	NA	–	NA	–	–
Feeding problems	80% +	53% +	–	NA	–	NA	+	+
Gastroesophageal reflux	68% +	–	–	NA	+	NA	–	–
Others			Prominent eyes; thin upper lip; C2–C3 vertebral fusion; cerebellar vermis hypoplasia; organomegaly	Thin upper lip; autism spectrum disorder; epileptiform abnormalities in the left fronto-temporal region	Early puberty (treated)	Thin lips	Thin lips; hearing loss; altered fine motor abilities; born at 35 weeks; pregnancy with a threatened miscarriage	Thin lips; kyphosis; abnormal ears

NA not assessed.

+ = Present (>30%).

– = Absent (unreported).

+/- = Present in a few cases (5–30%).

Caller module. Variants were classified as known or novel based on dbSNP146 and annotated using KGGSeq. Annotations were retrieved from dbNSFP v.3.0 and included positions in UCSC, RefGene, GENCODE, and ENSEMBL transcripts, OMIM and ClinVar annotations, allele frequency in dbSNP, ESP6500 (release SI-V2), 1000 Genomes Project (release 05/2013), ExAC and gnomAD, functional predictions for the amino-acid changes according to different models (SIFT, PolyPhen2, LRT, Pathogenic variantTaster, Pathogenic variantAssessor, and FATHMM). We filtered the identified variants according to recessive/dominant/*de novo* pattern of inheritance, gene features and $MAF < 1\%$ using as references dbSNP138, dbSNP141, 1000 Genomes, ESP6500, ExAC, and gnomAD. Subsequently, variants were evaluated for their phenotypic and biological impact.

Variants validation and segregation analysis

Variants of interest were confirmed by Sanger sequencing following PCR amplification and segregation analysis was performed in the available family trio. PCR reactions were ruled following the protocol for GoTaq Flexi DNA Polymerase (Promega) with patients' and variants' specific primer sets considering NG_027813.1 as reference for *KMT2A* gene. The same pairs of primers were used for Sanger sequencing. *KMT2A* exons are numbered like in ENST00000534358.8 reference. Sequence variants were described according to HGVS nomenclature guidelines (<https://varnomen.hgvs.org/>) and reported in LOVD (<https://databases.lovd.nl/shared/genes/KMT2A>) as individual IDs #00275545 (pt #208), #00275547 (pt #250), #00275548 (pt #187), #00275549 (pt #251), #00275550 (pt #243), and #00275551 (pt #221).

Results

KMT2A detected variants

CREBBP and *EP300* MLPA analysis was previously performed for all the six described patients and resulted negative. Patients #187, #208, and #221 underwent also *CREBBP* direct sequencing, without detecting pathogenic variants. Hence, we performed NGS analysis with a custom-made panel comprising 68 genes known as causative of chromatinopathies [25], including *CREBBP* and *EP300* genes, to 30 patients, including all the patients here described, except patient #187. NGS exome analysis was applied to #187 trio and additional nine patients. We detected in six patients (five out of 30 tested by multigene panel sequencing and one out of 10 analysed by WES) a novel heterozygous variant in *KMT2A* (Table 1).

In particular, patient #208 was found carrier of a *de novo* nucleotide substitution in exon 3: c.553C>T, predicted to cause a premature stop codon p.(Arg185*); patient #250 shows a 21 nucleotides insertion in exon 3: c.1697_1717dup, resulting in an aminoacidic in frame duplication p.(Leu566_Leu572dup). Patient #250 parents' DNA is not available for further testing.

Patients #187, #251, and #243 are carriers of three different *de novo* variants in exon 6: a single nucleotide change c.3596G>A leading to a premature stop codon p.(Trp1199*) in patient #187, a single nucleotide deletion c.3603del, causing a frameshift p.(Ser1202Profs*12) in patient #251 and a five nucleotides deletion c.3632_3634+2del involving the last three nucleotide of exon 6 and the first two bases of the following intronic sequence, suggesting a possible effect on the correct splicing, in patient #243.

Finally, patient #221 is carrier of a four nucleotides duplication in exon 7 c.3897_3900dup, leading to a frameshift p.(Leu1303Serfs24*). The patient is adopted, making impossible verifying the *de novo* origin of this variant.

According to ACMG guidelines, the clinical significance of the variants is pathogenic for patients #208, #187, #251, and #243 as all the variants meet the same ACMG criteria (PVS1, PM2, and PP3). Variant detected in patient #250 has been classified with uncertain significance (PM2, PM4, and BP4), probably due to the lack of predicted impact on gene product, while patient #221 was found carrier of a likely pathogenic variant (PVS1, PM2).

Clinical phenotypes

Patient #208

The patient is a 13 years old boy, born with normal birth parameters. Postnatal growth deficiency was reported. Minor facial anomalies were evident such as downslanting palpebral fissures, columella below the alae nasi, grimacing smile and hypertelorism, broad nasal bridge, long eyelashes, and prominent eyes. Angulated thumbs and broad halluces are present. He shows severe ID and behavioral issues, with aggression. In addition, C2–C3 vertebral fusion, organomegaly, and cerebellar vermis hypoplasia were reported.

Patient #250

Patient 250 is a 16 years old boy. A RSTS diagnosis was suspected for the presence of dysmorphisms such as columella below the alae nasi, grimacing smile, and for the skeletal anomalies of hand and feet (broad thumbs and halluces). Unfortunately, parents of patient 250 refuse a clinical reevaluation of their son and are unavailable to give



Fig. 1 Features of patients #187, #243, and #251, found carriers of *KMT2A* variants. Facies appearance of patient #187 was shown at neonatal age, at 2 and 10 years with particular of hand and foot (a).

Facies of patient #243 at 2, at 9 and 23 years and hands/feet particulars (b). Facies and foot (c) particular of patient #251 at 16 years.

their DNA making impossible test the *de novo* origin of *KMT2A* variant, detected in the son.

Patient #187

Patient 187 is a 17 years old boy, born after an uneventful pregnancy with normal birth parameters (weight 3.045 kg, length 47 cm; occipitofrontal circumference (OFC) 33.5 cm, APGAR 8/9). Neonatal hypotonia, a sacral dimple (S4–S5) and postnatal growth deficiency were described. He furthermore had a diagnosis of precocious puberty. Psychomotor development was delayed, with a moderate ID and some behavioral difficulty (anxiety in particular). Cerebral and medullary MRI showed craniocervical junction anomalies with a mild basilar impression. Clinical evaluation pointed out a relative macrocephaly, low anterior hairline, synophrys, long eyelashes, bulbous nose, low set ears, upturned corners of mouth, broad thumbs and halluces, and hirsutism.

Patient #251

Patient #251 is a 25 years old girl, born after an uneventful pregnancy with normal birth parameters (weight 3.100 kg). A gastroesophageal reflux was described. Psychomotor development was delayed, with a moderate ID. Cerebral and medullary MRI showed craniocervical junction anomalies with a mild basilar impression. Clinical evaluation pointed out long eyelashes, long and downslanting palpebral fissures, strabismus, epicanthal folds, hypertelorism, high nasal bridge, columella below alae nasi, upturned corners of mouth, broad halluces, and kyphoscoliosis.

Patient #243

Patient #243 is a 26 years old boy, born at 35 weeks of gestation. Parents were healthy and non-consanguineous.

The pregnancy showed several threatened miscarriages. Weight was 2.750 kg (+0.66 SD), APGAR score 7 and 8 at 1 and 5 min respectively. At the birth: transient polypnea of the newborn and cyanosis, jaundice treated with phototherapy are recorded. Around the age of 6 months, he showed growth and psychomotor retardation and hypotonia. At the auxological evaluation at 10 months of age: length was 67 cm (<3rd centile), weight 6.8 kg, OFC 44.3 cm. GH deficit was diagnosed at 2 years of life and GH therapy was started with good results and continued until 14.5 years. Early puberty was diagnosed at 7 years of life and treated with triptorelin therapy until 9.5 years. Final height was 164.8 cm (3rd centile), target height 171.5 cm (25th centile). At the clinical evaluation hypotonia, hypertrichosis, facial dysmorphism (telecanthus, downslanted and narrow palpebral fissures, and long eyelashes), broad thumbs, and broad distal fingertips were reported. Strabismus has been surgically corrected at 2.5 years of age. Speech language was delayed and he showed learning disability, mild ID and aggressive behavior. At the last examination at 21 years of age aggressive behavior with selective feeding has been confirmed.

Patient #221

Patient #221 is a 9 years old male child. He was adopted and the only information on biological family is that the parents were non-consanguineous. He showed dysmorphism such as coarse face, low anterior airline, synophrys, narrow forehead, hypertelorism, high arched and heavy eyebrows, long eyelashes, narrow and downslanting palpebral fissures, convex nasal bridge, short philtrum, thin lips, high-arched and narrow-palate, micrognathia and abnormal ears, and skeletal anomalies such as brachydactyly, broad and angulated thumbs, broad halluces and kyphosis. Clinical examination also reveals hirsutism, hypertrichosis, mobile testis and anamnestic record disclose

feeding problems, postnatal growth retardation, psychomotor delay (hypotonia, delayed erected head, sat and walked independently, and began speaking words at 4 years), and severe ID. At the age of 7.5 years his weight was 22.750 kg (10–25th pc), his height was 106 cm (<−3 SD), and his OFC measured 46.2 cm (<−4 SD). Electroencephalogram and cerebral MRI did not reveal any brain abnormalities; visual evoked potential and auditory brain stem responses to complex sounds (cABRs) were normal too. Ultrasound of the abdomen, ECG, and echocardiography were normal.

Table 1 summarizes the clinical features of six patients here described, comparing the clinical signs of each patient and the typical features of RSTS and WDSTS.

There are many clinical signs shared by RSTS and WDSTS patients described in the literature (growth retardation, ID, and specific dysmorphisms). The clinical reevaluation of patients shows that they display some typical RSTS features that appear more evident during childhood, but also various WDSTS specific signs with a peculiar global clinical presentation. All the described patients show the most frequent RSTS signs such as columella below alae nasi (5/5), broad thumbs/hallux (4/6, 5/6), and ptosis (4/6) (Fig. 1), but also typical WDSTS clinical features such as broad nasal tip (4/6), narrow palpebral fissures (5/6), and hirsutism (3/6).

Discussion

Chromatinopathies define a group of diseases caused by alterations in genes coding for components of the epigenetic apparatus termed “writers, erasers, readers, and remodelers”. These proteins act in concert to control the chromatin opening and closing thus, regulating gene expression by modification (i.e., methylation, acetylation, etc.) of histones and DNA methylation [25].

Due to the clinical overlap between different chromatinopathies and the functional network between the epigenetic components, pathogenic variants in a same “epigene” could be responsible for overlapping and/or slightly different clinical presentation cases.

Accordingly, in a recent work we found that some RSTS-like patients found negative for mutations in the two causative genes turned out to be carriers of variants in other chromatinopathies genes such as *KMT2D* (associated to Kabuki syndrome, KS; OMIM #147920), *ASXL1* (associated to Bohring–Opitz syndrome, BOS; OMIM #605039), and *KMT2A* (associated to Wiedemann–Steiner syndrome WDSTS; OMIM #605130) by WES analysis [24]. These results strongly suggest a possible implication of defective histone-modifying enzymes, other than CBP and p300, in the pathogenesis of RSTS-like phenotype. These findings

are in line with the known significant phenotypic overlap observed among Mendelian disorders involving the epigenetic machinery which likely reflects the interconnected pathways involved in the complex regulation of balance between open and closed chromatin [25, 31].

In the present study, we used a custom NGS panel or WES to screen RSTS patients who resulted negative for mutations in *CREBBP* and *EP300* and exome analysis in one trio. We identified six different novel variants in *KMT2A* (5/6 classified as pathogenic/likely pathogenic). Pathogenic variants in this gene, coding for a member of the Lysine methyltransferase 2 family cause the WDSTS.

The identified variants are *de novo* (for the 4/6 patients whose parents are available) and unreported, but indiscernible for type and localization from variants described in WDSTS patients. Interestingly, patients #208 and #221 display a more severe phenotype, although they are carriers of variants predicted pathogenic and likely pathogenic respectively. This is probably due to the involvement of protein domain affected by the *KMT2A* variant, which in patient #208 affects the AT hook domain, while in patient #221 any specific domain is involved. However, lack of a complete molecular picture for patient #221 (as adopted child) unfortunately prevents depth genotype–phenotype correlation. The clinical reevaluation shows that patients display the typical RSTS features, more evident in childhood, but also some WDSTS specific signs with a peculiar global clinical presentation, making difficult the correct diagnosis. WDSTS is a recently defined rare chromatinopathy (first description in 1989) and its clinical signs show several overlapping features with other chromatinopathies. Nevertheless, peculiar clinical signs such as hypertrichosis *cubiti* and a typical facial appearance are present in almost all the WDSTS reported patients [4]. *KMT2A* variants are reported also in one Coffin–Siris (CSS) patient (pt #K2431 in Bramswig et al. [20]), in two Cornelia de Lange syndrome (CdLS) patients (Yuan et al. [21], patient CdLS #3 and Parenti et al. [22], patient #1), in two patients with a diagnosis of Kabuki syndrome (KS) (patients KS8 and KS29 in Sobreira et al. [23]) and in another RSTS-like patient from our previous cohort (Negri et al. [24], pt #103). Recently, several papers [12–15, 17–19] report *KMT2A* pathogenic variants in patients without the “obligate” specific WDSTS clinical feature showing a broader phenotypic spectrum due to *KMT2A* alterations. All the above cited clinical conditions and in particular WDSTS and RSTS show several phenotypic overlapping (e.g., growth deficiency, neurological/cognitive impairment, similar dysmorphisms, and limb anomalies), as observed in our cohort, but we can envisage also a shared molecular cause. In all these cases, in fact, the causative variants affect a gene coding an epigenetic player that, by modulating the interconnected DNA methylation and histone acetylation/

methylation, define a correct and site-specific chromatin opening/closing balance. A loss of a specific player could perturb the equilibrium leading to similar consequences or to a spectrum of overlapping clinical conditions.

Reports in literature point out that variants in the same gene can lead to different phenotypes with a set of common features indicative of a group of disorders. On the other side, variants in different genes encoding proteins implicated in the same cellular pathway can lead to the same phenotype. The different clinical outcomes due to variants in the same gene can be attributed not only to specific genotype–phenotype correlations, but also, to stochastic events occurring during development and the different genetic background among patients [20, 32, 33].

In summary, using a NGS-dedicated approach, we found *KMT2A* variants in six patients with an initial RSTS clinical diagnosis, supporting that different mechanisms leading to imbalance of chromatin opening/closing can converge to a similar phenotype characterized by several overlapping RSTS/WDSTS clinical signs. Moreover, these patients show a moderately different spectrum of clinical findings, suggesting that different *KMT2A* variants or allelic heterogeneity could contribute to the wide variability of observed phenotypes of chromatinopathies.

Acknowledgements We thank the patients' families for participating in this study. CG thanks the Italian Association of Rubinstein–Taybi patients “RTS Una Vita Speciale ONLUS” for its support.

Funding This work was supported by Fondazione Cariplo (2015-0783 to VM), by intramural funding (Università degli Studi di Milano linea 2 to CG), by Associazione “RTS Una Vita Speciale ONLUS” (#DigiRare to CG), by grant “Aldo Ravelli Center” (to VM and CG); by Translational Medicine Ph.D.—Università degli Studi di Milano scholarship (to EDF); by Telethon—Italy (GGP13231 to GM), Italian Ministry of Health, Jerome Lejeune Foundation, Daunia Plast, Circolo Unione Apricena, Fidapa Apricena, and Associazione Italiana Sindrome Kabuki (AISK) (to GM).

Compliance with ethical standards

Conflict of interest The authors declare that they have no conflict of interest.

Ethical approval All the studies involving patients were in accordance with the 1964 Helsinki declaration and its later amendments or comparable ethical standards.

Informed consent Informed consent of patients was collected for biological samples studies and photographs publication (pts #187, #243, and #251).

Publisher's note Springer Nature remains neutral with regard to jurisdictional claims in published maps and institutional affiliations.

Open Access This article is licensed under a Creative Commons Attribution 4.0 International License, which permits use, sharing, adaptation, distribution and reproduction in any medium or format, as

long as you give appropriate credit to the original author(s) and the source, provide a link to the Creative Commons license, and indicate if changes were made. The images or other third party material in this article are included in the article's Creative Commons license, unless indicated otherwise in a credit line to the material. If material is not included in the article's Creative Commons license and your intended use is not permitted by statutory regulation or exceeds the permitted use, you will need to obtain permission directly from the copyright holder. To view a copy of this license, visit <http://creativecommons.org/licenses/by/4.0/>.

References

1. Lim DA, Huang YC, Swigut T, Mirick AL, Garcia-Verdugo JM, Wysocka J, et al. Chromatin remodelling factor Mll1 is essential for neurogenesis from postnatal neural stem cells. *Nature*. 2009;458:529–33.
2. Krivtsov AV, Armstrong SA. MLL translocations, histone modifications and leukaemia stem-cell development. *Nat Rev Cancer*. 2007;7:823–33.
3. Wiedemann HR, Kunze J, Grosse FR, Dibbern H. A syndrome of abnormal facies, short stature, and psychomotor retardation. In: Wiedemann HR, Kunze J, Grosse FR, Dibbern H (eds). *Atlas of clinical syndromes: a visual aid to diagnosis for clinicians and practicing physicians*. 2nd edn. (Wolfe Publishing Ltd, London, 1989), pp 198–199.
4. Jones WD, Dafou D, McEntagart M, Woollard WJ, Elmslie FV, Holder-Espinasse M, et al. *De novo* mutations in MLL cause Wiedemann–Steiner syndrome. *Am J Hum Genet*. 2012;91:358–64.
5. Aggarwal A, Rodriguez-Buritica DF, Northrup H. Wiedemann–Steiner syndrome: novel pathogenic variant and review of literature. *Eur J Med Genet*. 2017;60:285–8.
6. Enokizono T, Ohto T, Tanaka R, Tanaka M, Suzuki H, Sakai A, et al. Preaxial polydactyly in an individual with Wiedemann–Steiner syndrome caused by a novel nonsense mutation in *KMT2A*. *Am J Med Genet A*. 2017;173:2821–5.
7. Feldman HR, Dlouhy SR, Lah MD, Payne KK, Weaver DD. The progression of Wiedemann–Steiner syndrome in adulthood and two novel variants in the *KMT2A* gene. *Am J Med Genet A*. 2019;179:300–5.
8. Stoye G, Banka S, Langley C, Jones EA, Banerjee I. Growth hormone deficiency as a cause for short stature in Wiedemann–Steiner syndrome. *Endocrinol Diabetes Metab Case Rep*. 2018;2018. <https://doi.org/10.1530/edm-18-0085>.
9. Ramirez-Montañó D, Pachajoa H. Wiedemann–Steiner syndrome with a novel pathogenic variant in *KMT2A*: a case report. *Colomb Med*. 2019;50:40–5.
10. Grangeia A, Leão M, Moura CP. Wiedemann–Steiner syndrome in two patients from Portugal. *Am J Med Genet A*. 2019. <https://doi.org/10.1002/ajmg.a.61407>.
11. Chen M, Liu R, Wu C, Li X, Wang Y. A novel *de novo* mutation (p.Pro1310Glnfs*46) in *KMT2A* caused Wiedemann–Steiner syndrome in a Chinese boy with postnatal growth retardation: a case report. *Mol Biol Rep*. 2019;46:5555–9.
12. Martínez F, Caro-Llopis A, Roselló M, Oltra S, Mayo S, Monfort S, et al. High diagnostic yield of syndromic intellectual disability by targeted next-generation sequencing. *J Med Genet*. 2017;54:87–92.
13. Popp B, Ekici AB, Thiel CT, Hoyer J, Wiesener A, Kraus C, et al. Exome Pool-Seq in neurodevelopmental disorders. *Eur J Hum Genet*. 2017;25:1364–76.
14. Lebrun N, Giurgea I, Goldenberg A, Dieux A, Afenjar A, Ghomid J, et al. Molecular and cellular issues of *KMT2A* variants involved in Wiedemann–Steiner syndrome. *Eur J Hum Genet*. 2018;26:107–16.

15. Baer S, Afenjar A, Smol T, Piton A, Gérard B, Alembik Y, et al. Wiedemann-Steiner syndrome as a major cause of syndromic intellectual disability: a study of 33 French cases. *Clin Genet*. 2018;94:141–52.
16. Li N, Wang Y, Yang Y, Huang H, Xiong S, Sun L, et al. Description of the molecular and phenotypic spectrum of Wiedemann-Steiner syndrome in Chinese patients. *Orphanet J Rare Dis*. 2018;13. <https://doi.org/10.1186/s13023-018-0909-0>.
17. Helbig KL, Farwell Hagman KD, Shinde DN, Mroske C, Powis Z, Li S, et al. Diagnostic exome sequencing provides a molecular diagnosis for a significant proportion of patients with epilepsy. *Genet Med*. 2016;18:898–905.
18. Bogaert DJ, Dullaers M, Kuehn HS, Leroy BP, Niemela JE, De Wilde H, et al. Early-onset primary antibody deficiency resembling common variable immunodeficiency challenges the diagnosis of Wiedemann-Steiner and Roifman syndromes. *Sci Rep*. 2017;7. <https://doi.org/10.1038/s41598-017-02434-4>.
19. Zhang H, Xiang B, Chen H, Chen X, Cai T. A novel deletion mutation in *KMT2A* identified in a child with ID/DD and blood eosinophilia. *BMC Med Genet*. 2019;20. <https://doi.org/10.1186/s12881-019-0776-0>.
20. Bramswig NC, Lüdecke HJ, Alanay Y, Albrecht B, Barthelmie A, Boduroglu K, et al. Exome sequencing unravels unexpected differential diagnoses in individuals with the tentative diagnosis of Coffin-Siris and Nicolaides-Baraitser syndromes. *Hum Genet*. 2015;134:553–68.
21. Yuan B, Pehlivan D, Karaca E, Patel N, Charng WL, Gambin T, et al. Global transcriptional disturbances underlie Cornelia de Lange syndrome and related phenotypes. *J Clin Investig*. 2015;125:636–51.
22. Parenti I, Teresa-Rodrigo ME, Pozojevic J, Ruiz Gil S, Bader I, Braunholz D, et al. Mutations in chromatin regulators functionally link Cornelia de Lange syndrome and clinically overlapping phenotypes. *Hum Genet*. 2017;136:307–20.
23. Sobreira N, Brucato M, Zhang L, Ladd-Acosta C, Ongaco C, Romm J, et al. Patients with a Kabuki syndrome phenotype demonstrate DNA methylation abnormalities. *Eur J Hum Genet*. 2017;25:1335–44.
24. Negri G, Magini P, Milani D, Crippa M, Biamino E, Piccione M, et al. Exploring by whole exome sequencing patients with initial diagnosis of Rubinstein-Taybi syndrome: the interconnections of epigenetic machinery disorders. *Hum Genet*. 2019;138. <https://doi.org/10.1007/s00439-019-01985-y>.
25. Fahrner JA, Bjornsson HT. Mendelian disorders of the epigenetic machinery: postnatal malleability and therapeutic prospects. *Hum Mol Genet*. 2019. <https://doi.org/10.1093/hmg/ddz174>.
26. Valor LM, Viosca J, Lopez-Atalaya JP, Barco A. Lysine acetyltransferases CBP and p300 as therapeutic targets in cognitive and neurodegenerative disorders. *Curr Pharm Des*. 2013;19:5051–64.
27. Petrif F, Giles RH, Dauwerse HG, Saris JJ, Hennekam RCM, Masuno M, et al. Rubinstein-Taybi syndrome caused by mutations in the transcriptional co-activator CBP. *Nature*. 1995;376:348–51.
28. Hamilton MJ, Newbury-Ecob R, Holder-Espinasse M, Yau S, Lillis S, Hurst JA, et al. Rubinstein-Taybi syndrome type 2: report of nine new cases that extend the phenotypic and genotypic spectrum. *Clin Dysmorphol*. 2016;25:135–45.
29. RUBINSTEIN JH, TAYBI H. Broad thumbs and toes and facial abnormalities. A possible mental retardation syndrome. *Am J Dis Child*. 1963;105:588–608.
30. Hennekam RCM. Rubinstein-Taybi syndrome. *Eur J Hum Genet*. 2006;14:981–5.
31. Kleefstra T, Schenck A, Kramer JM, Van Bokhoven H. The genetics of cognitive epigenetics. *Neuropharmacology*. 2014;80:83–94.
32. Woods SA, Robinson HB, Kohler LJ, Agamanolis D, Sterbenz G, Khalifa M. Exome sequencing identifies a novel EP300 frame shift mutation in a patient with features that overlap Cornelia de Lange syndrome. *Am J Med Genet A*. 2014;164A:251–8.
33. Schulz Y, Freese L, Mänz J, Zoll B, Völter C, Brockmann K, et al. CHARGE and Kabuki syndromes: a phenotypic and molecular link. *Hum Mol Genet*. 2014;23:4396–405.



Article

Insights into the Role of the Microbiota and of Short-Chain Fatty Acids in Rubinstein–Taybi Syndrome

Elisabetta Di Fede ^{1,†}, Emerenziana Ottaviano ^{1,†}, Paolo Grazioli ¹, Camilla Ceccarani ^{1,2}, Antonio Galeone ³, Chiara Parodi ¹, Elisa Adele Colombo ¹, Giulia Bassanini ¹, Grazia Fazio ⁴, Marco Severgnini ², Donatella Milani ⁵, Elvira Verduci ^{1,6}, Thomas Vaccari ³, Valentina Massa ^{1,7,‡}, Elisa Borghi ^{1,‡} and Cristina Gervasini ^{1,7,*}

- ¹ Department of Health Sciences, Università degli Studi di Milano, 20142 Milan, Italy; elisabetta.difede@unimi.it (E.D.F.); emerenziana.ottaviano@unimi.it (E.O.); paolo.grazioli@unimi.it (P.G.); camilla.ceccarani@unimi.it (C.C.); chiara.parodi@unimi.it (C.P.); elisaadele.colombo@unimi.it (E.A.C.); giulia.bassanini@unimi.it (G.B.); elvira.verduci@unimi.it (E.V.); valentina.massa@unimi.it (V.M.); elisa.borghi@unimi.it (E.B.)
- ² Institute of Biomedical Technologies, Italian National Research Council, Segrate, 20054 Milan, Italy; marco.severgnini@itb.cnr.it
- ³ Department of Biosciences, Università degli Studi di Milano, 20133 Milano, Italy; antonio.galeone@unimi.it (A.G.); thomas.vaccari@unimi.it (T.V.)
- ⁴ Tettamanti Research Center, Department of Pediatrics, Università degli Studi di Milano-Bicocca, MBBM Foundation/San Gerardo Hospital, 20900 Monza, Italy; grazia.fazio@unimib.it
- ⁵ Fondazione IRCCS Ca' Granda Ospedale Maggiore Policlinico, 20122 Milan, Italy; donatella.milani@policlinico.mi.it
- ⁶ Department of Pediatrics, Vittore Buzzi Children's Hospital, University of Milan, 20154 Milan, Italy
- ⁷ "Aldo Ravelli" Center for Neurotechnology and Experimental Brain Therapeutics, Università degli Studi di Milano, 20142 Milan, Italy
- * Correspondence: cristina.gervasini@unimi.it; Tel.: +39-02-5032-3028
- † These authors contributed equally to this work.
- ‡ These authors contributed equally to this work.



Citation: Di Fede, E.; Ottaviano, E.; Grazioli, P.; Ceccarani, C.; Galeone, A.; Parodi, C.; Colombo, E.A.; Bassanini, G.; Fazio, G.; Severgnini, M.; et al. Insights into the Role of the Microbiota and of Short-Chain Fatty Acids in Rubinstein–Taybi Syndrome. *Int. J. Mol. Sci.* **2021**, *22*, 3621. <https://doi.org/10.3390/ijms22073621>

Academic Editor: Rustam Aminov

Received: 22 February 2021

Accepted: 27 March 2021

Published: 31 March 2021

Publisher's Note: MDPI stays neutral with regard to jurisdictional claims in published maps and institutional affiliations.



Copyright: © 2021 by the authors. Licensee MDPI, Basel, Switzerland. This article is an open access article distributed under the terms and conditions of the Creative Commons Attribution (CC BY) license (<https://creativecommons.org/licenses/by/4.0/>).

Abstract: The short-chain fatty acid butyrate, produced by the gut microbiota, acts as a potent histone deacetylase (HDAC) inhibitor. We assessed possible ameliorative effects of butyrate, relative to other HDAC inhibitors, in in vitro and in vivo models of Rubinstein–Taybi syndrome (RSTS), a severe neurodevelopmental disorder caused by variants in the genes encoding the histone acetyltransferases CBP and p300. In RSTS cell lines, butyrate led to the patient-specific rescue of acetylation defects at subtoxic concentrations. Remarkably, we observed that the commensal gut microbiota composition in a cohort of RSTS patients is significantly depleted in butyrate-producing bacteria compared to healthy siblings. We demonstrate that the effects of butyrate and the differences in microbiota composition are conserved in a *Drosophila melanogaster* mutant for CBP, enabling future dissection of the gut–host interactions in an in vivo RSTS model. This study sheds light on microbiota composition in a chromatinopathy, paving the way for novel therapeutic interventions.

Keywords: Rubinstein–Taybi syndrome; butyrate; microbiota; HDACi; histones

1. Introduction

Gene expression regulation is mediated by tightly balanced epigenetic mechanisms involving histone modifications, such as acetylation and methylation. Correct histone acetylation levels on lysine residues are fundamental for several physiological processes, including embryonic development [1,2]. Two classes of functionally antagonistic enzymes, the acetyltransferases (HAT) and deacetylases (HDAC), are known to modulate histone acetylation levels [3]. Histones hypoacetylation has been associated with alterations in synaptic plasticity, neuronal survival/regeneration, memory formation [4], while defects

in epigenetic components acting on acetylation status cause several neurodevelopmental/malformation syndromes [5]. Among them, Rubinstein–Taybi syndrome (RSTS, OMIM #180849, #613684) is a rare (1:125,000) autosomal-dominant disease characterized by a wide and heterogeneous spectrum of clinical signs [6]. These include intellectual disability of variable entity (ranging from mild to severe), postnatal growth deficiency, distinctive dysmorphisms, skeletal abnormalities (such as typical broad thumbs and large toes), multiple congenital anomalies (e.g., heart defects), and several additional clinical problems such as constipation [7]. Albeit the growth in height is constantly reduced in RSTS patients, growth in weight is reduced neonatally and in the first infancy, but at puberty an excessive weight gain is observed [8].

Most RSTS cases are caused by de novo monoallelic variants of one of two highly conserved genes: *CREBBP*, located at 16p13.3, coding for the CREB (cAMP response element-binding protein) binding protein (CBP) and *EP300*, mapping at 22q13.2, coding for the E1A-associated protein p300. *CREBBP* is found mutated in >50% RSTS patients, while *EP300* gene mutations have been described in a minor fraction of patients [9].

Somatic mutations in *CREBBP* and *EP300* are reported in different benign and malignant tumors, and an association between RSTS patients and tumor development has been investigated. This disorder is related to an increased risk of malignancies up to 5%, in particular involving cutaneous, hematological, and brain tumors such as pilomatrixoma, leukemia, and meningioma, respectively [10,11].

CBP and p300 have ubiquitously expressed paralog proteins belonging to the lysine acetyl transferases (HAT) family [12]. CBP and p300 act as co-factors for transcription and are required in multiple pathways controlling cell growth, DNA repair, cell differentiation, and tumor suppression [13–16]. Their acetylation of target histone tails enables the opening of chromatin, thus promoting gene expression [13,15,17].

In recent years, a novel class of compounds, termed HDAC inhibitors (HDACi), has been used to increase histone acetylation in different pathologies [18,19]. Preliminary studies testing the efficiency of HDACi to revert acetylation defects in RSTS lymphoblastoid cell lines (LCLs) supported the hypothesis that RSTS is caused by an acetylation imbalance [20]. Animal model studies introduced the idea that the chromatin alterations observed in RSTS could be reverted [21].

It has been demonstrated that protein acetylation can be modulated by the commensal microbial community (microbiota from here on) [22]. In fact, short-chain fatty acids (SCFAs), such as acetate, propionate, and butyrate, the most abundant products of anaerobic fermentation of the gut microbiota, can act as HDACi. Among SCFAs, butyrate is exclusively produced by commensal microorganisms and widely reported for its epigenetic activity, making it the most potent HDACi among natural compounds [23,24]. However, the role of butyrate or the composition of the microbiota in RSTS have not been investigated. Altered gut microbiota could itself affect the endogenous levels of SCFAs in patients, it could participate in their typical RSTS growth trend, characterized by a deficit in infancy and excessive weight gain after puberty, and/or it could contribute to the comorbidities often associated with RSTS, such as gastrointestinal discomfort [8].

On these premises, in the present study, we compared butyrate to other HDACi molecules in vitro on lymphoblastoid cell lines (LCLs) derived from RSTS patients. We have found it effective in modulating the acetylation impairment associated with reported CBP/p300 defects [20]. Remarkably, we also find that the microbiota of RSTS patients is poor in SCFA-producing bacteria, perhaps further contributing to acetylation imbalance. Finally, using *Drosophila melanogaster*, we model the effects of butyrate and microbiota alterations for future in vivo studies. Our work points to the importance of the microbiome in the pathogenesis and treatment of ultra-rare diseases.

2. Results

2.1. HDACi Exposure Counteracts Acetylation Imbalance in RSTS Lymphoblastoid Cell Lines (LCLs)

To investigate the effect of SCFAs as HDACi in RSTS, we exposed LCLs derived from eight patients, four with *CREBBP* and four with *EP300* mutations (Table S1) and seven healthy donors (HD) to sodium butyrate (NaB), and we compared the effect to that of three other HDACi: trichostatin A (TSA), suberoylanilide hydroxamic acid (SAHA), and valproic acid (VPA) (Table S2). By AlphaLISA[®] assay, we analyzed the acetylation levels of lysine 27 of histone H3 (H3K27ac) in LCLs upon three different conditions: HDACi treatments, exposure to the vehicle (DMSO or H₂O), and untreated cells (Figure 1).

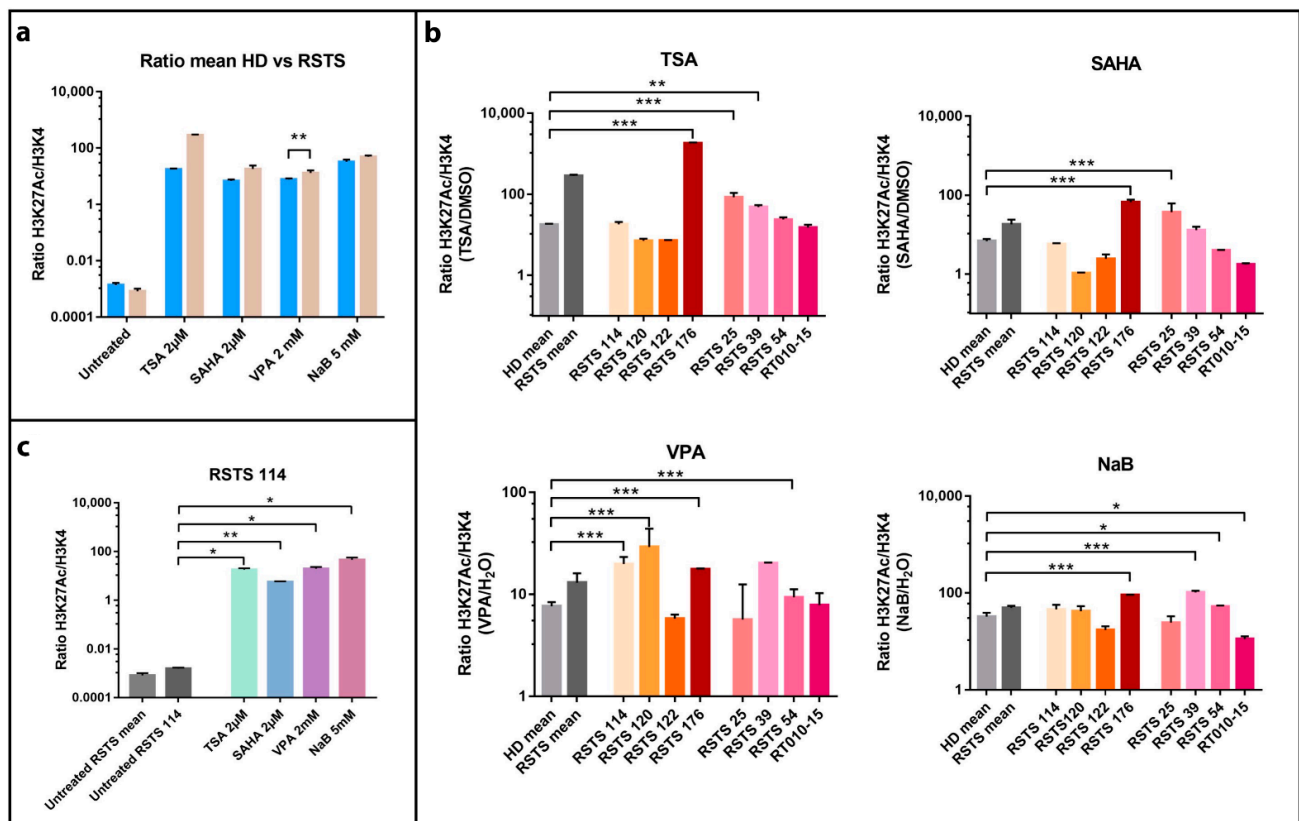


Figure 1. Histone acetylation on Rubinstein–Taybi syndrome (RSTS) lymphoblastoid cell lines (LCLs) upon acetyltransferases (HAT) and deacetylases (HDAC) inhibitors exposure. H3K27 acetylation levels normalized on H3K4 unmodified, assessed by AlphaLISA[®]; levels of acetylation upon HDAC inhibitors (HDACi) are expressed as a ratio between the treatment and respective vehicle (HDACi/vehicle); on the Log scale, Y-axis H3K27 acetylation levels normalized, on X-axis lists of epigenetic treatments or untreated/treated single LCL or LCLs means. (a) Means of values of H3K27 acetylation in healthy donors (HD, in blue) and patients LCLs (RSTS, in pale brown) untreated and exposed to four different HDACi (trichostatin A (TSA) 2 μM, suberoylanilide hydroxamic acid (SAHA) 2 μM, valproic acid (VPA) 2 mM, and sodium butyrate (NaB) 5 mM). (b) H3K27 acetylation in eight RSTS LCLs (*CREBBP* LCLs in shades of red, *EP300* LCLs in shades of pink) after exposure with the four different HDACi, compared to treated HD and RSTS means. (c) Insight on the single-patient response (RSTS 114) to the four compounds compared to untreated RSTS means and RSTS 114. Groups were compared using Student’s *t*-test as statistical method (* $p < 0.05$; ** $p < 0.01$; *** $p < 0.001$).

All the compounds succeeded in boosting histone acetylation in RSTS LCLs compared to healthy donor (HD) LCLs, with VPA exposure resulting highly significant ($p < 0.01$). This increment was particularly manifest in patient derived LCLs compared to untreated samples (Figure 1a).

We also observed that HDACi compounds induced a variable acetylation response, in a patient-specific manner when compared to treated HD LCLs (Figure 1b). As shown in Figure 1b, treatment with TSA 2 μ M boosted acetylation levels significantly in LCLs RSTS 176 ($p < 0.001$), RSTS 25 ($p < 0.001$) and RSTS 39 ($p < 0.01$), while SAHA 2 μ M showed highly significant effect on RSTS 176 and RSTS 25 ($p < 0.001$). VPA 2mM treatment particularly increased H3K27ac of RSTS 114, RSTS 120, RSTS 176, and RSTS 54 ($p < 0.001$), while exposure to NaB 5 mM significantly affected acetylation of RSTS 176 and RSTS 39 ($p < 0.001$), RSTS 54, and RT010-15 ($p < 0.05$).

Of note, when analyzing specific RSTS patient-derived LCLs response to HDACi compared to the relative untreated conditions, we observed that at least one HDACi significantly boosted acetylation and that RSTS-LCLs response varied among different drug treatments (Figure 1c and Figure S1). These data indicate that SCFAs as NaB show patient-specific acetylation increases, as is the case of other HDACi.

Considering HDACi applications as anticancer drugs for their role in cell cycle arrest, cell death, and immune-mediated mechanisms [25], we studied NaB and other HDACi effects on cell proliferation and apoptosis, performing Ki67 and Tunel assays upon exposure of LCLs with HDACi (Figures S2 and S3). For both assays, we did not observe a significant correlation with H3K27 acetylation (Figure S4), indicating that the HDACi rescue did not impair cell cycle progression or promote cell death under the experimental conditions used.

2.2. RSTS Patients Are Depleted in the Major Butyrate-Producer *Faecalibacterium* spp.

Because in vitro evaluation indicated that SCFAs can act as HDACi in RSTS, we focused on investigating the production of SCFAs by the commensal microbiota of the patients. To this end, we enrolled 23 RSTS subjects (mean age 10.2 ± 6.4 years; 12 females) and 16 healthy siblings (healthy donors, HD), mean age 12.7 ± 7.2 years; 6 females), as a control group to minimize environmental factors having a well-recognized role on gut microbiota. The dietary survey revealed no differences in intake of macronutrients. However, energy intake was lower in RSTS subjects when compared to HD controls ($p = 0.0054$). Nutritional parameters are detailed in the relative supplementary table (Table S3) [26].

Microbiota profiling was performed through 16S rRNA gene-targeted sequencing. After quality filtering processes, we obtained a mean count of 90,759 reads per sample. The alpha-diversity analysis of the gut microbiota showed no significant differences between RSTS and HD fecal samples in terms of richness (Observed species: $p = 0.255$; Phylogenetic Diversity (PD) whole tree: $p = 0.279$ —see Figure 2a) and of richness and evenness (Chao1: $p = 0.151$; Shannon: $p = 0.287$ —see Figure S5). Beta-diversity analysis, instead, showed that RSTS fecal microbiota differed significantly from that of HD according to both unweighted ($p = 0.013$) and weighted ($p = 0.022$) Unifrac distances (beta-diversity, Figure 2b).

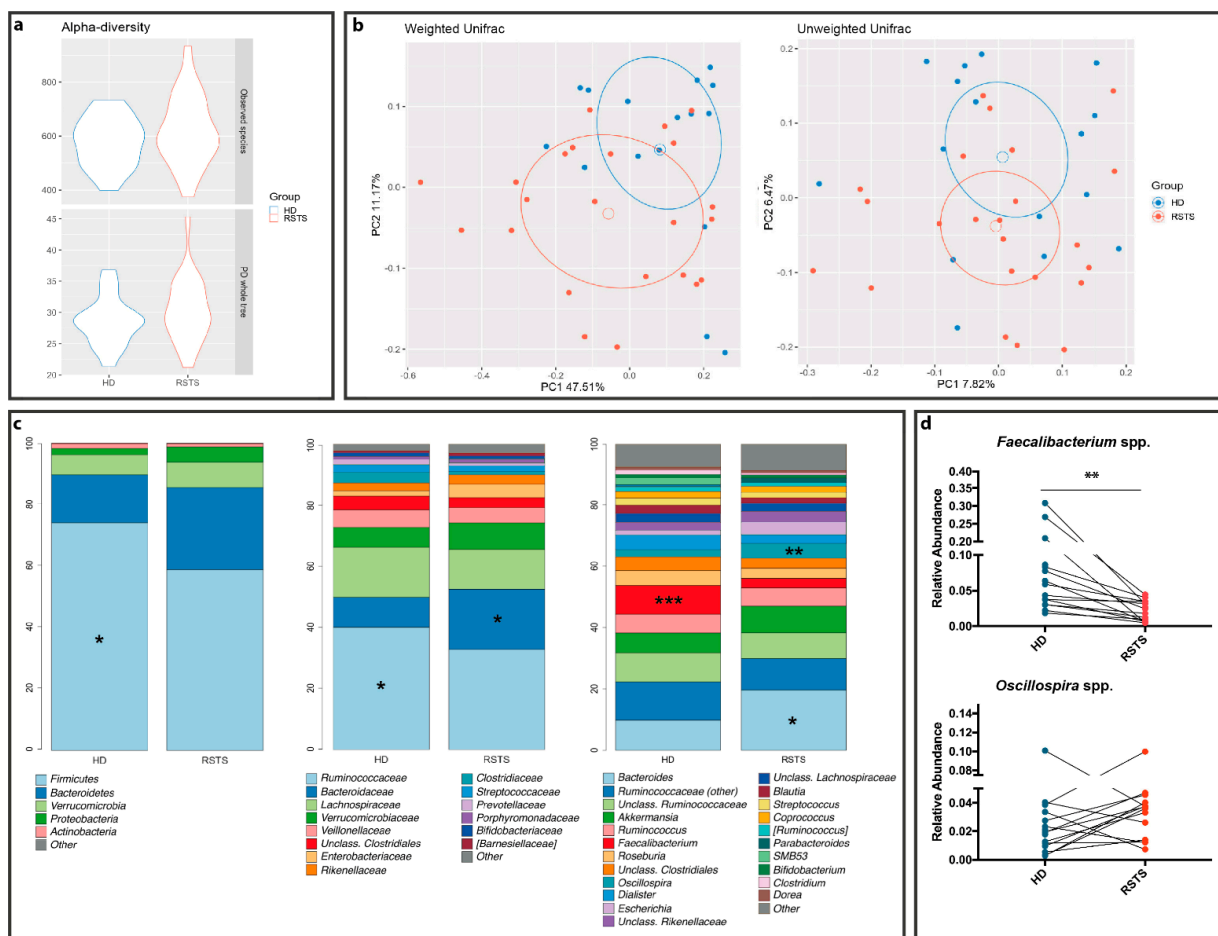


Figure 2. RSTS gut microbiota analysis. (a) alpha diversity. The violin plot shows biodiversity values for observed species and Faith's phylogenetic metrics. No statistically relevant differences were seen. (b) Principal coordinate analysis (PCoA) according to weighted and unweighted Unifrac distances. Microbial communities are statistically different (*Adonis* test: unweighted $p = 0.019$; weighted $p = 0.023$). The first and second principal coordinates are shown in the plot for both distances. (c) Bacterial composition of HD and RSTS groups. Relative taxonomic abundances are shown at phylum, family, and genus phylogenetic levels. All bacterial taxa present at <1% relative abundance were grouped into the "Other" classification. ***: $p < 0.005$; **: $p < 0.01$; *: $p < 0.05$. (d) *Faecalibacterium* spp. and *Oscillospira* spp. relative abundances (both significantly different between RSTS and HD) were compared within matched family members (patient/sibling, $n = 16$). For *Oscillospira* we did not observe a common pattern; *Faecalibacterium* spp. was significantly reduced in RSTS ($p = 0.0021$, Wilcoxon signed-rank test).

The overall composition of the intestinal microbiota (Figure 2c; Table S4) showed a decreased relative abundance of the Firmicutes phylum (58.5% in RSTS vs. 73.4% in HD, $p = 0.019$), of the *Ruminococcaceae* family (32.2% vs. 41.9%, $p = 0.049$) and of the SCFA-producing *Faecalibacterium* spp. (3.3% vs. 9.8% in HD, $p = 0.001$) in RSTS subjects. On the other hand, RSTS samples showed an enrichment in the *Bacteroidaceae* family and in *Bacteroides* spp. (21.1% vs. 10.3%, $p = 0.021$), as well as in *Oscillospira* spp. (5.1% vs. 2.4% in HD, $p = 0.007$). Matched-pair analysis (Wilcoxon signed-rank test), performed on RSTS/sibling pairs showed a significant and environment-independent decrease ($p = 0.0021$) in *Faecalibacterium* spp. (Figure 2d).

Afterward, we directly measured SCFA abundance in patient fecal samples. A decreasing trend in butyrate content was observed (4.13 ± 1.40 vs. 5.14 ± 1.79 mg/g feces, $p = 0.0741$, Mann–Whitney test), whereas acetate, propionate, and branched-chain fatty acids (iso-butyrate and iso-valerate) concentrations were similar ($p = 0.194$, $p = 0.874$, $p = 0.786$, and $p = 0.467$, respectively). These data indicate that RSTS patient microbiota produces low levels of endogenous butyrate.

2.3. HDACi Exposure Leads to Partial Rescue of RSTS Phenotype in *Drosophila* CBP Mutants

To establish an *in vivo* model to study the effect of SCFAs and the microbiome on RSTS pathogenesis, we analyzed *Drosophila melanogaster* mutants in the CBP homolog *nejire* (*nej*). Homozygous *nej* loss of function results in abnormal embryonic development leading to early lethality [27,28]. In particular, mutations in *nej* lead to defects in morphology caused by misregulation of wingless (*wg*) and other signaling pathways at stage 9 of embryonic development [27]. To test whether NaB, or VPA as a control HDACi, upon supplementation in the food could modulate emergence of *nej* mutant defects *in vivo*, we collected embryos deposited by females fed with the drugs and assessed their morphology at stages 8–12 (Figure 3 and Figure S6).

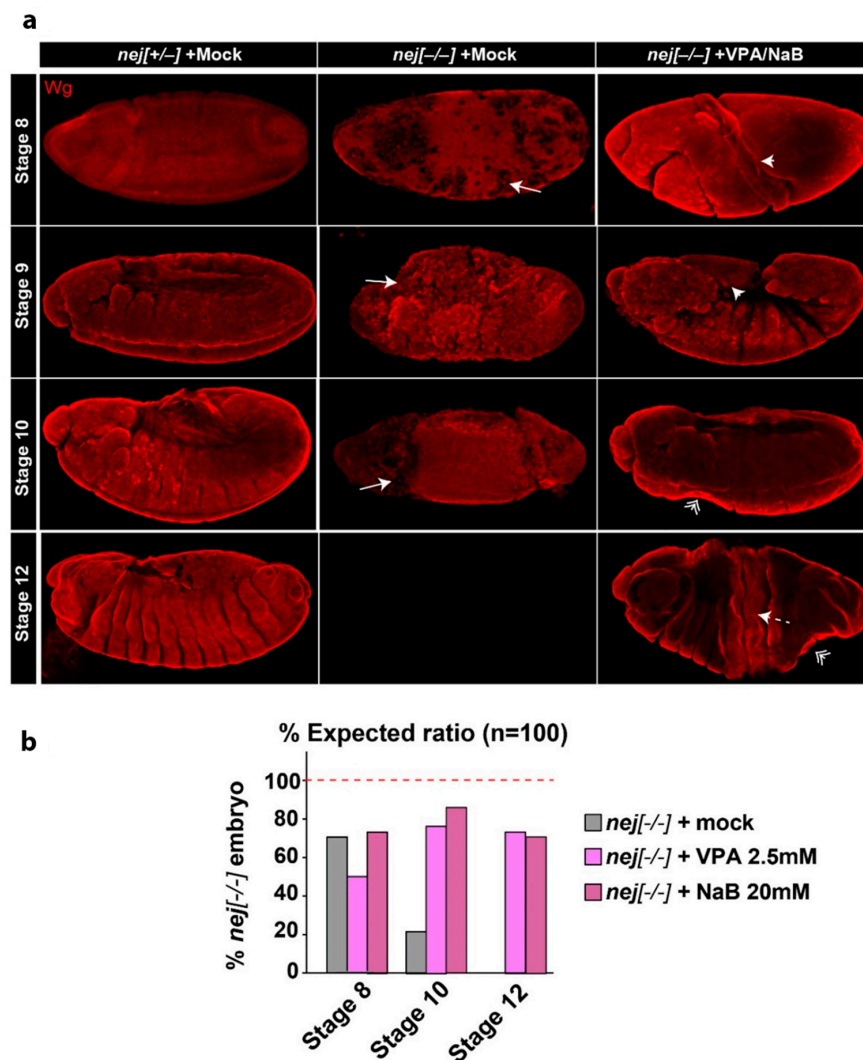


Figure 3. Developmental and morphological defects in *nej* mutant embryos are partially ameliorated by VPA or NaB treatment. (a) wingless (*wg*) staining of *nej* mutant embryos treated as indicated. Representative projections of confocal imaging from stages 8 to 12 are shown. The defects detected in *nej* mutant embryos with or without treatment include loss or uneven *wg* staining (Drilled, arrow), twisting (arrowhead), presence of bottlenecks (double-arrowheads), or cracks (dashed-arrow). (b) Quantification of embryo survival and of the above phenotypes in *nej* mutant embryos at stages 8 to 12. VPA or NaB treatments partially rescue embryo development, allowing *nej* mutant embryos to survive beyond stage 8 although with aberrant phenotypes, with significant embryo survival at stage 10 compared to untreated embryos ($p > 0.01$). Student's t-test was used as statistical method for comparing *nej* groups survival, with $p < 0.05$ considered significant.

Compared to $nej^{+/-}$ siblings, we have found that the majority of $nej^{-/-}$ embryos die between stages 8 and 10 with the reported twisting of embryo morphology [28] (Figure 3a, quantification in Figure 3b). Upon NaB or VPA treatment, $nej^{-/-}$ embryos display a partially rescued embryonic development, statistically significant at stage 10 ($p < 0.01$). Importantly, both treatments extended the survival of $nej^{-/-}$ embryos to stage 12, although twisting of the embryos is morphologically visible as bottleneck and cracks (Figure 3 and Figure S6). The reported twisting phenotype in treated $nej^{-/-}$ embryos is often less dramatic than in untreated $nej^{-/-}$ embryos allowing segmentation. Notably, both VPA and NaB treatment did not show any developmental delay or morphological defects in control embryos (data not shown). Altogether, these results indicate that NaB acts as a HDACi in vivo to ameliorate the developmental defects associated with acute loss of CBP homologs.

2.4. The Fly Gut Microbiota of Heterozygous *Drosophila* CBP Mutants

Because RSTS patients possess a defective microbiota, we analyzed that of heterozygous *nej* ($nej^{+/-}$) flies. In contrast to $nej^{-/-}$ embryos, $nej^{+/-}$ animals progress to adulthood and display no overt defects. However, they have been shown to reveal genetic interaction with genes involved in developmental processes regulated by CBP [28]. Hence, we reasoned that adult $nej^{+/-}$ animals could be used to investigate the fly gut microbiota.

A total of 10 samples were obtained from the two experimental groups (*yw* and $nej^{+/-}$), with five replicates each (three dissected guts in each replicate, with a total of 15 flies per group).

Alpha diversity metrics (Figure 4a) revealed that *nej* gut microbiota were enriched in low abundant species (Chao1 metric, $p = 0.005$), whereas the phylogenetic diversity between groups showed no significant differences (PD whole tree metric, $p = 0.668$).

Similarly, beta-diversity analysis (Figure 4b) highlighted clear discrimination between *yw* and *nej* microbial communities considering both abundant and rare species within the microbiota (unweighted Unifrac distance, $p = 0.007$),

As for the bacterial composition, the Firmicutes phylum was found more abundant in the *nej* flies (64.7% vs. 53.9% in *yw*), with a concurrent reduction of Proteobacteria (31.6 vs. 41.1% in *yw*). The taxonomic analysis revealed a remarkable increase in *Lactobacillaceae* (58.8% in *nej* vs. 7.5% in *yw*; $p = 0.0000254$), and a profound decrease in the *Enterococcaceae* family (0.2% vs. 12.9% in *yw*; $p = 0.00784$) (Figure 4c). These results were confirmed at genus level, with a significant enrichment in *Lactobacillus* (58.4% in *nej* vs. 3.4% in *yw*; $p = 0.00000806$) and a depletion in *Enterococcus* (0% vs. 3% in *yw*; $p = 0.00772$) (data not shown).

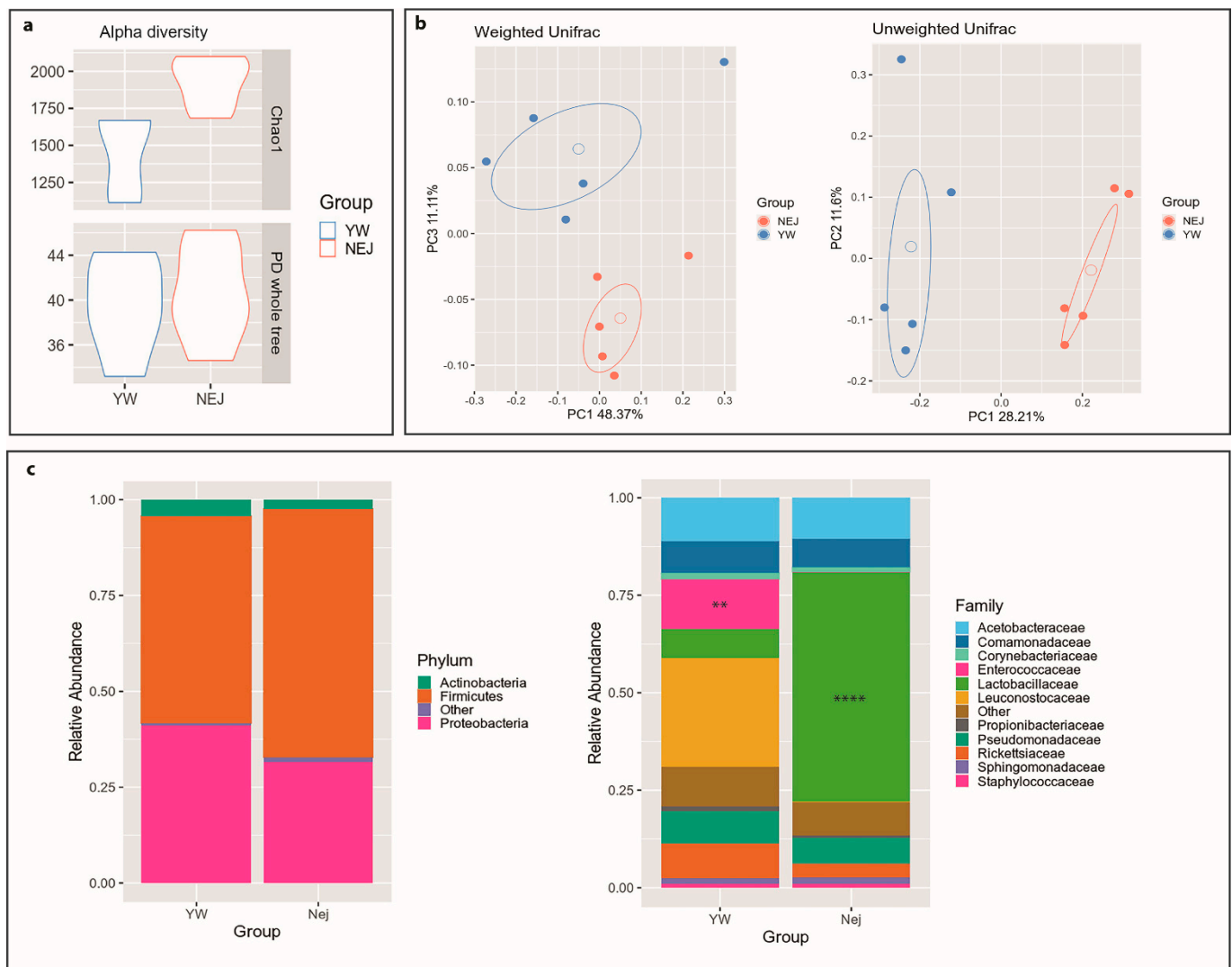


Figure 4. *Drosophila* gut microbiota analysis. Gut microbial communities were characterized by 16S rRNA gene sequencing. (a) Alpha diversity. Violin plots show biodiversity values for Chao1 ($p = 0.005$) and Faith's phylogenetic metrics (PD whole tree; $p = 0.668$). (b) Principal coordinate analysis (PCoA) for both Unifrac distances. (Adonis test: weighted $p = 0.216$; unweighted $p = 0.007$). (c) Relative taxonomic abundances of the gut bacterial composition in *yw* and *nej* flies at phylum and family levels. All bacterial taxa present at <1% relative abundance were grouped into the "Other" classification. ****: $p < 0.001$; **: $p < 0.01$.

3. Discussion

Current therapeutic approaches for RSTS patients are not targeted towards modulation of acetylation and are rather directed towards alleviating clinical symptoms and preventing possible known comorbidities. Common interventions include behavioral support and surgical procedures for the correction of orthopedic or cardiac malformations. In this context, exploring the effects of drugs with an established and specific molecular function in acetylation in preclinical studies is a fundamental step to devise effective future therapy. In the case of RSTS, HDACi are available and have already been used to treat neurological disorders [29]. Hence, the presented work explored the effects of HDAC inhibition in RSTS experimental models, focusing on natural SCFAs such as butyrate.

Treatment with a number of HDACi used in cancer therapy [30–33] showed a general boost in histone acetylation levels in RSTS patient-derived cell lines. Such increment was significant in a patient-specific manner. Each line derived from different RSTS patients with discrete pathogenic variants responded differently to tested compounds. These data provide evidence for HDACi's ability to restore acetylation levels in an in vitro model of

RSTS, strongly pointing to the possibility of future therapies tailored to individual patients, a central tenet of personalized medicine.

HDACi are tested in oncology trials for their ability to stop tumor cell proliferation by inducing selected and dose-dependent apoptosis [34]. Thus, our observation that selected HDACi dosing does not modulate cell proliferation or death in RSTS cells indicates that HDACi can boost acetylation at a sub-toxic concentration, at least in vitro.

Due to the HDACi function exerted by SCFAs, they have been tested in clinical trials for recurrent malignant gliomas or myelodysplastic syndrome and they have also been studied in vitro against Burkitt lymphoma, primary acute myeloid leukemia, retinoblastoma, medulloblastoma, prostate cancer, and hepatocellular and colon carcinoma [35,36].

Importantly, NaB, a natural SCFA with potent HDACi activity [37], performed on par with other HDACi in RSTS cells. We propose that it should be evaluated for the treatment of patients, considering that it is present in human diets as a product of the human microbiota or a well-tolerated supplement.

To investigate whether butyrate is normally produced by commensal bacteria of RSTS patients, we sequenced the V3–V4 hypervariable regions of the 16S rRNA genes and measured SCFAs as main microbial metabolites. While we scored no differences in nutritional parameters and in microbiota biodiversity in patients versus healthy siblings, we observed a distinct and highly interesting microbial signature characterized by loss of the butyrate-producer genus *Faecalibacterium* [38] in the microbiota of RSTS patients. Such change could participate in the syndrome comorbidity insurgence, perhaps in the gut, and further study should now aim at elucidation of possible genetic-microbial additive negative effects. Interestingly, a reduction of *Faecalibacterium* relative abundance was also reported in patients affected by Rett syndrome, autism spectrum disorder, and down syndrome, suggesting a shared microbiota signature in neurodevelopmental disorders [39].

A recent study reported that a ketogenic diet, highly impacting microbiota composition and metabolism [40], induces the production of deacetylase inhibitors in a mouse model of Kabuki syndrome (OMIM# 147920, # 300867), a rare disease sharing traits and histone modification defect with Rubinstein–Taybi syndrome [41]. Thus, nutritional interventions could also aim at rebalancing the microbiota of RSTS patients. In line with this approach, brain functions and behavior appear more and more influenced, through a bottom-up modulation, by the gut microbiota [42].

It is worth noting that carbohydrates, and in particular fermentable dietary fibers, the most important substrates for short-chain fatty acid production [43], were very similar in RSTS patients and healthy siblings, inconsistent with the reduction in the relative abundance of *Faecalibacterium* genus, or with the lower butyrate fecal concentration. Nutritional recommendations for RSTS comorbidity management are currently lacking as no studies focused on this. Our findings represent a starting point for the evaluation of specific nutritional regimens, which could also shed light on the basis of observed differences.

Studies with *nej* flies underscored the role of CBP during embryogenesis and as coactivators of critical signaling pathways involved in patterning [28,44]. In support of results from our in vitro RSTS model, we observed that rearing flies with food supplemented with NaB lead to partial rescue of embryogenesis and patterning, suggesting that nutritional intervention may ameliorate RSTS traits in vivo.

However, even if the *Drosophila* model has been used for investigating how different levels of nutrients and drugs influence the development and the metabolic phenotypes of emerging *Drosophila* embryos [45], our data are model behavior of oviparous animals, in which development occurs outside the mother's body. In mammals, maternal HDACi cross the placenta and affect embryogenesis; hence any future intervention should be envisaged after birth when the mammalian central nervous system is still developing.

Lack of an anoxic compartment in the *Drosophila* gut shapes a microaerophilic microbiota constituted, in laboratory strains, by few genera [46]. The most abundant taxa are *Firmicutes*, mainly *Lactobacillus* spp. and *alpha-Proteobacteria*, mainly *Acetobacteraceae*. Despite evolutionary divergence with the human microbiota, recent studies showed that an

altered relative abundance of these genera can result in gut homeostasis disturbance [47], growth delay [48], and behavioral changes [49]. Considering the results obtained from microbiota analysis of RSTS patients, we analyzed the microbial community of heterozygous *nej* insects compared to control animals. Results showed that, accounting for the species-specificity of the microbiota, the differences observed in RSTS patients compared to healthy siblings are recapitulated in RSTS flies compared to control animals, suggesting that patients–microbiota interactions could be modeled in *Drosophila*.

Overall, our results are in line with other studies [12,20,50], making a strong case for HDACi drug repurposing for future RSTS therapy. We envisage that the use of *Drosophila melanogaster* as an information rich in vivo RSTS model will speed up the transition from preclinical studies to clinical practice.

4. Materials and Methods

4.1. Cell Cultures

Lymphoblastoid cell lines (LCLs) from eight different RSTS patients (four carrying *CREBBP* mutations and four carrying *EP300* mutations, listed in Table S1) [20,51–53] and seven healthy donors were obtained in collaboration with the Gaslini Genetic Bank service (Telethon Network of Genetic Biobanks); their use was approved by Ethics Committee of Università degli Studi di Milano (Comitato Etico number 99/20, 17 November 2020). Cells were maintained in RPMI 1640 culture medium supplemented with L-glutamine (Euroclone, Pero, Italy), 20% fetal bovine serum (Euroclone, Pero, Italy), and penicillin/streptomycin (Euroclone, Pero, Italy), and cultured in an incubator with 5% CO₂ at 37 °C.

LCLs were exposed to four different HDAC inhibitors: Trichostatin A (TSA) (sc-3511, Santa Cruz Biotechnology, Dallas, TX, USA), Suberoylanilide hydroxamic acid (SAHA) (MK0683, Selleckchem, Houston, TX, USA), Valproic acid (VPA) (P4543, Sigma Aldrich, St. Louis, MO, USA), and Sodium Butyrate (NaB) (B5887, Sigma-Aldrich, St. Louis, MO, USA). We tested three different concentrations for each HDACi (Table S2) [54–59] and selected the maximum dose and timing of exposure, ensuring acceptable LCLs survival (data not shown). Cells were incubated with vehicles (H₂O or DMSO) at the maximum time (24 h), TSA 2 µM for 2 h, SAHA 2 µM for 24 h, VPA 2 mM for 24 h, or NaB 5 mM for 24 h as suggested from the literature (Table S2). Data were normalized on untreated cells and in vehicles for accounting for proliferation rate differences in basal condition between HD and RSTS lines.

4.2. AlphaLISA[®] Assay

After treatments, lymphoblastoid cellular pellets were obtained by centrifugation and frozen at –80 °C. An amount of 10,000 cells/well resuspended in 60 µL of culture media was used in order to perform AlphaLISA[®] assay (PerkinElmer, Waltham, MA, USA) according to the manufacturer’s protocol. Briefly, cells were incubated 15 min with Cell-Histone Lysis buffer and 10 min with Cell-Histone Extraction buffer; 30 µL of lysates were incubated with 10 µL of Acceptor mix 1h at room temperature (RT) and then 10 µL of Donor mix was added overnight at RT. Replicates were tested with both AlphaLISA Acetylated-Histone H3 Lysine 27 (H3K27ac) Cellular Detection Kit (AL720, PerkinElmer, Waltham, MA, USA) and AlphaLISA unmodified Histone H3 Lysine 4 (H3K4) Cellular Detection Kit (AL719, PerkinElmer, Waltham, MA, USA) for normalization. PerkinElmer EnSight[™] plate reader was used for the detection of the chemiluminescent signal.

4.3. Ki67 and TUNEL Assay

After treatments, at least 1.5×10^4 LCLs were seeded in duplicate on SuperFrost Plus slides (ThermoFisher Scientific, Waltham, MA, USA) through 5 min of cytospin at 500 rpm, followed by 10 min of incubation with PFA 4% and washed. Slides were stored at 4 °C until Ki67 or TUNEL assays were performed.

Briefly, for Ki67 assay slides, samples were put in a wet chamber and cells permeabilized with PBT buffer (Phosphate-Buffered Saline (PBS) with 0.2% Triton) for 10 min at room temperature (RT); blocking of non-specific sites was obtained by slide incubation with PBT supplemented with 10% FBS for 30 min at RT. Slides were first incubated overnight at 4 °C with the anti-Ki67 antibody (#9129 Cell Signaling, Danvers, MA, USA, 1:400), washed with PBT, and then incubated with Alexa-488 anti-Rabbit secondary antibody (#6441-30 SouthernBiotech, Birmingham, AL, USA, 1:250) for 2 h. Slides were washed with PBT and water, mounted with EverBrite Mounting Medium with DAPI (23002, Biotium, Landing Parkway Fremont, CA, USA), and fluorescent microscopic images of proliferative cells (Ki67+) were acquired and analyzed with ImageJ software (National Institute of Health, Bethesda, MD, USA).

Terminal deoxynucleotidyl transferase (TdT) dUTP Nick-End Labeling (TUNEL) assay was performed using In Situ Cell Death Detection kit, AP (Roche Diagnostics, Basilea, Switzerland), in order to detect apoptotic cells, according to manufacturer's protocol. Cells, previously seeded on slides were incubated with a permeabilization solution (0.1% Triton 100X and 0.1% sodium citrate) for 2 min at 4 °C, then washed with PBS and incubated with TUNEL mixture (composed by Enzyme Solution added to Label Solution) in a wet chamber for 1h at 37 °C. After 3 PBS washes, slides were incubated with Converter AP for 30 min at 37 °C and then with Substrate Solution (2% NBT/BCIP stock solution in NBT/BCIP Buffer) for 10 min at RT and dark. Finally, following PBS washes, mounted with DABCO mounting medium and brightfield microscopic images of apoptotic cells (TUNEL+) were acquired and analyzed with ImageJ software (National Institute of Health, Bethesda, MD, USA).

Both fluorescent and brightfield slide images were acquired by NanoZoomer S60 Digital Slide Scanner (Hamamatsu Photonics, Hamamatsu City, Japan) at 20× and 80× magnification, and two randomly selected fields for each experimental group at 20× were selected for blinded cells counts by three different operators. Panel images of Ki67+ cells were instead acquired by confocal microscopy A1/A1R (Nikon Corporation, Tokyo, Japan) at 60× and 100× magnification. The number of Ki67+ and TUNEL+ cells was normalized on the total cell number per image.

4.4. Subject Recruitment and Sampling for Gut Microbiota Profiling

For this study, 23 RSTS subjects and 16 healthy siblings were enrolled. All subjects were recruited in collaboration with the Italian family RSTS association "Associazione RTS Una Vita Speciale ONLUS".

For both patients and controls, exclusion criteria were treatments with antibiotic and/or probiotic/prebiotic assumption during the previous 3 months. For RSTS patients, inclusion criteria were confirmed clinical diagnosis with (20/23) or without (3/23) demonstrated *CREBBP/EP300* mutation. RSTS diagnosis of all patients was confirmed by an expert geneticist (DM) and genetic tests were performed in our laboratory (CG).

In conjunction with the stool sample collection, a 3 day dietary survey (preceding the sample collection) was filled by caregivers. Dietary food records were processed using commercially available software (ePhood V2, Openzone, Bresso, Italy).

The study was approved by the Ethics Committee of San Paolo Hospital in Milan (Comitato Etico Milano Area 1, Protocol number 2019/EM/076, 2 May 2019); written informed consent was obtained from enrolled subjects or caregivers.

4.5. Bacterial DNA Extraction and 16S rRNA Gene Sequencing of Human Gut Microbiota

Bacterial genomic DNA in stool samples was extracted as previously described [60] by using the Spin stool DNA kit (Stratec Molecular, Berlin, Germany), according to the manufacturer's instructions. Briefly, after homogenizing fecal samples in the lysis buffer for inactivating DNases, Zirconia Beads II were added for a complete lysis of bacterial cells by using TissueLyser LT. Bacterial lysates were then mixed with InviAdsorb reagent, a step designed to remove PCR inhibitors. Bacterial DNA was eventually eluted in 100 µL of buffer. Then, 25 ng of extracted DNA was used to construct the sequencing library. The V3–V4

hypervariable regions of the bacterial 16S rRNA were amplified with a two-step barcoding approach according to the Illumina 16S Metagenomic Sequencing Library Preparation (Illumina, San Diego, CA, USA). Library quantification was determined using the DNA High Sensitivity Qubit kit (ThermoFisher Scientific, Waltham, MA, USA) and Agilent 2100 Bioanalyzer System (Agilent, Santa Clara, CA, USA); libraries were pooled and sequenced on a MiSeq platform (Illumina, San Diego, CA, USA) in a 2×250 bp paired-end run. Obtained 16S rRNA gene sequences were analyzed using PANDAseq [61], and low-quality reads were filtered and discarded. Reads were then processed using the Quantitative Insights Into Microbial Ecology (QIIME) pipeline (release 1.8.0) [62] and clustered into Operational Taxonomic Unit (OTUs) at 97% identity level and discarding singletons (i.e., OTUs supported by only 1 read across all samples) as likely chimeras. Taxonomic assignment was performed via the Ribosomal Database Project (RDP) classifier [63] against the Greengenes database (version 13_8; ftp://greengenes.microbio.me/greengenes_release/gg_13_8_otus, accessed on 22 February 2021), with a 0.5 identity threshold. Alpha-diversity was computed using the Chao1, the number of OTUs, Shannon diversity, and Faith's Phylogenetic Diversity whole tree (PD whole tree) metrics throughout the QIIME pipeline. Beta-diversity was assessed by weighted and unweighted UniFrac distances [64] and principal coordinates analysis (PCoA).

4.6. Fecal Short-Chain Fatty Acid Quantification

Concentrations of acetate, propionate, iso-butyrate, butyrate, and iso-valerate were assessed according to Bassanini et al. [65]. The measurement of SCFAs was performed by gas chromatography, using a Varian model 3400 CX Gas chromatograph fitted with FID detector, split/splitless injector, and a SPB-1 capillary column (30 m \times 0.32 mm ID, 0.25 μ m film thickness; Supelco, Bellefonte, PA, USA). Calibration curves of SCFAs in concentration between 0.25 and 10 mM were constructed to obtain SCFAs quantification, and 10 mM 2-ethylbutyric acid was used as an internal standard. Results are expressed as mg/g of dry weight of feces.

4.7. *Drosophila Melanogaster* Stocks and HDACi Feeding

The following fly strains were used in this study: *Drosophila yw* strain used as control and $w[*] P\{w[+mC]=lacW\}nej[P]/FM7c$ known as *nejire* (*nejP/+*) mutant strain (#3728; Bloomington *Drosophila* Stock Center, Bloomington, IN, USA). *nejP* contains a P-element 347bp upstream of the second exon of *nej* gene and behaves as a loss of function mutant [27]. Flies were maintained and raised into vials containing a standard food medium composed of yeast, cornmeal, molasses, agar, propionic acid, tegosept, and water. All the strains were kept at 25 °C. To prepare food with HDACi, stock solutions of VPA (1 and 2.5 mM) and NaB (10 and 20 mM) solutions were diluted 1:10 in the food before solidification but under 65 °C to prevent heat damage of the compounds.

4.8. Fly Treatment and Embryo Immunostaining

To identify homozygous animals in sibling crosses, *nej* mutants were balanced over *FM7*, *kr-GAL4 UAS-GFP* chromosome. Adult *nej* mutant flies were life cycle-synchronized and treated with mock, VPA (2.5 mM) or NaB (20 mM) for four days. The drugs were mixed with standard food as described above at room temperature. For egg collection, adult flies were placed in cages for 4 h and then removed. Fertilized eggs were collected after 8h and stained as previously described [66]. Briefly, embryos were collected, dechorionated and fixed with a mixture of 4% paraformaldehyde and heptane. Following washes, embryos were permeabilized and blocked with PBT (PBS containing 0.1% Triton X-100 and 1% BSA) for 3 h. Staining was performed overnight with primary mouse anti-wg 1:50 (4D4, Developmental Studies Hybridoma Bank, Iowa City, IA, USA). Secondary goat anti-mouse-Cy3 (1:500) was used for 2 h. Images were taken with a Nikon AR1 confocal microscope using a 10X objective (Nikon Corporation, Tokyo, Japan).

4.9. Bacterial DNA Extraction and 16S rRNA Gene Sequencing of *Drosophila Melanogaster* Gut Microbiota

For microbiota sequencing, adult fly guts were dissected to avoid environmental contamination. Briefly, flies were anesthetized in ice for 5 min in a Petri dish and transferred, one by one, to the dissection dish and immersed in 50 μ L-drop of cold PBS. First, wings and legs were removed. Surgical forceps were used to gently separate the insect head from the body and exposing the foregut. The abdominal cuticle was then cut and dissected out, and the hindgut pulled outside the abdominal cavity. To completely free the entire gastrointestinal tract, the insect head and Malpighian tubes were removed. Only undamaged organs were further processed. Dissected guts, three per experimental condition, were immediately transferred into vials containing 100 μ L of cold PBS and kept at -80°C until use. A total of 15 *nej* and 15 *yw* flies were processed.

Bacterial DNA was extracted by means of QIAamp DNA Microbiome Kit (Qiagen, Hilden, Germany), designed to achieve enrichment of bacterial DNA from low biomass samples. Briefly, the depletion of host cells was performed by adding lysis buffer and benzonase to samples. Bacterial cell lysis was carried out by bead beating in the TissueLyser LT instrument (Qiagen, Hilden, Germany). Lysates were transferred to QIAamp UCP Mini Columns and processed according to the manufacturer's instructions. DNA was eluted in 30 μ L of the provided buffer. Library preparation and sequencing were performed as described above for human samples on the Illumina platform.

4.10. Statistical Analysis

Biological cell data were analyzed using Prism software (GraphPad Software, Sand Diego, CA, USA) and expressed as mean \pm Standard Deviation (SD). Student's t-tests were used to compare means between groups in AlphaLISA, Ki67, and TUNEL assays (LCLs acetylation, proliferation, and death rate), and in phenotypic evaluation (*Drosophila* embryo survival), with $p < 0.05$ considered significant (* $p < 0.05$; ** $p < 0.01$; *** $p < 0.001$ for graphics relative to in vitro model); the correlation between HDACi-induced acetylation and proliferative or apoptotic cells was calculated using Pearson correlation coefficient ($-1 < r < 1$) and Pearson correlation p -value, significant for $p < 0.05$.

For microbiota analysis, statistical evaluation among alpha-diversity indices was performed by a non-parametric Monte Carlo-based test, using 9999 random permutations. The PERMANOVA test (adonis function) in the R package vegan (version 2.0-10) was used to compare the microbial community structure of RSTS and HD subjects within the beta-diversity analysis. For evaluating differences in taxonomic relative abundances, the pairwise t-test from the package "rstatix" (version 0.6.0) in the RStudio software (version 1.2.1335; R version 3.6.3) was used. p -values < 0.05 were considered significant for each analysis.

Supplementary Materials: The following are available online at <https://www.mdpi.com/article/10.3390/ijms22073621/s1>, Figure S1: Insight on single-RSTS LCLs histone acetylation, Figure S2: HDAC inhibitors cytotoxicity analysis on RSTS LCLs, Figure S3: Insights on cell proliferation and cell death rate of RSTS LCLs upon HDAC inhibitors exposure, Figure S4: Correlation between HDACi-induced acetylation versus cell proliferation and apoptosis in RSTS LCLs, Figure S5: Gut microbiota composition in HD and RSTS subjects, Figure S6: Normal and altered phenotypes of *nej* mutant embryos from stage 8 to 12 treated or not with HDACi, Table S1: RSTS LCLs used for in vitro treatments, Table S2: Conditions of in vitro treatments used on LCLs, Table S3: Nutritional values of the enrolled patients, Table S4: Gut microbiota composition in HD and RSTS subjects.

Author Contributions: V.M., E.B. and C.G. conceived the project; E.D.F., E.O., P.G., A.G., C.P. and G.F. performed the experiments; C.C. and M.S. performed bioinformatics analyses; E.A.C. and G.B. contributed to molecular analyses; D.M. contributed to patient recruitment and clinical assessment; T.V. provided flies, reagents, animals, and design of in vivo experiments; E.D.F., E.O., V.M., E.B. and C.G. performed data analysis and interpretation; E.D.F., E.O., V.M., E.B. and C.G. wrote the manuscript; E.V., D.M. and T.V. provided guidance in the manuscript revision. All authors have read and agreed to the published version of the manuscript.

Funding: This work was supported by Fondazione Cariplo (2015-0783 to V.M.), by intramural funding (Università degli Studi di Milano linea 2 to C.G.), by Associazione “RTS Una Vita Speciale ONLUS” (#DigiRare to C.G.), by grant “Aldo Ravelli Center” (to V.M. and C.G.); by Translational Medicine PhD-Università degli Studi di Milano scholarship (to E.D.F. and C.P.); by Molecular and Translational Medicine PhD-Università degli Studi di Milano scholarship (to E.O., C.C. and P.G.), by H2020 Marie Skłodowska-Curie Actions (H2020-MSCA individual fellowship #844147) (to A.G.).

Institutional Review Board Statement: The study was conducted according to the guidelines of the Declaration of Helsinki and its later amendments. The use of lymphoblastoid cell lines was approved by Ethics Committee of Università degli Studi di Milano (Comitato Etico number 99/20). The study on gut microbiota profiling of the enrolled subjects was approved by Ethics Committee of San Paolo Hospital in Milan (Comitato Etico Milano Area 1, Protocol number 2019/EM/076).

Informed Consent Statement: Informed consent was obtained from all subjects involved in the study or their caregivers.

Data Availability Statement: Sequencing data of 16S rRNA amplicons have been deposited in NCBI Short-Read Archive (SRA) under accession number PRJNA616211 (<http://www.ncbi.nlm.nih.gov/bioproject/PRJNA616211>, accessed on 22 February 2021).

Acknowledgments: We thank the patients’ families for participating in this study. C.G. thanks the Italian Association of Rubinstein–Taybi patients “RTS Una Vita Speciale ONLUS” for its support. This work belongs to the ERN ITHACA network (DM). Microscopy observations were carried out at The Advanced Microscopy Facility Platform-UNitech NOLIMITS-University of Milan. All authors acknowledged support from the University of Milan through the APC initiative.

Conflicts of Interest: The authors declare no conflict of interest.

References



1. Atlasi, Y.; Stunnenberg, H.G. The interplay of epigenetic marks during stem cell differentiation and development. *Nat. Rev. Genet.* **2017**, *18*, 643–658. [[CrossRef](#)] [[PubMed](#)]
2. Xu, Q.; Xie, W. Epigenome in Early Mammalian Development: Inheritance, Reprogramming and Establishment. *Trends Cell Biol.* **2018**, *28*, 237–253. [[CrossRef](#)] [[PubMed](#)]
3. Grunstein, M. Histone acetylation in chromatin structure and transcription. *Nature* **1997**, *389*, 349–352. [[CrossRef](#)]
4. Uchida, S.; Shumyatsky, G.P. Epigenetic regulation of Fgf1 transcription by CRTCL1 and memory enhancement. *Brain Res. Bull.* **2018**, *141*, 3–12. [[CrossRef](#)]
5. Bjornsson, H.T. The Mendelian disorders of the epigenetic machinery. *Genome Res.* **2015**, *25*, 1473–1481. [[CrossRef](#)] [[PubMed](#)]
6. Rubinstein, J.H.; Taybi, H. Broad thumbs and toes and facial abnormalities. A possible mental retardation syndrome. *Am. J. Dis. Child.* **1963**, *105*, 588–608. [[CrossRef](#)] [[PubMed](#)]
7. Hennekam, R.C.M. Rubinstein–Taybi syndrome. *Eur. J. Hum. Genet.* **2006**, *14*, 981–985. [[CrossRef](#)]
8. Milani, D.; Manzoni, F.; Pezzani, L.; Ajmone, P.; Gervasini, C.; Menni, F.; Esposito, S. Rubinstein–Taybi syndrome: Clinical features, genetic basis, diagnosis, and management. *Ital. J. Pediatr.* **2015**, *41*, 4. [[CrossRef](#)]
9. Fergelot, P.; Van Belzen, M.; Van Gils, J.; Afenjar, A.; Armour, C.M.; Arveiler, B.; Beets, L.; Burglen, L.; Busa, T.; Collet, M.; et al. Phenotype and genotype in 52 patients with Rubinstein–Taybi syndrome caused by EP300 mutations. *Am. J. Med. Genet. Part A* **2016**, *170*, 3069–3082. [[CrossRef](#)]
10. Miller, R.W.; Rubinstein, J.H. Tumors in Rubinstein–Taybi syndrome. *Am. J. Med. Genet.* **1995**, *56*, 112–115. [[CrossRef](#)]
11. Boot, M.V.; van Belzen, M.J.; Overbeek, L.I.; Hijmering, N.; Mendeville, M.; Waisfisz, Q.; Wesseling, P.; Hennekam, R.C.; de Jong, D. Benign and malignant tumors in Rubinstein–Taybi syndrome. *Am. J. Med. Genet. Part A* **2018**, *176*, 597–608. [[CrossRef](#)]
12. Valor, L.M.; Viosca, J.; Lopez-Atalaya, J.P.; Barco, A. Lysine acetyltransferases CBP and p300 as therapeutic targets in cognitive and neurodegenerative disorders. *Curr. Pharm. Des.* **2013**, *19*, 5051–5064. [[CrossRef](#)] [[PubMed](#)]
13. Yao, T.P.; Oh, S.P.; Fuchs, M.; Zhou, N.D.; Ch’ng, L.E.; Newsome, D.; Bronson, R.T.; Li, E.; Livingston, D.M.; Eckner, R. Gene dosage-dependent embryonic development and proliferation defects in mice lacking the transcriptional integrator p300. *Cell* **1998**, *93*, 361–372. [[CrossRef](#)]
14. Oike, Y.; Hata, A.; Mamiya, T.; Kaname, T.; Noda, Y.; Suzuki, M.; Yasue, H.; Nabeshima, T.; Araki, K.; Yamamura, K. Truncated CBP protein leads to classical Rubinstein–Taybi syndrome phenotypes in mice: Implications for a dominant-negative mechanism. *Hum. Mol. Genet.* **1999**, *8*, 387–396. [[CrossRef](#)] [[PubMed](#)]
15. Chan, H.M.; La Thangue, N.B. p300/CBP proteins: HATs for transcriptional bridges and scaffolds. *J. Cell Sci.* **2001**, *114*, 2363–2373.
16. Dutto, I.; Scalera, C.; Prosperi, E. CREBBP and p300 lysine acetyl transferases in the DNA damage response. *Cell. Mol. Life Sci.* **2018**, *75*, 1325–1338. [[CrossRef](#)] [[PubMed](#)]

17. Weinert, B.T.; Narita, T.; Satpathy, S.; Srinivasan, B.; Hansen, B.K.; Schölz, C.; Hamilton, W.B.; Zucconi, B.E.; Wang, W.W.; Liu, W.R.; et al. Time-Resolved Analysis Reveals Rapid Dynamics and Broad Scope of the CBP/p300 Acetylome. *Cell* **2018**, *174*, 231–244.e12. [CrossRef]
18. Kazantsev, A.G.; Thompson, L.M. Therapeutic application of histone deacetylase inhibitors for central nervous system disorders. *Nat. Rev. Drug Discov.* **2008**, *7*, 854–868. [CrossRef] [PubMed]
19. Heerboth, S.; Lapinska, K.; Snyder, N.; Leary, M.; Rollinson, S.; Sarkar, S. Use of epigenetic drugs in disease: An overview. *Genet. Epigenet.* **2014**, *6*, 9–19. [CrossRef] [PubMed]
20. Lopez-Atalaya, J.P.; Gervasini, C.; Mottadelli, F.; Spena, S.; Piccione, M.; Scarano, G.; Selicorni, A.; Barco, A.; Larizza, L. Histone acetylation deficits in lymphoblastoid cell lines from patients with Rubinstein-Taybi syndrome. *J. Med. Genet.* **2012**, *49*, 66–74. [CrossRef]
21. Alarcón, J.M.; Malleret, G.; Touzani, K.; Vronskaya, S.; Ishii, S.; Kandel, E.R.; Barco, A. Chromatin Acetylation, Memory, and LTP Are Impaired in CBP+/- Mice. *Neuron* **2004**, *42*, 947–959. [CrossRef]
22. Simon, G.M.; Cheng, J.; Gordon, J.I. Quantitative assessment of the impact of the gut microbiota on lysine epsilon-acetylation of host proteins using gnotobiotic mice. *Proc. Natl. Acad. Sci. USA* **2012**, *109*, 11133–11138. [CrossRef]
23. Stilling, R.M.; van de Wouw, M.; Clarke, G.; Stanton, C.; Dinan, T.G.; Cryan, J.F. The neuropharmacology of butyrate: The bread and butter of the microbiota-gut-brain axis? *Neurochem. Int.* **2016**, *99*, 110–132. [CrossRef] [PubMed]
24. Astbury, S.M.; Corfe, B.M. Uptake and metabolism of the short-chain fatty acid butyrate, a critical review of the literature. *Curr. Drug Metab.* **2012**, *13*, 815–821. [CrossRef] [PubMed]
25. Eckschlager, T.; Plch, J.; Stiborova, M.; Hrabeta, J. Histone deacetylase inhibitors as anticancer drugs. *Int. J. Mol. Sci.* **2017**, *18*, 1414. [CrossRef] [PubMed]
26. Italian Society of Human Nutrition Nutrients and Energy Reference Intake Levels for Italian Population. Available online: <https://sinu.it/tabelle-larn-2014/> (accessed on 18 February 2021).
27. Akimaru, H.; Chen, Y.; Dai, P.; Hou, D.-X.; Nonaka, M.; Smolik, S.M.; Armstrong, S.; Goodman, R.H.; Ishii, S. Drosophila CBP is a co-activator of cubitus interruptus in hedgehog signalling. *Nature* **1997**, *386*, 735–738. [CrossRef] [PubMed]
28. Akimaru, H.; Hou, D.-X.; Ishii, S. Drosophila CBP is required for dorsal-dependent twist gene expression. *Nat. Genet.* **1997**, *17*, 211–214. [CrossRef] [PubMed]
29. Cobos, S.N.; Bennett, S.A.; Torrente, M.P. The impact of histone post-translational modifications in neurodegenerative diseases. *Biochim. Biophys. Acta Mol. Basis Dis.* **2019**, *1865*, 1982–1991. [CrossRef] [PubMed]
30. José-Enériz, E.S.; Gimenez-Camino, N.; Agirre, X.; Prosper, F. HDAC inhibitors in acute myeloid leukemia. *Cancers* **2019**, *11*, 1794. [CrossRef]
31. Spartalis, E.; Athanasiadis, D.I.; Chrysikos, D.; Spartalis, M.; Boutzios, G.; Schizas, D.; Garmpis, N.; Damaskos, C.; Paschou, S.A.; Ioannidis, A.; et al. Histone deacetylase inhibitors and anaplastic thyroid carcinoma. *Anticancer Res.* **2019**, *39*, 1119–1127. [CrossRef]
32. Tarnowski, M.; Tkacz, M.; Kopytko, P.; Bujak, J.; Piotrowska, K.; Pawlik, A. Trichostatin A Inhibits Rhabdomyosarcoma Proliferation and Induces Differentiation through MyomiR Reactivation. *Folia Biol.* **2019**, *65*, 43–52.
33. Lipska, K.; Gumieniczek, A.; Filip, A.A. Anticonvulsant valproic acid and other short-chain fatty acids as novel anticancer therapeutics: Possibilities and challenges. *Acta Pharm.* **2020**, *70*, 291–301. [CrossRef] [PubMed]
34. Yuan, X.G.; Huang, Y.R.; Yu, T.; Jiang, H.W.; Xu, Y.; Zhao, X.Y. Chidamide, a histone deacetylase inhibitor, induces growth arrest and apoptosis in multiple myeloma cells in a caspase-dependent manner. *Oncol. Lett.* **2019**, *18*, 411–419. [CrossRef] [PubMed]
35. Iannitti, T.; Palmieri, B. Clinical and experimental applications of sodium phenylbutyrate. *Drugs R D* **2011**, *11*, 227–249. [CrossRef]
36. Cappellacci, L.; Perinelli, D.R.; Maggi, F.; Grifantini, M.; Petrelli, R. Recent Progress in Histone Deacetylase Inhibitors as Anticancer Agents. *Curr. Med. Chem.* **2018**, *27*, 2449–2493. [CrossRef] [PubMed]
37. Davie, J.R. Inhibition of Histone Deacetylase Activity by Butyrate. *J. Nutr.* **2003**, *133*, 2485S–2493S. [CrossRef]
38. Louis, P.; Flint, H.J. Diversity, metabolism and microbial ecology of butyrate-producing bacteria from the human large intestine. *FEMS Microbiol. Lett.* **2009**, *294*, 1–8. [CrossRef]
39. Borghi, E.; Vignoli, A. Rett syndrome and other neurodevelopmental disorders share common changes in gut microbial community: A descriptive review. *Int. J. Mol. Sci.* **2019**, *20*, 4160. [CrossRef] [PubMed]
40. Lindefeldt, M.; Eng, A.; Darban, H.; Bjerkner, A.; Zetterström, C.K.; Allander, T.; Andersson, B.; Borenstein, E.; Dahlin, M.; Prast-Nielsen, S. The ketogenic diet influences taxonomic and functional composition of the gut microbiota in children with severe epilepsy. *Npj Biofilms Microbiomes* **2019**, *5*, 5. [CrossRef] [PubMed]
41. Benjamin, J.S.; Pilarowski, G.O.; Carosso, G.A.; Zhang, L.; Huso, D.L.; Goff, L.A.; Vernon, H.J.; Hansen, K.D.; Bjornsson, H.T. A ketogenic diet rescues hippocampal memory defects in a mouse model of Kabuki syndrome. *Proc. Natl. Acad. Sci. USA* **2017**, *114*, 125–130. [CrossRef] [PubMed]
42. Heijtz, R.D.; Wang, S.; Anuar, F.; Qian, Y.; Björkholm, B.; Samuelsson, A.; Hibberd, M.L.; Forsberg, H.; Pettersson, S. Normal gut microbiota modulates brain development and behavior. *Proc. Natl. Acad. Sci. USA* **2011**, *108*, 3047–3052. [CrossRef] [PubMed]
43. Bach Knudsen, K.E.; Lærke, H.N.; Hedemann, M.S.; Nielsen, T.S.; Ingerslev, A.K.; Gundelund Nielsen, D.S.; Theil, P.K.; Purup, S.; Hald, S.; Schioldan, A.G.; et al. Impact of Diet-Modulated Butyrate Production on Intestinal Barrier Function and Inflammation. *Nutrients* **2018**, *10*, 1499. [CrossRef]

44. Tanaka, Y.; Naruse, I.; Maekawa, T.; Masuya, H.; Shiroishi, T.; Ishii, S. Abnormal skeletal patterning in embryos lacking a single Cbp allele: A partial similarity with Rubinstein-Taybi syndrome. *Proc. Natl. Acad. Sci. USA* **1997**, *94*, 10215–10220. [[CrossRef](#)] [[PubMed](#)]
45. Matzkin, L.M.; Johnson, S.; Paight, C.; Markow, T.A. Preadult Parental Diet Affects Offspring Development and Metabolism in *Drosophila melanogaster*. *PLoS ONE* **2013**, *8*, e59530. [[CrossRef](#)]
46. Capo, F.; Wilson, A.; Di Cara, F. The intestine of *Drosophila melanogaster*: An emerging versatile model system to study intestinal epithelial homeostasis and host-microbial interactions in humans. *Microorganisms* **2019**, *7*, 336. [[CrossRef](#)] [[PubMed](#)]
47. Fast, D.; Duggal, A.; Foley, E. Monoassociation with *Lactobacillus plantarum* Disrupts Intestinal Homeostasis in Adult *Drosophila melanogaster*. *mBio* **2018**, *9*, e01114–e01118. [[CrossRef](#)]
48. Shin, S.C.; Kim, S.-H.; You, H.; Kim, B.; Kim, A.C.; Lee, K.-A.; Yoon, J.-H.; Ryu, J.-H.; Lee, W.-J. *Drosophila* microbiome modulates host developmental and metabolic homeostasis via insulin signaling. *Science* **2011**, *334*, 670–674. [[CrossRef](#)]
49. Sharon, G.; Segal, D.; Ringo, J.M.; Hefetz, A.; Zilber-Rosenberg, I.; Rosenberg, E. Commensal bacteria play a role in mating preference of *Drosophila melanogaster*. *Proc. Natl. Acad. Sci. USA* **2010**, *107*, 20051–20056. [[CrossRef](#)] [[PubMed](#)]
50. Babu, A.; Kamaraj, M.; Basu, M.; Mukherjee, D.; Kapoor, S.; Ranjan, S.; Swamy, M.M.; Kaypee, S.; Scaria, V.; Kundu, T.K.; et al. Chemical and genetic rescue of an ep300 knockdown model for Rubinstein Taybi Syndrome in zebrafish. *Biochim. Biophys. Acta Mol. Basis Dis.* **2018**, *1864*, 1203–1215. [[CrossRef](#)]
51. Spena, S.; Milani, D.; Rusconi, D.; Negri, G.; Colapietro, P.; Elcioglu, N.; Bedeschi, F.; Pilotta, A.; Spaccini, L.; Ficcidenti, A.; et al. Insights into genotype-phenotype correlations from CREBBP point mutation screening in a cohort of 46 Rubinstein-Taybi syndrome patients. *Clin. Genet.* **2015**, *88*, 431–440. [[CrossRef](#)]
52. Negri, G.; Milani, D.; Colapietro, P.; Forzano, F.; Della Monica, M.; Rusconi, D.; Consonni, L.; Caffi, L.G.; Finelli, P.; Scarano, G.; et al. Clinical and molecular characterization of Rubinstein-Taybi syndrome patients carrying distinct novel mutations of the EP300 gene. *Clin. Genet.* **2015**, *87*, 148–154. [[CrossRef](#)] [[PubMed](#)]
53. Negri, G.; Magini, P.; Milani, D.; Colapietro, P.; Rusconi, D.; Scarano, E.; Bonati, M.T.; Priolo, M.; Crippa, M.; Mazzanti, L.; et al. From Whole Gene Deletion to Point Mutations of EP300-Positive Rubinstein-Taybi Patients: New Insights into the Mutational Spectrum and Peculiar Clinical Hallmarks. *Hum. Mutat.* **2016**, *37*, 175–183. [[CrossRef](#)] [[PubMed](#)]
54. Schölz, C.; Weinert, B.T.; Wagner, S.A.; Beli, P.; Miyake, Y.; Qi, J.; Jensen, L.J.; Streicher, W.; McCarthy, A.R.; Westwood, N.J.; et al. Acetylation site specificities of lysine deacetylase inhibitors in human cells. *Nat. Biotechnol.* **2015**, *33*, 415–423. [[CrossRef](#)]
55. Chang, M.C.; Chen, Y.J.; Lian, Y.C.; Chang, B.E.; Huang, C.C.; Huang, W.L.; Pan, Y.H.; Jeng, J.H. Butyrate stimulates histone H3 acetylation, 8-isoprostane production, RANKL expression, and regulated osteoprotegerin expression/secretion in MG-63 osteoblastic cells. *Int. J. Mol. Sci.* **2018**, *19*, 4071. [[CrossRef](#)] [[PubMed](#)]
56. Freese, K.; Seitz, T.; Dietrich, P.; Lee, S.M.L.; Thasler, W.E.; Bosserhoff, A.; Hellerbrand, C. Histone deacetylase expressions in hepatocellular carcinoma and functional effects of histone deacetylase inhibitors on liver cancer cells in vitro. *Cancers* **2019**, *11*, 1587. [[CrossRef](#)]
57. Tarasenko, N.; Chekroun-Setti, H.; Nudelman, A.; Rephaeli, A. Comparison of the anticancer properties of a novel valproic acid prodrug to leading histone deacetylase inhibitors. *J. Cell. Biochem.* **2018**, *119*, 3417–3428. [[CrossRef](#)]
58. Gottlicher, M.; Minucci, S.; Zhu, P.; Krämer, O.H.; Schimpf, A.; Giavara, S.; Sleeman, J.P.; Lo Coco, F.; Nervi, C.; Pelicci, P.G.; et al. Valproic acid defines a novel class of HDAC inhibitors inducing differentiation of transformed cells. *PubMed NCBI EMBO J.* **2001**, *20*, 6969–6978. [[CrossRef](#)]
59. Chriett, S.; Dąbek, A.; Wojtala, M.; Vidal, H.; Balcerczyk, A.; Pirola, L. Prominent action of butyrate over β -hydroxybutyrate as histone deacetylase inhibitor, transcriptional modulator and anti-inflammatory molecule. *Sci. Rep.* **2019**, *9*, 742. [[CrossRef](#)] [[PubMed](#)]
60. Verduci, E.; Moretti, F.; Bassanini, G.; Banderali, G.; Rovelli, V.; Casiraghi, M.C.; Morace, G.; Borgo, F.; Borghi, E. Phenylketonuric diet negatively impacts on butyrate production. *Nutr. Metab. Cardiovasc. Dis.* **2018**, *28*, 385–392. [[CrossRef](#)] [[PubMed](#)]
61. Masella, A.P.; Bartram, A.K.; Truskowski, J.M.; Brown, D.G.; Neufeld, J.D. PANDAsseq: Paired-end assembler for illumina sequences. *BMC Bioinf.* **2012**, *13*, 31. [[CrossRef](#)] [[PubMed](#)]
62. Caporaso, J.G.; Kuczynski, J.; Stombaugh, J.; Bittinger, K.; Bushman, F.D.; Costello, E.K.; Fierer, N.; Pêa, A.G.; Goodrich, J.K.; Gordon, J.I.; et al. QIIME allows analysis of high-throughput community sequencing data. *Nat. Methods* **2010**, *7*, 335–336. [[CrossRef](#)] [[PubMed](#)]
63. Wang, Q.; Garrity, G.M.; Tiedje, J.M.; Cole, J.R. Naïve Bayesian classifier for rapid assignment of rRNA sequences into the new bacterial taxonomy. *Appl. Environ. Microbiol.* **2007**, *73*, 5261–5267. [[CrossRef](#)]
64. Lozupone, C.; Lladser, M.E.; Knights, D.; Stombaugh, J.; Knight, R. UniFrac: An effective distance metric for microbial community comparison. *ISME J.* **2011**, *5*, 169–172. [[CrossRef](#)] [[PubMed](#)]
65. Bassanini, G.; Ceccarani, C.; Borgo, F.; Severgnini, M.; Rovelli, V.; Morace, G.; Verduci, E.; Borghi, E. Phenylketonuria Diet Promotes Shifts in Firmicutes Populations. *Front. Cell. Infect. Microbiol.* **2019**, *9*, 101. [[CrossRef](#)] [[PubMed](#)]
66. Ashburner, M. *Drosophila: A Laboratory Handbook*; Cold Spring Harbor Laboratory Press: New York, NY, USA, 1989.

RESEARCH LETTER

SLC35F1 as a candidate gene for neurodevelopmental disorders resembling Rett syndrome

Elisabetta Di Fede¹ | Angela Peron^{2,3,4}  | Elisa Adele Colombo¹ |
Cristina Gervasini^{1,5} | Aglaia Vignoli³ 

¹Department of Health Sciences, Università degli Studi di Milano, Milan, Italy

²Human Pathology and Medical Genetics, ASST Santi Paolo e Carlo, San Paolo Hospital, Milan, Italy

³Child Neuropsychiatry Unit, Epilepsy Center, ASST Santi Paolo e Carlo, San Paolo Hospital, Department of Health Sciences, Università degli Studi di Milano, Milan, Italy

⁴Division of Medical Genetics, Department of Pediatrics, University of Utah School of Medicine, Salt Lake City, Utah

⁵“Aldo Ravelli” Center for Neurotechnology and Experimental Brain Therapeutics, Università degli Studi di Milano, Milan, Italy

Correspondence

Angela Peron, ASST Santi Paolo e Carlo, San Paolo Hospital, Department of Health Sciences, Università degli Studi di Milano, Milan, Italy.

Email: angela.peron@unimi.it

Funding information

Aldo Ravelli Center for Neurotechnology and Experimental Brain Therapeutics; Translational Medicine PhD scholarship; Università degli Studi di Milano - Linea 2 DiSS; Università degli Studi di Milano

To the Editor,

Rett syndrome (RTT, OMIM #312750) is a neurodevelopmental disorder with an incidence of 1 in 10,000 live female births. In classic RTT, affected girls present with psychomotor regression around age 6–18 months after initial normal development, and progressively develop a severe condition associated with motor, cognitive, and behavioral impairment. Most cases of classic RTT are related to pathogenic variants in the Methyl CpG-binding protein 2 gene (*MECP2*). Patients with atypical or variant forms of RTT exhibit many of the clinical signs of RTT, but do not necessarily show all the classic characteristics of the disorder (Neul et al., 2010). Among the atypical forms, individuals with the early seizure onset RTT variant (Scala et al., 2005), who manifest epilepsy before regression, have mutations in the cyclin-dependent kinase-like 5 gene (*CDKL5*), and patients with congenital RTT, who show early developmental delay, have molecular defects in the forkhead box G1 gene (*FOXG1*) (Ariani et al., 2008). However, no pathogenic variants in the aforementioned genes are identified in around 10% of patients clinically diagnosed as RTT.

Next generation sequencing (NGS) and especially exome sequencing have emerged as powerful tools for the identification of

additional new genes involved in rare genetic diseases (Zhu et al., 2015) and for the diagnosis of patients without a known genetic cause or with uncertain clinical manifestations (Negri et al., 2019). Indeed, several uncommon causative genes for classic/variant RTT or similar phenotypes (RTT-like) have been discovered in the last few years (Vidal et al., 2019).

We report on a 27-year-old woman recruited among the patients attending the RTT Clinic at the Child and Adolescent Neuro-Psychiatry Unit of ASST Santi Paolo Carlo Hospital (University of Milan, Italy). She exhibited an RTT-like phenotype but was negative after classic molecular analyses, and was found to carry a novel heterozygous missense variant in *SLC35F1*.

The patient was the third child of unrelated parents, born by caesarean section with 9/10 Apgar score.

Global developmental delay was noted since the age of 3 months; she sat unsupported at the age of 36 months.

At the age of 3 months, she experienced generalized tonic and tonic-clonic seizures, which became drug resistant, except for a seizure-free period between the age of 4 and 9 years. At the age of 9 years, tonic seizures with perioral cyanosis and clonic components in the face and upper limbs reappeared, presenting in clusters, with

This is an open access article under the terms of the Creative Commons Attribution-NonCommercial-NoDerivs License, which permits use and distribution in any medium, provided the original work is properly cited, the use is non-commercial and no modifications or adaptations are made.

© 2021 The Authors. *American Journal of Medical Genetics Part A* published by Wiley Periodicals LLC.

monthly frequency. Several antiepileptic drugs as well as vagal nerve stimulation did not control her seizures.

She never acquired independent walking and developed spastic tetraplegia in adulthood. Although not formally tested, she had severe intellectual disability (ID). Speech was limited to few intentional vocalizations. Intermittent stereotypies involving both hands, namely hand washing and mouthing, were present since the age of 2 years. Bruxism during wakefulness occurred almost daily.

Background electroencephalography (EEG) activity was diffusely slow with sharp-waves on both temporal regions. Brain magnetic resonance imaging (MRI) showed nonspecific abnormalities in the white matter on both hemispheres.

She experienced several episodes of pneumonia with severe respiratory deficit and received percutaneous endoscopic gastrostomy at the age of 24 years to prevent ab ingestis pneumonia. The patient recently passed away at the age of 27 years due to cardiac arrest during sleep.

Metabolic tests (plasma and urine amino acids, urine organic acids), genetic analyses (karyotype, chromosomal microarray, *MECP2*, *CDKL5*, and *STXBP1* sequencing and del/dup analyses), and transferrin isoelectrofocusing were normal.

DNA was then extracted from the patient's (blood and saliva) and parents' (blood) samples with the Wizard Genomic DNA Purification Kit (Promega, Madison, WI) and Quick-DNA Miniprep Plus Kit (Zymo Research, Freiburg im Breisgau, DE). Genomic DNA was enriched for the targeted exome with the Agilent SureSelect AllExon v7 kit according to the manufacturer's protocol and sequenced on the Illumina HiSeq3000 platform at CRS4 NGS Core facility. Data analysis was carried out as previously described in Di Fede et al. (2020). Exome sequencing identified a heterozygous missense variant in *SLC35F1*: c.1037T>C; p.(I346T) in exon 8 (RefSeq NC_000006.12, NM_001029858.4) in both the saliva and blood proband's samples. The variant was confirmed by Sanger sequencing in the trio, is *de novo*, and absent from population databases (now registered in the LOVD website as individual ID #00324959). This variant is predicted as damaging by several prediction tools (BayesDel_addAF, DANN, EIGEN, FATHMM-MKL, LIST-S2, MutationTaster, PrimateAI, and REVEL), and is classified as likely pathogenic (PS2, PM2, and PP3) according to the ACMG guidelines (Richards et al., 2015).

Little is known about *SLC35F1*, which is mainly expressed in the brain, and its protein product, which is thought to be a nucleotide sugar transporter (Song, 2013). However, in 2015, Szafranski and colleagues (Szafranski et al., 2015) showed that deletions in a chromosomal region including regulatory sequences of *SLC35F1* (6q22.1q22.31) are associated with pediatric epilepsy, thus suggesting a neurodevelopmental role for this gene. In addition, a recent study demonstrated that *Slc35f1* co-localizes in mouse with *Rab11*, a protein fundamental for dendritic spine formation and mutations in which in humans have been associated with developmental and epileptic encephalopathy (Farenholtz et al., 2019). These data support both the pathogenicity of the variant found in our patient and the presumed role of *SLC35F1* in synaptic plasticity.

Most of the previously described patients (Szafranski et al., 2015) showed variable severity of ID, stereotyped behaviors, and mild neurological signs. Epilepsy and EEG abnormalities were reported in half of the affected individuals, who frequently had drug-resistant seizures. Our patient exhibited a more severe phenotype characterized by spastic tetraplegia, absent speech, hand stereotypies, bruxism, drug-resistant seizures, and recurrent respiratory infections. We cannot exclude that these characteristics may appear or worsen with age, as our patient is the oldest reported thus far, or that different mechanisms in the same gene may cause slightly different phenotypes.

Although further work needs to be done, these premises together with our findings suggest *SLC35F1* as an excellent candidate gene for developmental and epileptic encephalopathies resembling Rett syndrome.

ACKNOWLEDGMENTS

This work was supported by intramural Department funding (Università degli Studi di Milano—Linea 2 DiSS, to Aglaia Vignoli and Cristina Gervasini), grant “Aldo Ravelli” Center for Neurotechnology and Experimental Brain Therapeutics (Università degli Studi di Milano, to Cristina Gervasini), Translational Medicine PhD scholarship (Università degli Studi di Milano, to Elisabetta Di Fede). The authors would like to thank the patient's family for participating in this study. This article is dedicated to the memory of our patient.

CONFLICT OF INTERESTS

The authors declare no conflicts of interest.

AUTHOR CONTRIBUTIONS

Aglaia Vignoli and Angela Peron critically recruited and clinically evaluated the patient; Elisabetta Di Fede, Elisa Adele Colombo, and Cristina Gervasini performed the variants analysis. All the authors wrote the text.

DATA AVAILABILITY STATEMENT

The variant is available in the LOVD website as individual ID #00324959. The raw data are available from the corresponding author upon reasonable request.

ORCID

Angela Peron  <https://orcid.org/0000-0002-1769-6548>

Aglaia Vignoli  <https://orcid.org/0000-0003-4638-4663>

REFERENCES

- Ariani, F., Hayek, G., Rondinella, D., Artuso, R., Mencarelli, M. A., Spanhol-Rosseto, A., Pollazzon, M., Buoni, S., Spiga, O., Ricciardi, S., Meloni, I., Longo, I., Mari, F., Broccoli, V., Zappella, M., & Renieri, A. (2008). *FOXG1* is responsible for the congenital variant of Rett syndrome. *American Journal of Human Genetics*, 83(1), 89–93. <https://doi.org/10.1016/j.ajhg.2008.05.015>
- Di Fede, E., Massa, V., Augello, B., Squeo, G., Scarano, E., Perri, A. M., Fischetto, R., Causio, F. A., Zampino, G., Piccione, M., Curridori, E., Mazza, T., Castellana, S., Larizza, L., Ghelma, F., Colombo, E. A., Gandini, M. C., Castori, M., Merla, G., ... Gervasini, C. (2020).

- Expanding the phenotype associated to KMT2A variants: Overlapping clinical signs between Wiedemann–Steiner and Rubinstein–Taybi syndromes. *European Journal of Human Genetics*, 29, 88–98. <https://doi.org/10.1038/s41431-020-0679-8>
- Farenholtz, J., Artelt, N., Blumenthal, A., Endlich, K., Kroemer, H. K., Endlich, N., & von Bohlen und Halbach, O. (2019). Expression of *Slc35f1* in the murine brain. *Cell and Tissue Research*, 377(2), 167–176. <https://doi.org/10.1007/s00441-019-03008-8>
- Negri, G., Magini, P., Milani, D., Crippa, M., Biamino, E., Piccione, M., Sotgiu, S., Perria, C., Vitiello, G., Frontali, M., Boni, A., di Fede, E., Gandini, M. C., Colombo, E. A., Bamshad, M. J., Nickerson, D. A., Smith, J. D., Loddo, I., Finelli, P., ... Gervasini, C. (2019). Exploring by whole exome sequencing patients with initial diagnosis of Rubinstein–Taybi syndrome: The interconnections of epigenetic machinery disorders. *Human Genetics*, 138(3), 257–269. <https://doi.org/10.1007/s00439-019-01985-y>
- Neul, J. L., Kaufmann, W. E., Glaze, D. G., Christodoulou, J., Clarke, A. J., Bahi-Buisson, N., Leonard, H., Bailey, M. E. S., Schanen, N. C., Zappella, M., Renieri, A., Huppke, P., Percy, A. K., & RettSearch Consortium. (2010). Rett syndrome: Revised diagnostic criteria and nomenclature. *Annals of Neurology*, 68(6), 944–950. <https://doi.org/10.1002/ana.22124>
- Richards, S., Aziz, N., Bale, S., Bick, D., Das, S., Gastier-Foster, J., Grody, W. W., Hegde, M., Lyon, E., Spector, E., Voelkerding, K., Reh, H. L., & ACMG Laboratory Quality Assurance Committee. (2015). Standards and guidelines for the interpretation of sequence variants: A joint consensus recommendation of the American College of Medical Genetics and Genomics and the Association for Molecular Pathology. *Genetics in Medicine*, 17(5), 405–424. <https://doi.org/10.1038/gim.2015.30>
- Scala, E., Ariani, F., Mari, F., Caselli, R., Pescucci, C., Longo, I., Meloni, I., Giachino, D., Bruttini, M., Hayek, G., Zappella, M., & Renieri, A. (2005). *CDKL5/STK9* is mutated in Rett syndrome variant with infantile spasms. *Journal of Medical Genetics*, 42(2), 103–107. <https://doi.org/10.1136/jmg.2004.026237>
- Song, Z. (2013, April). Roles of the nucleotide sugar transporters (SLC35 family) in health and disease. *Molecular Aspects of Medicine*, 34, 590–600. <https://doi.org/10.1016/j.mam.2012.12.004>
- Szafranski, P., Von Allmen, G. K., Graham, B. H., Wilfong, A. A., Kang, S. H. L., Ferreira, J. A., Upton, S. J., Moeschler, J. B., Bi, W., Rosenfeld, J. A., Shaffer, L. G., Cheung, S. W., Stankiewicz, P., & Lalani, S. R. (2015). 6q22.1 microdeletion and susceptibility to pediatric epilepsy. *European Journal of Human Genetics*, 23(2), 173–179. <https://doi.org/10.1038/ejhg.2014.75>
- Vidal, S., Xiol, C., Pascual-alonso, A., O'callaghan, M., Pineda, M., & Armstrong, J. (2019, August 2). Genetic landscape of Rett syndrome spectrum: Improvements and challenges. *International Journal of Molecular Sciences*, 20(16), 3925. <https://doi.org/10.3390/ijms20163925>
- Zhu, X., Petrovski, S., Xie, P., Ruzzo, E. K., Lu, Y. F., McSweeney, K. M., Ben-Zeev, B., Nissenkorn, A., Anikster, Y., Oz-Levi, D., Dhindsa, R. S., Hitomi, Y., Schoch, K., Spillmann, R. C., Heimer, G., Marek-Yagel, D., Tzadok, M., Han, Y., Worley, G., ... Goldstein, D. B. (2015). Whole-exome sequencing in undiagnosed genetic diseases: Interpreting 119 trios. *Genetics in Medicine*, 17(10), 774–781. <https://doi.org/10.1038/gim.2014.191>

How to cite this article: Di Fede E, Peron A, Colombo EA, Gervasini C, Vignoli A. *SLC35F1* as a candidate gene for neurodevelopmental disorders resembling Rett syndrome. *Am J Med Genet Part A*. 2021;1–3. <https://doi.org/10.1002/ajmg.a.62203>



Chromatin Imbalance as the Vertex Between Fetal Valproate Syndrome and Chromatinopathies

Chiara Parodi¹, Elisabetta Di Fede¹, Angela Peron^{2,3,4}, Ilaria Viganò¹, Paolo Grazioli¹, Silvia Castiglioni¹, Richard H. Finnell⁵, Cristina Gervasini^{1,6†}, Aglaia Vignoli^{1†} and Valentina Massa^{1,6*†}

¹ Department of Health Sciences, Università degli Studi di Milano, Milan, Italy, ² Human Pathology and Medical Genetics, ASST Santi Paolo e Carlo, San Paolo Hospital, Milan, Italy, ³ Child Neuropsychiatry Unit–Epilepsy Center, Department of Health Sciences, San Paolo Hospital, ASST Santi Paolo e Carlo, Università degli Studi di Milano, Milan, Italy, ⁴ Division of Medical Genetics, Department of Pediatrics, University of Utah School of Medicine, Salt Lake City, UT, United States, ⁵ Departments of Molecular and Cellular Biology, Molecular and Human Genetics and Medicine, Center for Precision Environmental Health, Baylor College of Medicine, Houston, TX, United States, ⁶ “Aldo Ravelli” Center for Neurotechnology and Experimental Brain Therapeutics, Università degli Studi di Milano, Milan, Italy

OPEN ACCESS

Edited by:

Xiajun Li,
ShanghaiTech University, China

Reviewed by:

Taiping Chen,
University of Texas MD Anderson
Cancer Center, United States
Alejandro Vaquero,
Josep Carreras Leukaemia Research
Institute (IJC), Spain

*Correspondence:

Valentina Massa
valentina.massa@unimi.it

†These authors have contributed
equally to this work and share last
authorship

Specialty section:

This article was submitted to
Developmental Epigenetics,
a section of the journal
Frontiers in Cell and Developmental
Biology

Received: 16 January 2021

Accepted: 01 April 2021

Published: 20 April 2021

Citation:

Parodi C, Di Fede E, Peron A,
Viganò I, Grazioli P, Castiglioni S,
Finnell RH, Gervasini C, Vignoli A and
Massa V (2021) Chromatin Imbalance
as the Vertex Between Fetal Valproate
Syndrome and Chromatinopathies.
Front. Cell Dev. Biol. 9:654467.
doi: 10.3389/fcell.2021.654467

Prenatal exposure to valproate (VPA), an antiepileptic drug, has been associated with fetal valproate spectrum disorders (FVSD), a clinical condition including congenital malformations, developmental delay, intellectual disability as well as autism spectrum disorder, together with a distinctive facial appearance. VPA is a known inhibitor of histone deacetylase which regulates the chromatin state. Interestingly, perturbations of this epigenetic balance are associated with chromatinopathies, a heterogeneous group of Mendelian disorders arising from mutations in components of the epigenetic machinery. Patients affected from these disorders display a plethora of clinical signs, mainly neurological deficits and intellectual disability, together with distinctive craniofacial dysmorphisms. Remarkably, critically examining the phenotype of FVSD and chromatinopathies, they shared several overlapping features that can be observed despite the different etiologies of these disorders, suggesting the possible existence of a common perturbed mechanism(s) during embryonic development.

Keywords: fetal valproate syndrome, chromatinopathies, anti-epileptic drugs, neurodevelopment, HDAC inhibitor

INTRODUCTION

Prenatal exposure to antiepileptic drugs (AEDs) are subject to the teratogenic effects associated with all of the frontline AED medications. Most women with epilepsy receiving adequate prenatal care will have uneventful pregnancies, but they are at a well-documented increased risk for having infants with congenital malformations compared to the general population (Viale et al., 2015). *In utero* AED exposure places their offspring at increased risk not only for major congenital malformations, but also for adverse neurological developmental outcomes. However, many of these risks can be mitigated through comprehensive prenatal maternal care by carefully selecting the type and dose of AEDs prior to conception and continuing to follow a proper therapeutic regimen throughout pregnancy (Tomson et al., 2011). Among all AEDs, valproate (2-propylpentanoic acid, VPA) exposure has been associated with the greatest risks of inducing severe teratogenicity (Lammer et al., 1987; Tomson et al., 2015). Several studies demonstrated a correlation between chronic exposure to VPA treatment and higher risk of displaying fetal anomalies—such as neural tube defects (NTDs), distinctive facial dysmorphia, craniofacial, and skeletal defects—in both in

humans and in animal models (Massa et al., 2005, 2006). Among the teratogen-induced congenital malformations, the most commonly observed include spina bifida, atrial septal defects, cleft palate, hypospadias, polydactyly, and craniosynostosis (Macfarlane and Greenhalgh, 2018).

Animal experiments demonstrated morphogenic anomalies throughout the entire axial skeleton and vertebral transformations in rat embryos due to VPA exposure, suggesting a possible compromise of the expression of genes involved in vertebral segments development (Menegola et al., 1998, 1999). In addition, an altered serotonergic differentiation, which correlates with autism-like behavioral abnormalities, was observed both in rodent and zebrafish models in response to prenatal valproate exposure (Dufour-Rainfray et al., 2010; Jacob et al., 2014). The amount of fetal harm appears to be linked to the maternal concentration of the drug (Nau et al., 1981; Nau, 1985), especially when it occurs in the first trimester during fetal organogenesis (Macfarlane and Greenhalgh, 2018). In animal models, such as *Xenopus* and *Hyperolius*, the beginning of gastrulation was delayed up to neurulation upon embryonic exposure to VPA, and eventually they displayed NTDs of different types and degree (Oberemm and Kirschbaum, 1992). To date, the correlation between typical dysmorphic facial features and developmental outcomes is unclear (Kini et al., 2006; Nicolini and Fahnestock, 2018).

Fetal valproate syndrome (FVS, OMIM #609442) is a condition resulting from the therapeutic management of epileptic mothers with VPA during their pregnancy, and it is observed in up to 20–30% of children exposed to high VPA dosage *in utero* (Nau et al., 1991; Ornoy, 2009; Tomson et al., 2011). FVS is characterized by a constellation of congenital malformations and developmental delay, with patients displaying intellectual disability (ID) as well as autism spectrum disorder (ASD), and a distinctive facial appearance strikingly similar to the one described in genetic disorders known as chromatinopathies (DiLiberti et al., 1984). A new term “fetal valproate spectrum disorder” (FVSD) has recently been proposed to describe the range of clinical and developmental effects that are attributed to *in utero* VPA exposure (Clayton-Smith et al., 2019).

Valproate has been commonly used as an anti-seizure medication for over half a century (Meunier et al., 1963). Given its broad antiepileptic effect, it has also been clinically utilized as a mood stabilizer in the treatment of bipolar disorders and in other neurological conditions—i.e., migraine and neuropathic pain, exposing many more women of reproductive age to this medication (Johannessen and Johannessen, 2003). In addition, this antiepileptic drug has shown anticancer properties for several tumors (Shah and Stonier, 2019), and its use in combination regimens with cytotoxic chemotherapy seems to be promising (Brodie and Brandes, 2014). VPA is also known to be a potent histone deacetylase inhibitor (HDACi) and therefore acts on chromatin. It is known to have dose-related teratogenic properties resulting in altered gene expression and potent inhibition of the histone deacetylases (HDAC) enzymes family (Schölz et al., 2015). Among the various hypotheses that have been proposed for the teratogenicity of VPA, its HDACi effects that is believed to be represent the principle underlying

teratogenic mechanism. VPA's anti-seizure activity can also be explained by its ability to modulate gene expression through the inhibition of HDAC enzymes (Göttlicher et al., 2001; Jacob et al., 2013; Brunton et al., 2018).

Valproate perturbs the cell's epigenetic machinery controlling its chromatin state. In this context, a group of heterogeneous genetic disorders known as the chromatinopathies, are believed to be caused by mutations in genes that regulate the conformation and function of chromatin, thus acting in concert with epigenetic mechanisms. Defects in the functional network between the complexes associated with chromatin could lead to alterations in gene expression and protein function. As estimated, there are over 80 Mendelian diseases associated with incorrect functioning of the “epigenetic machinery”, the majority of which presents with neurological defects and ID (Fahrner and Bjornsson, 2019). Kabuki syndrome (OMIM #147920 and #300867) (Niikawa et al., 1981) and CHARGE syndrome (OMIM #214800) (Pagon et al., 1981) are among the most well-known and studied chromatinopathies, for the cascading effect of the causative genes on different cell pathways. These syndromes are associated with ID and distinctive craniofacial dysmorphisms that are pathognomonic.

In this review, we explore shared features between FVSD and selected chromatinopathies, leading us to the hypothesis that these disorders, despite divergent etiologies (i.e., environmental or genetic), could operate through a common perturbed mechanism during embryonic development. As such, VPA-induced FVSD is a phenocopy of select chromatinopathies.

VALPROATE MECHANISM OF ACTION

Valproate has multiple cellular mechanisms of action consistent with its broad clinical efficacy. This compound appears to suppress repetitive high-frequency neuronal focus by blocking voltage-dependent sodium channels, but at sites that are different from other AEDs. VPA also appears to increase GABA concentrations in the brain at clinically relevant doses, without having direct effects on the GABA (A) receptors, potentiated by a presynaptic effect of valproate on GABA (B) receptors. In addition, VPA can increase GABA synthesis by activating the enzyme glutamic acid decarboxylase (GAD).

The molecular mechanisms underlying FVSD have not been fully established, although the consequences of *in utero* VPA exposure have been investigated for several decades. Such effects include apoptotic neurodegeneration observed in the developing rat brain (Bittigau et al., 2002), enhanced synaptic plasticity exhibited in the rat medial prefrontal cortex (Sui and Chen, 2012), and a decrease in folic acid (Wegner and Nau, 1992), suggesting that inadequate embryonic and fetal antioxidant defense mechanisms and consequent oxidative stress could be responsible for brain damage secondary to VPA teratogenicity (Ornoy, 2009).

Despite the fact that VPA has been shown to be neuroprotective in neurons through *Bcl-2* upregulation (Chen et al., 1999), its administration in critical developmental stages causes morphological defects and impaired social behavior in

rats (Kim et al., 2011). *In utero* VPA exposure in mouse pups on gestational day 11 leads to dysfunctional pre-weaning social behavior, together with delayed development, impaired olfactory discrimination and reduced cortical *Bdnf* expression, suggesting that VPA-driven perturbations in neuronal plasticity may underlie the behavioral phenotype (Rouillet et al., 2010). Similar to the results of VPA exposure of pregnant rats, neural progenitor cells (NPCs) of murine embryos exposed on gestational day E12 showed a reduced apoptotic cell death, which is fundamental to the proper regulation of NPCs during a developmentally critical period, suggesting another possible mechanism underlying FVSD defects (Go et al., 2011).

Alterations in embryonic gene expression following VPA exposure appears to be one of the primary mechanisms underlying VPA's teratogenicity. Previous studies showed that VPA alters Wnt signaling by inducing Wnt-dependent gene expression at doses that cause developmental effects (Phiel et al., 2001; Wiltse, 2005). This is due to its role as an HDAC inhibitor, which consists of deregulating class I HDACs, thus counteracting their normal activity of histone acetylation marks removal. This action induces chromatin changes converting segments of heterochromatin into euchromatin. VPA exposure can lead to hyperacetylation of histones and following activation of genes related to cell cycle and apoptosis, possibly explaining its teratogenic action (Göttlicher et al., 2001). For instance, hyperacetylation of all *Hoxb* developmental genes has been observed in mouse embryonic stem cells exposed to VPA, with increased levels of H3K9ac at upstream, promoter and coding regions across the entire *Hoxb* cluster (Boudadi et al., 2013).

Previous studies showed how HDACi is involved in early neuronal processes: exposure of neurulation-stage mouse embryos to VPA can cause NTDs and skeletal malformations (Finnell et al., 2002), supported by *in vivo* studies on chick embryos in which a complete failure of neural tube closure occurred (Murko et al., 2013). Since VPA exposure alters gene expression in the somitic tissues of mouse embryos (Massa et al., 2005) and an increased histone H4 acetylation in the caudal neural tube was observed, modulation of acetylation was hypothesized as mediating the effect of VPA on neurulation (Massa et al., 2005, 2009; Menegola et al., 2005).

VALPROATE IN CLINICAL PRACTICE

Valproate is a wide-spectrum anti-seizure medication that can be used to treat almost all types of seizure disorders (tonic clonic seizures, absence seizures, myoclonic seizures, less frequently in clonic seizures, tonic seizures and atonic seizures) (Perucca, 2002). It is used as first-line antiepileptic drug in generalized seizures; VPA may also be used in focal seizures, although it is no longer the first choice of neurologists (Tomson et al., 2015).

Valproate is also a mood stabilizer that is used in the treatment of bipolar disorders and other psychiatric conditions, including: anxiety disorders, post-traumatic stress disorder, substance abuse, and schizophrenia. VPA also appears to be an effective treatment for tardive dyskinesia thanks to its GABA-potentiating properties (Swann et al., 2002), for migraine prophylaxis, and for

the treatment of neuropathic pain, in particular for trigeminal neuralgia (Johannessen and Johannessen, 2003).

Typically, the initial dose of oral valproate is 10–15 mg/kg per day. If necessary, the dose can be increased with weekly increments of 5–10 mg/kg up to a maximum dose of 60 mg/kg/day. It is recommended to monitor VPA blood level during treatment, as well as blood count, liver enzymes, and coagulation tests, in order to avoid any potential side effects of the drug.

Valproate can alter vitamin D metabolism and affect bone mineral density, therefore 25-hydroxyvitamin D levels should be monitored. It may be useful to obtain serum amylase and lipase levels in cases where symptoms suggestive of pancreatitis, such as abdominal pain, nausea, vomiting and anorexia have occurred. Furthermore, ammonium levels should be monitored in patients receiving VPA who exhibit signs of vomiting or lethargy as the treatment inhibits *N*-acetyl glutamate, leading to systemic disruption and hyperammonemia (Bruni et al., 1979; Batshaw and Brusilow, 1982; Asconapé et al., 1993; Patsalos et al., 2008).

It is strongly recommended that VPA administration should be avoided during pregnancy; however, if necessary, a slow-release formulation that limits peak concentrations of the drug using the lowest efficacious dose possible should be given along with the administration of a high dose of folic acid. While folic acid has not been shown to be effective in reducing the prevalence of NTDs, it has been shown to be protective in limiting adverse cognitive consequences of VPA treatment, especially with respect to language skills (Meador et al., 2020).

CLINICAL FEATURES ASSOCIATED WITH FVSD

Studies conducted by Robert and Guibaud (1982) first drew attention to the increased risk of spina bifida after exposure to VPA in pregnancy. Subsequently, the initial reports of children suffering from FVSD were published (DiLiberti et al., 1984). FVSD is characterized by major and minor malformations, facial dysmorphism and impaired development with particular risks related to NTDs (Lindhout and Schmidt, 1986), congenital heart disease, ophthalmological, (Glover et al., 2002) and genitourinary abnormalities (DiLiberti et al., 1984; Ozkan et al., 2011), cleft palate (Jackson et al., 2016), overlapping fingers, and scalp defects (DiLiberti et al., 1984; Clayton-Smith and Donnai, 1995; Clayton-Smith et al., 2019).

Neurological development is impaired in many affected individuals. An increased risk of attention deficit hyperactivity disorder (ADHD) and ASD is often observed in these patients (Bromley et al., 2013, 2014, 2019; Christensen et al., 2013).

The typical facial features of FVSD include: swelling of the metopic suture, highly-arched eyebrows, hypertelorism, wide nasal bridge, short nose with anteverted nostrils, small mouth with thin upper lip and flat filament of the inverted lower lip (Ardinger et al., 1988; Clayton-Smith and Donnai, 1995; Kozma, 2001; Schorry et al., 2005; Kini et al., 2006; Chandane and Shah, 2014; Mohd Yunus and Green, 2018) (**Figure 1**).

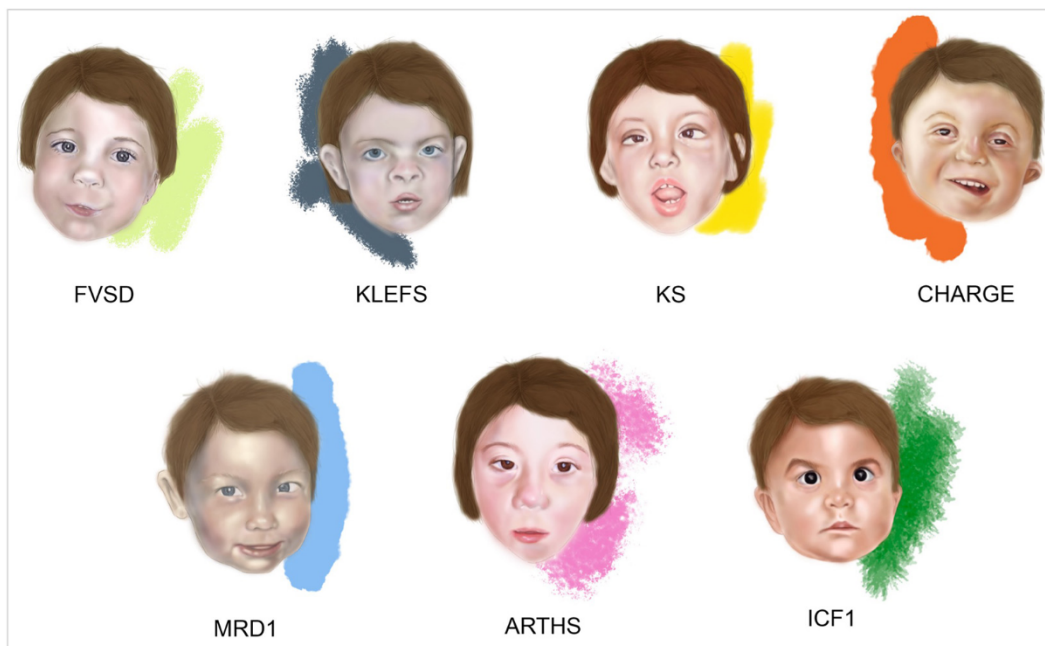


FIGURE 1 | Facies of fetal valproate spectrum disorders (FVSD) and related overlapping chromatinopathies. Distinctive facial phenotypes of patients affected by FVSD (Schorry et al., 2005), KLEFS (Willemsen et al., 2012), KS (Makrythanasis et al., 2013), CHARGE (Hefner and Fassi, 2017), MRD1 (Talkowski et al., 2011), ARTHS (Kennedy et al., 2019), and ICF1 (Gössling et al., 2017).

DIFFERENTIAL DIAGNOSES OF FVSD

Fetal valproate spectrum disorder diagnosis has been challenging in many ways, from gathering correct information about prenatal VPA exposure, to obtaining a comprehensive grasp of the clinically varied diagnostic phenotypic signs. Indeed, clinical presentations of affected patients show variability and the prevalence of neurocognitive dysfunction is higher than the prevalence of structural malformations, complicating the path toward reliable diagnosis (Clayton-Smith et al., 2019). In fact, not all the FVSD individuals even display dysmorphisms, which can be age dependent and rather subtle, thus recognizable only by experienced dysmorphologists. When FVSD signs are ascertained, physicians are often challenged by overlapping phenotypes associated with the following syndromes (Figure 1 and Table 1).

Kleefstra Syndrome

Kleefstra syndrome (KLEFS, OMIM #610253, #617768) is a rare condition characterized by heterozygous genomic deletions at chromosome 9q34.3 removing the *EHMT1* gene or *EHMT1* point mutations (KLEFS1), or pathogenic variants in *KMT2C* on chromosome 7q36.1 (KLEFS2), mostly *de novo*. *EHMT1* and *KMT2C* genes encode two histone methyltransferases. The prevalence is estimated to be 1:120,000 individuals affected by neurodevelopmental disorders. Patients with Kleefstra syndrome exhibit a distinctive phenotype including hypotonia; major anomalies such as congenital heart defects and genitourinary abnormalities; behavioral and developmental manifestations with

ID of variable severity, and in some cases severe speech delay. Typical facial dysmorphisms include: microcephaly, arched or straight with synophrys eyebrows, mildly up-slanted palpebral fissures, hypertelorism, short nose with anteverted nares and bulbous nasal tip, thick mouth, and everted lower lip (Kleefstra and De Leeuw, 1993; Kleefstra et al., 2006, 2012; Koemans et al., 2017) (Figure 1).

Fetal valproate spectrum disorders has been recently defined as a “phenocopy” of Kleefstra syndrome by Arora et al. (2018). Despite a preliminary diagnosis of FVSD—due to maternal intake of VPA during pregnancy and with clear facial characteristics that are typically attributable to FVSD—a more thorough examination of the facial features revealed subtle differences. Specific features of the proband included the presence of a broad forehead and brachycephaly in a child with FVSD, who had cephalic deformation due to the premature fusion of the metopic suture, scattered eyebrows, and pointed chin. Genetic testing revealed a *de novo* deletion on 9q34.3 that is known to cause Kleefstra syndrome. The convergent mechanism present in both conditions is their role in epigenetic modulation that mediates the modification (acetylation, methylation, etc.) of histone proteins and DNA demethylation, which might be responsible for the overlapping phenotype of FVSD and Kleefstra Syndrome (Willemsen et al., 2012; Hadzsiev et al., 2016; Arora et al., 2018) (Table 1).

Kabuki Syndrome

Specific dysmorphisms, postnatal growth delay, skeletal anomalies, and ID are typical features of another

TABLE 1 | Fetal valproate spectrum disorders (FVSD) clinical signs in chromatinopathies.

FVSD clinical signs	KLEFS	KS	CHARGE	MRD1	ARTHS	ICF
Facial dysmorphism						
Scalp defects	–	–	–	–	–	–
High/prominent forehead	+	–	+	Broad	–	±
Bitemporal narrowing	–	–	±	–	+	–
Arched eyebrows	+	+	–	+	–	±
Hypertelorism	+	±	±	–	–	+
Epicanthal folds	+	–	+	–	±	+
Ears abnormalities	+	+	+	+	±	+
Midface hypoplasia	+	–	+	±	–	–
Short nose	+	–	±	+	–	±
Broad/flat nasal bridge	+	+	–	+	Broad tip	+
Anteverted nostrils	+	–	–	–	–	±
Long smooth philtrum	+	–	–	–	–	–
Small mouth	–	–	–	–	–	–
Thin upper lip	–	–	±	+	+	–
Downturned corners of the mouth	+	–	–	+	±	–
Congenital anomalies						
Cleft palate	+	+	+	±	±	±
Macroglossia	–	–	+	–	–	±
Micro/retrognathia	–	+	+	+	±	±
Microcephaly	+	+	+	+	+	na
Trigonocephaly	–	–	–	–	–	–
Brachycephaly	+	–	–	+	±	–
Other malformations						
Neural tube or CNS defects	+	+	+	–	±	±
Ophthalmological defects	±	+	+	±	+	–
Muscoskeletal anomalies	–	+	+	+	±	–
Congenital heart defects	+	+	+	+	+	±
Genitourinary anomalies	+	+	+	±	±	–
Developmental delay	+	+	+	+	+	±
Intellectual disability	+	+	+	+	+	±
Speech delay	+	+	+	+	+	+
Behavioral problems	+	±	+	+	+	–
References						
DiLiberti et al., 1984; Ardinger et al., 1988; Kozma, 2001; Schorry et al., 2005; Kini et al., 2006; Chandane and Shah, 2014; Mohd Yunos and Green, 2018	Willemsen et al., 2012; Hadzsiev et al., 2016; Arora et al., 2018	Makrythanasis et al., 2013; Adam et al., 2019; Shangguan et al., 2019	Hefner and Fassi, 2017; van Ravenswaaij-Arts and Martin, 2017	Van Bon et al., 2010; Talkowski et al., 2011; Hodge et al., 2014; Mullegama et al., 2016	Arboleda et al., 2015; Tham et al., 2015; Millan et al., 2016; Murray et al., 2017; Kennedy et al., 2019	Hagleitner et al., 2008; Weemaes et al., 2013; van den Boogaard et al., 2017; Kamae et al., 2018

KLEFS, Kleefstra syndrome; KS, Kabuki syndrome; CHARGE, CHARGE syndrome; MRD1, mental retardation autosomal dominant 1; ARTHS, Arboleda-Tham syndrome; ICF1, immunodeficiency, centromeric instability, and facial anomalies syndrome 1; +, present; –, absent; ±, present in few cases; na, not available.

chromatinopathy such as Kabuki syndrome (KS, OMIM #147920 and #300867) (Kuroki et al., 1981; Niikawa et al., 1981; Adam et al., 2019). KS is caused by heterozygous pathogenic variants in *KMT2D* or *KDM6A* genes (Ng et al., 2010; Banka et al., 2012; Lederer et al., 2012; Miyake et al., 2013), on chromosome

12q13.12 and Xp11.3, causing KS1 and KS2, respectively. These genes altered in KS encode for a histone methyltransferase and a histone demethylase exerting their effect on different histone residues that favor the opening of chromatin and leading to the same downstream effects on gene expression, ultimately

resulting in the same condition. Aside from ID, developmental impairment and congenital heart defects, KS shares with FVSD specific craniofacial features such as arched eyebrows, wide nasal bridge, and cleft palate (Makrythanasis et al., 2013; Adam et al., 2019; Shangguan et al., 2019) (**Figure 1** and **Table 1**).

CHARGE Syndrome

CHARGE syndrome (OMIM #214800) is an acronym that summarizes the main clinical manifestations, namely Coloboma of the eye, Heart defect, choanal Atresia, Retardation of psychomotor development and growth, Genital hypoplasia, and Ear abnormalities. This syndrome is caused by heterozygous pathogenic variants in *CHD7* (OMIM # 608892), encoding an epigenetic regulator that is involved in the ATP-dependent remodeling of chromatin (Vissers et al., 2004; van Ravenswaaij-Arts and Martin, 2017). Interestingly, Shah et al. (2014) and Jackson et al. (2014) reported on five children affected by FVSD exhibiting unilateral or bilateral ocular coloboma, one of the main manifestations of CHARGE syndrome. Indeed, VPA acting as a HDAC inhibitor reduces the expression of *PAX2* and *PAX6*, which are implicated in ocular development (Pennati et al., 2001; Balmer et al., 2012). Of note, CHARGE syndrome shares autism-like disturbances, congenital anomalies and malformations together with specific facial features with FVSD (Hefner and Fassi, 2017; van Ravenswaaij-Arts and Martin, 2017) (**Figure 1** and **Table 1**).

Mental Retardation Autosomal Dominant 1

Mental retardation autosomal dominant 1 (*MRD1*, OMIM #156200) or *MBD5* haploinsufficiency is a neurodevelopmental disorder caused by heterozygous variants in *MBD5* or a deletion encompassing all or part of this gene sequence on chromosome 2q23.1 (Vissers et al., 2003; Talkowski et al., 2011). *MBD5* encodes for a methyl-CpG-binding domain protein. *MBD5* is part a class of proteins that bind to DNA with a transcriptional repressor activity. In Camarena et al. (2014) *MBD5* was shown to act as transcriptional activator *in vitro*. Hence, *MBD5* is considered a “reader” of the epigenetic machinery (Camarena et al., 2014). Patients display ID and developmental delay, sleep disturbances, seizures, severe speech impairment, behavioral problems, feeding difficulties, congenital anomalies mainly affecting the skeletal and cardiovascular systems, and dysmorphic signs. Among them, *MRD1* is characterized by broad forehead, highly arched eyebrows, outer ear abnormalities, short nose with broad nasal bridge, thin upper lip, and downturned mouth angles, which are remarkably overlapping with FVSD (Van Bon et al., 2010; Talkowski et al., 2011; Hodge et al., 2014; Mullegama et al., 2016) (**Figure 1** and **Table 1**).

Arboleda-Tham Syndrome

Pathogenic variants in the *KAT6A* gene, located on chromosome 8p11.21 cause Arboleda-Tham syndrome (ARTHS, OMIM #616268) or Mental retardation autosomal dominant 32 (MRD32), a recently described disorder affecting neurodevelopment and associated with ID (Arboleda et al., 2015;

Tham et al., 2015). *KAT6A* is a lysine-acetyltransferase involved in chromatin opening, transcriptional regulation, cellular replication and therefore, in multiple developmental programs (Voss et al., 2009). Kennedy et al. (2019) extensively described phenotypes of novel and previously reported ARTHS patients, who display distinctive clinical signs such as ID, developmental and speech delay, cardiac and ophthalmological defects, gastrointestinal problems, sleep disturbance, autism-like behavior and typical dysmorphisms (Arboleda et al., 2015; Tham et al., 2015; Millan et al., 2016; Murray et al., 2017), many of them overlapping with the FVSD phenotype (**Figure 1** and **Table 1**).

Immunodeficiency, Centromeric Instability and Facial Anomalies Syndrome

Immunodeficiency, centromeric instability and facial anomalies syndrome 1 (ICF1, #OMIM 602900) is a rare autosomal recessive disorder characterized by hypogammaglobulinemia leading to severe recurrent infections, instability of pericentromeric regions of chromosomes 1, 9, and 16 in mitogen-stimulated lymphocytes, and facial dysmorphisms (Maraschio et al., 1988; Ehrlich et al., 2006). When the mapping of a locus associated to ICF syndrome on chromosome 20 was performed in 1998 (Wijmenga et al., 1998), pathogenic variants in *de novo* DNA methyltransferase gene *DNMT3B* were identified, occurring in about half of ICF patients (Hansen et al., 1999; Xu et al., 1999). *DNMT3B* is involved in the establishment of DNA methylation patterns in early life and during cell differentiation. Hypomethylation of pericentromeric satellite 2 and 3 repeats represents the molecular hallmark of ICF syndrome (Jeanpierre et al., 1993), making it the first human disorder linked to a constitutive defect in DNA methylation. In addition to distinctive signs such as immunoglobulin deficiency and consequent recurrent infections (mainly respiratory and gastrointestinal), ICF1 patients also display some features that are common to FVSD: hypertelorism, epicanthus, flat nasal bridge, macroglossia, micrognathia, low-set ears, speech, and developmental delay, and—in a minority of affected individuals—CNS anomalies, congenital heart defects and ID (Hagleitner et al., 2008; Weemaes et al., 2013; van den Boogaard et al., 2017; Kamae et al., 2018) (**Figure 1** and **Table 1**).

Other Genetic Disorders

Qiao et al. (2019) recently described a 19 years-old man with ID and distinctive facial features who had a clinical diagnosis of FVSD and was later found to carry a *de novo* pathogenic variant in the *PURA* gene on chromosome 5q31. *PURA*-related neurodevelopmental disorders include Mental Retardation autosomal Dominant 31 (MRD31, #OMIM 616158) or *PURA* syndrome, caused by heterozygous mutations in the *PURA* gene or a 5q31.3 deletion affecting completely or partially eliminating the *PURA* sequence (Brown et al., 2013; Hunt et al., 2014; Lalani et al., 2014; Tanaka et al., 2015). This causative gene encodes for a DNA- and RNA-binding protein critical for survival and development of mammalian hematopoietic and central nervous systems (Daniel and Johnson, 2018). Shared phenotypic features between *PURA* disorders

and FVSD are ID and developmental delay, heart defects, urinary and ophthalmological abnormalities, and distinctive facial dysmorphism such as high/broad forehead, hypertelorism, wide nasal bridge, and thin upper lip (Reijnders et al., 2018). Furthermore, fetal valproate exposure has been reported to cause other malformation complexes such as Baller-Gerold syndrome (BGS, OMIM #218600), an ultra-rare disorder caused by pathogenic variants in the *RECQL4* gene on chromosome 8p24, and inherited in an autosomal recessive manner (Baller, 1950; Gerold, 1959). BGS patients display a plethora of phenotypic features (Van Maldergem et al., 1992), some of which are overlapping with FVSD. These include: ID, developmental delay, limb and congenital heart defects, genitourinary anomalies and facial dysmorphisms (Iype et al., 2008). Mutations in the *RECQL4* gene that codes for an ATP-dependent DNA helicase

essential for genome integrity and involved in DNA replication, recombination and repair (Bachrati and Hickson, 2008) have also been reported in Rothmund-Thomson (RTS, OMIM #268400) families (Kitao et al., 1999). In particular, children affected with type II RTS share a variety of clinical features with BGS patients (Rothmund, 1868; Thomson, 1936; Megarbane et al., 2000; Van Maldergem et al., 2006; Larizza et al., 2010). Considering the similarities among BGS and RTS patients, there are multiple overlapping features with FVSD that can be observed—e.g., head and nose dysmorphisms, developmental delay, cardiac defects and skeletal anomalies. Although these neurodevelopmental disorders are not considered chromatinopathies, it is worthy of note that *PURA* and *RECQL4* are transcriptional regulators, and helicases are considered a guardian of the genome, such that they are involved in proper chromatin maintenance.

TABLE 2 | Shared pathways between FVSD and chromatinopathies.

Shared pathways	KLFS	KS	CHARGE	MRD1	ARTHS	ICF1
Axon guidance						
Beta1 integrin cell surface interactions						
Cyclins and cell cycle regulation						
ECM-receptor interaction						
Ensemble of genes encoding core extracellular matrix including ECM glycoproteins, collagens and proteoglycans						
Ensemble of genes encoding extracellular matrix and extracellular matrix-associated proteins						
Epithelial cell signaling in Helicobacter pylori infection						
Eukaryotic translation elongation						
Eukaryotic translation termination						
Extracellular matrix organization						
Formation of a pool of free 40S subunits						
GABA receptor activation						
GABAergic synapse						
GTP hydrolysis and joining of the 60S ribosomal subunit						
HIF-1-alpha transcription factor network						
Interactions of neuroligins and neuroligins at synapses						
L13a-mediated translational silencing of ceruloplasmin expression						
L1CAM interactions						
MAPK signaling pathway						
Morphine addiction						
Neuronal system						
Non-sense mediated decay (NMD) enhanced by the exon junction complex (EJC)						
Non-sense mediated decay (NMD) independent of the exon junction complex (EJC)						
Non-sense-mediated decay (NMD)						
p73 transcription factor network						
Peptide chain elongation						
Protein-protein interactions at synapses						
Rac 1 cell motility signaling pathway						
Regulation of Commissural axon pathfinding by Slit and Robo						
Ribosome						
Selenoamino acid metabolism						
Selenocysteine synthesis						
SRP-dependent cotranslational protein targeting to membrane						
Transmission across chemical synapses						
Viral mRNA translation						

KLFS, Kleefstra syndrome; *KS*, Kabuki syndrome; *CHARGE*, CHARGE syndrome; *MRD1*, mental retardation autosomal dominant 1; *ARTHS*, Arboleda-Tham syndrome; *ICF1*, immunodeficiency, centromeric instability, and facial anomalies syndrome 1.

SHARED EPIGENETIC AND GENE EXPRESSION ALTERATIONS

Gene expression deregulation by VPA has been widely investigated over the last few decades (Marchion et al., 2005; Jergil et al., 2009, 2011; Chiu et al., 2013; Shinde et al., 2016; Balasubramanian et al., 2019; Kotajima-Murakami et al., 2019; Lin et al., 2019; Sanaei and Kavooosi, 2019). Interestingly, some of the causative genes of the aforementioned syndromes are dysregulated in different experimental models. *Ehmt1* was found to be downregulated in brains of mice exposed to VPA *in utero*, *Kdm6a*, and *Dnmt3b* appeared to be upregulated in the same model (Kotajima-Murakami et al., 2019), while *Chd7* was downregulated in embryonal carcinoma cells upon VPA exposure (Jergil et al., 2009). In addition, *Ehmt1* and its human orthologs were downregulated in neural stem/progenitor cells of a mouse model for KS1 (Carosso et al., 2019) and in lymphoblastoid cell lines derived from 2q23.1 deletion syndrome patients (Mullegama et al., 2016), respectively. Expression of *DNMT3B* was decreased in iPSCs derived from KS1 patient (Carosso et al., 2019). Furthermore, *Kdm6a* and *Chd7* have been reported to be interlinked in terms of gene expression regulation (Mansour et al., 2012; Hsu et al., 2020), and in a mouse model expressing catalytically inactive *Dnmt3b*, they share opposite behavior (Lopusna et al., 2021).

In **Table 2**, shared pathways with genes deregulated by VPA and downregulated in models of causative genes for KLEFS, KS, CHARGE, MRD1, and ARTHS or ICF1 are summarized (Katsumoto et al., 2006; Issaeva et al., 2007; Min et al., 2007; Fan, 2008; Gupta-Agarwal et al., 2012; Mansour et al., 2012; Balemans et al., 2014; Chen et al., 2014; Kim et al., 2014; Schulz et al., 2014; Turner-Ivey et al., 2014; Gigeek et al., 2015; Dhar et al., 2016, 2018; Fang et al., 2016; Mullegama et al., 2016; Sheikh et al., 2016, 2017; Feng et al., 2017a,b; Shpargel et al., 2017; Whittaker et al., 2017; Baell et al., 2018; Marie et al., 2018; Yao et al., 2018, 2020; Carosso et al., 2019; Machado et al., 2019; Nowialis et al., 2019; Cieslar-Pobuda et al., 2020; Frega et al., 2020; Hsu et al., 2020; Kong et al., 2020; Liu et al., 2020; Xu et al., 2020; Ying et al., 2020; Fei et al., 2021; Lopusna et al., 2021). Of note, the most commonly shared pathways involve either morphogenesis signals (for example, beta1 integrin cell surface interactions and extracellular matrix organization), or possible defects of the central nervous system (such as axon guidance and neuronal system). As such, given the recent description of ARTHS, it would be interesting to reassess this matter in the future utilizing state of the art molecular studies.

CONCLUSION

It is well established that the mammalian epigenome can change during embryonic development and be influenced by genetic and/or environmental factors, even though some molecular mechanisms underlying these modifications are yet not clear (Finnell et al., 2002; Xu and Xie, 2018). Chromatinopathies represent a heterogeneous group of Mendelian disorders with defects in the epigenetic apparatus, leading to an imbalance in

the chromatin state and consequent aberrant gene expression. As described above, these disorders share several overlapping clinical signs, though with some specific features allowing dysmorphologists to recognize each individual syndrome. We highlighted similarities between the discussed chromatinopathies and FVSD, pointing out shared features in these genetic- and teratogen-induced disorders. As reported in **Table 1**, overlapping clinical signs are primarily ID and developmental delay, present in 5 out of 5 chromatinopathies described herein (6/6), speech delay (6/6), ASD-like behavior (5/6), microcephaly (5/6), cardiac (6/6) and ophthalmological defects with different degree of severity (5/6), cleft palate (6/6), musculoskeletal anomalies (4/6), and dysmorphic features such as highly arched or thick eyebrows (4/6) and ears abnormalities (6/6).

Intriguingly, despite the different etiology of a FVSD and the chromatinopathies, the action of VPA—i.e., an HDACi acting on chromatin—can suggest a similar pathogenetic mechanism common to the other rare genetic disorders, giving rise to the observed shared phenotypic signs. Furthermore, recent work showed that recognition of FVSD *facies* can identify individuals with high risk of cognitive deficits, independently of VPA exposure and even in the absence of major malformations (Bromley et al., 2019). Taken together, these pieces of evidence support the hypothesis that FVSD may be considered as a phenocopy of chromatinopathy, caused in this case by environmental factors, and that a further investigation of this aspect could help elucidate the correlation between typical congenital anomalies and neurodevelopment.

AUTHOR CONTRIBUTIONS

CG, AV, and VM conceived the manuscript. CP and EDF wrote the manuscript. AP reviewed clinical information. IV wrote sections of the manuscript. PG and SC read and edited the manuscript. RHF reviewed and revised the manuscript. All authors contributed to manuscript revision, they have all read and approved the manuscript.

FUNDING

The authors are grateful to the following funding sources: Fondazione Cariplo (2015-0783 to VM); Intramural funding-Dipartimento DISS, Linea 2, Università degli Studi di Milano (to CG, AV, and VM); Translational Medicine Ph.D. scholarship-Università degli Studi di Milano (to CP and ED); Molecular and Translational Medicine Ph.D. scholarship-Università degli Studi di Milano (to PG); Nickel & Co S.p.A (to VM); and “Aldo Ravelli” Center for Neurotechnology and Experimental Brain Therapeutics-Università degli Studi di Milano (to CG and VM). The authors acknowledge support from the University of Milan through the APC initiative.

ACKNOWLEDGMENTS

The authors would like to thank Susanna Brusa for graphical support.

REFERENCES

- Adam, M. P., Banka, S., Bjornsson, H. T., Bodamer, O., Chudley, A. E., Harris, J., et al. (2019). Kabuki syndrome: international consensus diagnostic criteria. *J. Med. Genet.* 56, 89–95. doi: 10.1136/jmedgenet-2018-105625
- Arboleda, V. A., Lee, H., Dorrani, N., Zadeh, N., Willis, M., Macmurdo, C. F., et al. (2015). De novo nonsense mutations in KAT6A, a lysine acetyl-transferase gene, cause a syndrome including microcephaly and global developmental delay. *Am. J. Hum. Genet.* 96, 498–506. doi: 10.1016/j.ajhg.2015.01.017
- Ardinger, H. H., Atkin, J. F., Blackston, R. D., Elsas, L. J., Clarren, S. K., Livingstone, S., et al. (1988). Verification of the fetal valproate syndrome phenotype. *Am. J. Med. Genet.* 29, 171–185. doi: 10.1002/ajmg.1320290123
- Arora, V., Joshi, A., Lall, M., Agarwal, S., Bijarnia Mahay, S., Dua puri, R., et al. (2018). Fetal valproate syndrome as a phenocopy of Kleeftstra syndrome. *Birth Defects Res.* 110, 1205–1209. doi: 10.1002/bdr2.1379
- Asconapé, J. J., Penry, J. K., Dreifuss, F. E., Riela, A., and Mirza, W. (1993). Valproate-associated pancreatitis. *Epilepsia* 34, 177–183. doi: 10.1111/j.1528-1157.1993.tb02395.x
- Bachrati, C. Z., and Hickson, I. D. (2008). RecQ helicases: guardian angels of the DNA replication fork. *Chromosoma* 117, 219–233. doi: 10.1007/s00412-007-0142-4
- Baell, J. B., Leaver, D. J., Hermans, S. J., Kelly, G. L., Brennan, M. S., Downer, N. L., et al. (2018). Inhibitors of histone acetyltransferases KAT6A/B induce senescence and arrest tumour growth. *Nature* 560, 253–257. doi: 10.1038/s41586-018-0387-5
- Balasubramanian, D., Pearson, J. F., and Kennedy, M. A. (2019). Gene expression effects of lithium and valproic acid in a serotonergic cell line. *Physiol. Genomics* 51, 43–50. doi: 10.1152/physiolgenomics.00069.2018
- Balemans, M. C. M., Ansar, M., Oudakker, A. R., van Caam, A. P. M., Bakker, B., Vitters, E. L., et al. (2014). Reduced Euchromatin histone methyltransferase 1 causes developmental delay, hypotonia, and cranial abnormalities associated with increased bone gene expression in Kleeftstra syndrome mice. *Dev. Biol.* 386, 395–407. doi: 10.1016/j.ydbio.2013.12.016
- Baller, F. (1950). Radiusaplasie und Inzucht. *Z. Mensch. Vererb. Konstitutionsl.* 29, 782–790.
- Balmer, N. V., Weng, M. K., Zimmer, B., Ivanova, V. N., Chambers, S. M., Nikolaeva, E., et al. (2012). Epigenetic changes and disturbed neural development in a human embryonic stem cell-based model relating to the fetal valproate syndrome. *Hum. Mol. Genet.* 21, 4104–4114. doi: 10.1093/hmg/dd239
- Banka, S., Veeramachaneni, R., Reardon, W., Howard, E., Bunstone, S., Ragge, N., et al. (2012). How genetically heterogeneous is Kabuki syndrome: MLL2 testing in 116 patients, review and analyses of mutation and phenotypic spectrum. *Eur. J. Hum. Genet.* 20, 381–388. doi: 10.1038/ejhg.2011.220
- Batshaw, M. L., and Brusilow, S. W. (1982). Valproate-induced hyperammonemia. *Ann. Neurol.* 11, 319–321. doi: 10.1002/ana.410110315
- Bittigau, P., Siffringer, M., Genz, K., Reith, E., Pospischil, D., Govindarajalu, S., et al. (2002). Antiepileptic drugs and apoptotic neurodegeneration in the developing brain. *Proc. Natl. Acad. Sci. U.S.A.* 99, 15089–15094. doi: 10.1073/PNAS.222550499
- Boudadi, E., Stower, H., Halsall, J. A., Rutledge, C. E., Leeb, M., Wutz, A., et al. (2013). The histone deacetylase inhibitor sodium valproate causes limited transcriptional change in mouse embryonic stem cells but selectively overrides Polycomb-mediated Hoxb silencing. *Epigenet. Chromatin* 6:11. doi: 10.1186/1756-8935-6-11
- Brodie, S. A., and Brandes, J. C. (2014). Could valproic acid be an effective anticancer agent? The evidence so far. *Expert Rev. Anticancer Ther.* 14, 1097–1100. doi: 10.1586/14737140.2014.940329
- Bromley, R., Weston, J., Adab, N., Greenhalgh, J., Sanniti, A., McKay, A. J., et al. (2014). Treatment for epilepsy in pregnancy: neurodevelopmental outcomes in the child. *Cochrane Database Syst. Rev.* 2014:CD010236. doi: 10.1002/14651858.CD010236.pub2
- Bromley, R. L., Baker, G. A., Clayton-Smith, J., and Wood, A. G. (2019). Intellectual functioning in clinically confirmed fetal valproate syndrome. *Neurotoxicol. Teratol.* 71, 16–21. doi: 10.1016/j.ntt.2018.11.003
- Bromley, R. L., Mawer, G. E., Briggs, M., Cheyne, C., Clayton-Smith, J., Garcia-Fiñana, M., et al. (2013). The prevalence of neurodevelopmental disorders in children prenatally exposed to antiepileptic drugs. *J. Neurol. Neurosurg. Psychiatry* 84, 637–643. doi: 10.1136/jnnp-2012-304270
- Brown, N., Burgess, T., Forbes, R., McGillivray, G., Kornberg, A., Mandelstam, S., et al. (2013). 5q31.3 microdeletion syndrome: clinical and molecular characterization of two further cases. *Am. J. Med. Genet. Part A* 161, 2604–2608. doi: 10.1002/ajmg.a.36108
- Bruni, J., Wilder, B. J., Willmore, L. J., and Barbour, B. (1979). Valproic acid and plasma levels of phenytoin. *Neurology* 29, 904–905. doi: 10.1212/wnl.29.6.904
- Brunton, L. L., Hilal-Dandan, R., and Knollmann, B. C. (2018). *Goodman & Gilman's The Pharmacological Basis of Therapeutics*. New York, NY: McGraw-Hill.
- Camarena, V., Cao, L., Abad, C., Abrams, A., Toledo, Y., Araki, K., et al. (2014). Disruption of Mbd5 in mice causes neuronal functional deficits and neurobehavioral abnormalities consistent with 2q23.1 microdeletion syndrome. *EMBO Mol. Med.* 6, 1003–1015. doi: 10.15252/emmm.201404044
- Carosso, G. A., Boukas, L., Augustin, J. J., Nguyen, H. N., Winer, B. L., Cannon, G. H., et al. (2019). Precocious neuronal differentiation and disrupted oxygen responses in Kabuki syndrome. *JCI Insight* 4:e129375. doi: 10.1172/jci.insight.129375
- Chandane, P. G., and Shah, I. (2014). Fetal valproate syndrome. *Indian J. Hum. Genet.* 20, 187–188. doi: 10.4103/0971-6866.142898
- Chen, E. S., Gigeck, C. O., Rosenfeld, J. A., Diallo, A. B., Maussion, G., Chen, G. G., et al. (2014). Molecular convergence of neurodevelopmental disorders. *Am. J. Hum. Genet.* 95, 490–508. doi: 10.1016/j.ajhg.2014.09.013
- Chen, G., Zeng, W. Z., Yuan, P. X., Huang, L. D., Jiang, Y. M., Zhao, Z. H., et al. (1999). The mood-stabilizing agents lithium and valproate robustly increase the levels of the neuroprotective protein bcl-2 in the CNS. *J. Neurochem.* 72, 879–882. doi: 10.1046/j.1471-4159.1999.720879.x
- Chiu, C. T., Wang, Z., Hunsberger, J. G., and Chuang, D. M. (2013). Therapeutic potential of mood stabilizers lithium and valproic acid: beyond bipolar disorder. *Pharmacol. Rev.* 65, 105–142. doi: 10.1124/pr.111.005512
- Christensen, J., Grønberg, T. K., Sørensen, M. J., Schendel, D., Parner, E. T., Pedersen, L. H., et al. (2013). Prenatal valproate exposure and risk of autism spectrum disorders and childhood autism. *JAMA* 309, 1696–1703. doi: 10.1001/jama.2013.2270
- Cieslar-Pobuda, A., Ahrens, T. D., Caglayan, S., Behringer, S., Hannibal, L., and Staerk, J. (2020). DNMT3B deficiency alters mitochondrial biogenesis and α -ketoglutarate levels in human embryonic stem cells. *Stem Cells* 38, 1409–1422. doi: 10.1002/stem.3256
- Clayton-Smith, J., Bromley, R., Dean, J., Journal, H., Odent, S., Wood, A., et al. (2019). Diagnosis and management of individuals with fetal valproate spectrum disorder: a consensus statement from the European reference network for congenital malformations and intellectual disability. *Orphanet J. Rare Dis.* 14:180. doi: 10.1186/s13023-019-1064-y
- Clayton-Smith, J., and Donnai, D. (1995). Fetal valproate syndrome. *J. Med. Genet.* 32, 724–727. doi: 10.1136/jmg.32.9.724
- Daniel, D. C., and Johnson, E. M. (2018). PURA, the gene encoding Pur-alpha, member of an ancient nucleic acid-binding protein family with mammalian neurological functions. *Gene* 643, 133–143. doi: 10.1016/j.gene.2017.12.004
- Dhar, S. S., Lee, S. H., Chen, K., Zhu, G., Oh, W. K., Allton, K., et al. (2016). An essential role for UTX in resolution and activation of bivalent promoters. *Nucleic Acids Res.* 44, 3659–3674. doi: 10.1093/nar/gkv1516
- Dhar, S. S., Zhao, D., Lin, T., Gu, B., Pal, K., Wu, S. J., et al. (2018). MLL4 is required to maintain broad h3k4me3 peaks and super-enhancers at tumor suppressor genes. *Mol. Cell* 70, 825.e6–841.e6. doi: 10.1016/j.molcel.2018.04.028
- DiLiberti, J. H., Farndon, P. A., Dennis, N. R., and Curry, C. J. R. R. (1984). The fetal valproate syndrome. *Am. J. Med. Genet.* 19, 473–481. doi: 10.1002/ajmg.1320190308
- Dufour-Rainfray, D., Vourc'h, P., Le Guisquet, A. M., Garreau, L., Ternant, D., Bodard, S., et al. (2010). Behavior and serotonergic disorders in rats exposed prenatally to valproate: a model for autism. *Neurosci. Lett.* 470, 55–59. doi: 10.1016/j.neulet.2009.12.054
- Ehrlich, M., Jackson, K., and Weemaes, C. (2006). Immunodeficiency, centromeric region instability, facial anomalies syndrome (ICF). *Orphanet J. Rare Dis.* 1:2. doi: 10.1186/1750-1172-1-2
- Fahrner, J. A., and Bjornsson, H. T. (2019). Mendelian disorders of the epigenetic machinery: postnatal malleability and therapeutic prospects. *Hum. Mol. Genet.* 28, R254–R264. doi: 10.1093/hmg/ddz174

- Fan, H. (2008). Inhibition of de novo methyltransferase 3B is a potential therapy for hepatocellular carcinoma. *Gastroenterol. Res.* 1, 33–39. doi: 10.4021/gr2008.10.1240
- Fang, X., Poulsen, R. R., Wang-Hu, J., Shi, O., Calvo, N. S., Simmons, C. S., et al. (2016). Knockdown of DNA methyltransferase 3a alters gene expression and inhibits function of embryonic cardiomyocytes. *FASEB J.* 30, 3238–3255. doi: 10.1096/fj.201600346R
- Fei, D., Wang, Y., Zhai, Q., Zhang, X., Zhang, Y., Wang, Y., et al. (2021). KAT6A regulates stemness of aging bone marrow-derived mesenchymal stem cells through Nrf2/ARE signaling pathway. *Stem Cell Res. Ther.* 12:104. doi: 10.1186/s13287-021-02164-5
- Feng, W., Kawachi, D., Körkel-Qu, H., Deng, H., Serger, E., Sieber, L., et al. (2017a). Chd7 is indispensable for mammalian brain development through activation of a neuronal differentiation programme. *Nat. Commun.* 8:14758. doi: 10.1038/ncomms14758
- Feng, W., Shao, C., and Liu, H. K. (2017b). Versatile roles of the chromatin remodeler CHD7 during brain development and disease. *Front. Mol. Neurosci.* 10:309. doi: 10.3389/fnmol.2017.00309
- Finnell, R. H., Gelineau-van Waes, J., Eudy, J. D., and Rosenquist, T. H. (2002). Molecular basis of environmentally induced birth defects. *Annu. Rev. Pharmacol. Toxicol.* 42, 181–208. doi: 10.1146/annurev.pharmtox.42.083001.110955
- Frega, M., Selten, M., Mossink, B., Keller, J. M., Linda, K., Moerschen, R., et al. (2020). Distinct pathogenic genes causing intellectual disability and autism exhibit a common neuronal network hyperactivity phenotype. *Cell Rep.* 30, 173.e6–186.e6. doi: 10.1016/j.celrep.2019.12.002
- Gerold, M. (1959). Frakturheilung bei kongenitaler Anomalie der oberen Gliedmassen. *Zentralbl. Chir.* 84, 831–834.
- Gigek, C. O., Chen, E. S., Ota, V. K., Maussion, G., Peng, H., Vaillancourt, K., et al. (2015). A molecular model for neurodevelopmental disorders. *Transl. Psychiatry* 5:e565. doi: 10.1038/tp.2015.56
- Glover, S. J., Quinn, A. G., Barter, P., Hart, J., Moore, S. J., Dean, J. C. S., et al. (2002). Ophthalmic findings in fetal anticonvulsant syndrome(s). *Ophthalmology* 109, 942–947. doi: 10.1016/s0161-6420(02)00959-4
- Go, H. S., Seo, J. E., Kim, K. C., Han, S. M., Kim, P. K., Kang, Y. S., et al. (2011). Valproic acid inhibits neural progenitor cell death by activation of NF- κ B signaling pathway and up-regulation of Bcl-XL. *J. Biomed. Sci.* 18:48. doi: 10.1186/1423-0127-18-48
- Gössling, K. L., Schipp, C., Fischer, U., Babor, F., Koch, G., Schuster, F. R., et al. (2017). Hematopoietic stem cell transplantation in an infant with immunodeficiency, centromeric instability, and facial anomaly syndrome. *Front. Immunol.* 8:773. doi: 10.3389/fimmu.2017.00773
- Göttlicher, M., Minucci, S., Zhu, P., Krämer, O. H., Schimpf, A., Giavara, S., et al. (2001). Valproic acid defines a novel class of HDAC inhibitors inducing differentiation of transformed cells. *EMBO J.* 20, 6969–6978. doi: 10.1093/emboj/20.24.6969
- Gupta-Agarwal, S., Franklin, A. V., DeRamus, T., Wheelock, M., Davis, R. L., McMahon, L. L., et al. (2012). G9a/GLP histone lysine dimethyltransferase complex activity in the hippocampus and the entorhinal cortex is required for gene activation and silencing during memory consolidation. *J. Neurosci.* 32, 5440–5453. doi: 10.1523/jneurosci.0147-12.2012
- Hadzsviev, K., Komlosi, K., Czako, M., Duga, B., Szalai, R., Szabo, A., et al. (2016). Kleefstra syndrome in Hungarian patients: additional symptoms besides the classic phenotype. *Mol. Cytogenet.* 9:22. doi: 10.1186/s13039-016-0231-2
- Hagleitner, M. M., Lankester, A., Maraschio, P., Hultén, M., Fryns, J. P., Schuetz, C., et al. (2008). Clinical spectrum of immunodeficiency, centromeric instability and facial dysmorphism (ICF syndrome). *J. Med. Genet.* 45, 93–99. doi: 10.1136/jmg.2007.053397
- Hansen, R. S., Wijmenga, C., Luo, P., Stanek, A. M., Canfield, T. K., Weemaes, C. M. R., et al. (1999). The DNMT3B DNA methyltransferase gene is mutated in the ICF immunodeficiency syndrome. *Proc. Natl. Acad. Sci. U.S.A.* 96, 14412–14417. doi: 10.1073/pnas.96.25.14412
- Hefner, M. A., and Fassi, E. (2017). *Genetic Counseling in CHARGE Syndrome: Diagnostic Evaluation Through Follow Up*. Malden, MA: Blackwell Publishing Inc.
- Hodge, J. C., Mitchell, E., Pillalamarri, V., Toler, T. L., Bartel, F., Kearney, H. M., et al. (2014). Disruption of MBD5 contributes to a spectrum of psychopathology and neurodevelopmental abnormalities. *Mol. Psychiatry* 19, 368–379. doi: 10.1038/mp.2013.42
- Hsu, J., Huang, H. T., Lee, C. T., Choudhuri, A., Wilson, N. K., Abraham, B. J., et al. (2020). CHD7 and Runx1 interaction provides a braking mechanism for hematopoietic differentiation. *Proc. Natl. Acad. Sci. U.S.A.* 117, 23626–23635. doi: 10.1073/pnas.2003228117
- Hunt, D., Leventer, R. J., Simons, C., Taft, R., Swoboda, K. J., Gawne-Cain, M., et al. (2014). Whole exome sequencing in family trios reveals de novo mutations in PURA as a cause of severe neurodevelopmental delay and learning disability. *J. Med. Genet.* 51, 806–813. doi: 10.1136/jmedgenet-2014-102798
- Issaeva, I., Zonis, Y., Rozovskaia, T., Orlovsky, K., Croce, C. M., Nakamura, T., et al. (2007). Knockdown of ALR (MLL2) reveals ALR target genes and leads to alterations in cell adhesion and growth. *Mol. Cell. Biol.* 27, 1889–1903. doi: 10.1128/mcb.01506-06
- Iype, M., Henry, P., Aravind, C., and Arun, K. (2008). Baller-Gerold syndrome: further evidence for association with prenatal exposure to valproate. *Ann. Indian Acad. Neurol.* 11, 52–55. doi: 10.4103/0972-2327.40228
- Jackson, A., Bromley, R., Morrow, J., Irwin, B., and Clayton-Smith, J. (2016). In utero exposure to valproate increases the risk of isolated cleft palate. *Arch. Dis. Child. Fetal Neonatal Ed.* 101, F207–F211. doi: 10.1136/archdischild-2015-308278
- Jackson, A., Fryer, A., Clowes, V., and Clayton-Smith, J. (2014). Ocular coloboma and foetal valproate syndrome: four further cases and a hypothesis for aetiology. *Clin. Dysmorphol.* 23, 74–75. doi: 10.1097/MCD.0000000000000028
- Jacob, J., Ribes, V., Moore, S., Constable, S., Wilkinson, D., and Briscoe, J. (2013). *A Chemical-Genetics Approach to Study the Molecular Pathology of Central Serotonin Abnormalities in Fetal Valproate Syndrome*. Available online at: www.thelancet.com (accessed April 1, 2020).
- Jacob, J., Ribes, V., Moore, S., Constable, S. C., Sasaki, N., Gerety, S. S., et al. (2014). Valproic acid silencing of ascl1b/Ascl1 results in the failure of serotonergic differentiation in a zebrafish model of fetal valproate syndrome. *DMM Dis. Model. Mech.* 7, 107–117. doi: 10.1242/dmm.013219
- Jeanpierre, M., Turleau, C., Aurias, A., Prieur, M., Ledeist, F., Fischer, A., et al. (1993). An embryonic-like methylation pattern of classical satellite DNA is observed in ICF syndrome. *Hum. Mol. Genet.* 2, 731–735. doi: 10.1093/hmg/2.6.731
- Jergil, M., Forsberg, M., Salter, H., Stockling, K., Gustafson, A. L., Dencker, L., et al. (2011). Short-time gene expression response to valproic acid and valproic acid analogs in mouse embryonic stem cells. *Toxicol. Sci.* 121, 328–342. doi: 10.1093/toxsci/kfr070
- Jergil, M., Kultima, K., Gustafson, A. L., Dencker, L., and Stigson, M. (2009). Valproic acid-induced deregulation in vitro of genes associated in vivo with neural tube defects. *Toxicol. Sci.* 108, 132–148. doi: 10.1093/toxsci/kfp002
- Johannessen, C. U., and Johannessen, S. I. (2003). Valproate: past, present, and future. *CNS Drug Rev.* 9, 199–216. doi: 10.1111/j.1527-3458.2003.tb00249.x
- Kamae, C., Imai, K., Kato, T., Okano, T., Honma, K., Nakagawa, N., et al. (2018). Clinical and immunological characterization of ICF syndrome in Japan. *J. Clin. Immunol.* 38, 927–937. doi: 10.1007/s10875-018-0559-y
- Katsumoto, T., Aikawa, Y., Iwama, A., Ueda, S., Ichikawa, H., Ochiya, T., et al. (2006). MOZ is essential for maintenance of hematopoietic stem cells. *Genes Dev.* 20, 1321–1330. doi: 10.1101/gad.1393106
- Kennedy, J., Goudie, D., Blair, E., Chandler, K., Joss, S., McKay, V., et al. (2019). KAT6A Syndrome: genotype–phenotype correlation in 76 patients with pathogenic KAT6A variants. *Genet. Med.* 21, 850–860. doi: 10.1038/s41436-018-0259-2
- Kim, J. H., Sharma, A., Dhar, S. S., Lee, S. H., Gu, B., Chan, C. H., et al. (2014). UTX and MLL4 coordinately regulate transcriptional programs for cell proliferation and invasiveness in breast cancer cells. *Cancer Res.* 74, 1705–1717. doi: 10.1158/0008-5472.CAN-13-1896
- Kim, K. C., Kim, P., Go, H. S., Choi, C. S., Yang, S. I. L., Cheong, J. H., et al. (2011). The critical period of valproate exposure to induce autistic symptoms in Sprague-Dawley rats. *Toxicol. Lett.* 201, 137–142. doi: 10.1016/j.toxlet.2010.12.018
- Kini, U., Adab, N., Vinten, J., Fryer, A., and Clayton-Smith, J. (2006). Dysmorphic features: an important clue to the diagnosis and severity of fetal anticonvulsant syndromes. *Arch. Dis. Child. Fetal Neonatal Ed.* 91, 90–95. doi: 10.1136/adc.2004.067421

- Kitao, S., Shimamoto, A., Goto, M., Miller, R. W., Smithson, W. A., Lindor, N. M., et al. (1999). Mutations in RECQL4 cause a subset of cases of Rothmund-Thomson syndrome. *Nat. Genet.* 22, 82–84. doi: 10.1038/8788
- Kleefstra, T., Brunner, H. G., Amiel, J., Oudakker, A. R., Nillesen, W. M., Magee, A., et al. (2006). Loss-of-function mutations in Euchromatin histone methyltransferase 1 (EHMT1) cause the 9q34 subtelomeric deletion syndrome. *Am. J. Hum. Genet.* 79, 370–377. doi: 10.1086/505693
- Kleefstra, T., and De Leeuw, N. (1993). *Kleefstra Syndrome Synonyms: 9q Subtelomeric Deletion Syndrome, 9q34.3 Microdeletion Syndrome, 9qSTDS*. Available online at: <https://www.ncbi.nlm.nih.gov/books/> (accessed January 10, 2021).
- Kleefstra, T., Kramer, J. M., Neveling, K., Willemsen, M. H., Koemans, T. S., Vissers, L. E. L. M., et al. (2012). Disruption of an EHMT1-associated chromatin-modification module causes intellectual disability. *Am. J. Hum. Genet.* 91, 73–82. doi: 10.1016/j.ajhg.2012.05.003
- Koemans, T. S., Kleefstra, T., Chubak, M. C., Stone, M. H., Reijnders, M. R. F., de Munnik, S., et al. (2017). Functional convergence of histone methyltransferases EHMT1 and KMT2C involved in intellectual disability and autism spectrum disorder. *PLoS Genet.* 13:e1006864. doi: 10.1371/journal.pgen.1006864
- Kong, Q., Yu, M., Zhang, M., Wei, C., Gu, H., Yu, S., et al. (2020). Conditional Dnmt3b deletion in hippocampal dCA1 impairs recognition memory. *Mol. Brain* 13:42. doi: 10.1186/s13041-020-00574-9
- Kotajima-Murakami, H., Kobayashi, H., Kashii, H., Sato, A., Hagino, Y., Tanaka, M., et al. (2019). Effects of rapamycin on social interaction deficits and gene expression in mice exposed to valproic acid in utero. *Mol. Brain* 12:3. doi: 10.1186/s13041-018-0423-2
- Kozma, C. (2001). Valproic acid embryopathy: report of two siblings with further expansion of the phenotypic abnormalities and a review of the literature. *Am. J. Med. Genet.* 98, 168–175.
- Kuroki, Y., Suzuki, Y., Chyo, H., Hata, A., and Matsui, I. (1981). A new malformation syndrome of long palpebral fissures, large ears, depressed nasal tip, and skeletal anomalies associated with postnatal dwarfism and mental retardation. *J. Pediatr.* 99, 570–573. doi: 10.1016/S0022-3476(81)80256-9
- Lalani, S. R., Zhang, J., Schaaf, C. P., Brown, C. W., Magoulas, P., Tsai, A. C. H., et al. (2014). Mutations in PURA cause profound neonatal hypotonia, seizures, and encephalopathy in 5q31.3 microdeletion syndrome. *Am. J. Hum. Genet.* 95, 579–583. doi: 10.1016/j.ajhg.2014.09.014
- Lammer, E. J., Sever, L. E., and Oakley, G. P. (1987). Teratogen update: valproic acid. *Teratology* 35, 465–473. doi: 10.1002/tera.1420350319
- Larizza, L., Roversi, G., and Volpi, L. (2010). Rothmund-thomson syndrome. *Orphanet J. Rare Dis.* 5:2. doi: 10.1186/1750-1172-5-2
- Lederer, D., Grisart, B., Digilio, M. C., Benoit, V., Crespin, M., Ghariani, S. C., et al. (2012). Deletion of KDM6A, a histone demethylase interacting with MLL2, in three patients with kabuki syndrome. *Am. J. Hum. Genet.* 90, 119–124. doi: 10.1016/j.ajhg.2011.11.021
- Lin, Y. L., Bialer, M., Cabrera, R. M., Finnell, R. H., and Wlodarczyk, B. J. (2019). Teratogenicity of valproic acid and its constitutional isomer, amide derivative valnoctamide in mice. *Birth Defects Res.* 111, 1013–1023. doi: 10.1002/bdr2.1406
- Lindhout, D., and Schmidt, D. (1986). In-utero exposure to valproate and neural tube defects. *Lancet* 1, 1392–1393. doi: 10.1016/s0140-6736(86)91711-3
- Liu, C., Li, Q., Xiao, Q., Gong, P., and Kang, N. (2020). CHD7 regulates osteogenic differentiation of human dental follicle cells via PTH1R signaling. *Stem Cells Int.* 2020:8882857. doi: 10.1155/2020/8882857
- Lopusna, K., Nowialis, P., Opavska, J., Abraham, A., Riva, A., and Opavsky, R. (2021). Dnmt3b catalytic activity is critical for its tumour suppressor function in lymphomagenesis and is associated with c-Met oncogenic signalling. *EBioMedicine* 63:e103191. doi: 10.1016/j.ebiom.2020.103191
- Macfarlane, A., and Greenhalgh, T. (2018). Sodium valproate in pregnancy: what are the risks and should we use a shared decision-making approach? *BMC Preg. Childbirth* 18:200. doi: 10.1186/s12884-018-1842-x
- Machado, R. A. C., Schneider, H., DeOcesano-Pereira, C., Lichtenstein, F., Andrade, F., Fujita, A., et al. (2019). CHD7 promotes glioblastoma cell motility and invasiveness through transcriptional modulation of an invasion signature. *Sci. Rep.* 9:3952. doi: 10.1038/s41598-019-39564-w
- Makrythanasis, P., van Bon, B. W., Stehouwer, M., Rodríguez-Santiago, B., Simpson, M., Dias, P., et al. (2013). MLL2 mutation detection in 86 patients with Kabuki syndrome: a genotype-phenotype study. *Clin. Genet.* 84, 539–545. doi: 10.1111/cge.12081
- Mansour, A. A., Gafni, O., Weinberger, L., Zviran, A., Ayyash, M., Rais, Y., et al. (2012). The H3K27 demethylase Utx regulates somatic and germ cell epigenetic reprogramming. *Nature* 488, 409–413. doi: 10.1038/nature11272
- Maraschio, P., Zuffardi, O., Dalla Fior, T., and Tiepolo, L. (1988). Immunodeficiency, centromeric heterochromatin instability of chromosomes 1, 9, and 16, and facial anomalies: the ICF syndrome. *J. Med. Genet.* 25, 173–180. doi: 10.1136/jmg.25.3.173
- Marchion, D. C., Bicaku, E., Daud, A. I., Sullivan, D. M., and Munster, P. N. (2005). Valproic acid alters chromatin structure by regulation of chromatin modulation proteins. *Cancer Res.* 65, 3815–3822. doi: 10.1158/0008-5472.CAN-04-2478
- Marie, C., Clavairoly, A., Frah, M., Hmidan, H., Yan, J., Zhao, C., et al. (2018). Oligodendrocyte precursor survival and differentiation requires chromatin remodeling by Chd7 and Chd8. *Proc. Natl. Acad. Sci. U.S.A.* 115, E8246–E8255. doi: 10.1073/pnas.1802620115
- Massa, V., Cabrera, R. M., Menegola, E., Giavini, E., and Finnell, R. H. (2005). Valproic acid-induced skeletal malformations: associated gene expression cascades. *Pharmacogenet. Genomics* 15, 787–800. doi: 10.1097/01.fpc.0000170914.11898.3a
- Massa, V., Greene, N. D. E., and Copp, A. J. (2009). Do cells become homeless during neural tube closure? *Cell Cycle* 8, 2479–2480. doi: 10.4161/cc.8.16.9272
- Massa, V., Wlodarczyk, B., Giavini, E., and Finnell, R. H. (2006). Myo-inositol enhances teratogenicity of valproic acid in the mouse. *Birth Defects Res. Part A Clin. Mol. Teratol.* 76, 200–204. doi: 10.1002/bdra.20228
- Meador, K. J., Pennell, P. B., May, R. C., Brown, C. A., Baker, G., Bromley, R., et al. (2020). Effects of periconceptional folate on cognition in children of women with epilepsy: NEAD study. *Neurology* 94, e279–e740. doi: 10.1212/WNL.00000000000008757
- Megarbane, A., Melki, I., Souraty, N., Gerbaka, J., El Ghouzzi, V., Bonaventure, J., et al. (2000). Overlap between Baller-Gerold and Rothmund-Thomson syndrome. *Clin. Dysmorphol.* 9, 303–305. doi: 10.1097/00019605-200009040-00018
- Menegola, E., Broccia, M., Prati, M., and Giavini, E. (1999). Morphological alterations induced by sodium valproate on somites and spinal nerves in rat embryos. *Teratology* 59, 110–119.
- Menegola, E., Broccia, M. L., Prati, M., and Giavini, E. (1998). Stage-dependent skeletal malformations induced by valproic acid in rat. *Int. J. Dev. Biol.* 42, 99–102. doi: 10.1387/IJDB.9496792
- Menegola, E., Di Renzo, F., Broccia, M. L., Prudenziati, M., Minucci, S., Massa, V., et al. (2005). Inhibition of histone deacetylase activity on specific embryonic tissues as a new mechanism for teratogenicity. *Birth Defects Res. Part B Dev. Reprod. Toxicol.* 74, 392–398. doi: 10.1002/bdrb.20053
- Meunier, H., Carraz, G., Neunier, Y., Eymard, P., and Aimard, M. (1963). Pharmacodynamic properties of N-dipropylacetic acid. *Thérapie* 18, 435–438.
- Millan, F., Cho, M. T., Retterer, K., Monaghan, K. G., Bai, R., Vitazka, P., et al. (2016). Whole exome sequencing reveals de novo pathogenic variants in KAT6A as a cause of a neurodevelopmental disorder. *Am. J. Med. Genet. Part A* 170, 1791–1798. doi: 10.1002/ajmg.a.37670
- Min, G. L., Villa, R., Trojer, P., Norman, J., Yan, K. P., Reinberg, D., et al. (2007). Demethylation of H3K27 regulates polycomb recruitment and H2A ubiquitination. *Science* 318, 447–450. doi: 10.1126/science.1149042
- Miyake, N., Mizuno, S., Okamoto, N., Ohashi, H., Shiina, M., Ogata, K., et al. (2013). KDM6A point mutations cause kabuki syndrome. *Hum. Mutat.* 34, 108–110. doi: 10.1002/humu.22229
- Mohd Yunos, H., and Green, A. (2018). Fetal valproate syndrome: the Irish experience. *Ir. J. Med. Sci.* 187, 965–968. doi: 10.1007/s11845-018-1757-6
- Mullegamma, S. V., Mendoza-Londono, R., and Elsea, S. H. (2016). *MBD5 Haploinsufficiency*. Available online at: <http://www.ncbi.nlm.nih.gov/pubmed/27786435> (accessed December 2, 2020).
- Murko, C., Lagger, S., Steiner, M., Seiser, C., Schoefer, C., and Pusch, O. (2013). Histone deacetylase inhibitor Trichostatin A induces neural tube defects and promotes neural crest specification in the chicken neural tube. *Differentiation* 85, 55–66. doi: 10.1016/j.diff.2012.12.001
- Murray, C., Abel, S., McClure, M., Foster, J., Walke, M., Jayakar, P., et al. (2017). Novel causative variants in DYRK1A, KARS, and KAT6A associated with

- intellectual disability and additional phenotypic features. *J. Pediatr. Genet.* 06, 077–083. doi: 10.1055/s-0037-1598639
- Nau, H. (1985). Teratogenic valproic acid concentrations: infusion by implanted minipumps vs conventional injection regimen in the mouse. *Toxicol. Appl. Pharmacol.* 80, 243–250. doi: 10.1016/0041-008X(85)90081-X
- Nau, H., Hauck, R. S., and Ehlers, K. (1991). Valproic acid-induced neural tube defects in mouse and human: aspects of chirality, alternative drug development, pharmacokinetics and possible mechanisms. *Pharmacol. Toxicol.* 69, 310–321. doi: 10.1111/j.1600-0773.1991.tb01303.x
- Nau, H., Zierer, R., Spielmann, H., Neubert, D., and Gansau, C. (1981). A new model for embryotoxicity testing: teratogenicity and pharmacokinetics of valproic acid following constant-rate administration in the mouse using human therapeutic drug and metabolite concentrations. *Life Sci.* 29, 2803–2813. doi: 10.1016/0024-3205(81)90541-5
- Ng, S. B., Bigam, A. W., Buckingham, K. J., Hannibal, M. C., McMillin, M. J., Gildersleeve, H. I., et al. (2010). Exome sequencing identifies MLL2 mutations as a cause of Kabuki syndrome. *Nat. Genet.* 42, 790–793. doi: 10.1038/ng.646
- Nicolini, C., and Fahnstock, M. (2018). The valproic acid-induced rodent model of autism. *Exp. Neurol.* 299, 217–227. doi: 10.1016/j.expneurol.2017.04.017
- Niikawa, N., Matsuura, N., Fukushima, Y., Ohsawa, T., and Kajii, T. (1981). Kabuki make-up syndrome: a syndrome of mental retardation, unusual facies, large and protruding ears, and postnatal growth deficiency. *J. Pediatr.* 99, 565–569. doi: 10.1016/S0022-3476(81)80255-7
- Nowialis, P., Lopusna, K., Opavska, J., Haney, S. L., Abraham, A., Sheng, P., et al. (2019). Catalytically inactive Dnmt3b rescues mouse embryonic development by accessory and repressive functions. *Nat. Commun.* 10:4374. doi: 10.1038/s41467-019-12355-7
- Oberemm, A., and Kirschbaum, F. (1992). Valproic acid induced abnormal development of the central nervous system of three species of amphibians: implications for neural tube defects and alternative experimental systems. *Teratog. Carcinog. Mutagen.* 12, 251–262. doi: 10.1002/tcm.1770120603
- Ornoy, A. (2009). Valproic acid in pregnancy: how much are we endangering the embryo and fetus? *Reprod. Toxicol.* 28, 1–10. doi: 10.1016/J.REPROTOX.2009.02.014
- Ozkan, H., Cetinkaya, M., Köksal, N., and Yapici, S. (2011). Severe fetal valproate syndrome: combination of complex cardiac defect, multicystic dysplastic kidney, and trigonocephaly. *J. Matern. Fetal. Neonatal Med.* 24, 521–524. doi: 10.3109/14767058.2010.501120
- Pagon, R. A., Graham, J. M., Zonana, J., and Yong, S. L. (1981). Coloboma, congenital heart disease, and choanal atresia with multiple anomalies: CHARGE association. *J. Pediatr.* 99, 223–227. doi: 10.1016/S0022-3476(81)80454-4
- Patsalos, P. N., Berry, D. J., Bourgeois, B. F. D., Cloyd, J. C., Glauser, T. A., Johannessen, S. I., et al. (2008). Antiepileptic drugs - best practice guidelines for therapeutic drug monitoring: a position paper by the subcommission on therapeutic drug monitoring, ilae commission on therapeutic strategies. *Epilepsia* 49, 1239–1276. doi: 10.1111/j.1528-1167.2008.01561.x
- Pennati, R., Groppelli, S., De Bernardi, F., and Sotgia, C. (2001). Action of valproic acid on *Xenopus laevis* development: teratogenic effects on eyes. *Teratog. Carcinog. Mutagen.* 21, 121–133.
- Perucca, E. (2002). Pharmacological and therapeutic properties of valproate: a summary after 35 years of clinical experience. *CNS Drugs* 16, 695–714. doi: 10.2165/00023210-200216100-00004
- Phiel, C. J., Zhang, F., Huang, E. Y., Guenther, M. G., Lazar, M. A., and Klein, P. S. (2001). Histone deacetylase is a direct target of valproic acid, a potent anticonvulsant, mood stabilizer, and teratogen. *J. Biol. Chem.* 276, 36734–36741. doi: 10.1074/jbc.M101287200
- Qiao, Y., Bagheri, H., Tang, F., Badduke, C., Martell, S., Lewis, S. M. E., et al. (2019). Exome sequencing identified a de novo mutation of PURA gene in a patient with familial Xp22.31 microduplication. *Eur. J. Med. Genet.* 62, 103–108. doi: 10.1016/j.ejmg.2018.06.010
- Reijnders, M. R. F., Janowski, R., Alvi, M., Self, J. E., Van Essen, T. J., Vreeburg, M., et al. (2018). PURA syndrome: clinical delineation and genotype-phenotype study in 32 individuals with review of published literature. *J. Med. Genet.* 55, 104–113. doi: 10.1136/jmedgenet-2017-104946
- Robert, E., and Guibaud, P. (1982). Maternal valproic acid and congenital neural tube defects. *Lancet* 2:937. doi: 10.1016/s0140-6736(82)90908-4
- Rothmund, A. (1868). Ueber Cataracten in Verbindung mit einer eigenthümlichen Hautdegeneration. *Arch. für Ophthalmol.* 14, 159–182. doi: 10.1007/BF02720945
- Roulet, F. I., Wollaston, L., deCatanzaro, D., and Foster, J. A. (2010). Behavioral and molecular changes in the mouse in response to prenatal exposure to the anti-epileptic drug valproic acid. *Neuroscience* 170, 514–522. doi: 10.1016/j.neuroscience.2010.06.069
- Sanaei, M., and Kavoosi, F. (2019). Effect of 5-aza-2'-deoxycytidine in comparison to valproic acid and trichostatin a on histone deacetylase 1, dna methyltransferase 1, and cip/kip family (p21, p27, and p57) genes expression, cell growth inhibition, and apoptosis induction in colon cancer sw480 cell line. *Adv. Biomed. Res.* 8:52. doi: 10.4103/abr.abr_91_19
- Schölz, C., Weinert, B. T. B., Wagner, S. A. S., Beli, P., Miyake, Y., Qi, J., et al. (2015). Acetylation site specificities of lysine deacetylase inhibitors in human cells. *Cells* 33, 415–423.
- Schorry, E. K., Oppenheimer, S. G., and Saal, H. M. (2005). Valproate embryopathy: clinical and cognitive profile in 5 siblings. *Am. J. Med. Genet.* 133A, 202–206. doi: 10.1002/ajmg.a.30494
- Schulz, Y., Wehner, P., Opitz, L., Salinas-Riester, G., Bongers, E. M. H. F., van Ravenswaaij-Arts, C. M. A., et al. (2014). CHD7, the gene mutated in CHARGE syndrome, regulates genes involved in neural crest cell guidance. *Hum. Genet.* 133, 997–1009. doi: 10.1007/s00439-014-1444-2
- Shah, K. H., Shailaja, S., and Girisha, K. M. (2014). Is coloboma a feature of fetal valproate syndrome? *Clin. Dysmorphol.* 23, 24–25. doi: 10.1097/MCD.000000000000018
- Shah, R. R., and Stonier, P. D. (2019). Repurposing old drugs in oncology: opportunities with clinical and regulatory challenges ahead. *J. Clin. Pharm. Ther.* 44, 6–22. doi: 10.1111/jcpt.12759
- Shangguan, H., Su, C., Ouyang, Q., Cao, B., Wang, J., Gong, C., et al. (2019). Kabuki syndrome: novel pathogenic variants, new phenotypes and review of literature. *Orphanet J. Rare Dis.* 14:255. doi: 10.1186/s13023-019-1219-x
- Sheikh, B. N., Yang, Y., Schreuder, J., Nilsson, S. K., Bilardi, R., Carotta, S., et al. (2016). MOZ (KAT6A) is essential for the maintenance of classically defined adult hematopoietic stem cells. *Blood* 128, 2307–2318. doi: 10.1182/blood-2015-10-676072
- Sheikh, M. A., Malik, Y. S., and Zhu, X. (2017). RA-induced transcriptional silencing of checkpoint kinase-2 through promoter methylation by Dnmt3b is required for neuronal differentiation of P19 cells. *J. Mol. Biol.* 429, 2463–2473. doi: 10.1016/j.jmb.2017.07.005
- Shinde, V., Perumalivasan, S., Henry, M., Rotshteyn, T., Hescheler, J., Rahnenführer, J., et al. (2016). Comparison of a teratogenic transcriptome-based predictive test based on human embryonic versus inducible pluripotent stem cells. *Stem Cell Res. Ther.* 7:190. doi: 10.1186/s13287-016-0449-2
- Shpargel, K. B., Starmer, J., Wang, C., Ge, K., and Magnuson, T. (2017). UTX-guided neural crest function underlies craniofacial features of Kabuki syndrome. *Proc. Natl. Acad. Sci. U.S.A.* 114, E9046–E9055. doi: 10.1073/pnas.1705011114
- Sui, L., and Chen, M. (2012). Prenatal exposure to valproic acid enhances synaptic plasticity in the medial prefrontal cortex and fear memories. *Brain Res. Bull.* 87, 556–563. doi: 10.1016/J.BRAINRESBULL.2012.01.011
- Swann, A. C., Bowden, C. L., Calabrese, J. R., Dilsaver, S. C., and Morris, D. D. (2002). Pattern of response to divalproex, lithium, or placebo in four naturalistic subtypes of mania. *Neuropsychopharmacology* 26, 530–536. doi: 10.1016/S0893-133X(01)00390-6
- Talkowski, M. E., Mullegama, S. V., Rosenfeld, J. A., Van Bon, B. W. M., Shen, Y., Repnikova, E. A., et al. (2011). Assessment of 2q23.1 microdeletion syndrome implicates MBD5 as a single causal locus of intellectual disability, epilepsy, and autism spectrum disorder. *Am. J. Hum. Genet.* 89, 551–563. doi: 10.1016/j.ajhg.2011.09.011
- Tanaka, A. J., Bai, R., Cho, M. T., Anyane-Yeboah, K., Ahimaz, P., Wilson, A. L., et al. (2015). De novo mutations in PURA are associated with hypotonia and developmental delay. *Mol. Case Stud.* 1:a000356. doi: 10.1101/mcs.a000356
- Tham, E., Lindstrand, A., Santani, A., Malmgren, H., Nesbitt, A., Dubbs, H. A., et al. (2015). Dominant mutations in KAT6A cause intellectual disability with recognizable syndromic features. *Am. J. Hum. Genet.* 96, 507–513. doi: 10.1016/j.ajhg.2015.01.016
- Thomson, M. S. (1936). POIKILODERMA CONGEXITALE. *Br. J. Dermatol.* 48, 221–234. doi: 10.1111/j.1365-2133.1936.tb10332.x
- Tomson, T., Battino, D., Bonizzoni, E., Craig, J., Lindhout, D., Perucca, E., et al. (2015). Dose-dependent teratogenicity of valproate in mono- and polytherapy. *Neurology* 85, 866–872. doi: 10.1212/WNL.0000000000001772

- Tomson, T., Battino, D., Bonizzoni, E., Craig, J., Lindhout, D., Sabers, A., et al. (2011). Dose-dependent risk of malformations with antiepileptic drugs: an analysis of data from the EURAP epilepsy and pregnancy registry. *Lancet Neurol.* 10, 609–617. doi: 10.1016/S1474-4422(11)70107-7
- Turner-Ivey, B., Guest, S. T., Irish, J. C., Kappler, C. S., Garrett-Mayer, E., Wilson, R. C., et al. (2014). KAT6A, a chromatin modifier from the 8p11-p12 amplicon is a candidate oncogene in luminal breast cancer. *Neoplasia* 16, 644–655. doi: 10.1016/j.neo.2014.07.007
- Van Bon, B. W. M., Koolen, D. A., Brueton, L., McMullan, D., Lichtenbelt, K. D., Adès, L. C., et al. (2010). The 2q23.1 microdeletion syndrome: clinical and behavioural phenotype. *Eur. J. Hum. Genet.* 18, 163–170. doi: 10.1038/ejhg.2009.152
- van den Boogaard, M. L., Thijssen, P. E., Aytekin, C., Licciardi, F., Kiyoku, A. A., Sposito, L., et al. (2017). Expanding the mutation spectrum in ICF syndrome: evidence for a gender bias in ICF2. *Clin. Genet.* 92, 380–387. doi: 10.1111/cge.12979
- Van Maldergem, L., Siitonen, H. A., Jalkh, N., Chouery, E., De Roy, M., Delague, V., et al. (2006). Revisiting the craniosynostosis-radial ray hypoplasia association: baller-gerold syndrome caused by mutations in the RECQL4 gene. *J. Med. Genet.* 43, 148–152. doi: 10.1136/jmg.2005.031781
- Van Maldergem, L., Verloes, A., Lejeune, L., and Gillerot, Y. (1992). The Baller-Gerold syndrome. *J. Med. Genet.* 29, 266–268. doi: 10.1136/jmg.29.4.266
- van Ravenswaaij-Arts, C., and Martin, D. M. (2017). New insights and advances in CHARGE syndrome: diagnosis, etiologies, treatments, and research discoveries. *Am. J. Med. Genet. Part C Semin. Med. Genet.* 175, 397–406. doi: 10.1002/ajmg.c.31592
- Viale, L., Allotey, J., Cheong-See, F., Arroyo-Manzano, D., McCorry, D., Bagary, M., et al. (2015). Epilepsy in pregnancy and reproductive outcomes: a systematic review and meta-analysis. *Lancet* 386, 1845–1852. doi: 10.1016/S0140-6736(15)00045-8
- Vissers, L. E. L. M., De Vries, B. B. A., Osoegawa, K., Janssen, I. M., Feuth, T., Choy, C. O., et al. (2003). Array-based comparative genomic hybridization for the genome-wide detection of submicroscopic chromosomal abnormalities. *Am. J. Hum. Genet.* 73, 1261–1270. doi: 10.1086/379977
- Vissers, L. E. L. M., Van Ravenswaaij, C. M. A., Admiraal, R., Hurst, J. A., De Vries, B. B. A., Janssen, I. M., et al. (2004). Mutations in a new member of the chromodomain gene family cause CHARGE syndrome. *Nat. Genet.* 36, 955–957. doi: 10.1038/ng1407
- Voss, A. K., Collin, C., Dixon, M. P., and Thomas, T. (2009). Moz and retinoic acid coordinately regulate H3K9 acetylation, hox gene expression, and segment identity. *Dev. Cell* 17, 674–686. doi: 10.1016/j.devcel.2009.10.006
- Weemaes, C. M., Van Tol, M. J., Wang, J., Van Ostaijen-Ten Dam, M. M., Van Eggermond, M. C., Thijssen, P. E., et al. (2013). Heterogeneous clinical presentation in icf syndrome: correlation with underlying gene defects. *Eur. J. Hum. Genet.* 21, 1219–1225. doi: 10.1038/ejhg.2013.40
- Wegner, C., and Nau, H. (1992). Alteration of embryonic folate metabolism by valproic acid during organogenesis: implications for mechanism of teratogenesis - PubMed. *Neurology* 42, 17–24.
- Whittaker, D. E., Riegman, K. L. H., Kasah, S., Mohan, C., Yu, T., Sala, B. P., et al. (2017). The chromatin remodeling factor CHD7 controls cerebellar development by regulating reelin expression. *J. Clin. Invest.* 127, 874–887. doi: 10.1172/JCI83408
- Wijmenga, C., Van Den Heuvel, L. P. W. J., Strengman, E., Luyten, J. A. F. M., Van Der Burgt, I. J. A. M., De Groot, R., et al. (1998). Localization of the ICF syndrome to chromosome 20 by homozygosity mapping. *Am. J. Hum. Genet.* 63, 803–809. doi: 10.1086/302021
- Willemsen, M. H., Vulto-Van Silfhout, A. T., Nillesen, W. M., Wissink-Lindhout, W. M., Van Bokhoven, H., Philip, N., et al. (2012). Update on Kleeftstra syndrome. *Mol. Syndromol.* 2, 202–212. doi: 10.1159/000335648
- Wiltse, J. (2005). Mode of action: inhibition of histone deacetylase, altering WNT-dependent gene expression, and regulation of beta-catenin—developmental effects of valproic acid. *Crit. Rev. Toxicol.* 35, 727–738. doi: 10.1080/10408440591007403
- Xu, B., Mulvey, B., Salie, M., Yang, X., Matsui, Y., Nityanandam, A., et al. (2020). UTX/KDM6A suppresses AP-1 and a gliogenesis program during neural differentiation of human pluripotent stem cells. *Epigenet. Chromatin* 13:38. doi: 10.1186/s13072-020-00359-3
- Xu, G. L., Bestor, T. H., Bourc'His, D., Hsieh, C. L., Tommerup, N., Bugge, M., et al. (1999). Chromosome instability and immunodeficiency syndrome caused by mutations in a DNA methyltransferase gene. *Nature* 402, 187–191. doi: 10.1038/46052
- Xu, Q., and Xie, W. (2018). Epigenome in early mammalian development: inheritance, reprogramming and establishment. *Trends Cell Biol.* 28, 237–253. doi: 10.1016/j.tcb.2017.10.008
- Yao, H., Hannum, D. F., Zhai, Y., Hill, S. F., Albanus, R. D., Lou, W., et al. (2020). CHD7 promotes neural progenitor differentiation in embryonic stem cells via altered chromatin accessibility and nascent gene expression. *Sci. Rep.* 10:17445. doi: 10.1038/s41598-020-74537-4
- Yao, H., Hill, S. F., Skidmore, J. M., Sperry, E. D., Swiderski, D. L., Sanchez, G. J., et al. (2018). CHD7 represses the retinoic acid synthesis enzyme ALDH1A3 during inner ear development. *JCI Insight* 3:e97440. doi: 10.1172/jci.insight.97440
- Ying, J., Xu, T., Wang, C., Jin, H., Tong, P., Guan, J., et al. (2020). Dnmt3b ablation impairs fracture repair through upregulation of Notch pathway. *JCI Insight* 5:e131816. doi: 10.1172/jci.insight.131816

Conflict of Interest: RF formerly held a leadership position in TeratOmic Consulting LLC. This now dissolved organization provided expert consulting support in birth defects litigation.

The remaining authors declare that the research was conducted in the absence of any commercial or financial relationships that could be construed as a potential conflict of interest.

Copyright © 2021 Parodi, Di Fedè, Peron, Viganò, Grazioli, Castiglioni, Finnell, Gervasini, Vignoli and Massa. This is an open-access article distributed under the terms of the Creative Commons Attribution License (CC BY). The use, distribution or reproduction in other forums is permitted, provided the original author(s) and the copyright owner(s) are credited and that the original publication in this journal is cited, in accordance with accepted academic practice. No use, distribution or reproduction is permitted which does not comply with these terms.



OPEN ACCESS

EDITED BY

Ronja Hollstein,
University Hospital Bonn, Germany

REVIEWED BY

Binnaz Yalcin,
Institut National de la Santé et de la
Recherche Médicale, France
Vanja Nagy,
Ludwig Boltzmann Institute for Rare and
Undiagnosed Diseases, Austria

*CORRESPONDENCE

Valentina Massa,
valentina.massa@unimi.it

§PRESENT ADDRESS

Chiara Parodi,
EHS Department, Columbia University,
New York, NY, United States

[†]These authors have contributed equally
to this work and share first authorship

[‡]These authors have contributed equally
to this work and share last authorship

SPECIALTY SECTION

This article was submitted to Molecular
and Cellular Pathology,
a section of the journal
Frontiers in Cell and Developmental
Biology

RECEIVED 27 June 2022

ACCEPTED 05 September 2022

PUBLISHED 26 September 2022

CITATION

Di Fede E, Grazioli P, Lettieri A, Parodi C,
Castiglioni S, Taci E, Colombo EA,
Ancona S, Priori A, Gervasini C and
Massa V (2022), Epigenetic disorders:
Lessons from the animals–animal
models in chromatinopathies.
Front. Cell Dev. Biol. 10:979512.
doi: 10.3389/fcell.2022.979512

COPYRIGHT

© 2022 Di Fede, Grazioli, Lettieri, Parodi,
Castiglioni, Taci, Colombo, Ancona,
Priori, Gervasini and Massa. This is an
open-access article distributed under
the terms of the [Creative Commons
Attribution License \(CC BY\)](https://creativecommons.org/licenses/by/4.0/). The use,
distribution or reproduction in other
forums is permitted, provided the
original author(s) and the copyright
owner(s) are credited and that the
original publication in this journal is
cited, in accordance with accepted
academic practice. No use, distribution
or reproduction is permitted which does
not comply with these terms.

Epigenetic disorders: Lessons from the animals–animal models in chromatinopathies

Elisabetta Di Fede^{1†}, Paolo Grazioli^{1†}, Antonella Lettieri¹,
Chiara Parodi^{1§}, Silvia Castiglioni¹, Esi Taci¹,
Elisa Adele Colombo¹, Silvia Ancona¹, Alberto Priori^{1,2},
Cristina Gervasini^{1,2‡} and Valentina Massa^{1,2*†}

¹Department of Health Sciences, Università Degli Studi di Milano, Milan, Italy, ²“Aldo Ravelli” Center for Neurotechnology and Experimental Brain Therapeutics, Università Degli Studi di Milano, Milan, Italy

Chromatinopathies are defined as genetic disorders caused by mutations in genes coding for protein involved in the chromatin state balance. So far 82 human conditions have been described belonging to this group of congenital disorders, sharing some molecular features and clinical signs. For almost all of these conditions, no specific treatment is available. For better understanding the molecular cascade caused by chromatin imbalance and for envisaging possible therapeutic strategies it is fundamental to combine clinical and basic research studies. To this end, animal modelling systems represent an invaluable tool to study chromatinopathies. In this review, we focused on available data in the literature of animal models mimicking the human genetic conditions. Importantly, affected organs and abnormalities are shared in the different animal models and most of these abnormalities are reported as clinical manifestation, underlying the parallelism between clinics and translational research.

KEYWORDS

chromatinopathies, animal models, rare diseases, mus musculus, drosophila melanogaster, *Danio rerio*

Introduction

Rare diseases are defined as conditions having a prevalence lower than 1:2000 and, nevertheless, they are estimated to be over 6,000, deeply impacting patients, families, caregivers, and health systems (Eurordis 2005). Among rare diseases, some have recently been ascribed to the so-called chromatinopathies, a heterogeneous group of Mendelian disorders affecting the epigenetic machinery (Fahrner and Bjornsson, 2014). By 2019, 70 epigenetic machinery genes have been identified, when mutated these genes are responsible for 82 human conditions. These genes were further expanded to 295 by Bjornsson and colleagues (Boukas et al., 2019), and a review on monogenetic neurodevelopmental disorders (Ciptasari and van Bokhoven, 2020) is available. In this review we will focus on the 70 firstly described and better characterized causative genes. Such genes code for different epigenetic components presenting protein domains exerting

writer, eraser, reader, and remodeler activities or a combination of these functions (e.g., a protein could include both a writer and a reader domain) (Fahrner and Bjornsson, 2019). Patients affected by chromatinopathies display shared clinical features, such as intellectual disability (ID) and abnormal growth, and shared etiology, which mainly relies on disruption of dosage-sensitive genes leading to haploinsufficiency (Bjornsson, 2015; Fahrner and Bjornsson, 2019).

Considering the advent of next generation sequencing (NGS) technologies, which led to the identification of a growing number of candidate variants, validation of pathogenicity can be difficult. Considering that many of the epigenetic machinery disorders are rare and/or “ultrarare”, human-based studies are often intrinsically challenging (Shen et al., 2015).

Among *in vivo* models, mice (*Mus musculus*) are the most commonly used for human genetic diseases mainly for their homology to human genome, their size, their strains that are highly inbred giving uniformed experimental conditions and reproducibility, their lifespan and for the possibility to perform genetic manipulation to obtain models of monogenic diseases, through available transgenic technologies (Dow and Lowe, 2012). Despite these advantages, mice have high husbandry costs which make them suboptimal for candidate variants assessment and drug screening. For these purposes fruit flies (*Drosophila melanogaster*) represent another valid option, considering the rapid generation time, relatively low-cost housing, and high experimental manipulability, even if evolutionary more distant from humans compared to mammals (Moulton and Letsou, 2016). Another animal commonly used for high-throughput studies is zebrafish (*Danio rerio*), which is a vertebrate with a high homology in the genome. It can be exploited for a deep characterization of disorders involving embryogenesis, due to its transparent embryos and larvae, and it represents a valid model for studying organs and structures shared with humans (Santoriello and Zon, 2012). For example, this model has been used to evaluate 3D genome organization of the epigenetic machinery (Labudina and Horsfield, 2021).

In this work we report on animal models for chromatinopathies, focusing on how these models recapitulate genotype-phenotype correlation and analyzing affected functions; moreover, we highlight the importance of an integrative approach for epigenetic machinery disorders.

Animal models for chromatinopathies

In the last 30 years many animal models have been used to study chromatinopathies. The possibility to exploit animal models for studying the molecular mechanisms underlying a disorder, is a pivotal step for confirming etiology and pathogenic variants validation, and a valuable tool for preclinical analysis of possible therapeutic approaches. To date, the majority of

translational research in this field mainly focuses on mouse (*Mus musculus*), zebrafish (*Danio rerio*) and invertebrates as fruit fly (*Drosophila melanogaster*). We also included studies on other modeling systems such as *Caenorhabditis elegans*, medaka fish (*Oryzias latipes*), *Xenopus laevis*, rat (*Rattus norvegicus*), chicken (*Gallus gallus domesticus*), rabbit (*Oryctolagus cuniculus*) and monkey (*Macaca fascicularis*). In [Supplementary Table S1](#) animal models discussed in this review are detailed.

Genetic heterogenous syndromes

Some chromatinopathies are known to be caused by mutations in different components of the epigenetic machinery, such as Rubinstein-Taybi (RSTS1, OMIM #180849; RSTS2, OMIM #613684), Kleeftstra (KLEFS1, OMIM #610253; KLEFS2, OMIM #617768) and Kabuki (KS1, OMIM #147920; KS2 OMIM #300867) syndromes. In this cases, “canonical causative genes” exert the same function on the open/close chromatin equilibrium (Figure 1). Patients affected by these syndromes show a recognizable phenotype, which can vary in severity depending on the mutated gene. Therefore, it is interesting to investigate animal models-related phenotypes recapitulating syndromes with these molecular/clinical features (below 3 examples are discussed in details) for understanding whether the human genotype-phenotype correlations are well translated *in vivo* ([Supplementary Table S1](#)).

Rubinstein-Taybi syndrome

RSTS is a rare neurodevelopmental multisystem malformation syndrome characterized by developmental delay and intellectual disability, growth retardation, skeletal anomalies including broad/short thumbs and/or big toes and distinctive facial features. RSTS causative genes CREBBP and EP300 code for two writers of the epigenetic machinery, CBP and p300, both histone acetyltransferases (HAT) which alterations are responsible respectively for the 60% (RSTS1) and 10% (RSTS2) of cases; p300 disruption is associated with milder phenotypes in humans (Cohen et al., 2020). Homozygous mice for *Cbp* or p300 (ortholog genes of human CREBBP and EP300, respectively) show embryonic lethality (Tanaka et al., 1997) and, interestingly, it has been observed also in p300 heterozygous mutants by Yao and colleagues (Yao et al., 1998). *Cbp* heterozygous mice are viable although displaying skeletal and cardiac abnormalities, growth retardation and memory deficits (Oike et al., 1999). In addition, craniofacial aspects and developmental delay associated with RSTS have been reported in p300 mutant mice (Viosca et al., 2010). Therefore, loss of function of *Cbp* and p300 leads to these similar defects in mouse models (Tanaka et al., 1997; Yao et al., 1998; Oike et al., 1999; Viosca et al., 2010) together with multilineage defects in hematopoiesis (Kung et al., 2000; Kasper et al., 2002), which in

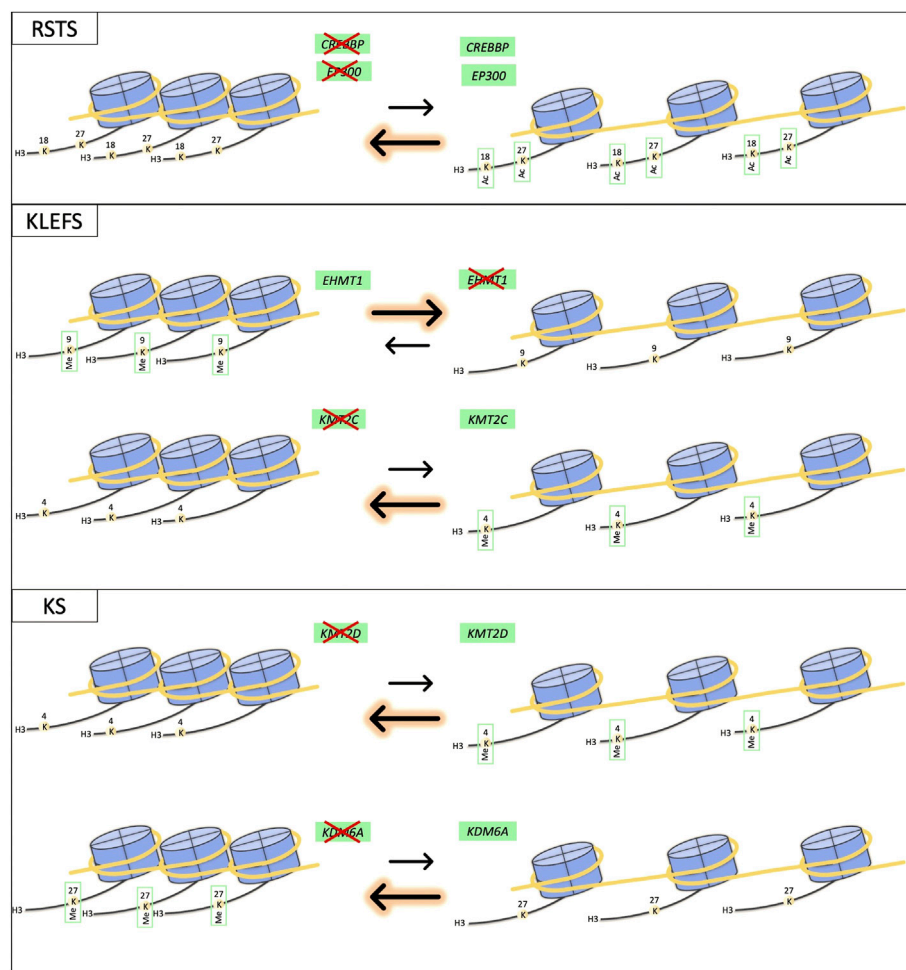


FIGURE 1

Schematic representation of effects on chromatin equilibrium for RSTS, KLEFS and KS syndromes. The drawing shows the impact of abnormal function of proteins coded by different genes having common effects on chromatin state equilibrium.

Cbp ± mice can increase the incidence of hematologic malignancies, as observed in RSTS patients (Kung et al., 2000; Boot et al., 2018). Mice lacking normal Cbp functions have been well characterized for memory and behavior capabilities, displaying synaptic plasticity deficits (Bourtchouladze et al., 2003; Alarcón et al., 2004; Wood et al., 2005), long-term memory (Tanaka et al., 1997; Oike et al., 1999; Korzus et al., 2004; Wood et al., 2006) and neuroadaptation impairment (Lopez-Atalaya et al., 2011), ASD-relevant repetitive behaviors, hyperactivity, and social interaction deficits (Zheng et al., 2016). Furthermore, Cbp seems to play a role in energy homeostasis, with mice showing increased insulin sensitivity and glucose tolerance (Yamauchi et al., 2002). In zebrafish, specific inhibition of cbp/p300 leads to a muscular dystrophy-like phenotype (Fauquier et al., 2018), while ep300 knockdown causes skeletal, cardiac and neural abnormalities (Babu et al., 2018) modelling defects present in patients. Conversely, a

Drosophila model for EP300-related RSTS phenotype does not exist, leaving the study of dCBP mutant flies, named nejire (nejP/+), as the only option for *Drosophila* studies of RSTS. Hemizygous nej are embryonic lethal (Akimaru et al., 1997; Di Fede et al., 2021), while nejire mutants affect the eye specification and cell fate determination (Kumar et al., 2004). Similarly to what happens in mouse, knockdown of dCBP causes behavioral alterations (Boyles et al., 2010; Sethi et al., 2019), affects nervous system development (Kirilly et al., 2011) and learning, due to altered development of mushroom bodies, associative center in invertebrate brains (Li et al., 2018).

Kleefstra syndrome

Another chromatinopathy caused by variants in two known causative genes coding for proteins members of the epigenetic machinery is Kleefstra syndrome (KLEFS) characterized by a variable phenotype including severe intellectual disability,

hypotonia, brachy (micro)cephaly, seizures, heart defects, and typical facies. Patients affected from this disorder present pathogenic variants in EHMT1 or KMT2C/MLL3, coding for two methyltransferases and epigenetic writers (respectively EHMT1 and KMT2C/MLL3), which give rise to clinically overlapping phenotypes in human (KLEFS1 and KLEFS2) (Koemans et al., 2017). However, this does not seem to be reflected in mouse models, observing on the one hand severe growth retardation and embryonic lethality in Ehmt1 knockout mice (Tachibana et al., 2005), on the other hand only partial embryonic lethality and features such as stunted growth, lower fertility, very little white fat, unusual hyperproliferation, hydronephrosis, kidney abnormalities and even ureter epithelial tumors, upon Mll3 inactivation in mice (Lee et al., 2009). Despite a mouse model heterozygous for Kmt2c (Kmt2c^{+/-}) has never been described, Ehmt1 ± mice recapitulate closely KLEFS phenotype, displaying autistic-like features (Balemans et al., 2010), learning deficits and synaptic dysfunction (Balemans et al., 2013), delayed postnatal development and increased expression of bone developmental genes (Balemans et al., 2014), increased adult cell proliferation in the hippocampus and enhanced pattern separation ability (Benevento et al., 2017), impaired cognitive abilities and hypoactive behavior (Iacono et al., 2018). Loss of *Drosophila* EHMT1 and KMT2C orthologs, G9a and trr respectively, appears to be rather convergent in flies, leading to neurodevelopmental impairment, with defects of peripheral dendrite development, larval locomotor behavior, non-associative learning, and courtship memory observed in Ehmt1 mutants (Kramer et al., 2011), short-term memory impairment caused by trr knockdown in mushroom bodies (Koemans et al., 2017) and developmental phenotypes in trr catalytic mutant alleles after environmental stress (Rickels et al., 2017).

Kabuki syndrome

Kabuki syndrome (KS) is a genetic condition characterized by growth deficiency, intellectual disability, minor skeletal anomalies and distinctive facial features caused by mutations in KMT2D (60% of cases) or in KDM6A (6% of cases), coding for two different components of the epigenetic machinery, a writer and an eraser respectively. Although the affected proteins are a histone methyltransferase and a histone demethylase, they lead to indistinguishable conditions (KS1 and KS2). This could be explained by the role of these two proteins: KMT2D methylates lysine 4 of histone 3 (H3K4), while KDM6A demethylates lysine 27 of histone 3 (H3K27), both enzymes operating two epigenetic modifications associated to a common downstream effect on chromatin state (open) (Fahrner and Bjornsson, 2014). Between KS1 and KS2 only slight phenotypic differences were found in a large cohort of patients, with a major incidence of hypotonia for KMT2D patients and postnatal growth retardation for KDM6A

mutation group (Miyake et al., 2013). Also, mice models for KS1 and KS2 show similarities recapitulating some aspects of the human disorder. Homozygous mice deficient for the orthologs of human KMT2D and KDM6A, Kmt2d/Mll2 and Utx respectively, show both embryonic lethality and developmental retardation (Glaser et al., 2006; Lee et al., 2012, 2013; Welstead et al., 2012; Thieme et al., 2013). In addition to these features, loss of Utx leads also to heart malformations and defective cardiovascular development (Lee et al., 2012; Shpargel et al., 2012; Welstead et al., 2012; Thieme et al., 2013), neural tube closure defects (Welstead et al., 2012) and cranioschisis (Thieme et al., 2013). Conditional mouse knockouts show that both Kmt2d and Utx are involved in myogenesis (Lee et al., 2013; Faralli et al., 2016) and in neural development since their loss can lead to hippocampal memory defects (Bjornsson, 2015) and post-migratory embryonic neural crest deficiencies (Shpargel et al., 2017). Furthermore, Utx depletion in adult females leads to myelodysplasia (Thieme et al., 2013) and in females neural crest induces severe craniofacial abnormalities (Shpargel et al., 2017), annexing tumorigenesis and dysmorphisms to the features shared with human phenotypes. Particularly, one of the most interesting mouse models is the N-ethyl-N-nitrosourea (ENU)-induced mutant mouse named bate palmas (bapa) which presents a missense mutation in Kmt2d and features such as psychomotor and behavior impairments (i.e., hypotonia), fine motor coordination and hyperactivity, closely modelling brain-associated aspects of KS1 (Yamamoto et al., 2019). To date, only *Drosophila* model for KDM6A (dUTX) loss has been studied, which results in semi-lethality and Trithorax-like phenotype (Herz et al., 2010), while both kmt2d and kdm6a zebrafish morphants have been generated, displaying skeletal and craniofacial abnormalities (Bögershausen et al., 2015; Van Laarhoven et al., 2015; Tsai et al., 2018), impairment of cardiac and angiogenic development (Van Laarhoven et al., 2015; De Los Angeles Serrano et al., 2019) and neurodevelopmental defects (Van Laarhoven et al., 2015; Tsai et al., 2018), resembling the ones observed in KS patients.

The three chromatinopathies cited above clearly represent a good example of how alterations in different genes can result in the same phenotype and, by extension, in the same disorder. This is possible in case of either common protein functions, as for RSTS and KLEFS, or different epigenetic actors, as for KS, with shared effect on chromatin balance.

Genetic convergence for divergent phenotypes

Another important feature of chromatinopathies is the blurred limit among syndromes: in some cases molecular diagnosis does not coincide with the initial clinical one, complicating genotype-phenotype correlation for these disorders. Below three examples of overlapping

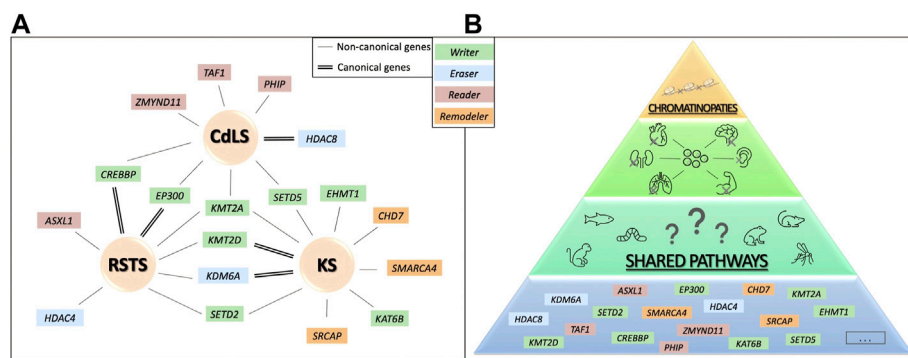


FIGURE 2

Genetic convergence for different human phenotype. In (A), canonical and non-canonical causative genes are shown for RSTS, CdLS and KS. In (B) a schematic representation of the hypothesis of possible shared molecular pathways upon chromatin balance disruption resulting in organ abnormal development that could be studied combining animal models and human data.

molecular/clinical syndromes (i.e. genes coding for proteins of the epigenetic machinery “canonical” for one chromatinopathy, found altered in other chromatinopathies) are discussed in details (Figure 2A). For these cases, animal models could be an extremely relevant tool for elucidating pathogenetic mechanisms of these human disorders. ⁃

Rubinstein-Taybi syndrome

Indeed, clinically diagnosed RSTS patients found negative for CREBBP/EP300 mutations resulted in presenting pathogenic variants in genes causative of other chromatinopathies such as Bohring-Opitz syndrome (BOPS, OMIM #605039) (pts #80 and #173 in (Negri et al., 2019)), KS (pt #95 in (Negri et al., 2019)), Wiedemann-Steiner syndrome (WDSTS, OMIM #605130) (pt #103 in (Negri et al., 2019) and six patients in (Di Fede et al., 2020)), Brachydactyly-Mental Retardation syndrome (BDMR, OMIM #600430) (pt #GDB1427 in (Squeo et al., 2020)) and Luscan-Lumish syndrome (LLS, OMIM #616831) (pt #18–2,798 in (Squeo et al., 2020)). Causative genes of these syndromes are not all writers of the epigenetic machinery as those responsible for RSTS (CREBBP and EP300). Indeed, only KS (KMT2D), WDSTS (KMT2A) and LLS (SETD2) genes share their epigenetic function with CREBBP and EP300, while the other KS causative gene KDM6A, BDMR gene HDAC4 and BOPS gene ASXL1 are two erasers and a reader, respectively. Despite molecular differences some patients were found to have common clinical signs and interestingly similarities can be observed in animals modelling these human disorders (Supplementary Table S1, Table 1). *In vivo* systems found in literature for all these syndromes show that if mutated, those genes impact on viability and growth (Sinclair et al., 1992; Yu et al., 1995; Akimaru et al., 1997; Tanaka et al., 1997; Sinclair et al., 1998; Yao et al., 1998; Katsani et al., 2001; Kumar et al., 2004; Vega et al., 2004; Glaser et al., 2006; Herz et al., 2010; Hu et al., 2010; Viosca et al., 2010; Lee et al., 2012; Abdel-Wahab

et al., 2013; Thieme et al., 2013; Wang et al., 2014; Hsu et al., 2017; Tsai et al., 2018; Gjini et al., 2019; Liu et al., 2020), neural and brain development (Tanaka et al., 1997; Sinclair et al., 1998; Yao et al., 1998; Oike et al., 1999; Bourtchouladze et al., 2003; Wood et al., 2006; Boyles et al., 2010; Gupta et al., 2010; Hu et al., 2010; Kirilly et al., 2011; Lopez-Atalaya et al., 2011; Welstead et al., 2012; Huang et al., 2015; Van Laarhoven et al., 2015; Zheng et al., 2016; Babu et al., 2018; Li et al., 2018; Tsai et al., 2018; Yamamoto et al., 2019), hematopoiesis (Kung et al., 2000; Kasper et al., 2002; Fisher et al., 2010; Wan et al., 2011; Thieme et al., 2013; Gjini et al., 2019), and lead to skeletal and craniofacial abnormalities (Sinclair et al., 1992; Yu et al., 1995; Tanaka et al., 1997; Sinclair et al., 1998; Vega et al., 2004; Hu et al., 2010; Viosca et al., 2010; Welstead et al., 2012; Abdel-Wahab et al., 2013; Bögershausen et al., 2015; Van Laarhoven et al., 2015; Babu et al., 2018; Tsai et al., 2018), resembling human phenotypes.

Kabuki syndrome

As described for RSTS patients, initial clinical diagnosis for Kabuki syndrome (KS) was not always confirmed at molecular level. KS patients negative for mutations in KMT2D or KDM6A were found carriers of pathogenic variants in genes related to WDSTS, KLEFS, Mental Retardation Autosomal Dominant 23 (MRD23, OMIM #615761), Say-Barber-Biesecker-Young-Simpson or Ohdo syndrome (SBBYSS, OMIM #603736), Coffin-Siris syndrome-4 (CSS4, OMIM #614609), Floating Harbor syndrome (FLHS, OMIM #136140), CHARGE syndrome (CHARGE, OMIM #214800) and LLS (e.g. pts GDB1054, GDB1405, GDB1400, #18–2,261, GDB1128, GDB1185, GDB1311, GDB1404, GDB1422, GDB1154, GDB1406, GDB1433 in (Squeo et al., 2020)). As KMT2D, most of the causative genes of the aforementioned syndromes are writers of the epigenetic machinery (KMT2A, EHMT1, SETD5, KAT6B and SETD2), except for the remodelers SMARCA4 (CSS4), SRCAP (FLHS) and CHD7 (CHARGE).

TABLE 1 Correlation between function/organ involvement and genes belonging to the writers-erasers-readers-remodelers groups.

Function/Organ involvement	Writers	Erasers	Readers	Remodelers
A Viability	ASH1L - CREBBP - DNMT1 - DNMT3A- DNMT3B- EHMT1 - EP300 - EZH2 - KAT6A- KMT2A- KMT2B- KMT2D - KMT5B- PRDM16 - SETD2 - SETD5	KDM5B- KDM5C - KDM6A	ASXL1 - ASXL2 - BPTF - BRPF1 - BRWD3 - CBX2 - EED - LBR - MBD5 - MECP2 - ORC1 - PHF6 - RAI1 - RERE - SMN1 - TAF1	ATRX - CHD2 - CHD3 - CHD7 - CHD8 - SMARCA4 - SRCAP
Neural and Brain Development	CREBBP - DNMT3A- DNMT3B- EHMT1 - EP300 - EZH2 - KAT6B- KMT2A- KMT2C - KMT2D - KMT5B- PRDM12 - SETD2 - SETD5 - WHSC1	KDM5B- KDM5C - KDM6A- PHF8	ALG13 - ASXL1 - BRPF1 - BRWD3 - EED - MBD5 - MECP2 - ORC1 - PHF6 - RAG2 - RAI1 - RERE - SMN1 - TAF1	ATRX - CHD2 - CHD7 - CHD8 - SMARCA2 - SMARCA4 - SRCAP
Growth	ASH1L - CREBBP - DNMT1 - DNMT3A- DNMT3B- EHMT1 - EP300 - EZH2 - KMT2A- KMT2C - KMT2D - KMT2E - KMT5B- NSD1 - SETD2 - SETD5 - WHSC1	HDAC8 - HR - KDM5C - KDM6A	AIRE - ASXL1 - ASXL2 - BPTF - CBX2 - EED - LBR - MBD5 - MECP2 - ORC1 - RAI1 - RERE - TAF1	ATRX - CHD2
Skeletal and Craniofacial Development	ASH1L - CREBBP - DNMT3B- EP300 - EZH2 - KAT6A- KAT6B- KMT2A- KMT2D - KMT5B- PRDM16 - WHSC1	KDM6A- HDAC4 - HDAC8 - KDM5B	ASXL1 - ASXL2 - BPTF - BRPF1 - CBX2 - EED - LBR - ORC1 - RAI1 - RERE - ZMYND11	ATRX - CHD2 - CHD7 - CHD8
Heart and Vascular Development	CREBBP - DNMT3B- EP300 - EZH2 - KAT6A- KMT2B- KMT2D - PRDM16 - SETD2 - SETD5 - WHSC1	KDM6A	ASXL2 - BRPF1 - EED - RERE	CHD2 - CHD7 - SMARCA4
Hematopoiesis	CREBBP - DNMT3A- EP300 - EZH2- KAT6A- KMT2A- KMT2E	KDM6A	ASXL1 - BPTF - BRPF1 - CBX2 - EED - LBR - PHF6 - TAF1	SRCAP
Eyes	CREBBP - DNMT3A- EZH2 - KMT2B- KMT2C - KMT5B- NSD1 - SETD5 - WHSC1	KDM5B	BRWD3 - RERE - TAF1 - TDRD7	CHD7 - SMARCA4
Memory	CREBBP - DNMT1 - DNMT3A- EHMT1 - KMT2A- KMT2B- KMT2C - KMT2D - NSD1	PHF8	BRPF1 - RAI1	CHD1 - CHD2 - CHD7 - SMARCA2
Behavior	CREBBP - EHMT1 - KMT2C - KMT2D - SETD5	KDM5C	MECP2 - PHF6 - RAG2 - RAI1	ATRX - CHD2 - CHD8 - SMARCA2
B Fertility	ASH1L - DNMT3A- KMT2C - KMT2E	-	AIRE - CBX2 - MORC2 - ORC1 - RAI1 - TAF1 - TDRD7	CHD1 - SRCAP
Tumorigenesis	CREBBP - DNMT1 - DNMT3B- KMT2C	KDM6A	ASXL1 - ASXL2 - BPTF - MORC2 - MSH6 - PHF6	SMARCA4
Immunity	KMT2A	KDM1A	AIRE - MECP2 - RAG2 - SMN1	SMARCA4
Muscle	CREBBP - EP300 - KMT5B	KDM6A	SMN1	-
Energy Homeostasis	CREBBP - EHMT1 - SETD2	-	ASXL2	CHD8
Insulinemia and Glucose Homeostasis	EZH2 - KMT2B	-	ASXL2 - EED - MBD5	-
Gut	EZH2	-	ASXL1	CHD8
Obesity	EHMT1	-	RAI1 - MECP2	-
Kidney	NSD1	-	EED - RERE	-
Hair/Skin	-	HR	-	-

Animal models mimicking these disorders (Supplementary Table S1, Table 1) do not reach adulthood when ortholog genes are depleted, as observed in mouse (Yu et al., 1995; Bultman et al., 2000; Bosman et al., 2005; Tachibana et al., 2005; Glaser et al., 2006; Hu et al., 2010; Lee et al., 2012; Thieme et al., 2013; Osipovich et al., 2016), zebrafish (Thieme et al., 2013; Tsai et al., 2018) and fruit fly (Braun et al., 1997; Ruhf et al., 2001; Herz et al., 2010), with the only exception of KAT6B mutant mice getting through the postnatal period (Thomas et al., 2000; Merson et al., 2006). Interestingly, despite the variety of mutants used for studying these disorders, they display anomalies impacting similar neural aspects: neural tube closure in mouse (Hu et al., 2010; Welstead et al., 2012; Osipovich et al., 2016); neuronal differentiation in zebrafish (Van Laarhoven et al., 2015) and *Xenopus* (Seo et al., 2005); neural development and neurogenesis in rodents (Merson et al., 2006; Layman et al., 2009; Clayton-Smith et al., 2011; Moore et al., 2019; Sessa et al., 2019), zebrafish (Huang et al., 2015; Van Laarhoven et al., 2015; Tsai et al., 2018) and fruit flies (Braun et al., 1997; Melicharek et al., 2010; Kramer et al., 2011); cognitive ability and synaptic functions in mice (Layman et al., 2009; Gupta et al., 2010; Balemans et al., 2013; Iacono et al., 2018; Sessa et al., 2019) and *Drosophila* (Melicharek et al., 2010; Kramer et al., 2011); psychomotor functions and autistic-like behavior in mice (Balemans et al., 2010; Deliu et al., 2018; Moore et al., 2019; Sessa et al., 2019; Yamamoto et al., 2019) and *Drosophila* (Melicharek et al., 2010; Kramer et al., 2011). In addition, patients affected from syndromes such as KS, MRD32, CSS4 and CHARGE often display heart defects and cardiovascular anomalies (Kosho et al., 2014; Koemans et al., 2017; van Ravenswaaij-Arts and Martin, 2017; Powis et al., 2018) as well as animals modelling these disorders (Bosman et al., 2005; Takeuchi et al., 2011; Lee et al., 2012; Shpargel et al., 2012; Welstead et al., 2012; Thieme et al., 2013; Van Laarhoven et al., 2015; Osipovich et al., 2016; De Los Angeles Serrano et al., 2019). Although similar defects have been observed also in WDSTS, KLEFS1 and SBBYSS patients (Lemire et al., 2012; Willemssen et al., 2012; Baer et al., 2018), *in vivo* systems for these syndromes do not show anomalies in this organ.

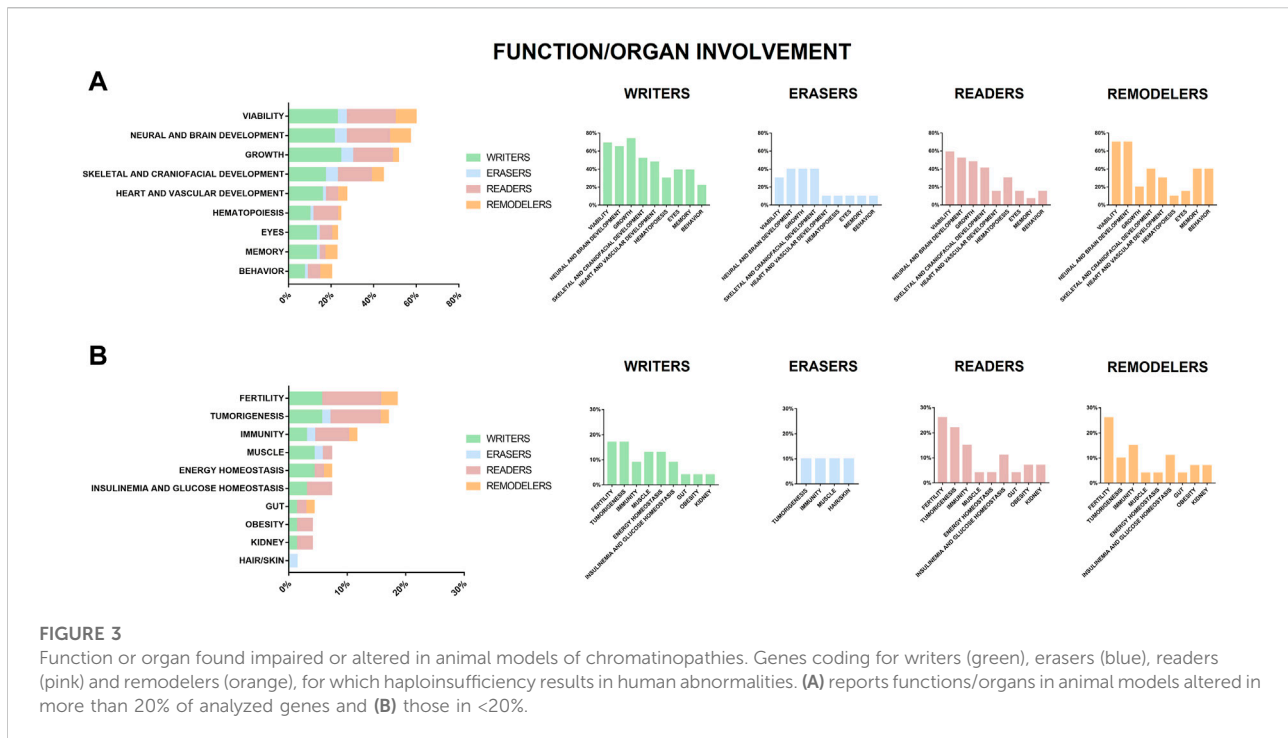
Cornelia de lange syndrome

CdLS is a rare heterogenous developmental disorder characterized by multiorgan abnormalities leading to severe growth delay, distinctive facial feature, psychomotor deficit, intellectual disability, behavioral problems, and limb malformations. Patients firstly diagnosed by geneticists for having CdLS (CdLS1, OMIM #122470; CdLS2, OMIM #300590; CdLS3, OMIM #610759; CdLS4, OMIM #614701; CdLS5, OMIM #300882), not always carried mutations in one of the seven known genes causative of this syndrome. Instead, the genetic alteration can be found in a gene associated with another syndrome even though patients display typical characteristics described in the CdLS consensus (Kline et al., 2018). As a matter of fact, CdLS is now considered a “clinical spectrum” rather than

an isolated syndrome with unique features (Selicorni et al., 2021). Genes found mutated in patients with an initial diagnosis of CdLS are: EP300 ((Aoi et al., 2019) - Patient 6; (Cucco et al., 2020); - Patient A; (Squeo et al., 2020); - GDB1418; (Woods et al., 2014); - Case Report)), KMT2A ((Yuan et al., 2015) - CdLS-3 (BAB4964); (Parenti et al., 2017); - Patient 12; (Aoi et al., 2019); - Patient 27; (Demir et al., 2021); - Case Report)); TAF1 ((O’Rawe et al., 2015) - Individual 4A; (Cheng et al., 2020); - Individual 13) causative of Mental Retardation X-Linked Syndromic 33 (MRXS33, OMIM #300966); ZMYND11((Aoi et al., 2019) - Patient 53) causative of Mental Retardation Autosomal Dominant 30 (MRD30, OMIM #616083)); PHIP ((Aoi et al., 2019) - Patient 56) associated to Developmental Delay Intellectual Disability Obesity and Dysmorphism or Chung-Jansen syndrome (CHUJANS, OMIM #617991)), CREBBP ((Tang et al., 2019) - Patient 3)); SETD5 ((Squeo et al., 2020) - GDB1400) causative of MRD23). These genes, involved in chromatin regulation, are associated with syndromes different from CdLS, but studies conducted exploiting animal models highlighted some similar characteristics that can be found in the human patients affected with CdLS. Almost all animals mutated in the above mentioned genes display impaired viability or overall defects in growth (HDAC8, EP300, KMT2A, TAF1, CREBBP, SETD5) (Yu et al., 1995; Akimaru et al., 1997; Tanaka et al., 1997; Yao et al., 1998; Wassarman et al., 2000; Katsani et al., 2001; Kumar et al., 2004; Haberland et al., 2009; Viosca et al., 2010; Osipovich et al., 2016; Deliu et al., 2018; Gudmundsson et al., 2019), usually with mild to severe problems affecting the embryonic neurodevelopment (HDAC8, EP300, KMT2A, TAF1, CREBBP, SETD5) (Tanaka et al., 1997; Yao et al., 1998; Oike et al., 1999; Bourtchouladze et al., 2003; Wood et al., 2006; Haberland et al., 2009; Boyles et al., 2010; Gupta et al., 2010; Kirilly et al., 2011; Lopez-Atalaya et al., 2011; Huang et al., 2015; O’Rawe et al., 2015; Osipovich et al., 2016; Zheng et al., 2016; Babu et al., 2018; Deliu et al., 2018; Li et al., 2018; Gudmundsson et al., 2019; Sessa et al., 2019) and skeletal abnormalities often found in the craniofacial district (Yu et al., 1995; Tanaka et al., 1997; Haberland et al., 2009; Viosca et al., 2010; Babu et al., 2018; Sun et al., 2018; Sessa et al., 2019) (HDAC8, EP300, KMT2A, ZMYND11, CREBBP, SETD5) (Supplementary Table S1, Table 1).

Lessons from the models

In vivo systems representative of depletion or alteration of chromatin regulators, listed in Supplementary Table S1, show many parallelisms with patients affected by chromatinopathies. As shown in Figure 3 genes causative of human chromatinopathies impact common organ function/development also in different animal models. As portrayed in Figure 3A and Table 1, the most compromised functions in most animal models we found reported for all the players of the epigenetic machinery (writers, erasers, readers, and remodelers)



resulted to be viability, growth, and neural and skeletal development. These features can be identified in patients who often present main clinical signs such as growth delay, intellectual disability (ID), facial dysmorphisms and skeletal anomalies (Fahrner and Bjornsson, 2014). In addition, most individuals affected by chromatinopathies have loss of function mutations leading to haploinsufficiency, due to the fundamental role of causative genes in embryonic development whose complete loss would be often at odds with life (Bjornsson, 2015). Of note, the vascular system together with organs such as heart and eyes seem particularly affected in writers models (Figure 3A), memory in writers and remodelers models (Figure 3A), while fertility resulted mostly altered in readers models (Figure 3B). Furthermore, about 20% of these *in vivo* systems display defects in hematopoiesis and altered mechanisms leading to tumorigenesis (Figure 3 and Table 1). Interestingly, although somatic mutations in genes of the epigenetic apparatus have been found in different types of tumors, cancer predisposition due to germline mutations is a feature common to some chromatinopathies. For instance, a peculiar aspect of RSTS is the increased incidence of benign and malignant tumors (Boot et al., 2018), which can be observed in the Cbp ± mouse model for this syndrome (Kung et al., 2000). Tumors susceptibility has been studied also for BOPS and was found that, although isolated reports on BOPS children seem to suggest a greater risk for Wilms tumor, sporadic malignancies in absence of other BOPS findings more frequently harbor somatic ASXL1 pathogenetic variants (Russell et al., 2018) which increase the risk of myelodysplastic syndrome as

shown in mice (Abdel-Wahab et al., 2013; Wang et al., 2014). A tumor predisposition was also found in patients positive for germline mutation in MSH6 and SMARCA4 who developed respectively Hereditary nonpolyposis colorectal cancer type 5 and rhabdoid tumors (Biegel et al., 2014; Lepore Signorile et al., 2021) and this increased risk of developing malignancies was observed also in their corresponding animal models (Edelmann et al., 1997; De Wind et al., 1999; Bultman et al., 2000; Feitsma et al., 2008; Peled et al., 2010). Conversely, for Immunodeficiency-centromeric instability-facial anomalies syndrome 1 (ICF1, OMIM #242860), Borjeson-Forssmann-Lehmann syndrome (BFLS, OMIM #301900) and KS a cancer association has only been hypothesized so far, as patients who developed Hodgkin lymphoma, adrenocortical adenoma, acute lymphoblastic leukemia, Burkitt's lymphoma and solid tumors (Ijichi et al., 1996; Scherer et al., 2003; Ehrlich et al., 2008; Chao et al., 2010a,b; Wang et al., 2019), and animal models presenting hematopoietic tumors (Shah et al., 2010; Thieme et al., 2013; Hsu et al., 2019) have been reported for these syndromes.

Conclusion

In vivo models require genetic manipulation and shared homology with the human genome, leading to the possibility of mimicking the human genetic disease for studying for possibly shared molecular mechanisms responsible for clinical phenotypes and examine physically or temporarily inaccessible

tissues (Figure 2B). Animal models for chromatinopathies have proved to be a valuable tool for dissecting mechanisms underlying these disorders and altered functions due to mutations in genes of the epigenetic apparatus. More variants in genes that can be grouped in the chromatinopathies are increasingly reported as well as animal models for their study. Hence, we propose a table with details of the first 70 well characterized genes, with the possibility of expanding such collection in an open science format (<https://www.shorturl.at/nuV78>). Importantly, affected organs and abnormalities are shared in the different animal models (listed in Supplementary Table S1), generated for a better understanding for the effects of loss or alteration of epigenetic genes (represented in Figure 3 and Table 1). Most of these abnormalities can also be found in patients affected by chromatinopathies, pointing out once again the parallelism between clinics and translational research. Importantly, for better dissecting each organ/function abnormalities in these rare conditions many studies are undergoing exploiting also stem cells and organoids for combining human data and animal model information. Interestingly, Boukas and colleagues (Boukas et al., 2019) recently demonstrated that a large subset of genes belonging to the epigenetic machinery are highly co-expressed, intolerant to variation and independently enriched for genes affecting neurological function. This suggests a link between these properties, highlighting once again the interconnection between epigenetic regulators. This aspect can be observed in applied research, where modelling disorders leads to phenotypes resembling not only the human disease but also shared features among chromatinopathies. Thus, to ensure the understanding of molecular mechanisms characterizing these disorders an integrative approach should be supported.

Author contributions

EDF and PG literature review; EDF, PG, CG, and VM manuscript writing; AL, CP, SC, ET, EAC, SA, and AP critical revision.

References

- Abdel-Wahab, O., Gao, J., Adli, M., Dey, A., Trimarchi, T., Chung, Y. R., et al. (2013). Deletion of *Asx1* results in myelodysplasia and severe developmental defects *in vivo*. *J. Exp. Med.* 210, 2641–2659. doi:10.1084/jem.20131141
- Akimaru, H., Chen, Y., Dai, P., Hou, D. X., Nonaka, M., Smolik, S. M., et al. (1997). *Drosophila* CBP is a co-activator of *cubitus interruptus* in hedgehog signalling. *Nature* 386, 735–738. doi:10.1038/386735a0
- Alarcón, J. M., Malleret, G., Touzani, K., Vronskaya, S., Ishii, S., Kandel, E. R., et al. (2004). Chromatin acetylation, memory, and ltp are impaired in CBP[±] mice: A model for the cognitive deficit in rubinstein-taybi syndrome and its amelioration. *Neuron* 42, 947–959. doi:10.1016/j.neuron.2004.05.021
- Aoi, S., Ohashi, T., Bamba, R., Fujiki, S., Tamura, D., Funato, T., et al. (2019). Neuromusculoskeletal model that walks and runs across a speed range with a few

Funding

The authors are grateful to the following funding sources: “Aldo Ravelli” Center for Neurotechnology and Experimental Brain Therapeutics - Università degli Studi di Milano (to AL, AP, CG and VM), Intramural funding - Dipartimento DISS, Linea 2, Università degli Studi di Milano (to CG and VM).

Acknowledgments

Translational Medicine Ph.D. scholarship - Università degli Studi di Milano (to ED, PG and CP) and Fondazione Umberto Veronesi fellowship (to AL).

Conflict of interest

The authors declare that the research was conducted in the absence of any commercial or financial relationships that could be construed as a potential conflict of interest.

Publisher's note

All claims expressed in this article are solely those of the authors and do not necessarily represent those of their affiliated organizations, or those of the publisher, the editors and the reviewers. Any product that may be evaluated in this article, or claim that may be made by its manufacturer, is not guaranteed or endorsed by the publisher.

Supplementary material

The Supplementary Material for this article can be found online at: <https://www.frontiersin.org/articles/10.3389/fcell.2022.979512/full#supplementary-material>

motor control parameter changes based on the muscle synergy hypothesis. *Sci. Rep.* 9, 369. doi:10.1038/s41598-018-37460-3

Babu, A., Kamaraj, M., Basu, M., Mukherjee, D., Kapoor, S., Ranjan, S., et al. (2018). Chemical and genetic rescue of an ep300 knockdown model for Rubinstein Taybi Syndrome in zebrafish. *Biochim. Biophys. Acta. Mol. Basis Dis.* 1864, 1203–1215. doi:10.1016/j.bbdis.2018.01.029

Baer, S., Afenjar, A., Smol, T., Piton, A., Gérard, B., Alembik, Y., et al. (2018). Wiedemann-steiner syndrome as a major cause of syndromic intellectual disability: A study of 33 French cases. *Clin. Genet.* 94, 141–152. doi:10.1111/cge.13254

Balemans, M. C. M., Ansar, M., Oudakker, A. R., van Caam, A. P. M., Bakker, B., Vitters, E. L., et al. (2014). Reduced Euchromatin histone methyltransferase 1 causes developmental delay, hypotonia, and cranial abnormalities associated with increased bone gene expression in Kleeftstra syndrome mice. *Dev. Biol.* 386, 395–407. doi:10.1016/j.ydbio.2013.12.016

- Balemans, M. C. M., Huibers, M. M. H., Eikelenboom, N. W. D., Kuipers, A. J., van Summeren, R. C. J., Pijpers, M. M. C. A., et al. (2010). Reduced exploration, increased anxiety, and altered social behavior: Autistic-like features of euchromatin histone methyltransferase 1 heterozygous knockout mice. *Behav. Brain Res.* 208, 47–55. doi:10.1016/j.bbr.2009.11.008
- Balemans, M. C. M., Nadif kasri, N., Kopanitsa, M. V., Afinowi, N. O., Ramakers, G., Peters, T. A., et al. (2013). Hippocampal dysfunction in the Euchromatin histone methyltransferase 1 heterozygous knockout mouse model for Kleeftstra syndrome. *Hum. Mol. Genet.* 22, 852–866. doi:10.1093/hmg/ddt490
- Benevento, M., Oomen, C. A., Horner, A. E., Amiri, H., Jacobs, T., Pauwels, C., et al. (2017). Haploinsufficiency of EHMT1 improves pattern separation and increases hippocampal cell proliferation. *Sci. Rep.* 7, 40284. doi:10.1038/srep40284
- Biegel, J. A., Busse, T. M., and Weissman, B. E. (2014). SWI/SNF chromatin remodeling complexes and cancer. *Am. J. Med. Genet. C Semin. Med. Genet.* 166C, 350–366. doi:10.1002/AJMG.C.31410
- Bjornsson, H. T. (2015). The Mendelian disorders of the epigenetic machinery. *Genome Res.* 25, 1473–1481. doi:10.1101/gr.190629.115
- Bögershausen, N., Tsai, I. C., Pohl, E., Kiper, P. O. S., Beleggia, F., Ferda Percin, E., et al. (2015). RAP1-mediated MEK/ERK pathway defects in Kabuki syndrome. *J. Clin. Invest.* 125, 3585–3599. doi:10.1172/JCI80102
- Boot, M. V., van Belzen, M. J., Overbeek, L. I., Hijmering, N., Mendeville, M., Waaisfz, Q., et al. (2018). Benign and malignant tumors in Rubinstein–Taybi syndrome. *Am. J. Med. Genet. A* 176, 597–608. doi:10.1002/ajmg.a.38603
- Bosman, E. A., Penn, A. C., Ambrose, J. C., Kettleborough, R., Stemple, D. L., and Steel, K. P. (2005). Multiple mutations in mouse Chd7 provide models for CHARGE syndrome. *Hum. Mol. Genet.* 14, 3463–3476. doi:10.1093/hmg/ddi375
- Boukas, L., Havrilla, J. M., Hickey, P. F., Quinlan, A. R., Bjornsson, H. T., and Hansen, K. D. (2019). Coexpression patterns define epigenetic regulators associated with neurological dysfunction. *Genome Res.* 29, 532–542. doi:10.1101/gr.239442.118
- Bourtchouladze, R., Lidge, R., Catapano, R., Stanley, J., Gossweiler, S., Romashko, D., et al. (2003). A mouse model of Rubinstein–Taybi syndrome: Defective long-term memory is ameliorated by inhibitors of phosphodiesterase 4. *Proc. Natl. Acad. Sci. U. S. A.* 100, 10518–10522. doi:10.1073/pnas.1834280100
- Boyles, R. S., Lantz, K. M., Poertner, S., Georges, S. J., and Andres, A. J. (2010). Presenilin controls CBP levels in the adult *Drosophila* central nervous system. *PLoS One* 5, e14332. doi:10.1371/journal.pone.0014332
- Braun, A., Lemaître, B., Lanot, R., Zachary, D., and Meister, M. (1997). *Drosophila* immunity: Analysis of larval hemocytes by P-element-mediated enhancer trap. *Genetics* 147, 623–634. doi:10.1093/genetics/147.2.623
- Bultman, S., Gebuhr, T., Yee, D., La Mantia, C., Nicholson, J., Gilliam, A., et al. (2000). A Brg1 null mutation in the mouse reveals functional differences among mammalian SWI/SNF complexes. *Mol. Cell.* 6, 1287–1295. doi:10.1016/S1097-2765(00)00127-1
- Chao, H. T., Chen, H., Samaco, R. C., Xue, M., Chahrour, M., Yoo, J., et al. (2010a). Dysfunction in GABA signalling mediates autism-like stereotypies and Rett syndrome phenotypes. *Nature* 468, 263–269. doi:10.1038/nature09582
- Chao, M. M., Todd, M. A., Kontny, U., Neas, K., Sullivan, M. J., Hunter, A. G., et al. (2010b). T-cell acute lymphoblastic leukemia in association with Börjeson–Forssman–Lehmann syndrome due to a mutation in PHF6. *Pediatr. Blood Cancer* 55, 722–724. doi:10.1002/PBC.22574
- Cheng, C., Deng, P. Y., Ikeuchi, Y., Yuede, C., Li, D., Rensing, N., et al. (2018). Characterization of a mouse model of börjeson-forssman-lehmann syndrome. *Cell. Rep.* 25, 1404–1414. e6. doi:10.1016/j.celrep.2018.10.043
- Cheng, H., Capponi, S., Wakeling, E., Marchi, E., Li, Q., Zhao, M., et al. (2020). Missense variants in TAF1 and developmental phenotypes: Challenges of determining pathogenicity. *Hum. Mutat.* 41, 449–464. doi:10.1002/HUMU.23936
- Ciptasari, U., and van Bokhoven, H. (2020). The phenomenal epigenome in neurodevelopmental disorders. *Hum. Mol. Genet.* 29, R42–R50. doi:10.1093/HMG/DDAA175
- Clayton-Smith, J., O’Sullivan, J., Daly, S., Bhaskar, S., Day, R., Anderson, B., et al. (2011). Whole-exome-sequencing identifies mutations in histone acetyltransferase gene KAT6B in individuals with the say-barber-biesecker variant of Ohdo syndrome. *Am. J. Hum. Genet.* 89, 675–681. doi:10.1016/j.ajhg.2011.10.008
- Cohen, J. L., Schrier Vergano, S. A., Mazzola, S., Strong, A., Keena, B., McDougall, C., et al. (2020). EP300-related Rubinstein–Taybi syndrome: Highlighted rare phenotypic findings and a genotype–phenotype meta-analysis of 74 patients. *Am. J. Med. Genet. A* 182, 2926–2938. doi:10.1002/ajmg.a.61883
- Cucco, F., Sarogni, P., Rossato, S., Alpa, M., Patimo, A., Latorre, A., et al. (2020). Pathogenic variants in EP300 and ANKRD11 in patients with phenotypes overlapping Cornelia de Lange syndrome. *Am. J. Med. Genet. A* 182, 1690–1696. doi:10.1002/AJMG.A.61611
- De Los Angeles Serrano, M., Demarest, B. L., Tone-Pah-Hote, T., Tristani-Firouzi, M., and Joseph Yost, H. (2019). Inhibition of notch signaling rescues cardiovascular development in Kabuki Syndrome. *PLoS Biol.* 17, e3000087. doi:10.1371/journal.pbio.3000087
- De Wind, N., Dekker, M., Claij, N., Jansen, L., Van Klink, Y., Radman, M., et al. (1999). HNPCC-like cancer predisposition in mice through simultaneous loss of Msh3 and Msh6 mismatch-repair protein functions. *Nat. Genet.* 23, 359–362. doi:10.1038/15544
- Deliu, E., Arecco, N., Morandell, J., Dotter, C. P., Contreras, X., Girardot, C., et al. (2018). Haploinsufficiency of the intellectual disability gene SETD5 disturbs developmental gene expression and cognition. *Nat. Neurosci.* 21, 1717–1727. doi:10.1038/s41593-018-0266-2
- Demir, S., Gürkan, H., Öz, V., Yalçın, S., Atll, E., and Atll, E. (2021). Wiedemann–Steiner syndrome as a differential diagnosis of cornelia de Lange syndrome using targeted next-generation sequencing: A case report. *Mol. Syndromol.* 12, 46–51. doi:10.1159/000511971
- Di Fede, E., Massa, V., Augello, B., Squeo, G., Scarano, E., Perri, A. M., et al. (2020). Expanding the phenotype associated to KMT2A variants: Overlapping clinical signs between wiedemann–steiner and rubinstein–taybi syndromes. *Eur. J. Hum. Genet.* 29, 88–98. doi:10.1038/s41431-020-0679-8
- Di Fede, E., Ottaviano, E., Grazioli, P., Ceccarani, C., Galeone, A., Parodi, C., et al. (2021). Insights into the role of the microbiota and of short-chain fatty acids in rubinstein–taybi syndrome. *Int. J. Mol. Sci.* 22, 3621. doi:10.3390/IJMS22073621
- Dow, L. E., and Lowe, S. W. (2012). Life in the fast lane: Mammalian disease models in the genomics era. *Cell.* 148, 1099–1109. doi:10.1016/j.cell.2012.02.023
- Edelmann, W., Yang, K., Umar, A., Heyer, J., Lau, K., Fan, K., et al. (1997). Mutation in the mismatch repair gene Msh6 causes cancer susceptibility. *Cell.* 91, 467–477. doi:10.1016/S0092-8674(00)80433-X
- Ehrlich, M., Sanchez, C., Shao, C., Nishiyama, R., Kehrl, J., Kuick, R., et al. (2008). ICF, an immunodeficiency syndrome: DNA methyltransferase 3B involvement, chromosome anomalies, and gene dysregulation. *Autoimmunity* 41, 253–271. doi:10.1080/08916930802024202
- Eurordis, November (2005). Rare Diseases : Understanding this Public Health Priority” – www.eurordis.org.
- Fahrner, J. A., and Bjornsson, H. T. (2019). Mendelian disorders of the epigenetic machinery: Postnatal malleability and therapeutic prospects. *Hum. Mol. Genet.* 28, R254–R264. doi:10.1093/HMG/DDZ174
- Fahrner, J. A., and Bjornsson, H. T. (2014). Mendelian disorders of the epigenetic machinery: Tipping the balance of chromatin States. *Annu. Rev. Genomics Hum. Genet.* 15, 269–293. doi:10.1146/annurev-genom-090613-094245
- Faralli, H., Wang, C., Nakka, K., Benyoucef, A., Sebastian, S., Zhuang, L., et al. (2016). UTX demethylase activity is required for satellite cell-mediated muscle regeneration. *J. Clin. Invest.* 126, 1555–1565. doi:10.1172/JCI83239
- Fauquier, L., Azzag, K., Parra, M. A. M., Quillien, A., Boulet, M., Diouf, S., et al. (2018). CBP and P300 regulate distinct gene networks required for human primary myoblast differentiation and muscle integrity. *Sci. Rep.* 8, 12629. doi:10.1038/s41598-018-31102-4
- Feitsma, H., Kuiper, R. V., Korving, J., Nijman, I. J., and Cuppen, E. (2008). Zebrafish with mutations in mismatch repair genes develop neurofibromas and other tumors. *Cancer Res.* 68, 5059–5066. doi:10.1158/0008-5472.CAN-08-0019
- Fisher, C. L., Pineault, N., Brookes, C., Helgason, C. D., Ohta, H., Bodner, C., et al. (2010). Loss-of-function additional sex combs like 1 mutations disrupt hematopoiesis but do not cause severe myelodysplasia or leukemia. *Blood* 115, 38–46. doi:10.1182/blood-2009-07-230698
- Gjini, E., Jing, C. B., Nguyen, A. T., Reyon, D., Gans, E., Kesarsing, M., et al. (2019). Disruption of asxl1 results in myeloproliferative neoplasms in zebrafish. *Dis. Model. Mech.* 12, dmm035790. doi:10.1242/dmm.035790
- Glaser, S., Schaff, J., Lubitz, S., Vintersten, K., van der Hoeven, F., Tufteland, K. R., et al. (2006). Multiple epigenetic maintenance factors implicated by the loss of Mll2 in mouse development. *Development* 133, 1423–1432. doi:10.1242/dev.02302
- Gudmundsson, S., Wilbe, M., Filipek-Górniok, B., Molin, A. M., Ekvall, S., Johansson, J., et al. (2019). TAF1, associated with intellectual disability in humans, is essential for embryogenesis and regulates neurodevelopmental processes in zebrafish. *Sci. Rep.* 9, 10730. doi:10.1038/s41598-019-46632-8
- Gupta, S., Kim, S. Y., Artis, S., Molfese, D. L., Schumacher, A., Sweatt, J. D., et al. (2010). Histone methylation regulates memory formation. *J. Neurosci.* 30, 3589–3599. doi:10.1523/JNEUROSCI.3732-09.2010
- Haberland, M., Mokalled, M. H., Montgomerie, R. L., and Olson, E. N. (2009). Epigenetic control of skull morphogenesis by histone deacetylase 8. *Genes. Dev.* 23, 1625–1630. doi:10.1101/gad.1809209

- Herz, H.-M., Madden, L. D., Chen, Z., Bolduc, C., Buff, E., Gupta, R., et al. (2010). The H3K27me3 demethylase dUTX is a suppressor of notch- and Rb-dependent tumors in *Drosophila*. *Mol. Cell. Biol.* 30, 2485–2497. doi:10.1128/mcb.01633-09
- Hsu, Y. C., Chen, T. C., Lin, C. C., Yuan, C. T., Hsu, C. L., Hou, H. A., et al. (2019). Phf6-null hematopoietic stem cells have enhanced self-renewal capacity and oncogenic potentials. *Blood Adv.* 3, 2355–2367. doi:10.1182/bloodadvances.2019000391
- Hsu, Y. C., Chiu, Y. C., Lin, C. C., Kuo, Y. Y., Hou, H. A., Tzeng, Y. S., et al. (2017). The distinct biological implications of Asx1 mutation and its roles in leukemogenesis revealed by a knock-in mouse model. *J. Hematol. Oncol.* 10, 139. doi:10.1186/s13045-017-0508-x
- Hu, M., Sun, X. J., Zhang, Y. L., Kuang, Y., Hu, C. Q., Wu, W. L., et al. (2010). Histone H3 lysine 36 methyltransferase Hpyb/Setd2 is required for embryonic vascular remodeling. *Proc. Natl. Acad. Sci. U. S. A.* 107, 2956–2961. doi:10.1073/PNAS.0915033107
- Huang, Y. C., Shih, H. Y., Lin, S. J., Chiu, C. C., Ma, T. L., Yeh, T. H., et al. (2015). The epigenetic factor Kmt2a/Mll1 regulates neural progenitor proliferation and neuronal and glial differentiation. *Dev. Neurobiol.* 75, 452–462. doi:10.1002/dneu.22235
- Iacono, G., Dubos, A., Méziane, H., Benevento, M., Habibi, E., Mandoli, A., et al. (2018). Increased H3K9 methylation and impaired expression of Protocadherins are associated with the cognitive dysfunctions of the Kleefstra syndrome. *Nucleic Acids Res.* 46, 4950–4965. doi:10.1093/nar/gky196
- Ijichi, O., Kawakami, K., Matsuda, Y., Ikarimoto, N., Miyata, K., Takamatsu, H., et al. (1996). A case of Kabuki make-up syndrome with EBV+Burkitt's lymphoma. *Acta Paediatr. Jpn.* 38, 66–68. doi:10.1111/J.1442-200X.1996.TB03439.X
- Kasper, L. H., Boussouar, F., Ney, P. A., Jackson, C. W., Reh, J., Van Deursen, J. M., et al. (2002). A transcription-factor-binding surface of coactivator p300 is required for haematopoiesis. *Nature* 419, 738–743. doi:10.1038/nature01062
- Katsani, K. R., Arredondo, J. J., Kal, A. J., and Verrijzer, C. P. (2001). A homeotic mutation in the trithorax SET domain impedes histone binding. *Genes. Dev.* 15, 2197–2202. doi:10.1101/gad.201901
- Kirilly, D., Wong, J. J. L., Lim, E. K. H., Wang, Y., Zhang, H., Wang, C., et al. (2011). Intrinsic epigenetic factors cooperate with the steroid hormone ecdysone to govern dendrite pruning in *Drosophila*. *Neuron* 72, 86–100. doi:10.1016/j.neuron.2011.08.003
- Kline, A. D., Moss, J. F., Selicorni, A., Bisgaard, A. M., Deardorff, M. A., Gillett, P. M., et al. (2018). Diagnosis and management of cornelia de Lange syndrome: First international consensus statement. *Nat. Rev. Genet.* 19, 649–666. doi:10.1038/s41576-018-0031-0
- Koemans, T. S., Kleefstra, T., Chubak, M. C., Stone, M. H., Reijnders, M. R. F., de Munick, S., et al. (2017). Functional convergence of histone methyltransferases EHMT1 and KMT2C involved in intellectual disability and autism spectrum disorder. *PLoS Genet.* 13, e1006864. doi:10.1371/journal.pgen.1006864
- Korzus, E., Rosenfeld, M. G., and Mayford, M. (2004). CBP histone acetyltransferase activity is a critical component of memory consolidation. *Neuron* 42, 961–972. doi:10.1016/j.neuron.2004.06.002
- Kosho, T., Okamoto, N., Imai, Y., Ohashi, H., van Eerde, A. M., Chrzanoska, K., et al. (2014). Genotype-phenotype correlation of coffin-siris syndrome caused by mutations in SMARCB1, SMARCA4, SMARCE1, and ARID1A. *Am. J. Med. Genet. C Semin. Med. Genet.* 166, 262–275. doi:10.1002/ajmg.c.31407
- Kramer, J. M., Kochinke, K., Oortveld, M. A. W., Marks, H., Kramer, D., de Jong, E. K., et al. (2011). Epigenetic regulation of learning and memory by *Drosophila* EHMT/G9a. *PLoS Biol.* 9, e1000569. doi:10.1371/journal.pbio.1000569
- Kumar, J. P., Jamal, T., Doetsch, A., Turner, F. R., and Duffy, J. B. (2004). CREB binding protein functions during successive stages of eye development in *Drosophila*. *Genetics* 168, 877–893. doi:10.1534/genetics.104.029850
- Kung, A. L., Rebel, V. I., Bronson, R. T., Ch'ng, L. E., Sieff, C. A., Livingston, D. M., et al. (2000). Gene dose-dependent control of hematopoiesis and hematologic tumor suppression by CBP. *Genes. Dev.* 14, 272–277. doi:10.1101/gad.14.3.272
- Labudina, A., and Horsfield, J. A. (2021). The three-dimensional genome in zebrafish development. *Brief. Funct. Genomics* 20, elab008–377. doi:10.1093/BFGP/ELAB008
- Layman, W. S., McEwen, D. P., Beyer, L. A., Lalani, S. R., Fernbach, S. D., Oh, E., et al. (2009). Defects in neural stem cell proliferation and olfaction in Chd7 deficient mice indicate a mechanism for hyposmia in human CHARGE syndrome. *Hum. Mol. Genet.* 18, 1909–1923. doi:10.1093/hmg/ddp112
- Lee, J. E., Wang, C., Xu, S., Cho, Y. W., Wang, L., Feng, X., et al. (2013). H3K4 mono- and di-methyltransferase MLL4 is required for enhancer activation during cell differentiation. *Elife* 2, e01503. doi:10.7554/eLife.01503
- Lee, S., Kim, D. H., Goo, Y. H., Lee, Y. C., Lee, S. K., and Lee, J. W. (2009). Crucial roles for interactions between MLL3/4 and INI1 in nuclear receptor transactivation. *Mol. Endocrinol.* 23, 610–619. doi:10.1210/me.2008-0455
- Lee, S., Lee, J. W., and Lee, S. K. (2012). UTX, a histone H3-lysine 27 demethylase, acts as a critical switch to activate the cardiac developmental program. *Dev. Cell.* 22, 25–37. doi:10.1016/j.devcel.2011.11.009
- Lemire, G., Campeau, P. M., and Lee, B. H. (2012). KAT6B disorders. Available at: <https://www.ncbi.nlm.nih.gov/books/NBK114806/> (Accessed December 28, 2020).
- Lepore Signorile, M., Disciglio, V., Di Carlo, G., Pisani, A., Simone, C., and Ingravalo, G. (2021). From genetics to histomolecular characterization: An insight into colorectal carcinogenesis in lynch syndrome. *Int. J. Mol. Sci.* 22, 6767. doi:10.3390/IJMS22136767
- Li, K. L., Zhang, L., Yang, X. M., Fang, Q., Yin, X. F., Wei, H. M., et al. (2018). Histone acetyltransferase CBP-related H3K23 acetylation contributes to courtship learning in *Drosophila*. *BMC Dev. Biol.* 18, 20. doi:10.1186/s12861-018-0179-z
- Liu, D. J., Zhang, F., Chen, Y., Jin, Y., Zhang, Y. L., Chen, S. B., et al. (2020). setd2 knockout zebrafish is viable and fertile: differential and developmental stress-related requirements for Setd2 and histone H3K36 trimethylation in different vertebrate animals. *Cell. Discov.* 6, 72–15. doi:10.1038/s41421-020-00203-8
- Lopez-Atalaya, J. P., Ciccirelli, A., Viosca, J., Valor, L. M., Jimenez-Minchan, M., Canals, S., et al. (2011). CBP is required for environmental enrichment-induced neurogenesis and cognitive enhancement. *EMBO J.* 30, 4287–4298. doi:10.1038/emboj.2011.299
- Melicharek, D. J., Ramirez, L. C., Singh, S., Thompson, R., and Marendra, D. R. (2010). Kismet/CHD7 regulates axon morphology, memory and locomotion in a *Drosophila* model of CHARGE syndrome. *Hum. Mol. Genet.* 19, 4253–4264. doi:10.1093/hmg/ddq348
- Merson, T. D., Dixon, M. P., Collin, C., Rietze, R. L., Bartlett, P. F., Thomas, T., et al. (2006). The transcriptional coactivator Querkopf controls adult neurogenesis. *J. Neurosci.* 26, 11359–11370. doi:10.1523/JNEUROSCI.2247-06.2006
- Miyake, N., Mizuno, S., Okamoto, N., Ohashi, H., Shiina, M., Ogata, K., et al. (2013). KDM6A point mutations cause Kabuki syndrome. *Hum. Mutat.* 34, 108–110. doi:10.1002/humu.22229
- Moore, S. M., Seidman, J. S., Ellegood, J., Gao, R., Savchenko, A., Troutman, T. D., et al. (2019). Setd5 haploinsufficiency alters neuronal network connectivity and leads to autistic-like behaviors in mice. *Transl. Psychiatry* 9, 24. doi:10.1038/s41398-018-0344-y
- Moulton, M. J., and Letsou, A. (2016). Modeling congenital disease and inborn errors of development in *Drosophila melanogaster*. *Dis. Model. Mech.* 9, 253–269. doi:10.1242/dmm.023564
- Negri, G., Magini, P., Milani, D., Crippa, M., Biamino, E., Piccione, M., et al. (2019). Exploring by whole exome sequencing patients with initial diagnosis of rubinstein-taybi syndrome: The interconnections of epigenetic machinery disorders. *Hum. Genet.* 138, 257–269. doi:10.1007/s00439-019-01985-y
- Oike, Y., Hata, A., Mamiya, T., Kaname, T., Noda, Y., Suzuki, M., et al. (1999). Truncated CBP protein leads to classical rubinstein-taybi syndrome phenotypes in mice: Implications for a dominant-negative mechanism. *Hum. Mol. Genet.* 8, 387–396. doi:10.1093/HMG/8.3.387
- O'Rawe, J. A., Wu, Y., Dörfel, M. J., Rope, A. F., Au, P. Y. B., Parboosingh, J. S., et al. (2015). TAF1 variants are associated with dysmorphic features, intellectual disability, and neurological manifestations. *Am. J. Hum. Genet.* 97, 922–932. doi:10.1016/j.ajhg.2015.11.005
- Ospovich, A. B., Gangula, R., Vianna, P. G., and Magnuson, M. A. (2016). Setd5 is essential for mammalian development and the co-transcriptional regulation of histone acetylation. *Development* 143, 4595–4607. doi:10.1242/dev.141465
- Parenti, I., Teresa-Rodrigo, M. E., Pozojevic, J., Ruiz Gil, S., Bader, I., Braunholz, D., et al. (2017). Mutations in chromatin regulators functionally link Cornelia de Lange syndrome and clinically overlapping phenotypes. *Hum. Genet.* 136, 307–320. doi:10.1007/S00439-017-1758-Y
- Peled, J. U., Sellers, R. S., Iglesias-Ussel, M. D., Shin, D. M., Montagna, C., Zhao, C., et al. (2010). Msh6 protects mature B cells from lymphoma by preserving genomic stability. *Am. J. Pathol.* 177, 2597–2608. doi:10.2353/ajpath.2010.100234
- Powis, Z., Farwell Hagman, K. D., Mroske, C., McWalter, K., Cohen, J. S., Colombo, R., et al. (2018). Expansion and further delineation of the SETD5 phenotype leading to global developmental delay, variable dysmorphic features, and reduced penetrance. *Clin. Genet.* 93, 752–761. doi:10.1111/cge.13132
- Rickels, R., Herz, H. M., Sze, C. C., Cao, K., Morgan, M. A., Collings, C. K., et al. (2017). Histone H3K4 monomethylation catalyzed by Trr and mammalian COMPASS-like proteins at enhancers is dispensable for development and viability. *Nat. Genet.* 49, 1647–1653. doi:10.1038/ng.3965
- Ruhf, M. L., Braun, A., Papoulas, O., Tamkun, J. W., Randsholt, N., and Meister, M. (2001). The domino gene of *Drosophila* encodes novel members of the SWI2/

- SNF2 family of DNA-dependent ATPases, which contribute to the silencing of homeotic genes. *Development* 128, 1429–1441. doi:10.1242/dev.128.8.1429
- Russell, B., Tan, W.-H., and Graham, J. M. (2018). “Bohring-opitz syndrome,” in *GeneReviews (qeios)*. doi:10.32388/uq2hhr
- Santoriello, C., and Zon, L. I. (2012). Hooked! modeling human disease in zebrafish. *J. Clin. Invest.* 122, 2337–2343. doi:10.1172/JCI60434
- Scherer, S., Theile, U., Beyer, V., Ferrari, R., Kreck, C., and Rister, M. (2003). Patient with Kabuki syndrome and acute leukemia. *Am. J. Med. Genet. A* 122A, 76–79. doi:10.1002/AJMG.A.20261
- Selicorni, A., Mariani, M., Lettieri, A., and Massa, V. (2021). Cornelia de Lange syndrome: From a disease to a broader spectrum. *Genes*. 12, 1075. doi:10.3390/GENES12071075
- Seo, S., Richardson, G. A., and Kroll, K. L. (2005). The SWI/SNF chromatin remodeling protein Brg1 is required for vertebrate neurogenesis and mediates transactivation of Ngn and NeuroD. *Development* 132, 105–115. doi:10.1242/dev.01548
- Sessa, A., Fagnocchi, L., Mastrototaro, G., Massimino, L., Zaghi, M., Indrigo, M., et al. (2019). SETD5 regulates chromatin methylation state and preserves global transcriptional fidelity during brain development and neuronal wiring. *Neuron* 104, 271–289. e13. doi:10.1016/j.neuron.2019.07.013
- Sethi, S., Lin, H. H., Shepherd, A. K., Volkan, P. C., Su, C. Y., and Wang, J. W. (2019). Social context enhances hormonal modulation of pheromone detection in *Drosophila*. *Curr. Biol.* 29, 3887–3898. e4. doi:10.1016/j.cub.2019.09.045
- Shah, M. Y., Vasanthakumar, A., Barnes, N. Y., Figueroa, M. E., Kamp, A., Hendrick, C., et al. (2010). DNMT3B7, a truncated DNMT3B isoform expressed in human tumors, disrupts embryonic development and accelerates lymphomagenesis. *Cancer Res.* 70, 5840–5850. doi:10.1158/0008-5472.CAN-10-0847
- Shen, T., Lee, A., Shen, C., and Lin, C. J. (2015). The long tail and rare disease research: The impact of next-generation sequencing for rare Mendelian disorders. *Genet. Res.* 97, e15. doi:10.1017/S0016672315000166
- Shpargel, K. B., Sengoku, T., Yokoyama, S., and Magnuson, T. (2012). UTX and UTY demonstrate histone demethylase-independent function in mouse embryonic development. *PLoS Genet.* 8, e1002964. doi:10.1371/journal.pgen.1002964
- Shpargel, K. B., Starmer, J., Wang, C., Ge, K., and Magnuson, T. (2017). UTX-guided neural crest function underlies craniofacial features of Kabuki syndrome. *Proc. Natl. Acad. Sci. U. S. A.* 114, E9046–E9055. doi:10.1073/pnas.1705011114
- Sinclair, D. A., Campbell, R. B., Nicholls, F., Slade, E., and Brock, H. W. (1992). Genetic analysis of the additional sex combs locus of *Drosophila melanogaster*. *Genetics* 130, 817–825. doi:10.1093/genetics/130.4.817
- Sinclair, D. A., Milne, T. A., Hodgson, J. W., Shellard, J., Salinas, C. A., Kyba, M., et al. (1998). The Additional sex combs gene of *Drosophila* encodes a chromatin protein that binds to shared and unique Polycomb group sites on polytene chromosomes. *Development* 125, 1207–1216. doi:10.1242/dev.125.7.1207
- Squeo, G. M., Augello, B., Massa, V., Milani, D., Colombo, E. A., Mazza, T., et al. (2020). Customised next-generation sequencing multigene panel to screen a large cohort of individuals with chromatin-related disorder. *J. Med. Genet.* 57, 760–768. doi:10.1136/jmedgenet-2019-106724
- Sun, X., Chen, J., Zhang, Y., Munisha, M., Dougan, S., and Sun, Y. (2018). Mga modulates Bmpr1a activity by antagonizing Bsg9 in zebrafish. *Front. Cell. Dev. Biol.* 6, 126. doi:10.3389/fcell.2018.00126
- Tachibana, M., Ueda, J., Fukuda, M., Takeda, N., Ohta, T., Iwanari, H., et al. (2005). Histone methyltransferases G9a and GLP form heteromeric complexes and are both crucial for methylation of euchromatin at H3-K9. *Genes. Dev.* 19, 815–826. doi:10.1101/gad.1284005
- Takeuchi, J. K., Lou, X., Alexander, J. M., Sugizaki, H., Delgado-Olguin, N. P., Holloway, A. K., et al. (2011). Chromatin remodeling complex dosage modulates transcription factor function in heart development. *Nat. Commun.* 2, 187. doi:10.1038/ncomms1187
- Tanaka, Y., Naruse, I., Maekawa, T., Masuya, H., Shiroishi, T., and Ishii, S. (1997). Abnormal skeletal patterning in embryos lacking a single cbp allele: A partial similarity with rubinstein-taybi syndrome. *Proc. Natl. Acad. Sci. U. S. A.* 94, 10215–10220. doi:10.1073/pnas.94.19.10215
- Tang, H., Guo, J., Linpeng, S., and Wu, L. (2019). Next generation sequencing identified two novel mutations in NIPBL and a frame shift mutation in CREBBP in three Chinese children. *Orphanet J. Rare Dis.* 14, 45. doi:10.1186/S13023-019-1022-8
- Thieme, S., Gyárfás, T., Richter, C., Özhan, G., Fu, J., Alexopoulou, D., et al. (2013). The histone demethylase UTX regulates stem cell migration and hematopoiesis. *Blood* 121, 2462–2473. doi:10.1182/blood-2012-08-452003
- Thomas, T., Voss, A. K., Chowdhury, K., and Gruss, P. (2000). Querkopf, a MYST family histone acetyltransferase, is required for normal cerebral cortex development. *Development* 127, 2537–2548. doi:10.1242/dev.127.12.2537
- Tsai, I. C., McKnight, K., McKinstry, S. U., Maynard, A. T., Tan, P. L., Golzio, C., et al. (2018). Small molecule inhibition of RAS/MAPK signaling ameliorates developmental pathologies of Kabuki Syndrome. *Sci. Rep.* 8, 10779. doi:10.1038/s41598-018-28709-y
- Van Laarhoven, P. M., Neitzel, L. R., Quintana, A. M., Geiger, E. A., Zackai, E. H., Clouthier, D. E., et al. (2015). Kabuki syndrome genes KMT2D and KDM6A: Functional analyses demonstrate critical roles in craniofacial, heart and brain development. *Hum. Mol. Genet.* 24, 4443–4453. doi:10.1093/hmg/ddv180
- van Ravenswaaij-Arts, C., and Martin, D. M. (2017). New insights and advances in CHARGE syndrome: Diagnosis, etiologies, treatments, and research discoveries. *Am. J. Med. Genet. C Semin. Med. Genet.* 175, 397–406. doi:10.1002/AJMG.C.31592
- Vega, R. B., Matsuda, K., Oh, J., Barbosa, A. C., Yang, X., Meadows, E., et al. (2004). Histone deacetylase 4 controls chondrocyte hypertrophy during skeletogenesis. *Cell*. 119, 555–566. doi:10.1016/j.cell.2004.10.024
- Viosca, J., Lopez-Atalaya, J. P., Olivares, R., Eckner, R., and Barco, A. (2010). Syndromic features and mild cognitive impairment in mice with genetic reduction on p300 activity: Differential contribution of p300 and CBP to Rubinstein-Taybi syndrome etiology. *Neurobiol. Dis.* 37, 186–194. doi:10.1016/j.nbd.2009.10.001
- Wan, X., Hu, B., Liu, J. X., Feng, X., and Xiao, W. (2011). Zebrafish mll gene is essential for hematopoiesis. *J. Biol. Chem.* 286, 33345–33357. doi:10.1074/JBC.M111.253252
- Wang, J., Li, Z., He, Y., Pan, F., Chen, S., Rhodes, S., et al. (2014). Loss of Asxl1 leads to myelodysplastic syndrome-like disease in mice. *Blood* 123, 541–553. doi:10.1182/blood-2013-05-500272
- Wang, Y. R., Xu, N. X., Wang, J., and Wang, X. M. (2019). Kabuki syndrome: Review of the clinical features, diagnosis and epigenetic mechanisms. *World J. Pediatr.* 15, 528–535. doi:10.1007/S12519-019-00309-4
- Wasserman, D. A., Aoyagi, N., Pile, L. A., and Schlag, E. M. (2000). TAF250 is required for multiple developmental events in *Drosophila*. *Proc. Natl. Acad. Sci. U. S. A.* 97, 1154–1159. doi:10.1073/pnas.97.3.1154
- Welstead, G. G., Creighton, M. P., Bilodeau, S., Cheng, A. W., Markoulaki, S., Young, R. A., et al. (2012). X-linked H3K27me3 demethylase Utx is required for embryonic development in a sex-specific manner. *Proc. Natl. Acad. Sci. U. S. A.* 109, 13004–13009. doi:10.1073/pnas.1210787109
- Willemsen, M. H., Vulto-Van Silfhout, A. T., Nillesen, W. M., Wissink-Lindhout, W. M., Van Bokhoven, H., Philip, N., et al. (2012). Update on Kleeftstra syndrome. *Mol. Syndromol.* 2, 202–212. doi:10.1159/000335648
- Wood, M. A., Attner, M. A., Oliveira, A. M. M., Brindle, P. K., and Abel, T. (2006). A transcription factor-binding domain of the coactivator CBP is essential for long-term memory and the expression of specific target genes. *Learn. Mem.* 13, 609–617. doi:10.1101/lm.213906
- Wood, M. A., Kaplan, M. P., Park, A., Blanchard, E. J., Oliveira, A. M. M., Lombardi, T. L., et al. (2005). Transgenic mice expressing a truncated form of CREB-binding protein (CBP) exhibit deficits in hippocampal synaptic plasticity and memory storage. *Learn. Mem.* 12, 111–119. doi:10.1101/lm.86605
- Woods, S. A., Robinson, H. B., Kohler, L. J., Agamanolis, D., Sterbenz, G., and Khalifa, M. (2014). Exome sequencing identifies a novel EP300 frame shift mutation in a patient with features that overlap Cornelia de Lange syndrome. *Am. J. Med. Genet. A* 164A, 251–258. doi:10.1002/AJMG.A.36237
- Yamamoto, P. K., de Souza, T. A., Antiorio, A. T. F. B., Zanatto, D. A., Garcia-Gomes, M. de S. A., Alexandre-Ribeiro, S. R., et al. (2019). Genetic and behavioral characterization of a Kmt2d mouse mutant, a new model for Kabuki Syndrome. *Genes. Brain Behav.* 18, e12568. doi:10.1111/gbb.12568
- Yamauchi, T., Oike, Y., Kamon, J., Waki, H., Kameda, K., Tsuchida, A., et al. (2002). Increased insulin sensitivity despite lipodystrophy in Crebbp heterozygous mice. *Nat. Genet.* 30, 221–226. doi:10.1038/ng829
- Yao, T. P., Oh, S. P., Fuchs, M., Zhou, N. D., Ch'ng, L. E., Newsome, D., et al. (1998). Gene dosage-dependent embryonic development and proliferation defects in mice lacking the transcriptional integrator p300. *Cell*. 93, 361–372. doi:10.1016/S0092-8674(00)81165-4
- Yu, B. D., Hess, J. L., Horning, S. E., Brown, G. A. J., and Korsmeyer, S. J. (1995). Altered Hox expression and segmental identity in Mll-mutant mice. *Nature* 378, 505–508. doi:10.1038/378505A0
- Yuan, B., Pehlivan, D., Karaca, E., Patel, N., Charng, W. L., Gambin, T., et al. (2015). Global transcriptional disturbances underlie Cornelia de Lange syndrome and related phenotypes. *J. Clin. Invest.* 125, 636–651. doi:10.1172/JCI77435
- Zheng, F., Kasper, L. H., Bedford, D. C., Lerach, S., Teubner, B. J. W., and Brindle, P. K. (2016). Mutation of the CH1 domain in the histone acetyltransferase CREBBP results in autism-relevant behaviors in mice. *PLoS One* 11, e0146366. doi:10.1371/journal.pone.0146366